AD-A279 292

②

AD_____

GRANT NO: DAMD17-92-J-2025

TITLE: NON-INVASIVE DETECTION OF INCREASED INTRACRANIAL
        PRESSURE USING ACOUTICAL TECHNIQUES

PRINCIPAL INVESTIGATOR: George R. Wodicka, Ph.D.

CONTRACTING ORGANIZATION: Purdue Research Foundation
                           Purdue University
                           West Lafayette, Indiana 47907

REPORT DATE: March 7, 1994

DTIC
SELECTE
MAY 17. 1994
B **D**

TYPE OF REPORT: Final Report

PREPARED FOR: U.S. Army Medical Research, Development,
               Acquisition and Logistics Command (Provisional),
               Fort Detrick, Frederick, Maryland 21702-5012

DISTRIBUTION STATEMENT: Approved for public release;
                         distribution unlimited

The views, opinions and/or findings contained in this report are
those of the author(s) and should not be construed as an official
Department of the Army position, policy or decision unless so
designated by other documentation.

94-14769

94 5 17 002

REPORT DOCUMENTATION PAGE

1. AGENCY USE ONLY (Leave blank)	2. REPORT DATE 7 March 1994	3. REPORT TYPE AND DATES COVERED Final Report (9/8/92 - 2/7/94)

4. TITLE AND SUBTITLE
Non-Invasive Detection of Increased Intracranial
Pressure Using Acoutical Techniques

5. FUNDING NUMBERS
Grant No.
DAMD17-92-J-2025

6. AUTHOR(S)
George R. Wodicka, Ph.D., Joe D. Bourland,
Gary C. Lantz, Willis A. Tacker

7. PERFORMING ORGANIZATION NAME(S) AND ADDRESS(ES)
Purdue Research Foundation
Purdue University
West Lafayette, Indiana 47907

8. PERFORMING ORGANIZATION REPORT NUMBER

9. SPONSORING/MONITORING AGENCY NAME(S) AND ADDRESS(ES)
U.S. Army Medical Research, Development,
Acquisition and Logistics Command (Provisional),
Fort Detrick
Frederick, Maryland 21702-5012

10. SPONSORING/MONITORING AGENCY REPORT NUMBER

11. SUPPLEMENTARY NOTES

12a. DISTRIBUTION/AVAILABILITY STATEMENT
Approved for public release; distribution unlimited

12b. DISTRIBUTION CODE

13. ABSTRACT (Maximum 200 words)

This study was undertaken to determine the relationships between intracranial pressure (ICP) and the acoustic response of the head. Potentially fatal increases in ICP can occur in soldiers afflicted with Acute Mountain Sickness at high-altitude, yet there is no reliable and noninvasive procedure to monitor ICP changes in uncontrolled conditions. In this investigation, an ovine animal model was used in which incremental increases in ICP were elicited and directly measured through intraventricular cannulae. At each ICP increment, a vibration source elicited a flexural response of the animal's head, and this acoustic response was measured at four locations on the skull using accelerometers. Spectral analysis of the response showed numerous changes in proportion to ICP up to roughly 20 cmH$_2$O above normal; a clinically significant range. For example, changes in magnitude and phase at frequencies between 4 and 7 kHz each correlated well (> 0.92) with ICP across the study group. Thus, alterations in ICP give rise to measurable acoustic changes that can potentially be used to noninvasively monitor afflicted soldiers in uncontrolled environments.

14. SUBJECT TERMS
Altitude, Cerebral Edema, Acoustics, Mountain Sickness
RAD III

15. NUMBER OF PAGES

16. PRICE CODE

17. SECURITY CLASSIFICATION OF REPORT	18. SECURITY CLASSIFICATION OF THIS PAGE	19. SECURITY CLASSIFICATION OF ABSTRACT	20. LIMITATION OF ABSTRACT
Unclassified	Unclassified	Unclassified	Unlimited

FOREWORD

Opinions, interpretations, conclusions and recommendations are those of the author and are not necessarily endorsed by the US Army.

_____ Where copyrighted material is quoted, permission has been obtained to use such material.

_____ Where material from documents designated for limited distribution is quoted, permission has been obtained to use the material.

GRW Citations of commercial organizations and trade names in this report do not constitute an official Department of Army endorsement or approval of the products or services of these organizations.

GRW In conducting research using animals, the investigator(s) adhered to the "Guide for the Care and Use of Laboratory Animals," prepared by the Committee on Care and Use of Laboratory Animals of the Institute of Laboratory Resources, National Research Council (NIH Publication No. 86-23, Revised 1985).

_____ For the protection of human subjects, the investigator(s) adhered to policies of applicable Federal Law 45 CFR 46.

_____ In conducting research utilizing recombinant DNA technology, the investigator(s) adhered to current guidelines promulgated by the National Institutes of Health.

_____ In the conduct of research utilizing recombinant DNA, the investigator(s) adhered to the NIH Guidelines for Research Involving Recombinant DNA Molecules.

_____ In the conduct of research involving hazardous organisms, the investigator(s) adhered to the CDC-NIH Guide for Biosafety in Microbiological and Biomedical Laboratories.

Accession For		
NTIS GRA&I	☑	
DTIC TAB	☐	
Unannounced	☐	
Justification		
By		
Distribution/		
Availability Codes		
Dist	Avail and/or Special	
A-1		

PI - Signature   _James R Woodcock_   Date _3/4/94_

i

TABLE OF CONTENTS

I. INTRODUCTION

A. *Problem Statement*

Acute Mountain Sickness (AMS) is a failure to adapt to high altitude and usually occurs at elevations of 8,000 feet or more. Although the onset of this syndrome in any one individual is unpredictable, staging the ascent to allow for acclimatization to altitude and avoiding over-exertion can prevent or reduce the severity of AMS. These precautions are probably not realistic for the majority of military exercises and missions held at high altitude. The definitive treatment for severe cases of AMS is to take the affected person to lower altitude (Elnicki 1990, Jacobson 1988, Mountain 1987, Hamilton 1986 b, Houston 1984).

A spectrum of medical problems can occur in this syndrome, with one of the most frequent and serious conditions being cerebral edema with associated increased intracranial pressure (ICP) (Houston 1975, Wilson 1973, Singh 1969). Although the exact etiology of the edema and increased ICP is not known, their progression to dangerous levels can occur rapidly. Delayed recognition and treatment of this syndrome may likely lead to disability or death, and in fact, cerebral edema is found in the vast majority of fatal cases of acute AMS (Levine 1989).

Early recognition of the increased ICP associated with cerebral edema is essential to protect an individual's life as well as to help insure the success of a mission at high altitude. The most commonly-used techniques for ICP measurement are: 1) intraventricular catheters, 2) subarachnoid or epidural pressure sensors, or 3) the lumbar puncture (Luchka, 1991). Each of these techniques is invasive and requires a controlled environment and a skilled physician to successfully perform the procedure. Currently, there is not a reliable noninvasive technique to monitor changes in ICP in an uncontrolled environment .

B. A Potential Acoustic Solution

The analysis of sound transmitted through a structure or system is a commonly-used engineering technique to assess underlying physical properties. The attributes of even highly heterogeneous systems such as the undersea environment can be determined by probing the system over a wide range of sonic frequencies and measuring the acoustic response. In the case of constrained structures such as the human head, the response to sound (or equivalently, vibration) typically exhibits well-defined spectral and spatial patterns which are determined by the inherent geometry, weight, pressure, and losses in a predictable manner. Thus, it is likely that increases in ICP would be reflected in the overall acoustical properties of the head and that ICP can potentially be monitored noninvasively using acoustical techniques.

C. Literature Review

In a preliminary study by Semmlow and Fisher (1982) using two canine pups, the response of the head to low-level audible vibrations was observed to correlate with ICP. In the protocol, the animals developed a chronically elevated ICP over a six-week period due to initial autogenous blood injections into the cisterna magna, with a maximum ICP increase of roughly 11 cm H_2O. An electro-mechanical solenoid was employed before and after increased ICP development to introduce vibrations into the heads of the animals, and the acoustical responses were measured on the opposite side of the skull using a contact accelerometer. Significant alterations in the initial timing, frequency content, and temporal decay of the response were noted after increased ICP development, and the decay was observed to be a roughly linear function of ICP. Although there is no statistical significance of these measurements due to the small study group and the possible effects of skull growth over the six-week period complicate the interpretation of the results, the significant changes in the measured acoustical parameters of the head strongly suggest a sensitive relationship between these (and possibly other) parameters and ICP.

The mechanical properties of the head have been studied extensively to understand the effects of the large forces and displacements associated with traumatic injury. In response to these large forces, the action of the head is highly non-linear and significant structural damage can often be observed. The response of the head to low-level acoustical vibrations, however, has been the topic of relatively few studies. To investigate the mechanisms of bone-conducted sound on hearing, the human skull (Franke 1956) and head (Hakansson 1986, Franke 1956, Bekesy 1951) have been vibrated using various techniques, and measurements of the acoustical response performed. Similar studies have also been performed on the human skull (Khalil 1979), cadaver head (Stalnaker 1971, Gurdjian 1970, Hodgson 1967) and human head (Gurdjian 1970, Hodgson 1968) as a prelude to further studies using larger forces.

Although each study employed a unique range of perturbation forces and frequencies, measurement sites, mechanical boundary conditions, etc., some consistencies in the observations are evident. The first consistent observation is that the head exhibits measurable acoustical resonance behavior over the frequency range between 100 and 2,000 cycles per second (Hz). In this context, resonance can be loosely defined as the frequency at which a large acoustical response of the system occurs for a given input acoustical perturbation. For various skulls, the first excitable (fundamental) resonance occurred at frequencies above 500 Hz, and the effects of the intracranial tissues was to decrease the observed resonance frequencies by roughly a factor of two to a range of approximately 250 - 500 Hz. The acoustical effects of the extracranial tissues was to slightly decrease the resonance frequency even further and also to significantly increase the overall losses, or damping, of the response. It is clear from these measurements that the exact locations of both the transducers and the mechanical boundary (support) conditions on the head significantly affect the overall measured response. The former observation indicates that the head exhibits a flexural response (mode) to the vibrations since as the head flexes its measured response would exhibit strong spatial dependence. These flexural responses are also consistent with the strong dependence of the measurements on the mechanical support (or lack thereof) employed for the head in each study

since the exact flexural mode of a structure is a strong function of the imposed boundary conditions.

To better understand the complex response of the head to acoustical vibrations, the head has been modeled from a theoretical perspective as a vibrating spherical shell (Wilkinson 1965 a,b, Baker 1961). A vibrating shell may exhibit various modes of vibration which are dependent upon the spatial and spectral attributes of the applied acoustical perturbation. For example, there are translational modes (resonances) that reflect bulk movement of the shell, so-called spherical modes which can only be excited via a spatially uniform perturbation about the sphere, and flexural modes of different types which are dependent upon the location of the perturbation, the boundary conditions which surround the sphere, and the mechanical properties of the shell and its interior.

The application of theories which describe the spherical shell toward understanding the acoustical properties of the human skull have met with some success (Khalil 1982). Comparing the predicted resonance frequencies of fundamental flexural modes from a spherical model with those observed in an *in vitro* preparation using a human skull results in an over-estimation of the resonance frequency by about a factor of two. If one assumes, however, that the effective overall compliance of the skull is roughly 50% greater than that for an intact sphere because of sutures and openings in the skull, the measured resonance frequencies are predicted reasonably well by this approach. These findings suggest that while employing a spherical geometry to model the head is clearly a simplification of the actual anatomy, it may provide some useful information concerning the physical determinants of the acoustic response.

D. Goals of the Research Project

The principle objective of this research project was to quantitatively determine the acoustical properties of the head and their relation to ICP. The study incorporated an acute

ovine model in which accurate acoustical measurements were made as a function of elevated ICP over a wide pathological range. Sophisticated signal analysis and acoustical techniques were employed to elucidate the key parameters to measure as sensitive and reliable correlates of ICP. The results provide a framework upon which to develop a novel instrument that could be easily employed to noninvasively monitor ICP elevations in the field.

II. BODY

A. *Animal Surgery*

An ovine animal model was employed to experimentally vary ICP and measure the resulting changes in the acoustical properties of the head. This model has been successfully used in surgical studies of the cerebrospinal fluid (CSF) system (Hamilton 1986 a) and was chosen since its skull size and shape facilitated the application of transducers to measure both ICP and the acoustical response. An acute protocol that mimiced the clinical syndrome found in AMS and allowed for a wide range of generated ICP in a single animal was used.

As detailed in the quarterly progress reports on this project, a total of 8 sheep (ovis aries) were studied. Complete acoustical and ICP data were obtained from four sheep(#4, 5, 6, 8), control data at normal ICP was taken over time in one of the sheep (#3), and limited or no data was obtained from three sheep due to computer difficulties (#1), intermittent catheter blockage (#2), and hemorrhage (#7), during this complex protocol. Each sheep was fasted for 24 hours with free-choice water before anesthesia induction. Anesthesia was induced with pentobarbital sodium (Anthony Products, Arcadia, CA) 25 to 30 mg/kg, too effect, administered intravenously and maintained with intravenous pentobarbital sodium and oxygen administered via an endotracheal tube. A ventilator assisted respiration. A right femoral arterial catheter was placed for direct continuous physiograph blood pressure monitoring. The sheep were place in sternal recumbancy. A midline cranial incision was made from the level of the medial canthi to 2.0 cm caudal to the external occipital protruberance. Soft tissues were subperiosteally elevated and retracted. A hole was drilled and tapped at the level of the internal
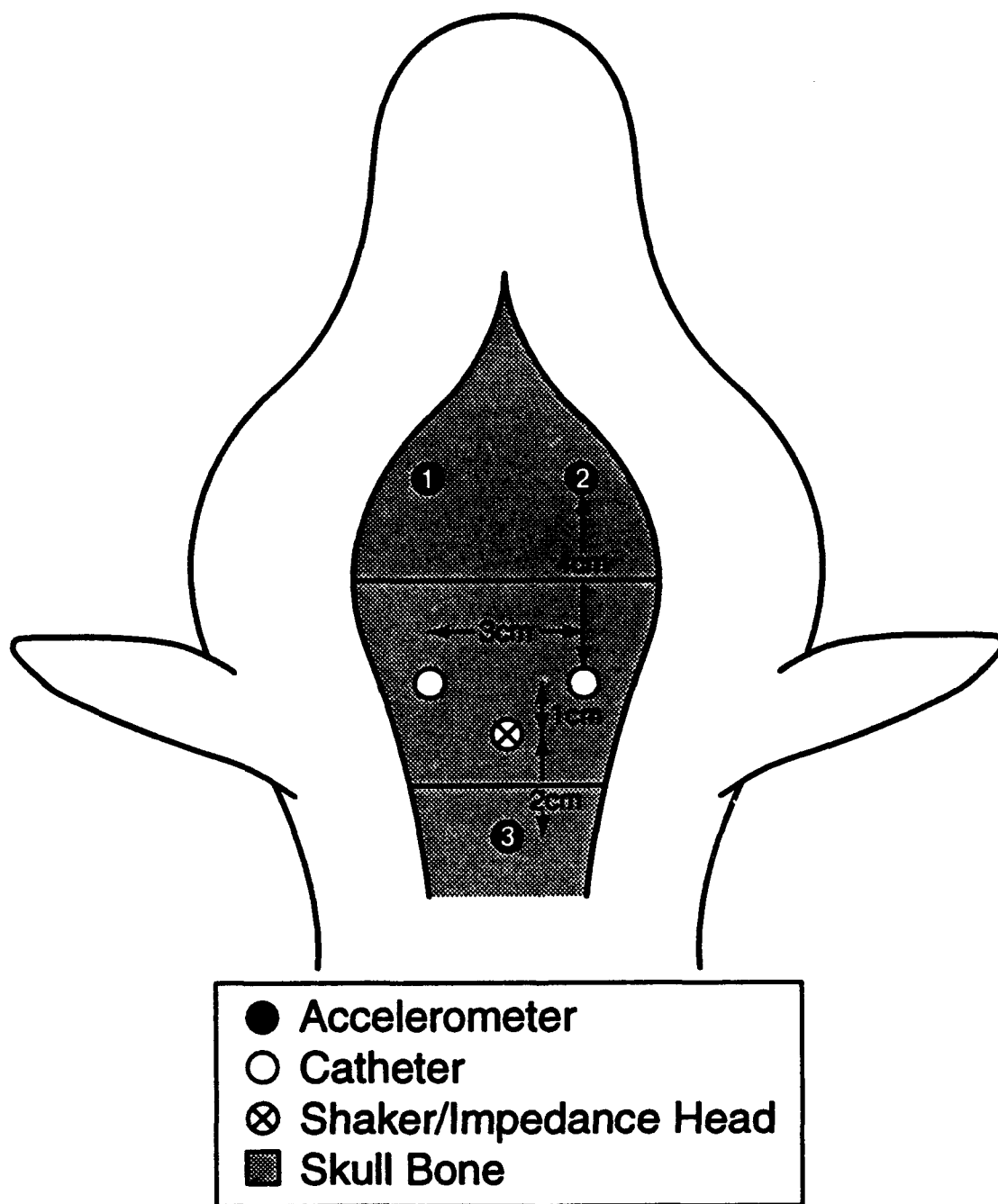
Figure 1: Diagram of catheter and transducer locations on the ovine skull.

occipital protruberance for screw mounting of the shaker head (see Figure 1). The external bone cortex at this level was contoured with a bone burr to ensure maximal contact between the shaker head and bone. Three accelerometers were mounted on the skull with screws placed in drilled and tapped holes located on the external occipital protruberance, and on each frontal bone. Two holes were drilled and tapped for the mounting of a wire frame to which the inflow and outflow lines attached to the ventricular catheters would be mounted. None of the six holes that were drilled entered the cranial cavity. Trephine holes (0.5 cm diameter) were then made with a bone burr in the parietal bone 1.0 cm caudal to the coronal suture and 1.5 cm lateral to each side of the mideline (Pappenheimer 1962). The external dura mater remained intact. Teflon catheters (Angiocath, 19 gauge, 1 1/4", Becton-Dickinson, Sandy, UT) were modified by the addition of 2 side ports. The catheters with stylets were advanced until the respective lateral ventricle was penetrated about 12 to 15 mm ventral to the external dura. Removal of the stylet and return to the catheter hub of cerebrospinal fluid (CSF) confirmed placement of the catheters. The catheters were held in position with epoxy (5 Minute Epoxy Gel, Devion Corp., Davners, MA). The wire frame was attached to the skull with screws. After attaching the catheter hubs to their respective inflow and outflow lines, the lines were secured to the frame with silk ties. This prevented the weight of the lines from contributing to kinking of the ventricular catheters.

Needle trocarization was performed as necessary during the protocol to relieve ruminal tympany. At the completion of each experiment, while each sheep was under general anesthesia, potassium chloride was administered and the ECG tracing monitored until all cardiac activity was stopped.

B. Measurement and Control of Intracranial Pressure

The tubing from the catheters leading to each lateral ventricle was connected to an infusion pump (model 994, Harvard Apparatus) and a pressure transducer (model CDX, Cobe Laboratories). Initially, the infusion rate of artificial CSF (Lactated Ringer's Injection USP,

Baxter Heathcare, Deerfield, IL) was set extremely low, 0.00494 ml/min, so as to not elevate

ICP but yet insure catheter patency. The output of each pressure transducer was monitored

using a chart recorder (model Physiograph CPM, Narco Biosystems) and both cardiac and

respiratory variations as well as agreement between ICP values were noted. One of the

catheters was chosen at random as the channel where the infusion rate would be increased to

elevate ICP, and the ICP signal from the other catheter was connected to the computer for

subsequent measurement. In this manner, ICP was elevated in a controlled manner via

infusion into one lateral ventricle and measured via a catheter in the other ventricle. Infusion

rates up to 0.494 ml/min were used during the protocol to allow acoustical measurements to be

made at roughly 5 cmH$_2$0 increments in ICP, up to a maximum value of approximately 100

cmH$_2$0.

C. Acoustic Measurements and Signal Processing

To elicit measurable vibrations of the head, noise with equal energy at frequencies

between 100 and 10,000 Hz was generated (model WSB-100, QuaTech), amplified (model NS

B-2, Yamaha) and input to an electromechanical shaker (model 203, Ling). The shaker was

mounted in a free-standing frame (see Figure 2) that also served to immobilize the ovine head

and thereby insure no bulk translation in response to the vibrational excitation. The shaker

armature was connected to the proximal end of an impedance head (model Z11, Wilcoxen) that

measures both force and acceleration, with the distal end mounted in the skull. The force and

acceleration signals from the impedance head along with the signals from the three

accelerometers mounted at the other skull locations (model 303A, PCB) were amplified using

charge (model 422D03, PCB) and voltage (model 483B07, PCB) amplifiers and then bandpass

filtered (4-pole Butterworth type) with cutoff frequencies of 50 and 10,000 Hz. Each of the

five acoustic signals (one force and four acceleration) were digitized with the ICP signal at a

rate of 32,768 samples/sec (model DAS-16F, Metrabyte) for a duration of 1 s.
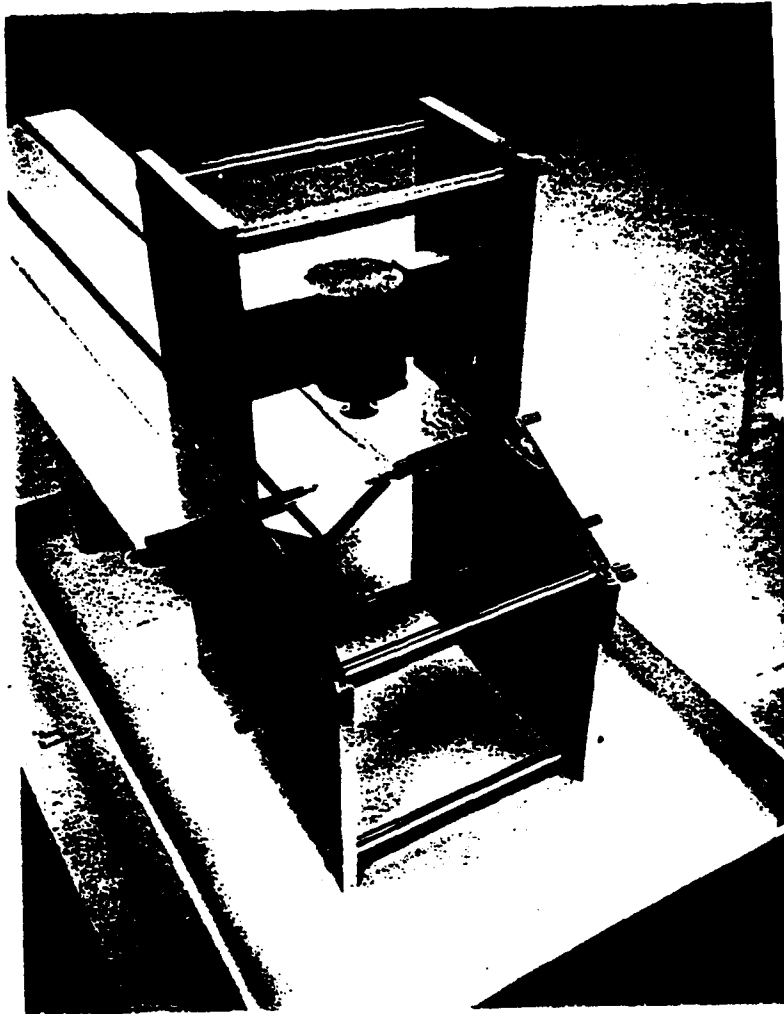
Figure 2: Photograph of shaker mount and frame used to immobilize the ovine head.

To simplify the interpretation of the signal processing (Labview, National Instruments), the four acceleration signals ($i = 0, 1, 2, 3$) were considered as outputs and processed relative to the force signal input. Initially, the coherence $\alpha(f)$ between each output and the input was estimated and found to be very close to unity (> 0.95) over the entire frequency f range of the excitation and measurements. This finding indicates a strong linear dependence of the acceleration response of the skull to low-amplitude audible vibrations as well as a high signal to background noise ratio of the measurements.

The output acceleration signals were each digitally integrated (summed) to form the equivalent velocity. Spectral estimates of the velocity of each output $V_i(f)$ and the input force $F(f)$ were performed using the method described by Welch (Kay 1988). In particular, each time-domain digital signal was parsed into 14 epochs of 4096 samples in duration with 50% overlap between successive epochs, windowed with a Hanning function, transformed to the frequency domain, and then averaged to form the spectal estimate. Calibration and mass data from each transducer were used to minimize transducer sensitivity differences and loading effects, respectively.

The absolute transfer impedance $Z_i(f) = F(f)/V_i(f)$ to each output site was calculated and placed in magnitude $|Z_i(f)|$ and phase $\measuredangle Z_i(f)$ form. $Z_i(f)$ is a measure, as a function of frequency, of the relationship between the applied force and the resulting velocity. To assess how $Z_i(f)$ changed with elevations in ICP, the relative impedance magnitude $|\overline{Z}_i(f, ICP)|$ and phase $\measuredangle \overline{Z}_i(f, ICP)$ with respect to the estimates at normal ICP were determined

$$\left|\overline{Z}_i(f, ICP)\right| = \frac{\left|Z_i(f, ICP)\right|}{\left|Z_i(f, \text{ normal ICP})\right|}$$

$$\measuredangle \overline{Z}_i(f, ICP) = \measuredangle Z_i(f, ICP) - \measuredangle Z_i(f, \text{ normal ICP})$$

Changes in the relative spectral magnitude or phase can be quantified in numerous ways such as calculating heights of spectral peaks or valleys. However, these measures fail to yield consistent results if the exact spectral shapes or peak locations change - as was observed to be the case for ICP induced spectral changes. Thus, we decided to quantify the changes in each magnitude and phase spectra by calculating the standard deviation of each over specific frequency bands. In this context, since $\overline{Z}_i(f, ICP)$ is relative to that at normal ICP, the standard deviation represents a global measure of the spectral energy in the band due to ICP evelation that is not sensitive to the exact spectral shape. This measure was observed to follow a roughly linear trend with ICP up to 20 cmH$_2$O above normal. Thus, a least-squares minimization procedure was used to fit a line passing through the origin to represent the standard deviation vs. ICP elevation data. The correlation coefficient and slope of this line were examined to assess the linearity and variability of the acoustic response to ICP.

D. Results

A representative set of absolute impedance spectral estimates in magnitude | $Z_i(f)$ | and phase $\measuredangle Z_i(f)$ form for the 4 measurements sites at normal ICP is shown in Figure 3. The phase change from slightly positive to negative in the driving point impedance at very low frequencies is consistent with the study by Hakansson (1986) where the acoustic response of the skull was modeled as a simple resonant structure with mass, resistance and compliance. Also at very lower frequencies, all of the responses have similar phases indicative of nearly in-phase vibrational motion of the entire head. At higher frequencies, the relative motion of the sites becomes out of phase indicating that the head exhibited a flexural response to the broadband excitation. Eliciting a flexural response was a key goal of the experimentation, and to our knowledge represents the first experimental measurements of this phenomenon. This finding lead us to focus our subsequent analysis on frequencies above 1000 Hz where flexural modes occur and where we had hypothesized that the response would be most sensitive to changes in ICP.

IMPEDANCE MAGNITUDES FROM FOUR SITES AT NORMAL ICP

IMPEDANCE PHASES FROM FOUR SITES AT NORMAL ICP
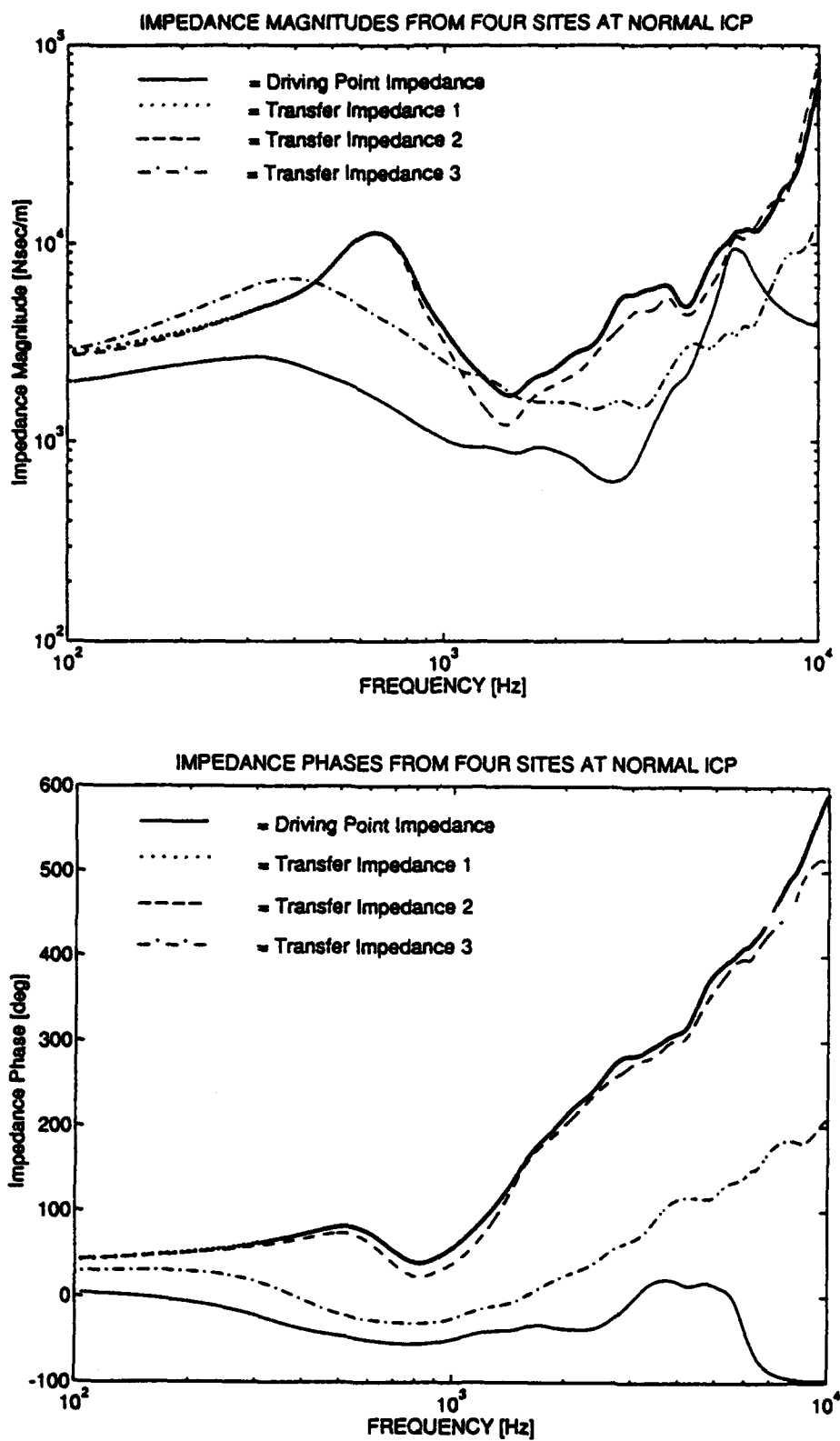
Figure 3: Absolute impedance magnitude | $Z_i(f)$ | and phase $\angle Z_i(f)$ at the four measurements
sites at normal ICP.
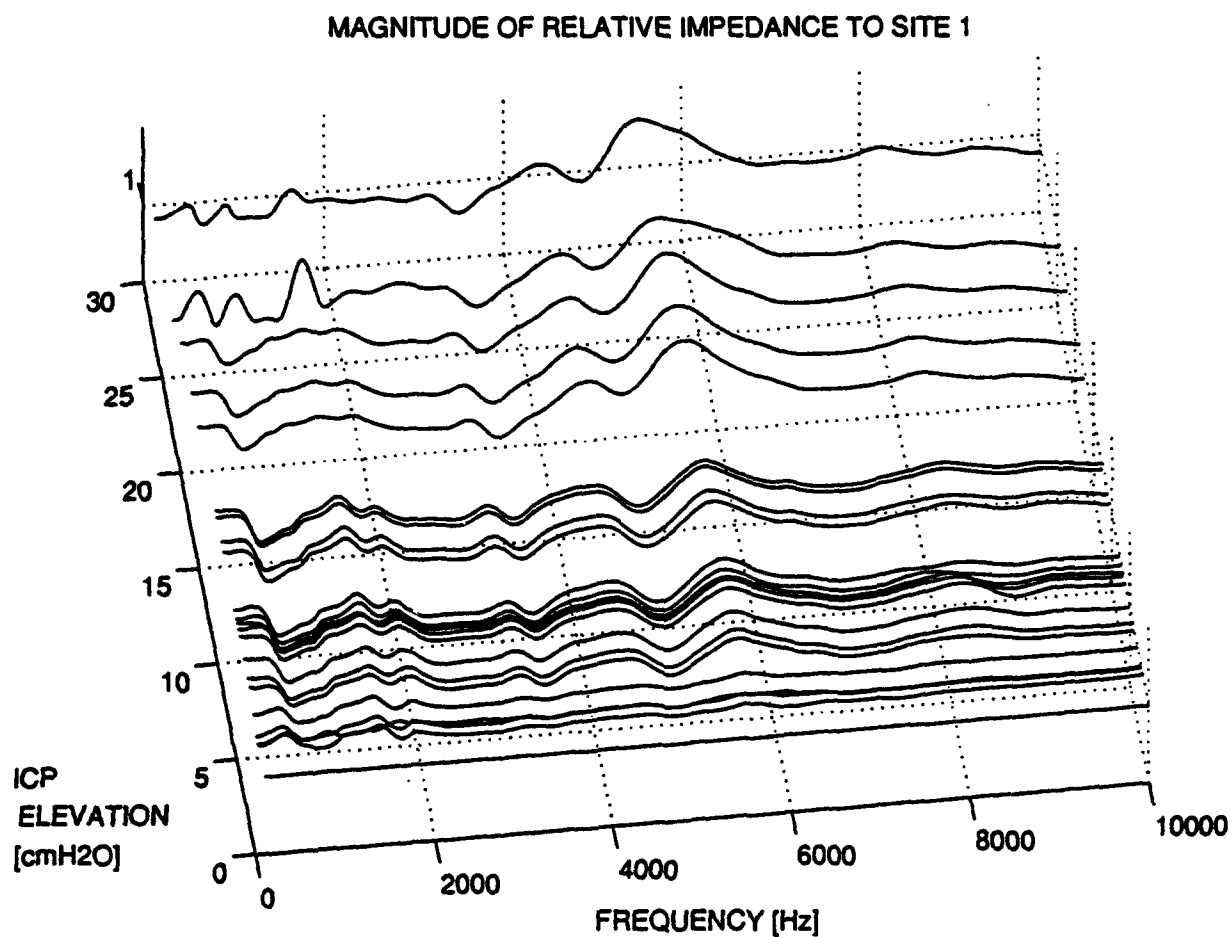
Figure 4: Relative impedance magnitude $| Z_i(f, ICP) |$ vs. frequency and ICP for sheep #8.
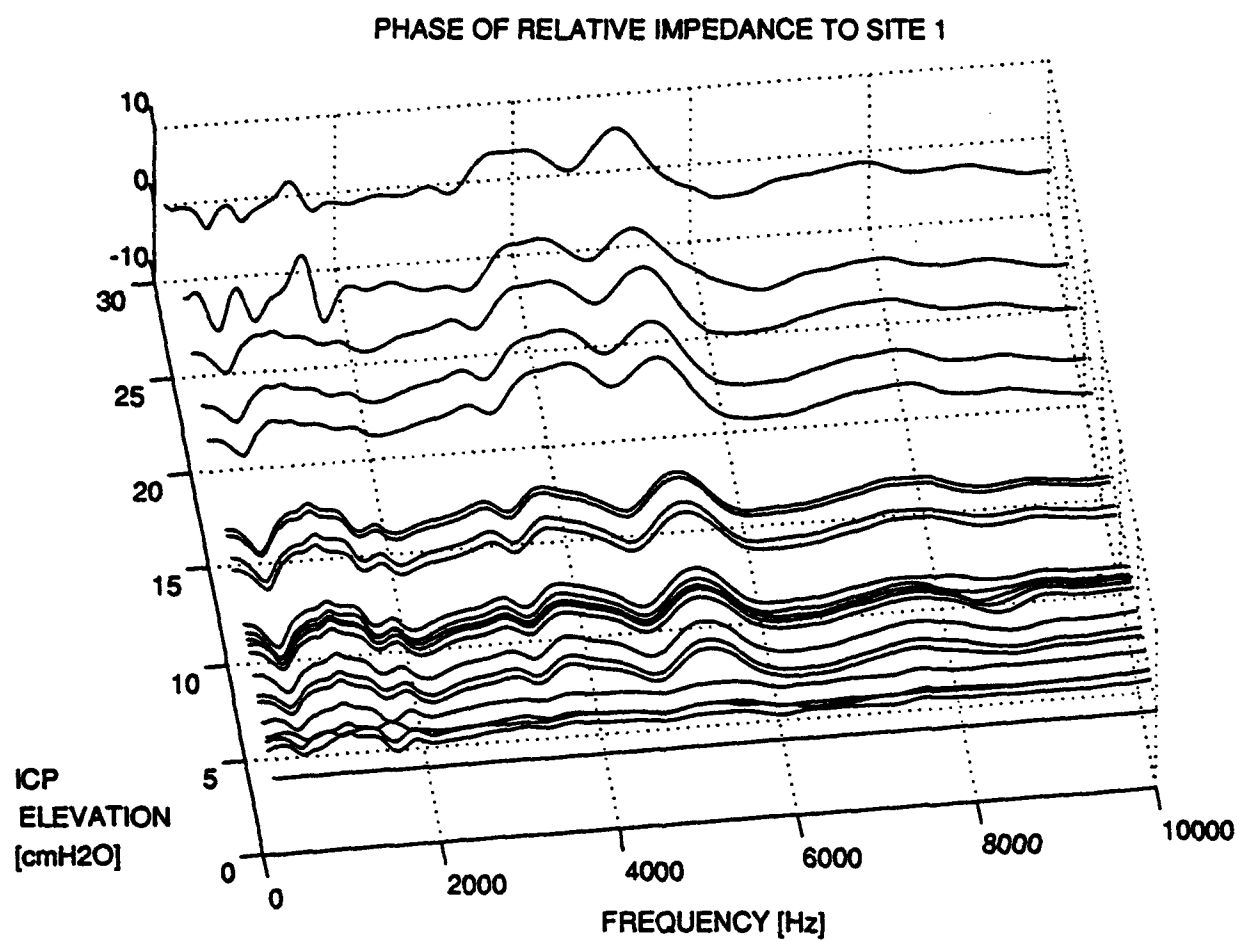
Figure 5:   Relative impedance phase ∡ $\overline{Z}_i$(f, ICP) vs. frequency and ICP for sheep #8.

Figure 4 depicts a representative magnitude of the relative transfer impedance to the #1 site, $| \overline{Z}_1(f, ICP) |$, as a function of frequency and elevated ICP in a three-dimensional plotting form. At normal ICP, $| \overline{Z}_1(f, ICP) |$ is unity at all frequencies representing the reference spectrum. As ICP increases, a number of observable spectral changes occur in proportion up to about 20 cmH_2O above normal where the responses reach a plateau and do not change further. The magnitude of the maximum spectral changes are roughly 50% of the normal ICP spectral value of unity and are reliably measured given the accuracy of the instrumentation and the signal processing. These changes do not occur over time if ICP is not elevated as observed in the control sheep. In the control case, even after 3 hours of elapsed time the spectral values were within 4% of unity over the entire frequency range.

Similar spectral changes in proportion to ICP were observed in the phase of the relative transfer impedance, $\angle \overline{Z}_i(f, ICP)$. Figure 5 shows the phase spectra as a function of ICP for the same subject and site as in Figure 4. The resultant phase changes are measureable and also do not change significantly after ICP reaches roughly 20 cmH_2O above normal. Thus, it appears as though nearly equivalent ICP information is contained in both the magnitude and phase of the acoustic response from a particular measurement site.

Extraction of the standard deviation as a measure of spectral change from either $| \overline{Z}_i(f, ICP) |$ or $\angle Z_i(f, ICP)$ over designated frequency bands yielded a reliable and sensitive index of ICP. Plots of the standard deviation vs. ICP elevation derived from the relative magnitude and phase spectra in each sheep over the 4000 - 7000 Hz frequency range are presented in Figures 6 (magnitude) and 7 (phase). A linear trend with ICP is observed and the correlation coefficients approach unity (> 0.92) in each case and for the group. Table A summarizes the dynamics of this particular variable for the 4 sheep in which complete data were obtained. Although the exact range of ICP values over which a linear trend is found varied across sheep, high overall correlations between this acoustic variable and ICP were observed.
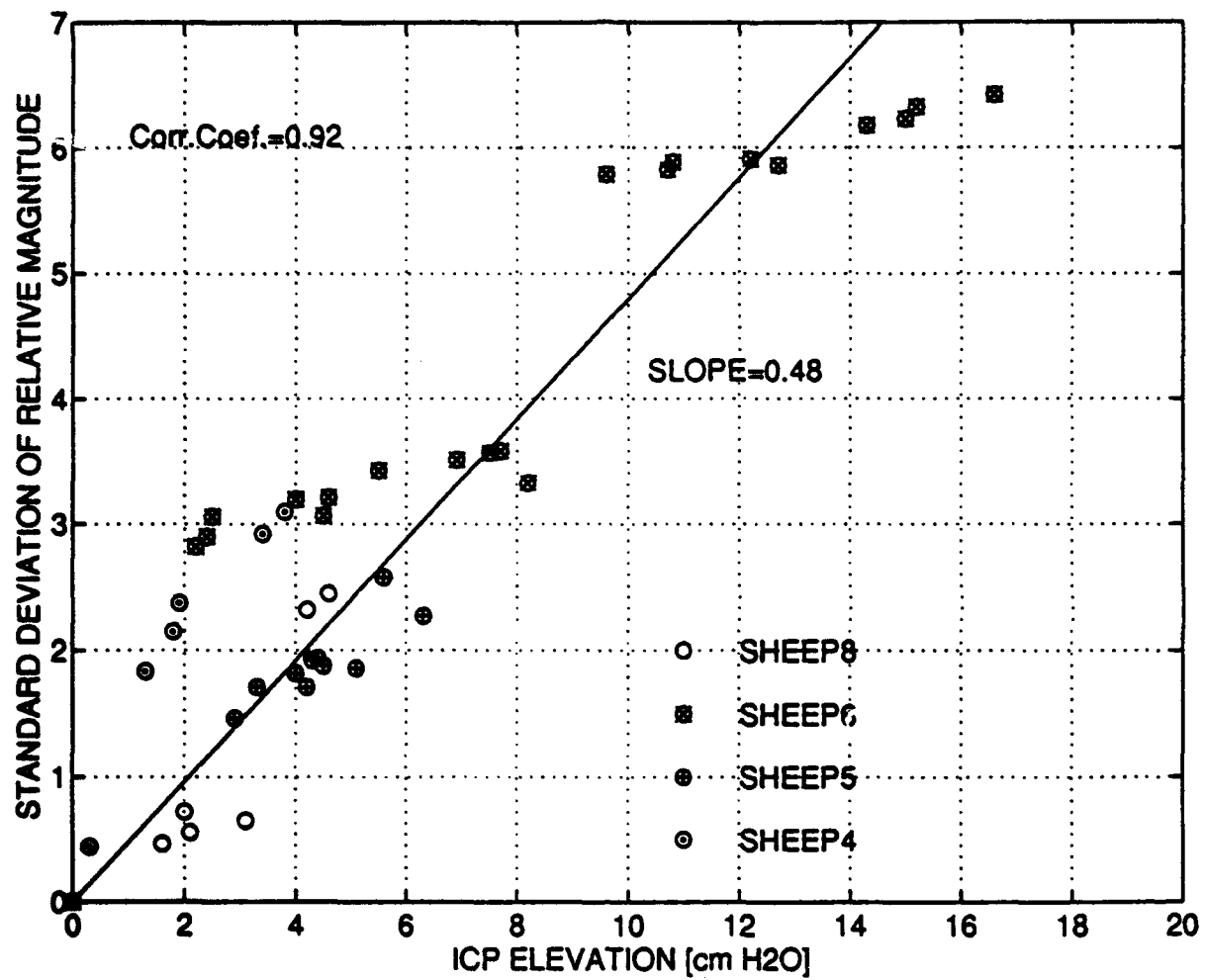
Figure 6: Standard deviation of relative magnitude at mid frequencies vs. ICP for the 4 sheep studied. The line through the origin represents a least-squares fit to the data.
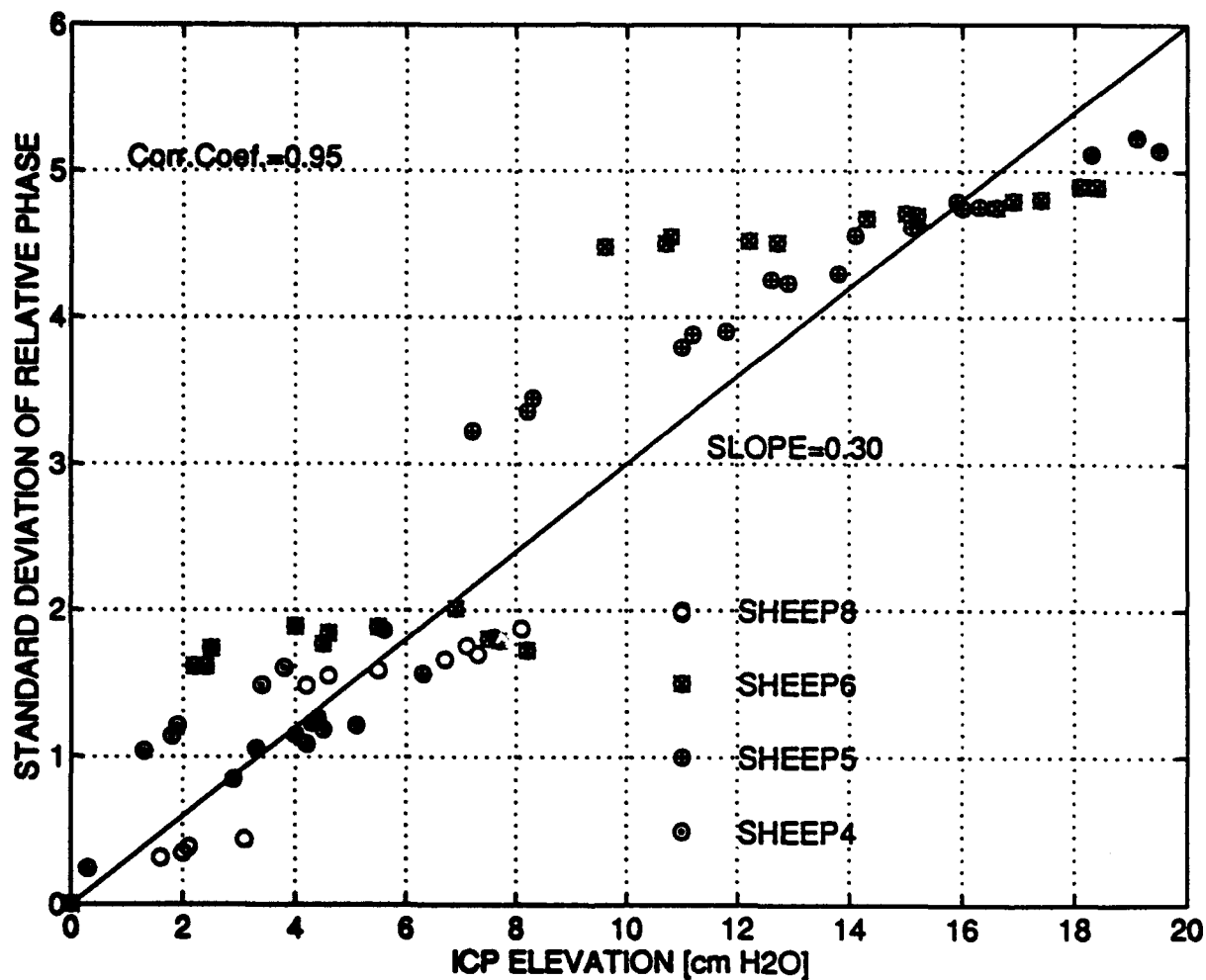
Figure 7: Standard deviation of relative phase at mid-frequencies vs. ICP for the 4 sheep studied. The line through the origin represents a least-square fit to the data.

SHEEP	MAGNITUDE		PHASE	
	Slope	Corr. Coef.	Slope	Corr. Coef.
4	0.94	0.95	0.46	0.95
5	0.42	0.95	0.30	0.97
6	0.47	0.93	0.30	0.92
8	0.38	0.93	0.23	0.92
GROUP	0.48	0.92	0.30	0.95

Table A. Sensitivity (slopes) and correlation coefficient data for each sheep and the study group.

E. Discussion

The goal of determining if and to what degree the acoustic response of the head changes with elevations in ICP was accomplished in this study. The broadband excitation elicited a flexural response that exhibited numerous changes with ICP up to 20 cmH_2O; a clinically significant range. Subsequent data analysis showed that at least one extractable acoustic parameter, the standard deviation over middle frequencies, correlated well with ICP.

The experimental protocol presented a number of challenges that were overcome during the study. Correct catheter placement near the center of the lateral ventricle was essential to insure catheter patency. The attachment of pumps for infusion at very slow rates immediately after placements also acted to keep the catheters patent. However, the possibility remains that this procedure caused some increase in ICP above normal to occur before the acoustic measurements began. This may explain why the acoustic response reached a plateau earlier in some of the sheep, as their ICP may have been prematurely elevated to some degree. This phenomenon was evident in sheep #7 where a surgical error caused a hemhorrage that increased the baseline ICP to almost 45 cmH_2O. Changes in the acoustic response of this

animal due to small ICP elevations above this high baseline were relatively diminished, as was observed in the response plateau of the other sheep. Thus, the data from this sheep was not included in any subsequent analysis.

The use of the specially-constructed shaker mount and frame was necessary to insure that the weight of the shaker did not significantly load the skull, and that there was no bulk movement of the animals head. Also, tapping a hole in the skull and using epoxy for each transducer attachment provided direct measurements of the skull's vibration without the potentially confounding effects of the extracranial tissues.

The observed acoustic responses were a strong function of frequency and a weaker function of the measurement site. There appeared to be three regions (which were termed low, mid, and high) of relative spectral changes that correlated with elevations in ICP. The analytical focus was placed on the mid range primarily because we had hypothesized that flexural modes of the head might be most effected by ICP changes. Initially, a number of acoustic parameters such as peak height were extracted and related to ICP, but the standard deviation measure proved most robust since it was less sensitive to the exact relative spectral shape changes with ICP, and was also computationally simple to determine. As is evident by the wealth of acoustic spectral changes that occurred as presented in the Appendix, there may be other extractable measures that will prove to be even more reliable and sensitive indicies of elevated ICP.

Relating the measurable response of the head directly to underlying structural changes due to ICP elevation is difficult at frequencies above 1000 Hz. However, the general trend of increasing impedance magnitude with ICP suggests that the overall stiffness of the head increased in proportion as would be predicted from a simple spherical shell model. The response plateau above roughly 20 cmH2O of pressure increase cannot be explained simply through this interpretation though, and this suggests that small pressure elevations resulted in some net expansion or relative movement of the skull and brain which stops after reaching an elastic limit. Further investigations into the measured response, especially at lower frequencies

where more direct ties to structure can be made, are needed to fully understand and interpret these positive findings.

III. CONCLUSIONS

Although it is clear that measurable acoustic parameters correlate well with elevations in ICP, a number of key efforts are necessary to determine the clinical utility of this method.

1. Further processing of the acoustic data to quantitate the spatial effects of the response. This effort will determine if spatially separated vibration excitation and measurement sites are required, or if one anatomical site can be used for both and thereby simplify the measurement system.

2. Measurement of the effects of the scalp tissues overlying the skull on the vibrational response. As these tissues have been observed to exhibit a highly-damped low pass response, the ability to measure the response on the scalp at high frequencies needs to be assessed. This information could be obtained in the same ovine animal model used in this research project, with additional measurements made simultaneously on the scalp. Also, the advantages of excitation and/or measurements on bony structures such as the upper teeth could be readily assessed.

3. Investigation of the utility of impulsive or sinusoidal excitation and subsequent time domain data analysis to extract acoustic variables that correlate well with elevations in ICP. These methods have the advantage of being experimentally and computationally simpler than using noise excitation and spectral estimation, but in general do not elicit the wealth of information that was observed in this study.

4. Design and construction of a vibration excitation and measurement device that can easily be attached to and used on the intact head. Initial designs would need to be evaluated to determine their effect on such factors as sensitivity, bandwidth and reproducibility, and this would be accomplished using the ovine model. Subsequent design improvements to

facilitate use and patient comfort would be validated through measurements on healthy human subjects.

5. Clinical testing of the device using neurosurgical patients who have direct ICP monitoring. We have had discussions with physicians in both the Neurological Surgery and Neurology Departments at Indiana University Medical Center, and they have agreed to collaborate with us on the clinical stages of this research. Comparisons between acoustically estimated ICP with direct measurements for various pathologies would define the clinical scope of the methods capabilities.

These five key efforts would develop and refine this technology into a device that would reliably and noninvasively quantify ICP elevations in afflicted soldiers.

IV. REFERENCES

Baker, W. E., "Axisymmetric modes of vibration of thin spherical shell", J. Acoust. Soc. Am., Vol. 33, pp. 1749-1758, 1961.

Bekesy, G. V., "Response of the human skull to mechanical vibrations", in *Handbook of Experimental Psychology*, Stevens, S. S., ed., New York: John Wiley and Sons, 1951.

Elliott, K. A. C. and Jasper H. H., "Physiological salt solutions for brain surgery", J. Neurosurg., Vol. 6, pp. 140-143, 1949.

Elnicki, D. M., "Mountain sickness", W. V. Med. J., Vol. 86, pp. 246-249, 1990.

Franke, E. K., "Response of the human skull to mechanical vibrations", J. Acoust. Soc. Am., Vol. 28., pp. 1277-1284, 1956.

Gurdjian, E. S., Hodgson, V. R. and Thomas, L. M., "Studies on mechanical impedance of the human skull: preliminary report", J. Biomechonics, Vol. 2, pp. 239-247, 1970.

Hakansson, B. and Carlsson, P., "The mechanical point impedance of the human head, with and without skin penetration", J. Acoust. Soc. Am., Vol. 80, pp. 1065-1075, 1986.

Hamilton, A. J., Black P. M., Madsen, J. and Carr, D. B., "Neuropeptide investigations with an ovine surgical model", Neuosurg., Vol. 18, pp. 748-755, 1986.

Hamilton, A. J., Cymmerman, A. and Black, P. M., "High altitude cerebral edema", Neurosurg., Vol. 19, pp. 841-849, 1986.

Hodgson, V. R., Gurdjian, E. S. and Thomas, L. M., "The determination of the response characteristics of the head with emphasis on mechanical impedance techniques", in Proc. 11th Stapp Car Crash Conf., pp. 125-138, 1967.

Hodgson, V. R. and Patrick, L. M., "Dynamic response of the human cadaver head compared to a simple mathematical model", Proc. 12th Stapp Car Crash Conf., pp. 280-301, 1968.

Houston, C. S. and Dickinson, J., "Cerebral form of high altitude illness", Lancet., Vol. 2, pp. 758-761, 1975.

Houston, C. S., "Altitude illness", Emerg. Med. Clin. North Am., Vol. 2, pp. 503-512, 1984.

Jacobson, N. D., "Acute high-altitude illness", Am. Fam. Physician, Vol. 38, pp.135-144, 1988.

Kay, S. M., *Modern Spectral Estimation: Theory and Application*, New York: Prentice-Hall, 1988.

Khalil, T. B. and Viano, D. C., "Experimental analysis of the vibrational characteristics of the human skull", J. Sound Vibration, Vol. 63, pp. 351-376, 1979.

Khalil, T. B. and Viano, D. C., "Comparison of human skull and spherical shell vibrations - implications for head injury modeling", J. Sound Vibration, Vol. 82, pp. 95-110, 1982.

Kinsler, L. E., Frey, A. R., Coppens, A. B., Sanders, J. V., Fundamentals of Acoustics, New York, John Wiley and Sons, 1982.

Levine, B. D., Yoshimura, K., Kobayashi, T., Fukushima, M., Shibamoto, T. and Veda, G., "Dexamethasone in the treatment of accute mountain sickness", N. Engl. J. Med., Vol. 321, pp. 1707-1713, 1989.

Luchka, S., "Working with ICP monitors", R.N., Vol. April, pp. 34-37, 1991.

Mountain, R. D., "High-altitude medical problems", Clin. Orthop., Vol. 216, pp. 50-54, 1987.

Pappenheimer, J. R., Heisey, S. R., Jordan, E. F., Downer J. DeC., "Perfusion of the cerebral ventricular system in unanesthetized goats", Am. J. Physiol, Vol. 203, pp. 763-774, 1962.

Semmlow, J. L. and Fisher, R., "A noninvasive approach to intracranial pressure monitoring", J. Clin. Eng., Vol. 7, pp. 73-78, 1982.

Singh, I., Khanna, K. , Srivastava, M. C., Lal, M., Roy, S. B., and Subramanyam, C. S. V., "Acute mountain sickness", New Engl. J. Med., Vol. 280, pp. 175-184, 1969.

Stalnaker, R. L., Fogle, J. L. and McElhaney, J. H., "Driving point impedance characteristics of the head", J. Biomechanics, Vol. 4, pp. 127-139, 1971.

Wilkinson, J. P., "Natural frequencies of closed spherical shells", J. Acoust. Soc. Am., Vol. 38, pp. 367-368, 1965.

Wilkinson, J. P. and Kalnins, A., "On nonsymmetric dynamic problems of elastic spherical shells", J. Appl. Math., Vol. 9, pp. 525-532, 1965.

Wilson, R., "Acute high-altitude illness in mountaineers and problems of rescue", Ann. Int. Med., Vol. 78, pp. 421-428, 1973.

Wood, J. H., "Technical aspects of clinical and experimental cerebrospinal fluid investigations", in *Neurobiology of Cerebrospinal Fluid*, Wood, J. H., ed., New York: Plenum Press, pp. 71-96, 1980.

V. APPENDIX

The organization of this appendix is as follows. For each sheep (#4, 5, 6 or 8), the relative spectra at a particular site (driving point, 1, 2 or 3) is presented first in terms of magnitude. After each relative magnitude spectral plot, the frequency range over which the standard deviation was extracted is highlighted in bold, followed by a plot of the dependence of the standard deviation upon ICP. As noted in the body of this report, this parameter correlated well with ICP elevation up to roughly 20 cmH$_2$O above normal and reached a plateau at higher frequencies. This same procedure is used to present the magnitude data over various frequency ranges (low, mid or high). The phase spectra and resultant standard deviation measures are then presented in the same progression.

MAGNITUDE OF RELATIVE DRIVING POINT IMPEDANCE, SHEEP4
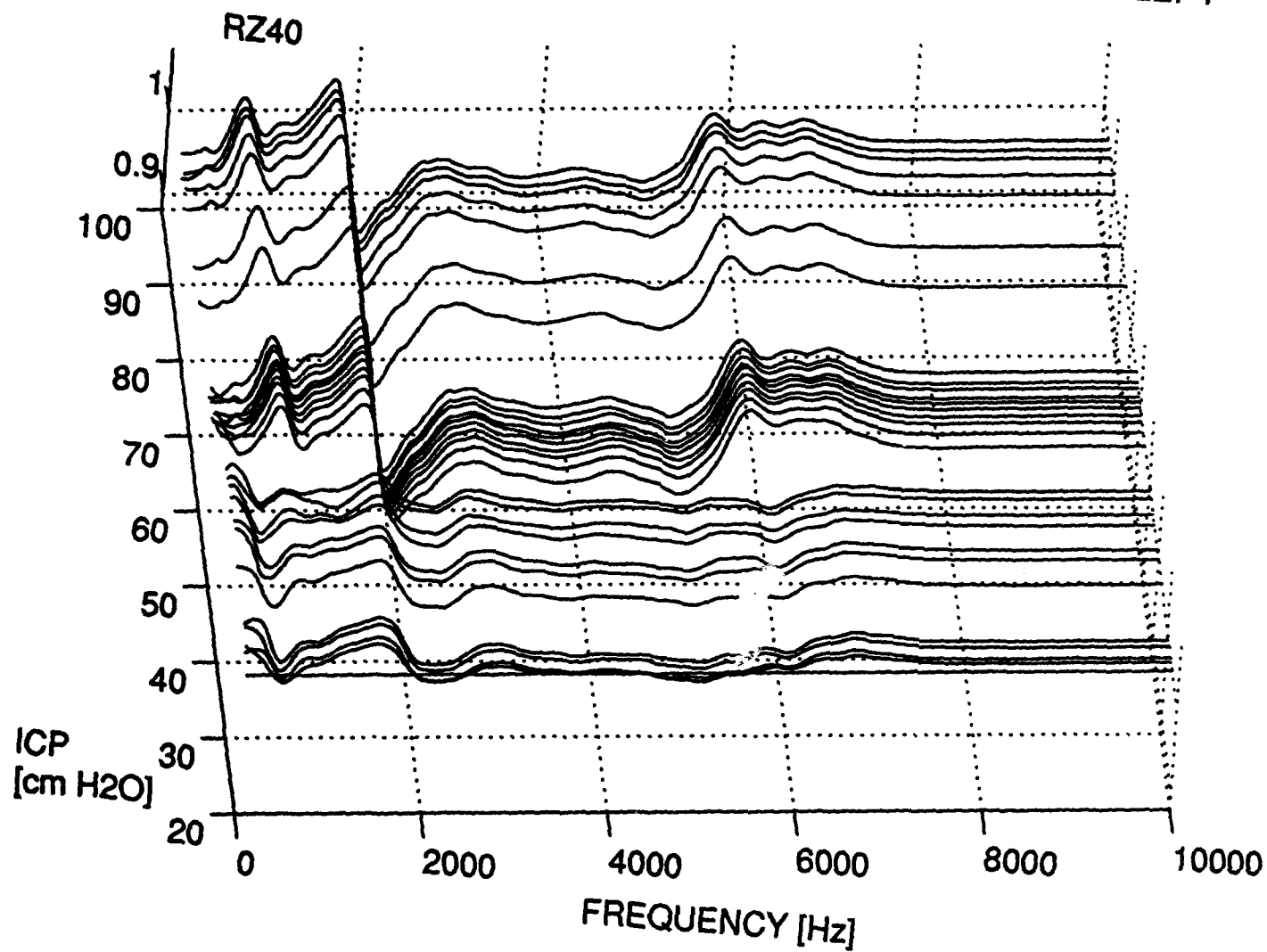
MAGNITUDE OF RELATIVE DRIVING POINT IMPEDANCE, SHEEP4
FREQUENCY RANGE (104 - 2096 Hz)
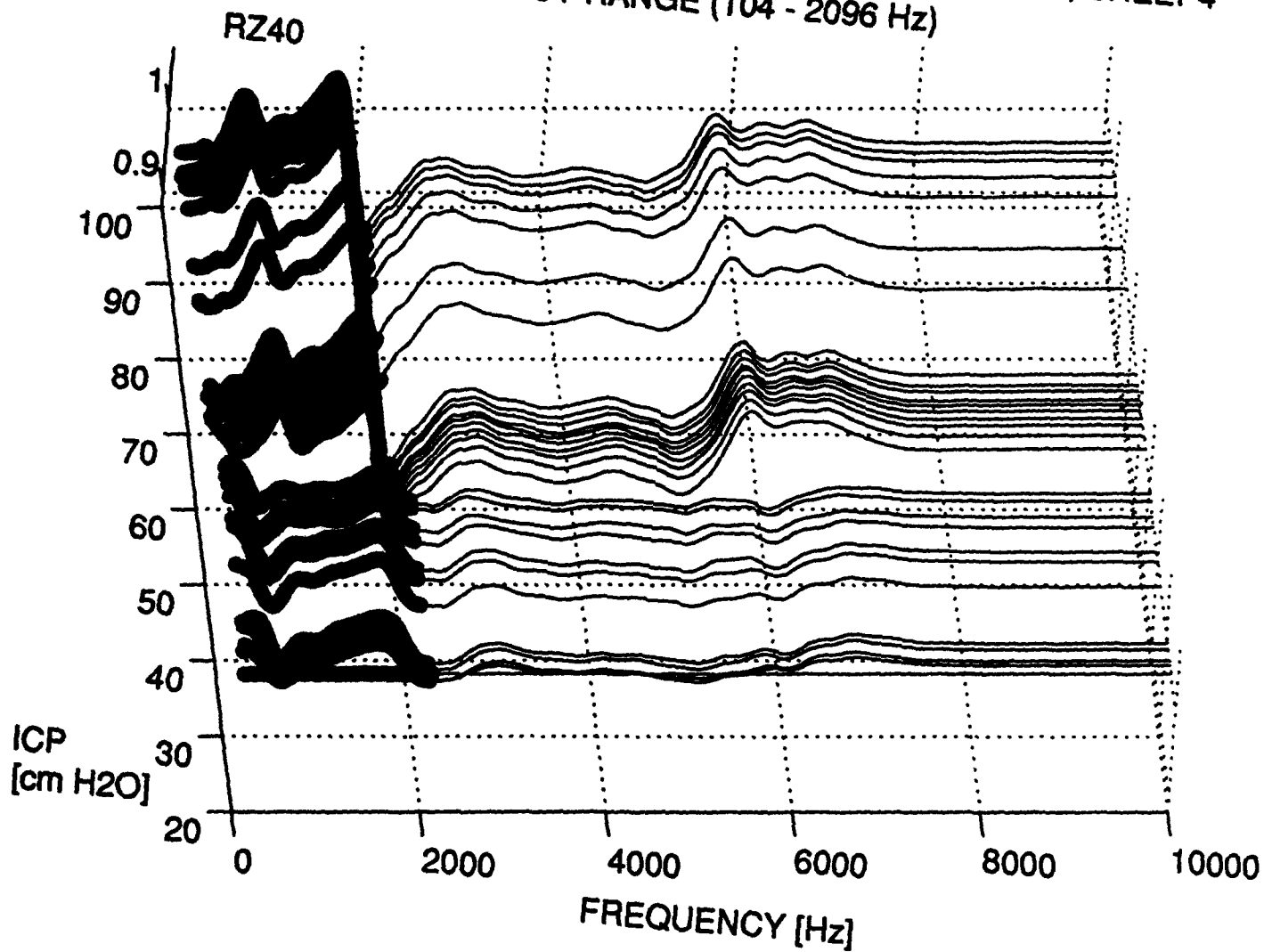
MAGNITUDE STANDARD DEVIATION vs. ICP
SHEEP4: Mag.Rel.DP.   FREQUENCY RANGE (104 - 2096 Hz)

MAGNITUDE OF RELATIVE DRIVING POINT IMPEDANCE, SHEEP4
FREQUENCY RANGE (2016 - 3296 Hz)
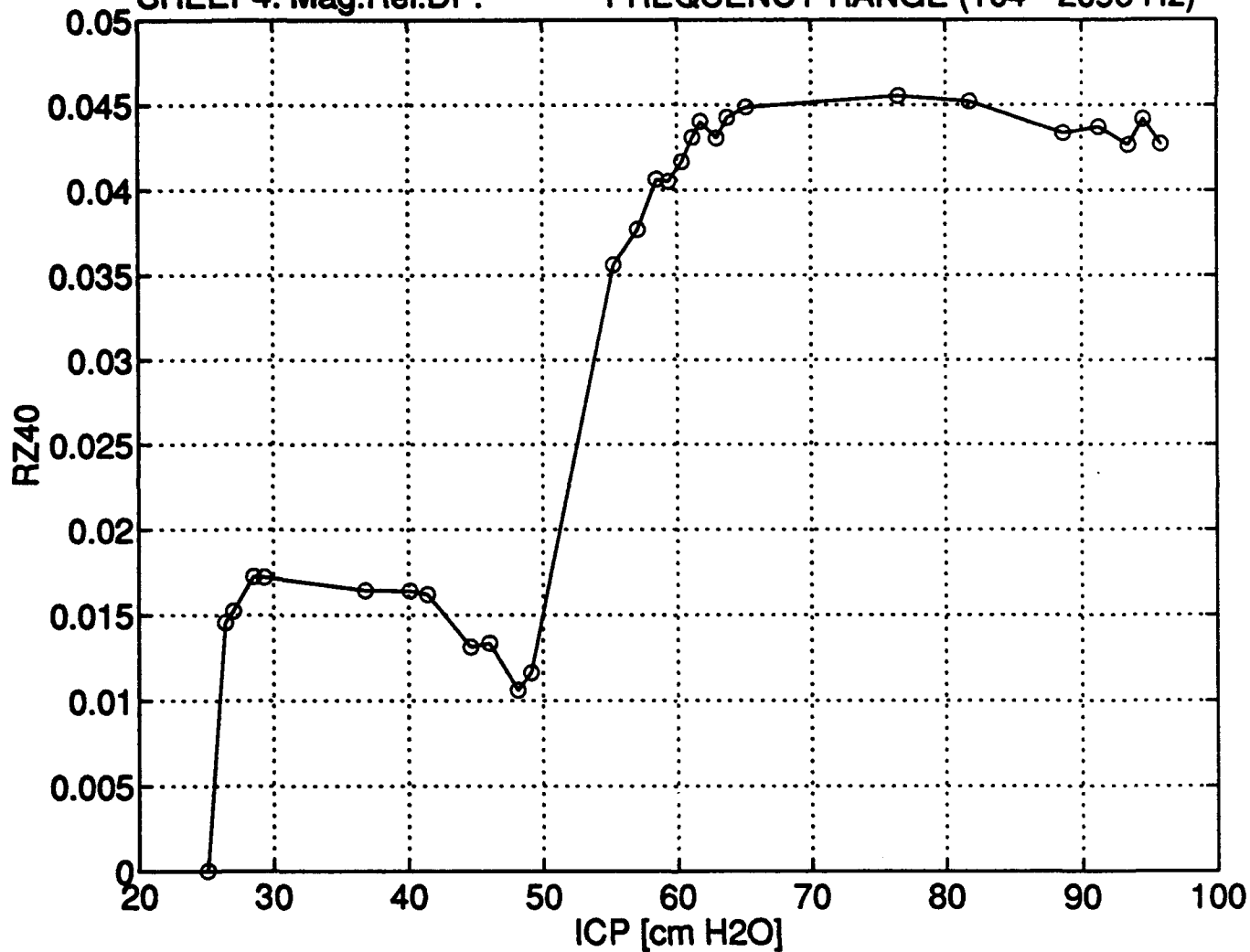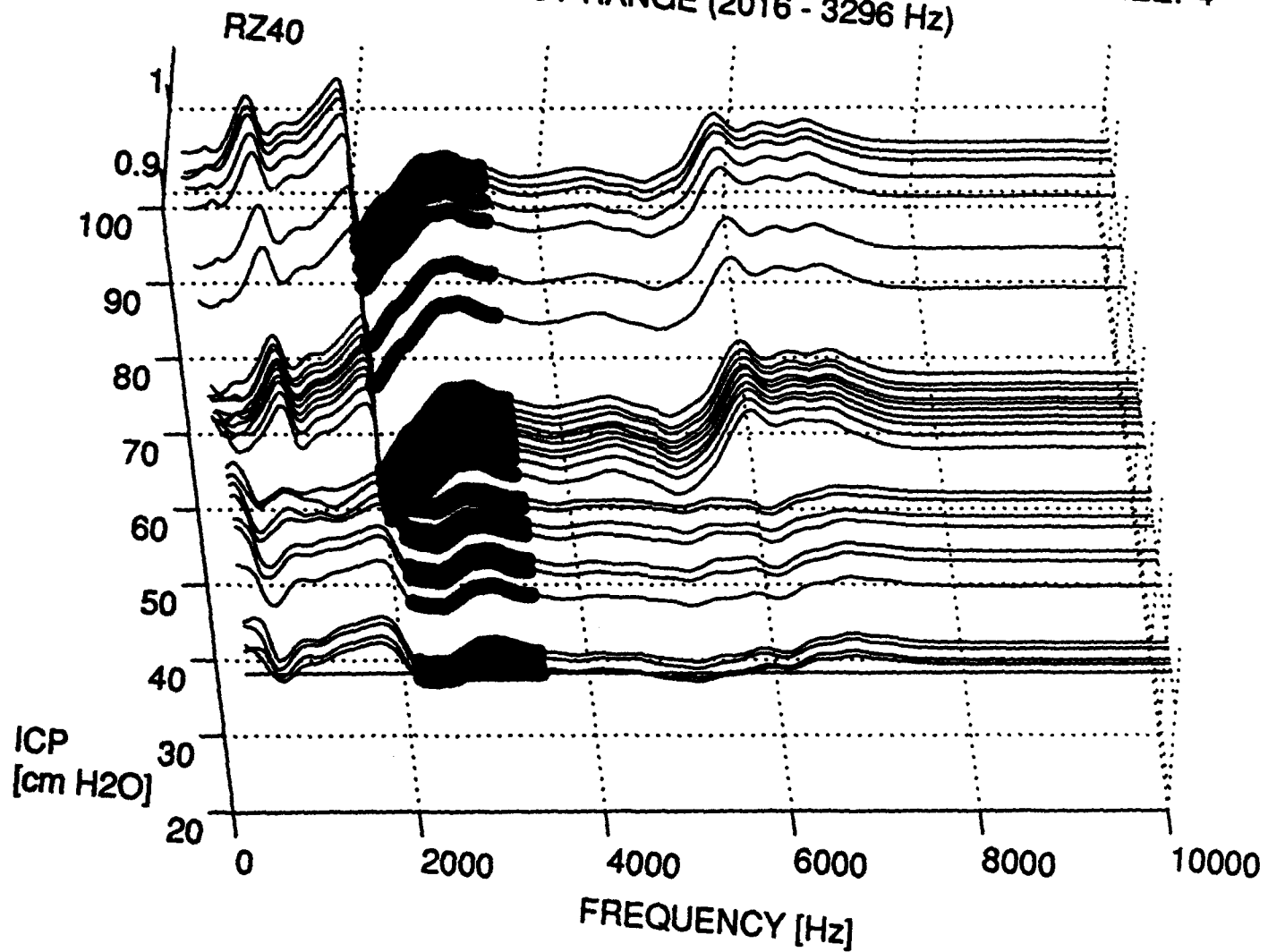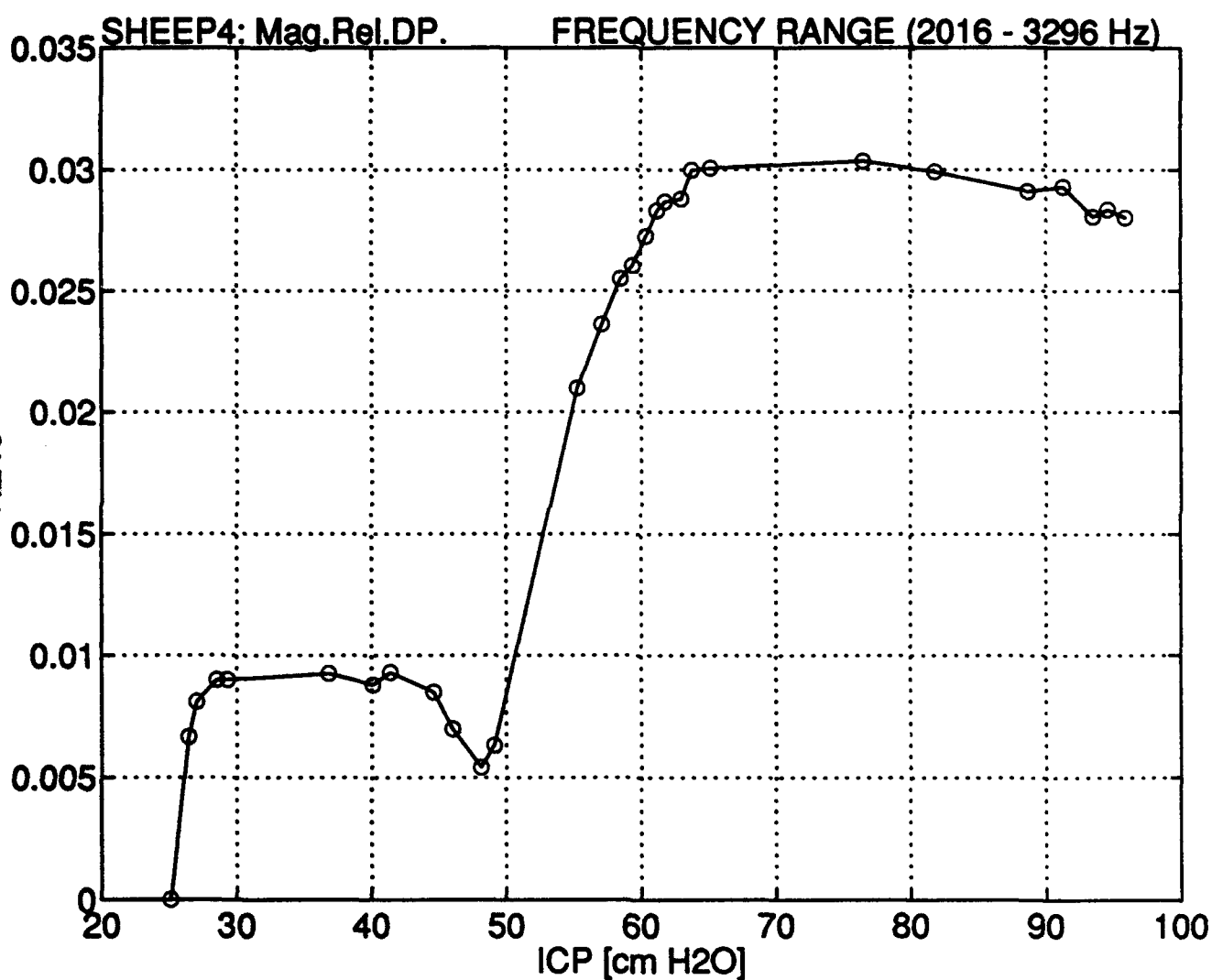
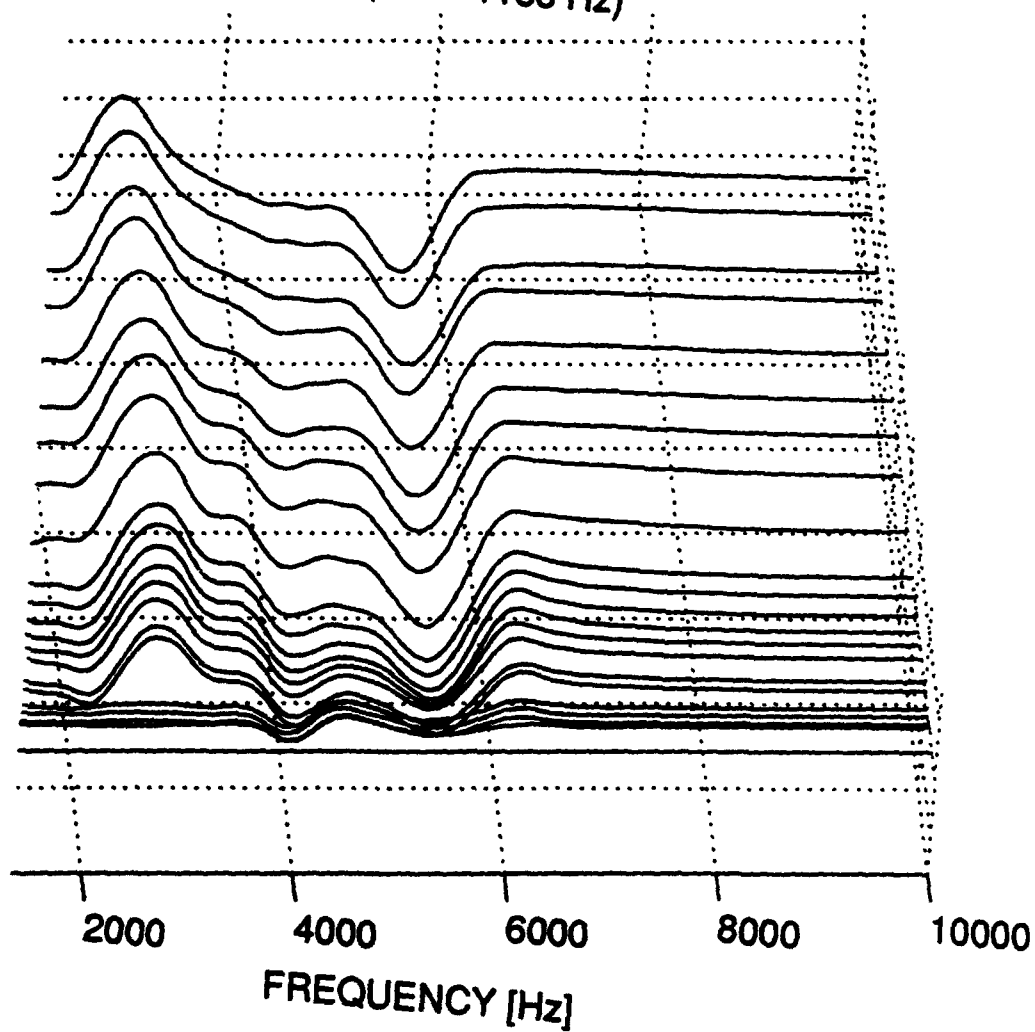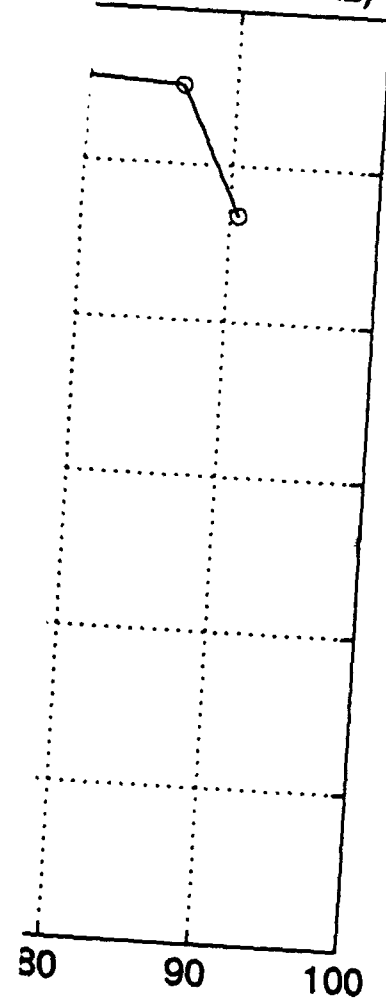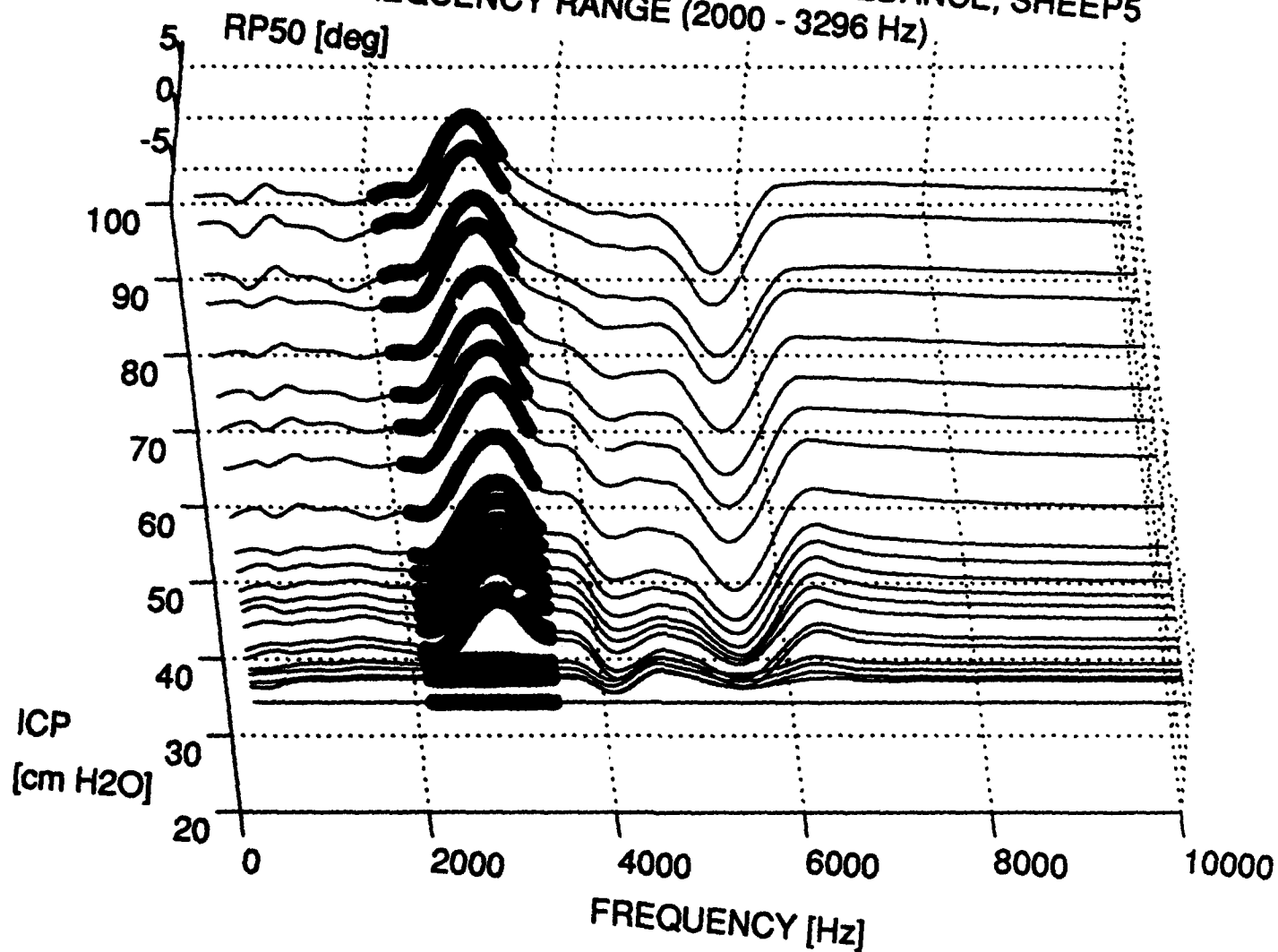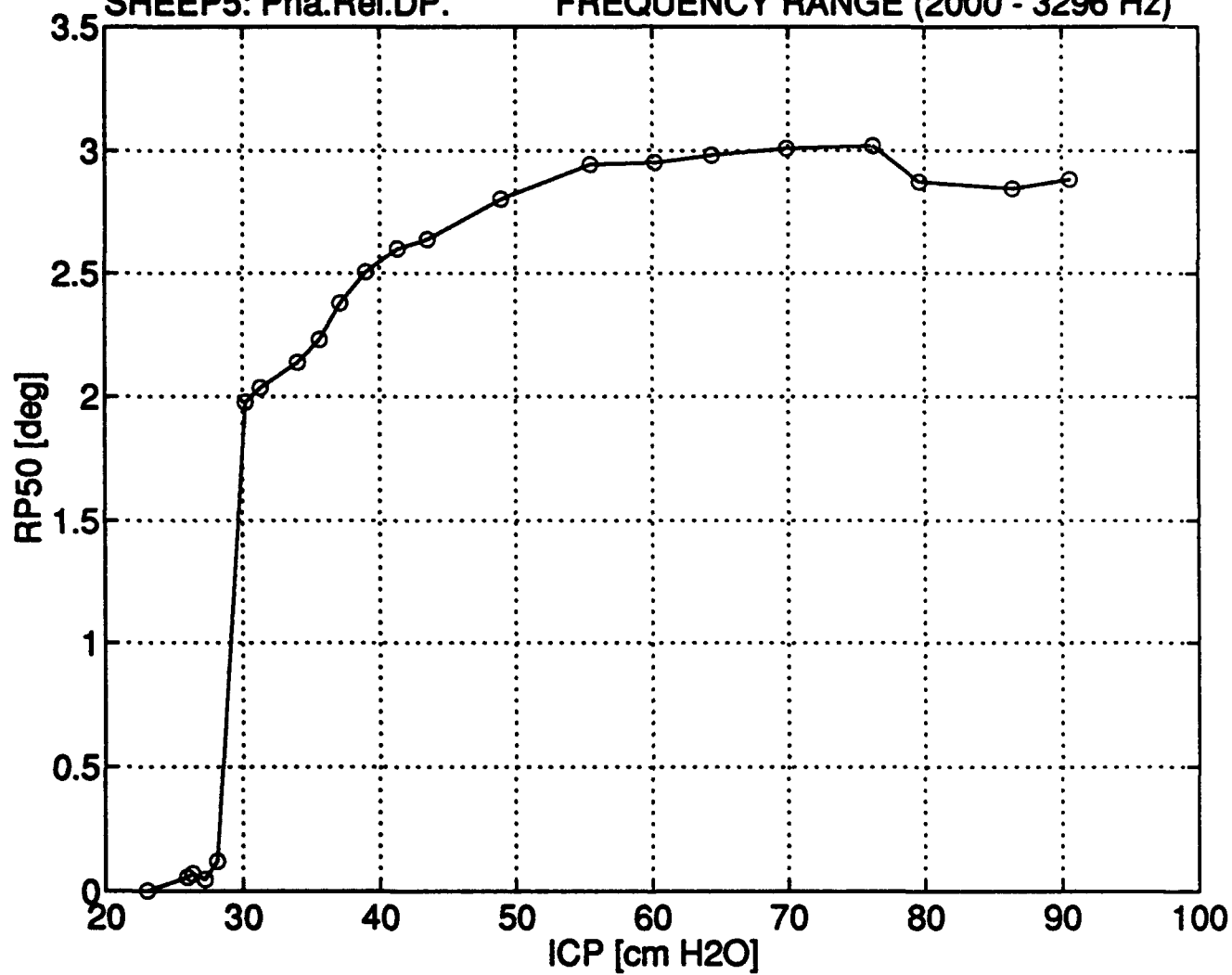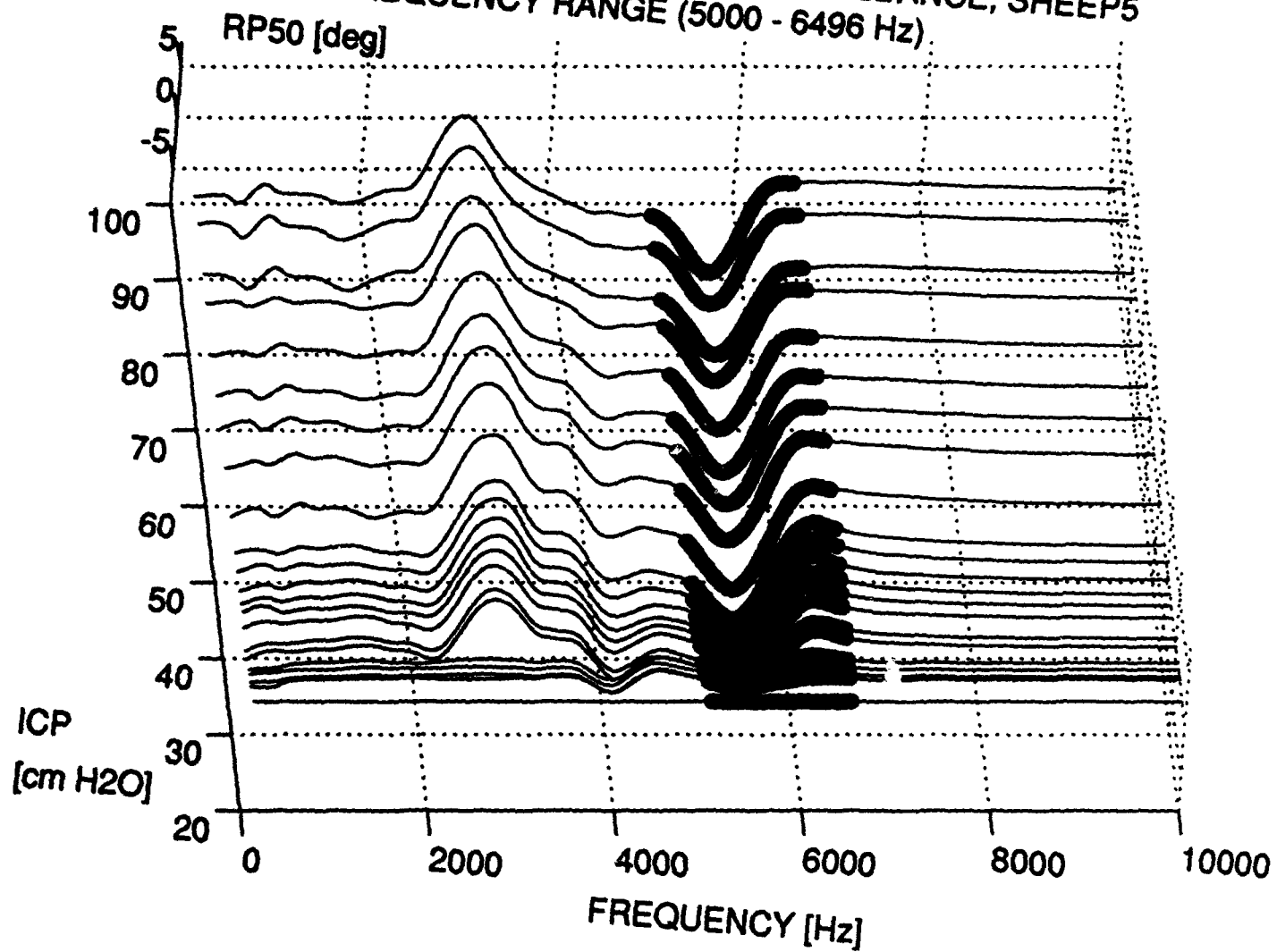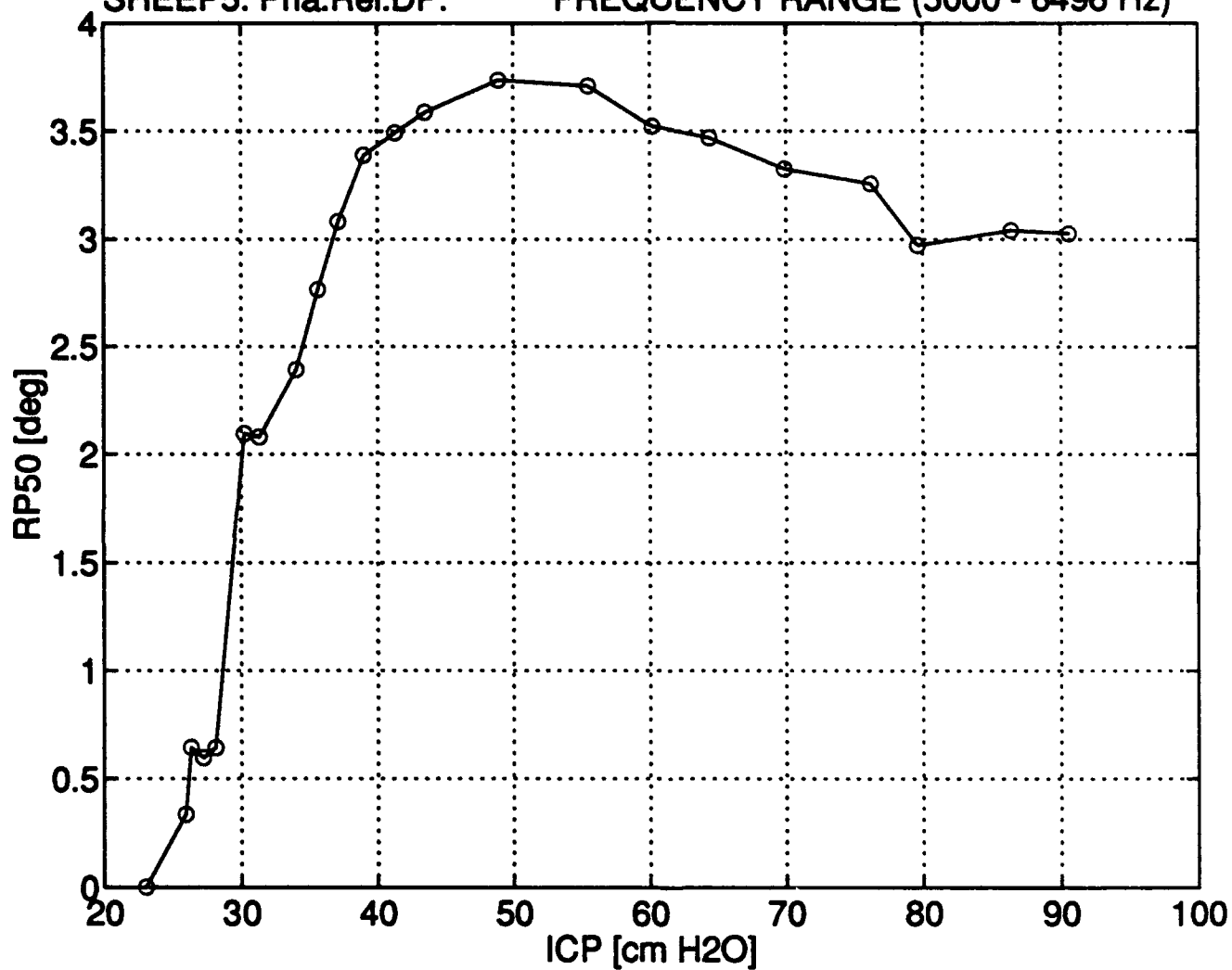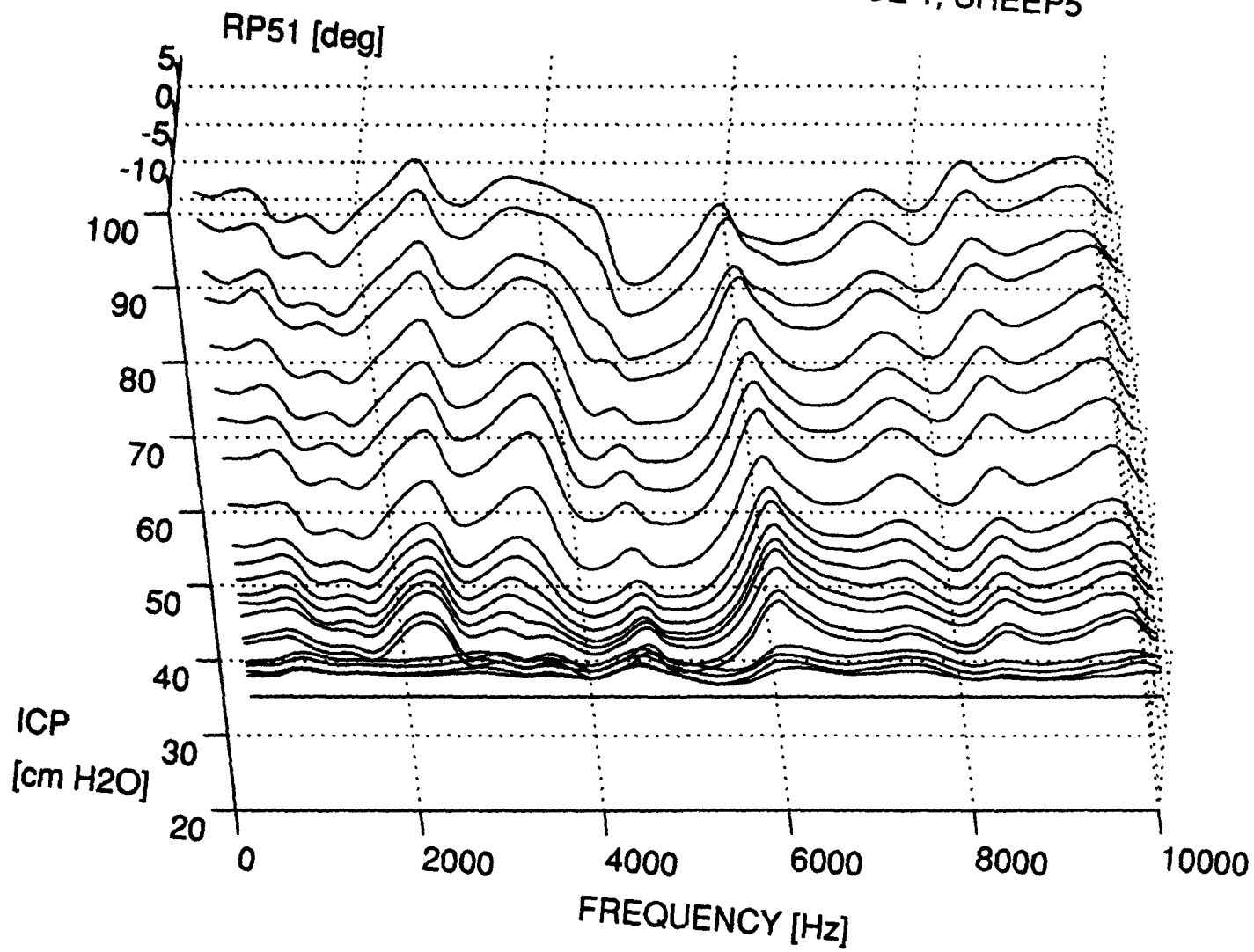MAGNITUDE STANDARD DEVIATION vs. ICP

SHEEP4: Mag.Rel.DP.   FREQUENCY RANGE (2016 - 3296 Hz)

MAGNITUDE OF RELATIVE DRIVING POINT IMPEDANCE, SHEEP4
FREQUENCY RANGE (4896 - 7296 Hz)
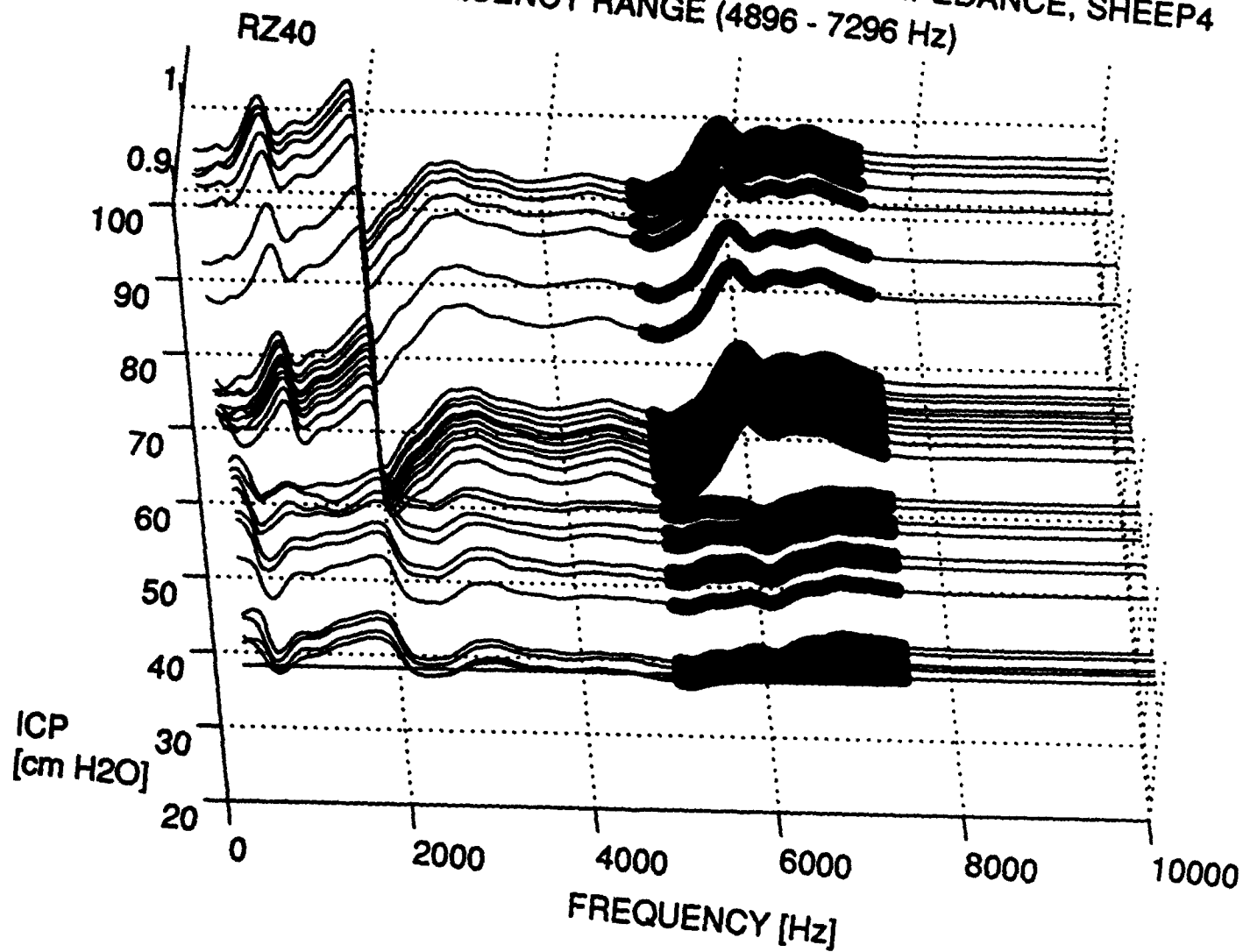
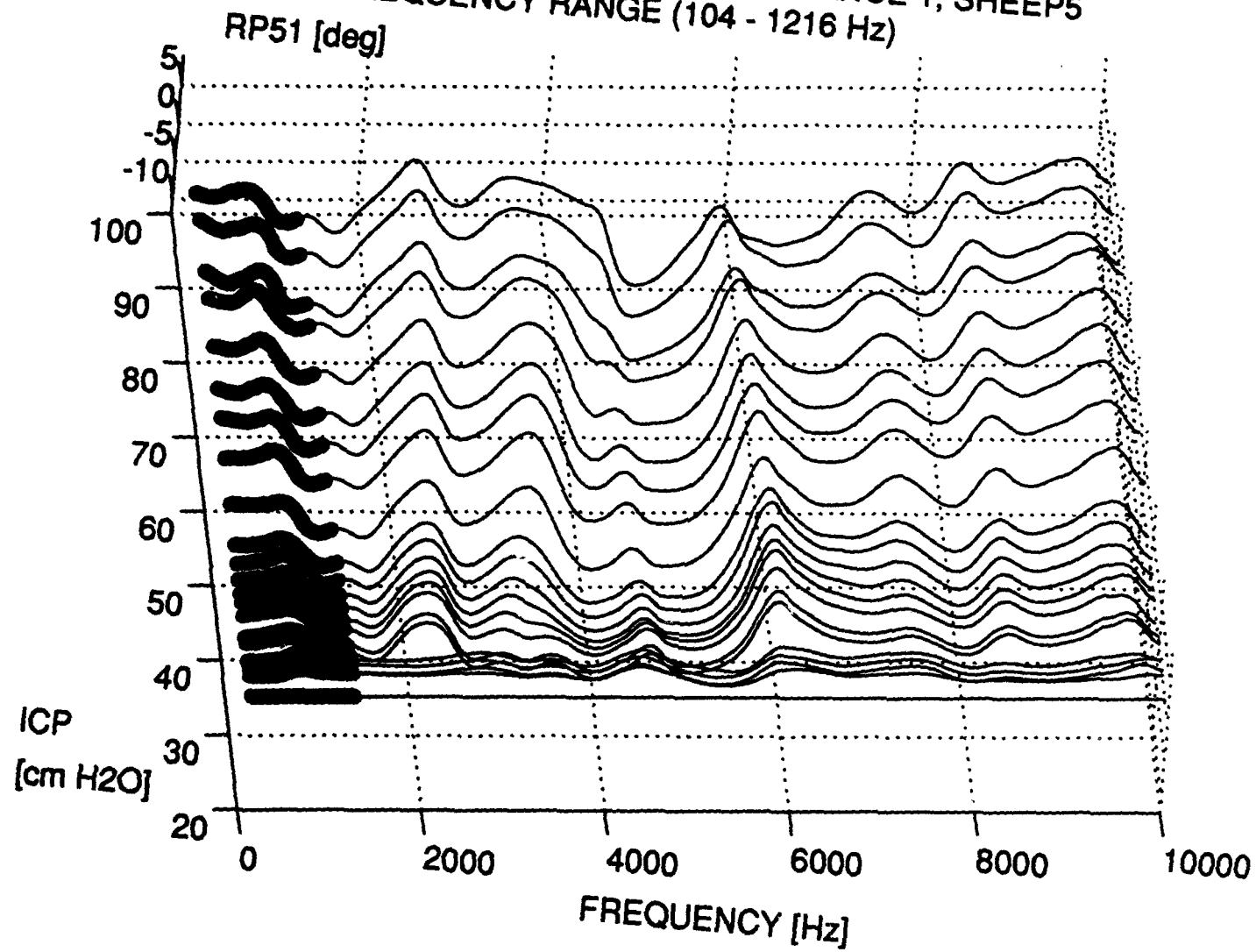MAGNITUDE STANDARD DEVIATION vs. ICP
SHEEP4: Mag.Rel.DP.   FREQUENCY RANGE (4896 - 7296 Hz)
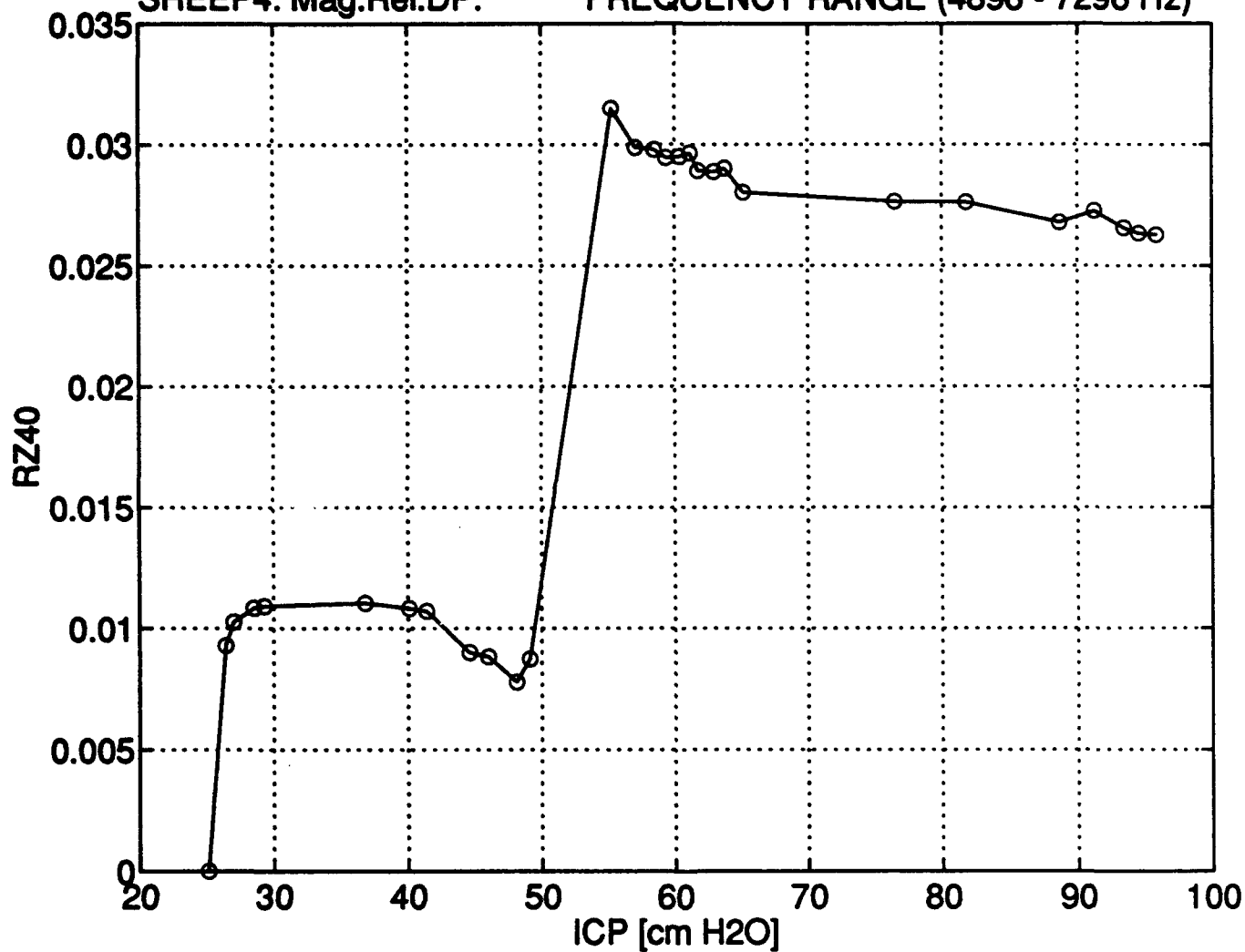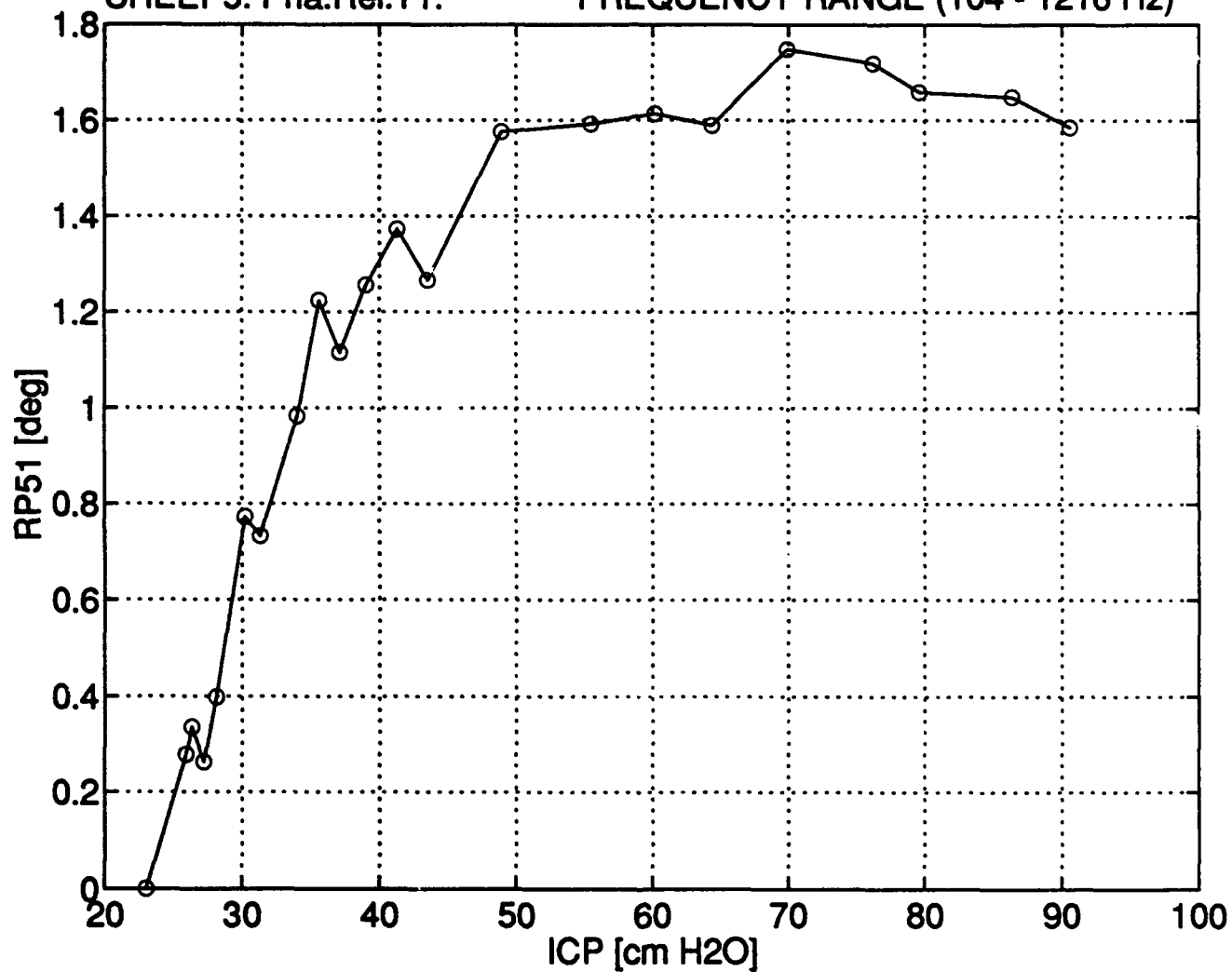
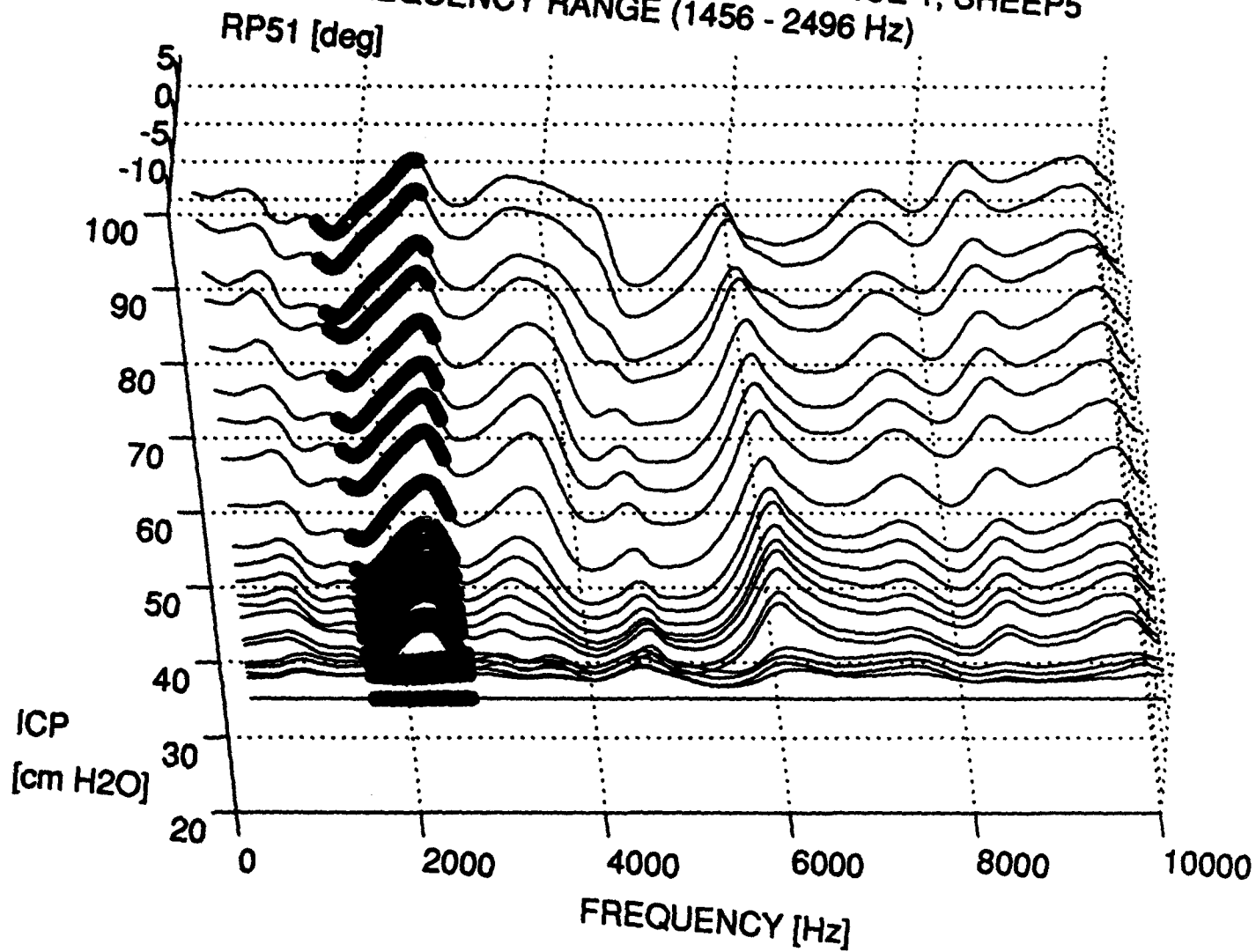MAGNITUDE OF RELATIVE TRANSFER IMPEDANCE 1, SHEEP4
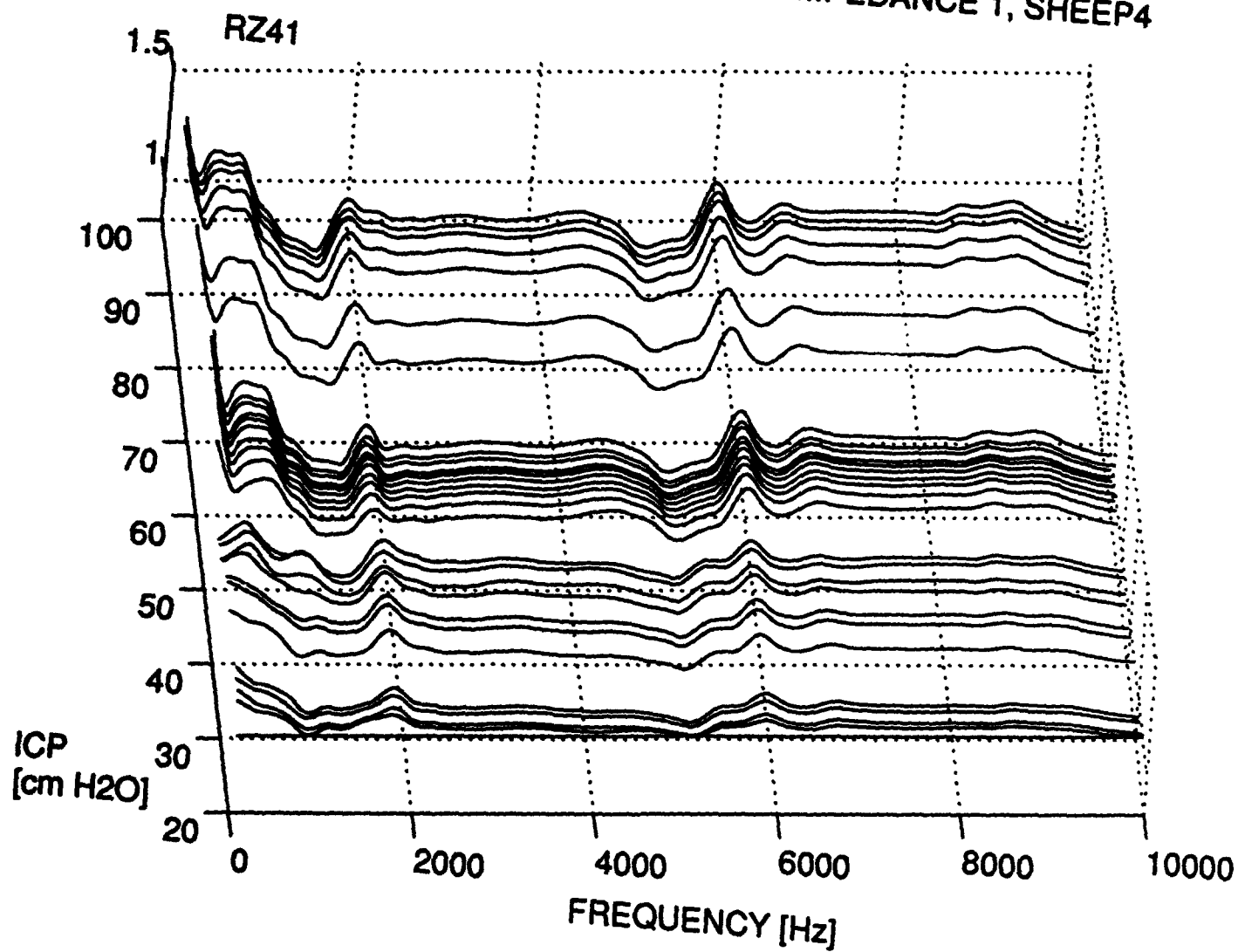
MAGNITUDE OF RELATIVE TRANSFER IMPEDANCE 1, SHEEP4
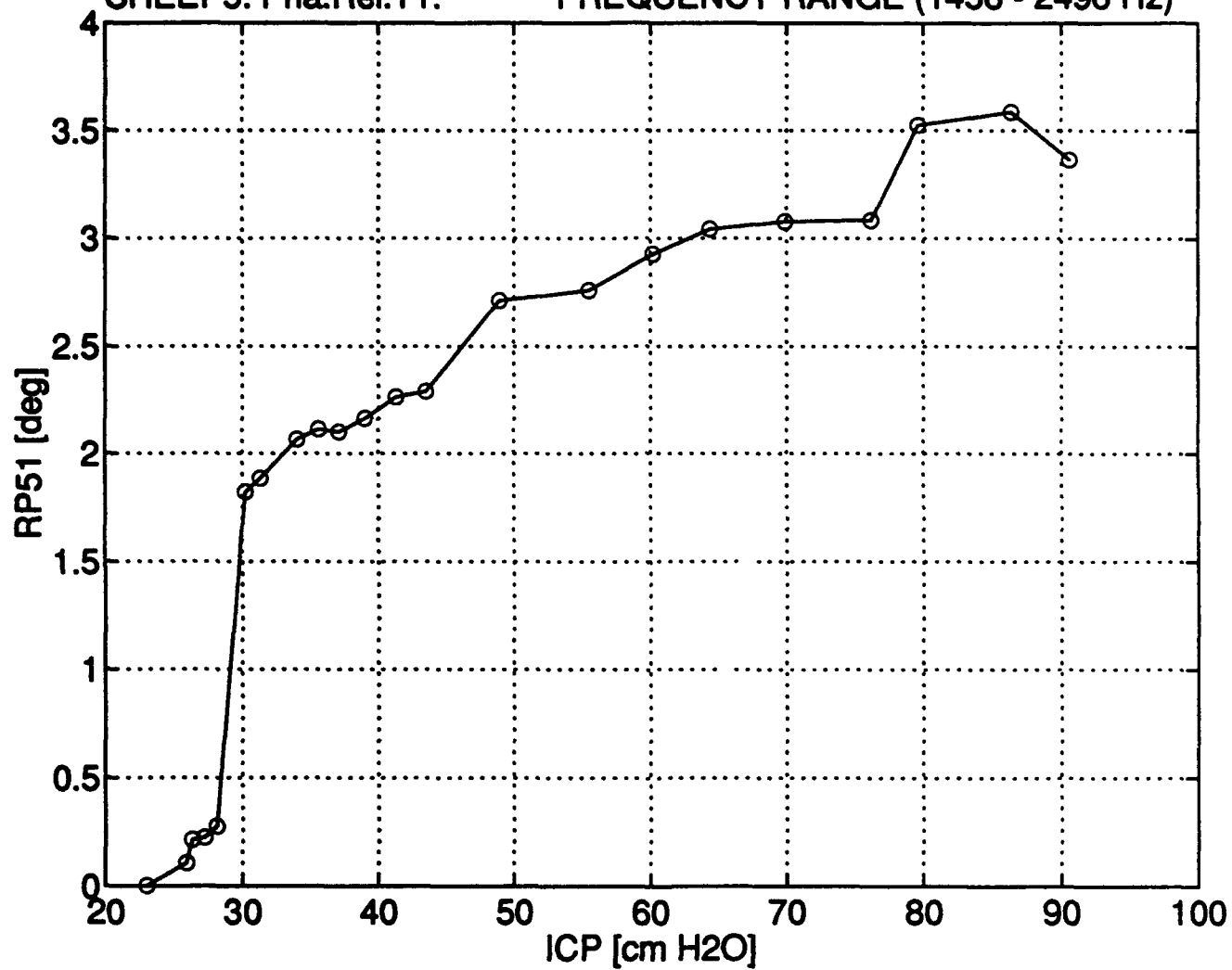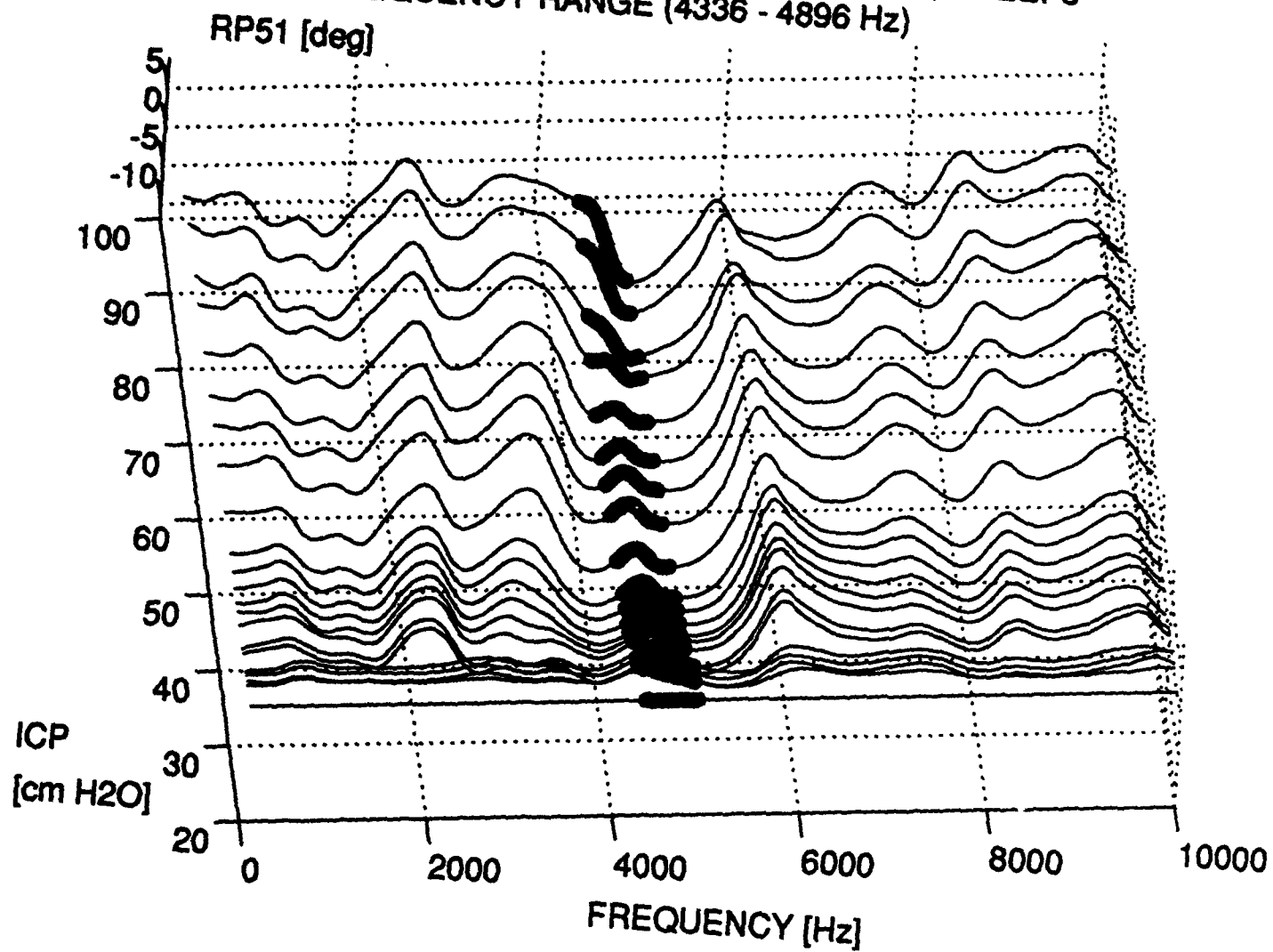FREQUENCY RANGE (1376 - 2256 Hz)
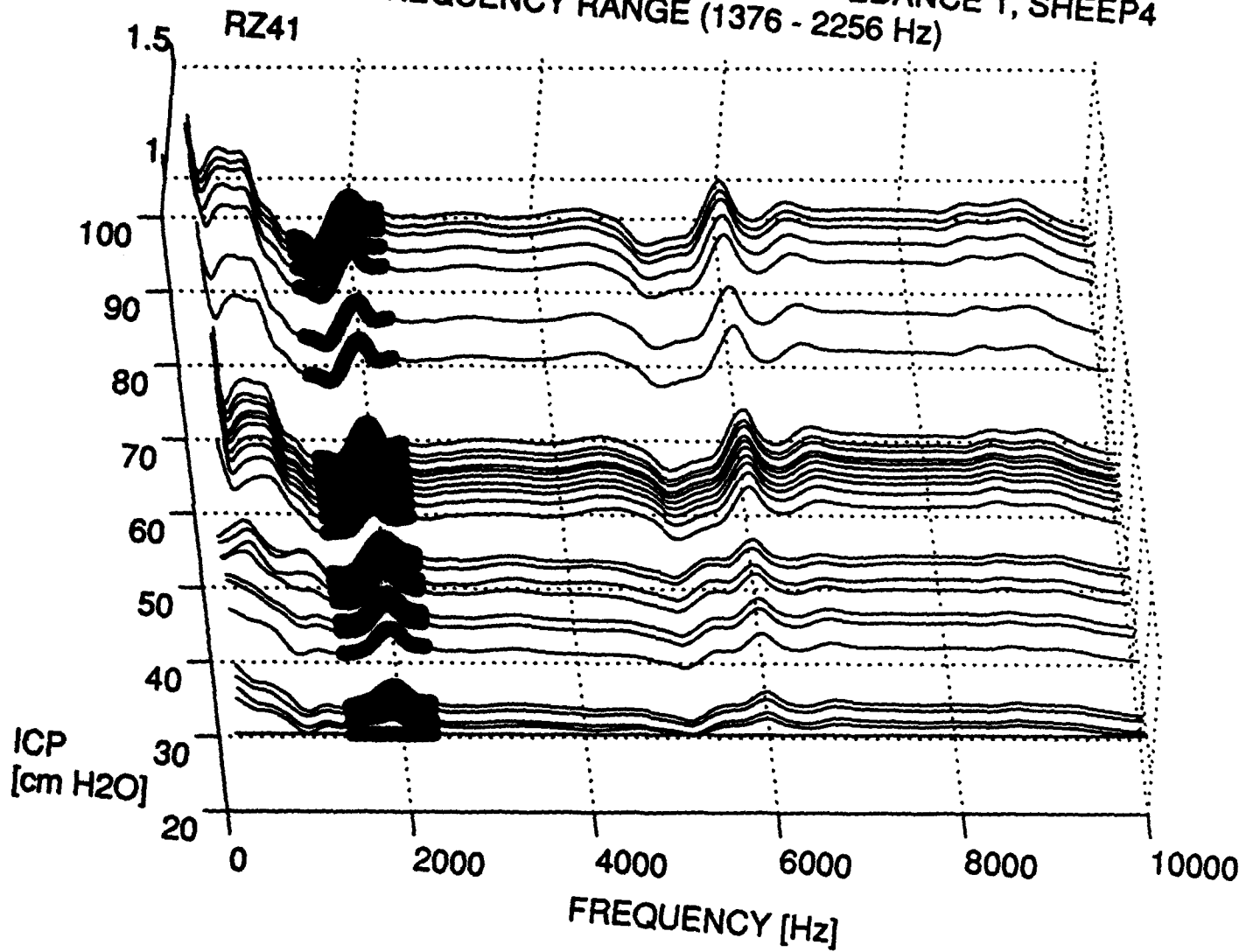
MAGNITUDE STANDARD DEVIATION vs. ICP
SHEEP4: Mag.Rel.T1.   FREQUENCY RANGE (1376 - 2256 Hz)
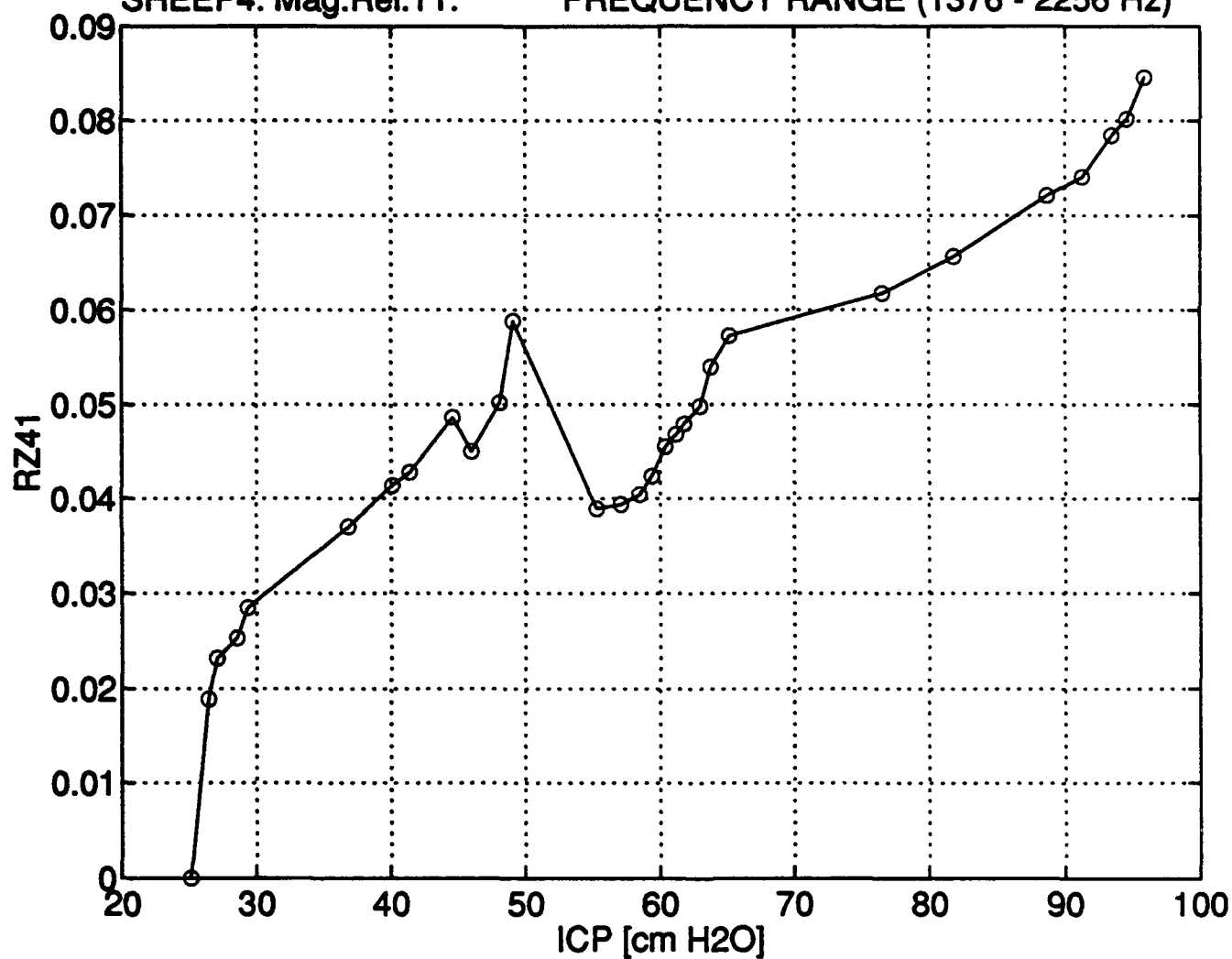
MAGNITUDE OF RELATIVE TRANSFER IMPEDANCE 1, SHEEP4
FREQUENCY RANGE (4896 - 7296 Hz)
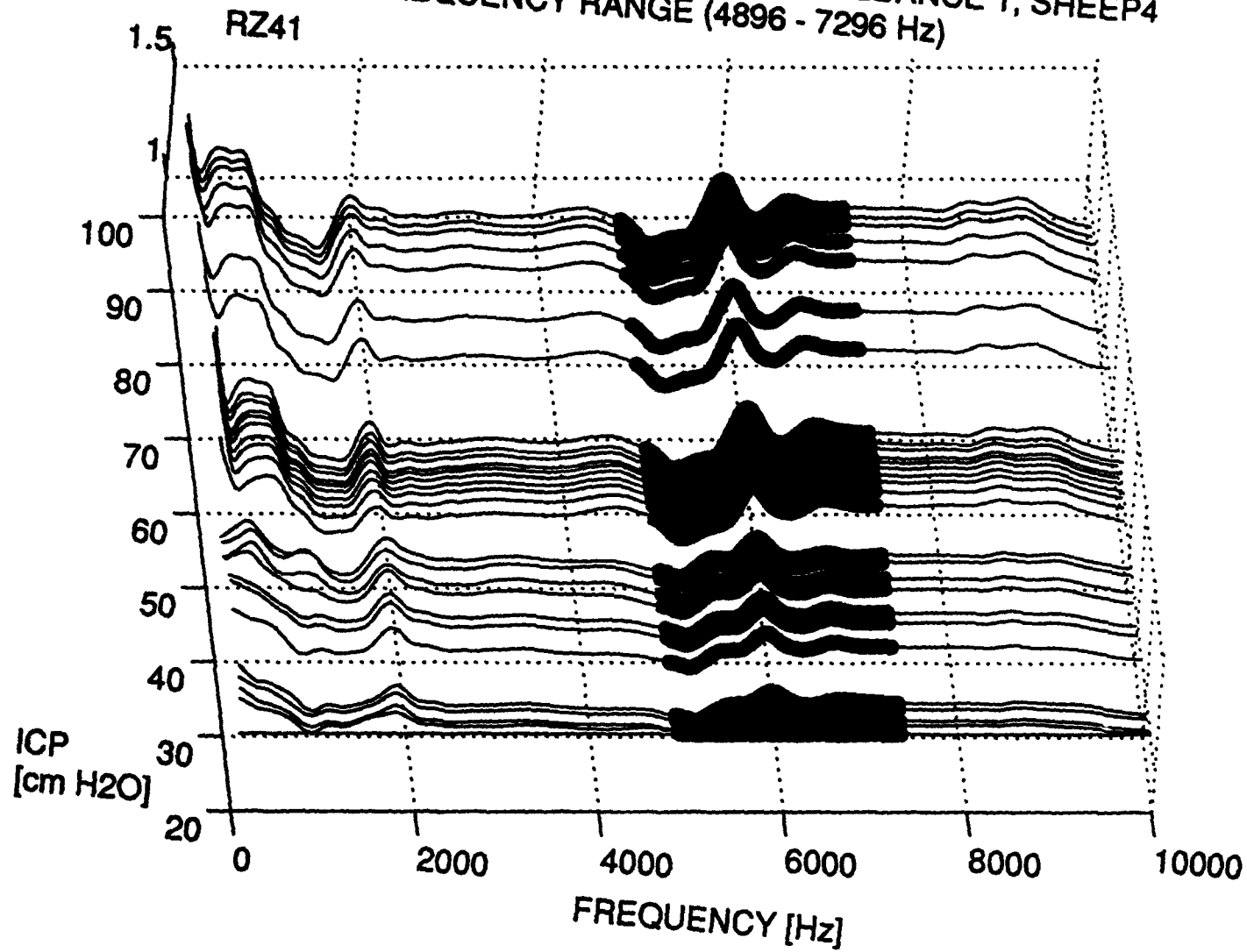
MAGNITUDE STANDARD DEVIATION vs. ICP
SHEEP4: Mag.Rel.T1.   FREQUENCY RANGE (4896 - 7296 Hz)
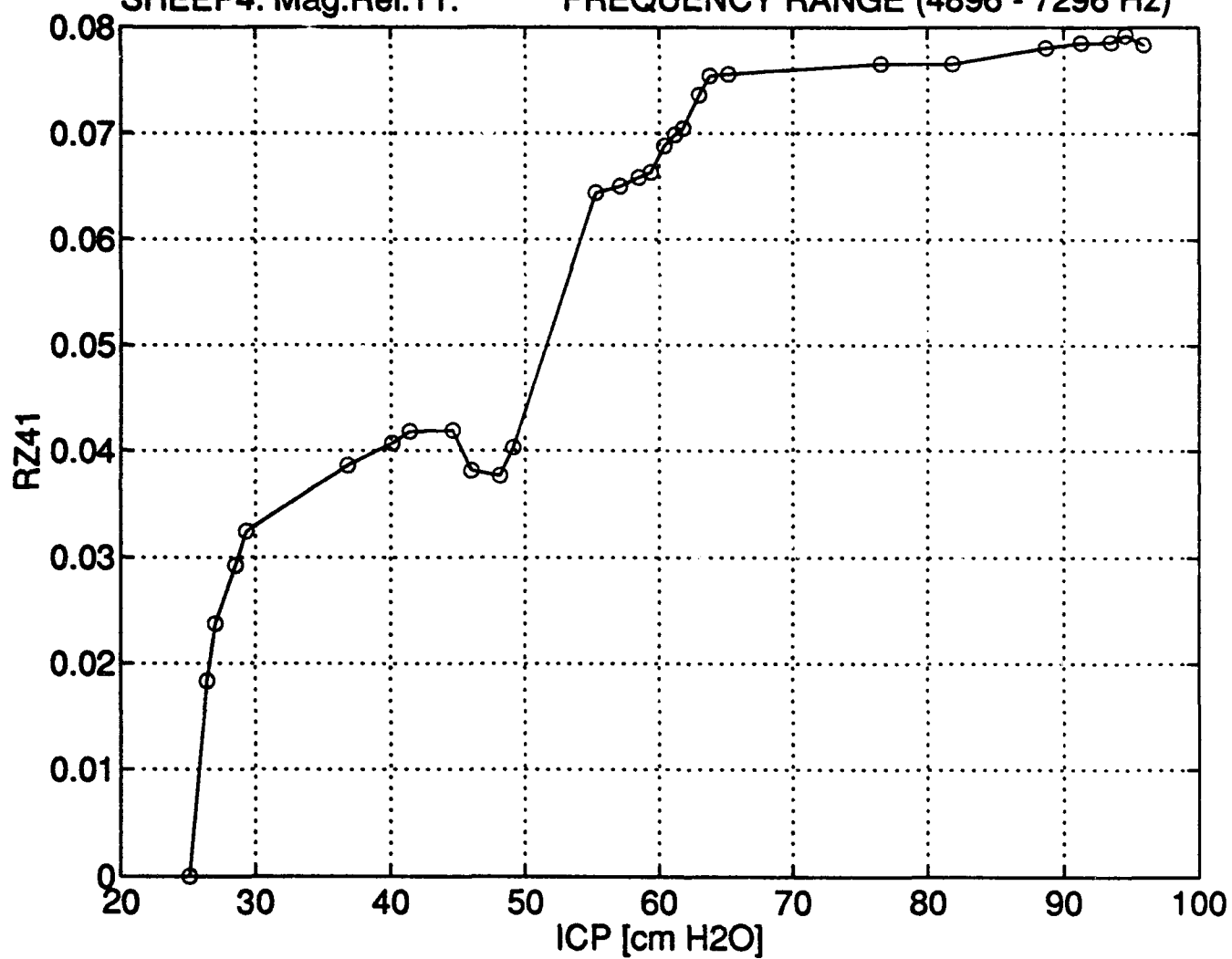
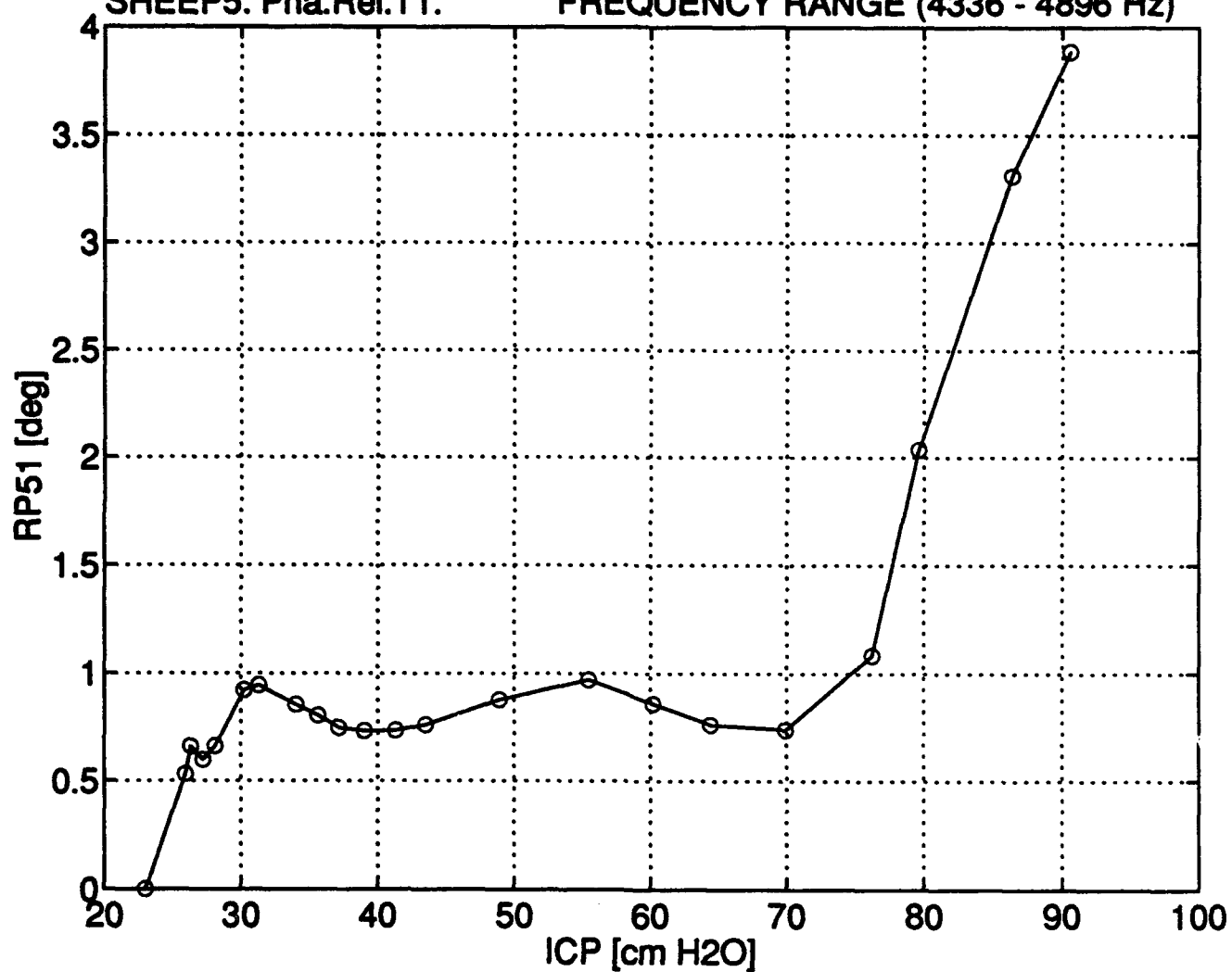MAGNITUDE OF RELATIVE TRANSFER IMPEDANCE 2, SHEEP4

MAGNITUDE OF RELATIVE TRANSFER IMPEDANCE 2, SHEEP4
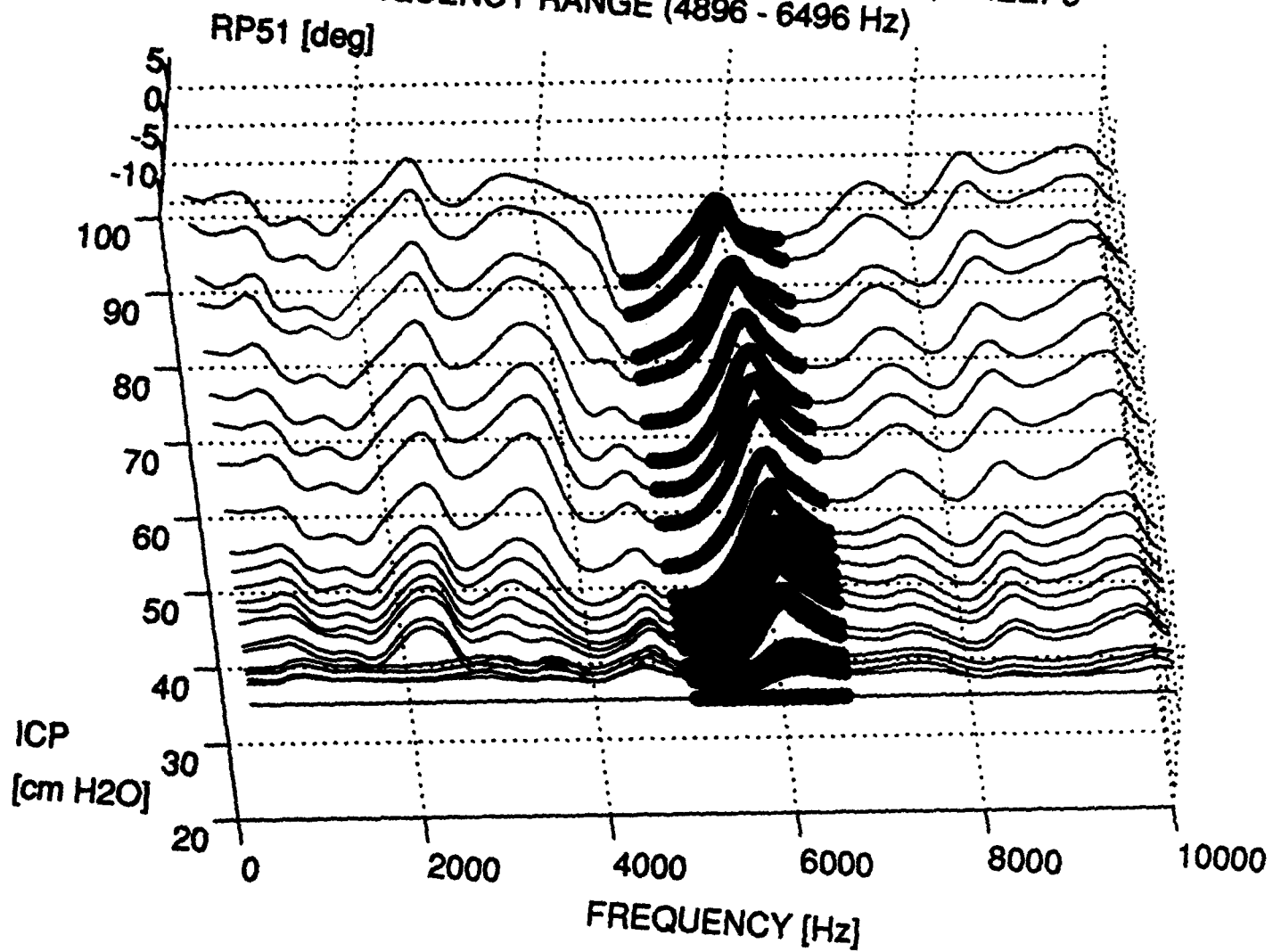FREQUENCY RANGE (104 - 1056 Hz)
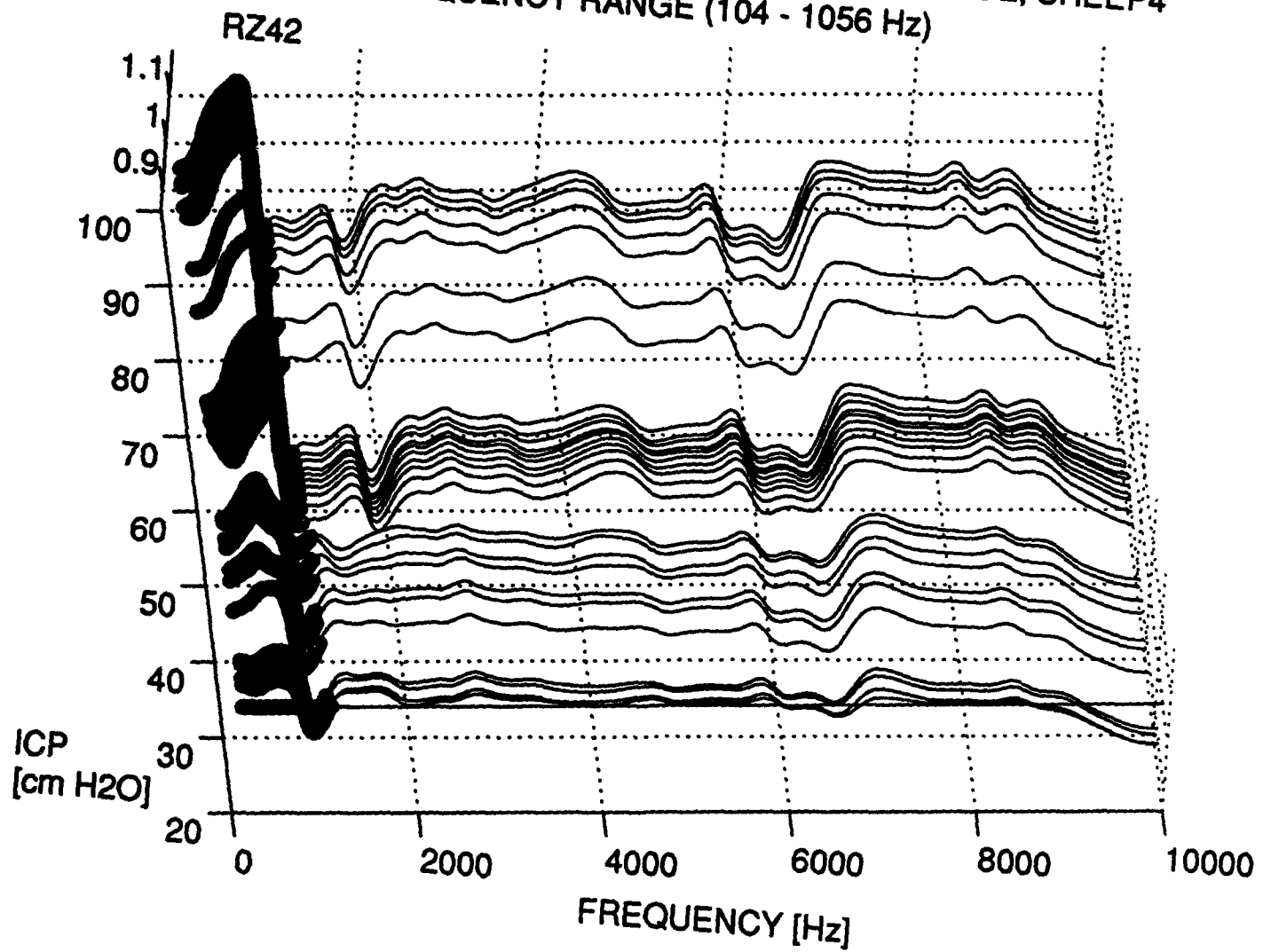
MAGNITUDE STANDARD DEVIATION vs. ICP
SHEEP4: Mag.Rel.T2.   FREQUENCY RANGE (104 - 1056 Hz)
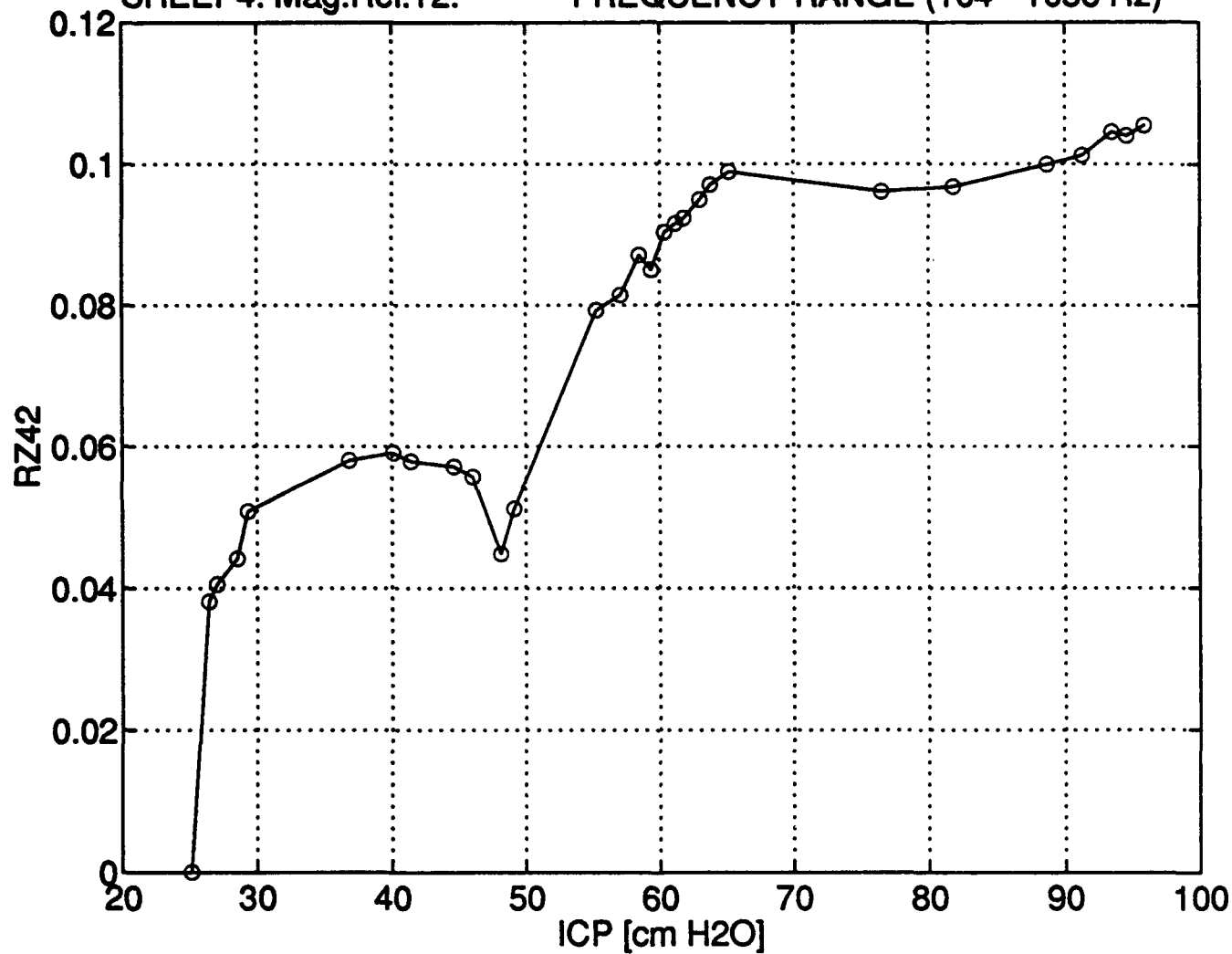
MAGNITUDE OF RELATIVE TRANSFER IMPEDANCE 2, SHEEP4
FREQUENCY RANGE (1296 - 2496 Hz)
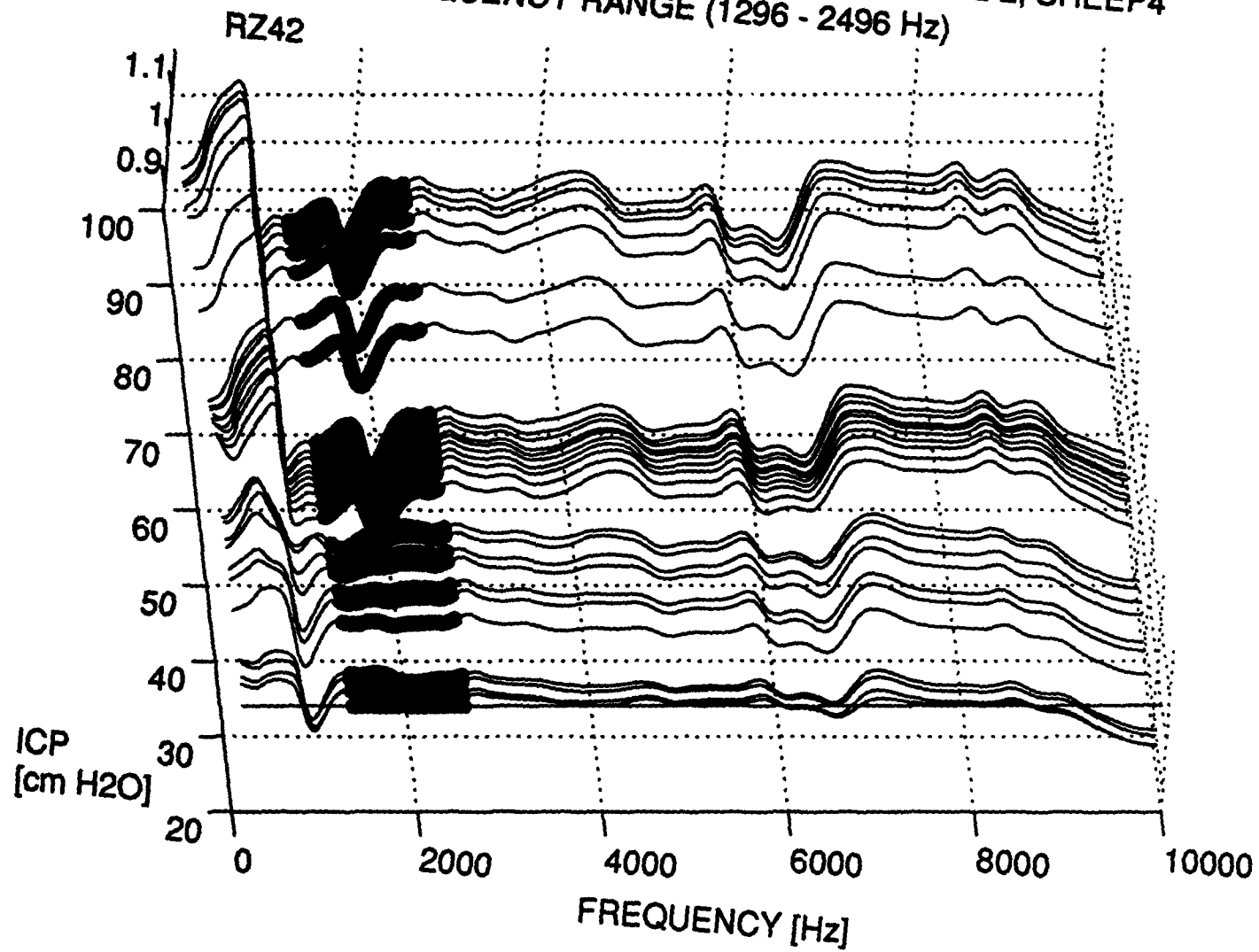
RZ42

ICP
[cm H2O]

FREQUENCY [Hz]

MAGNITUDE STANDARD DEVIATION vs. ICP
SHEEP4: Mag.Rel.T2.   FREQUENCY RANGE (1296 - 2496 Hz)
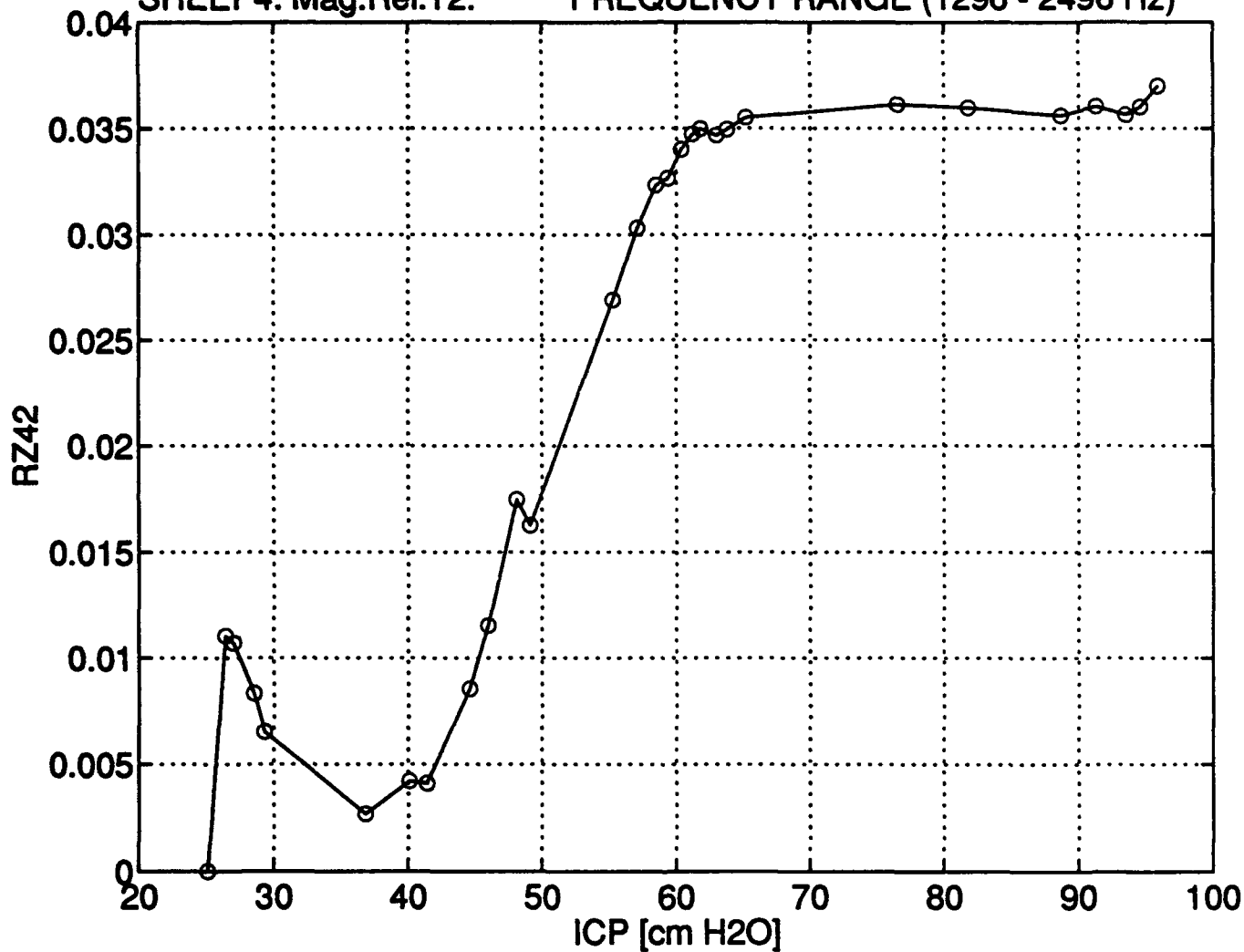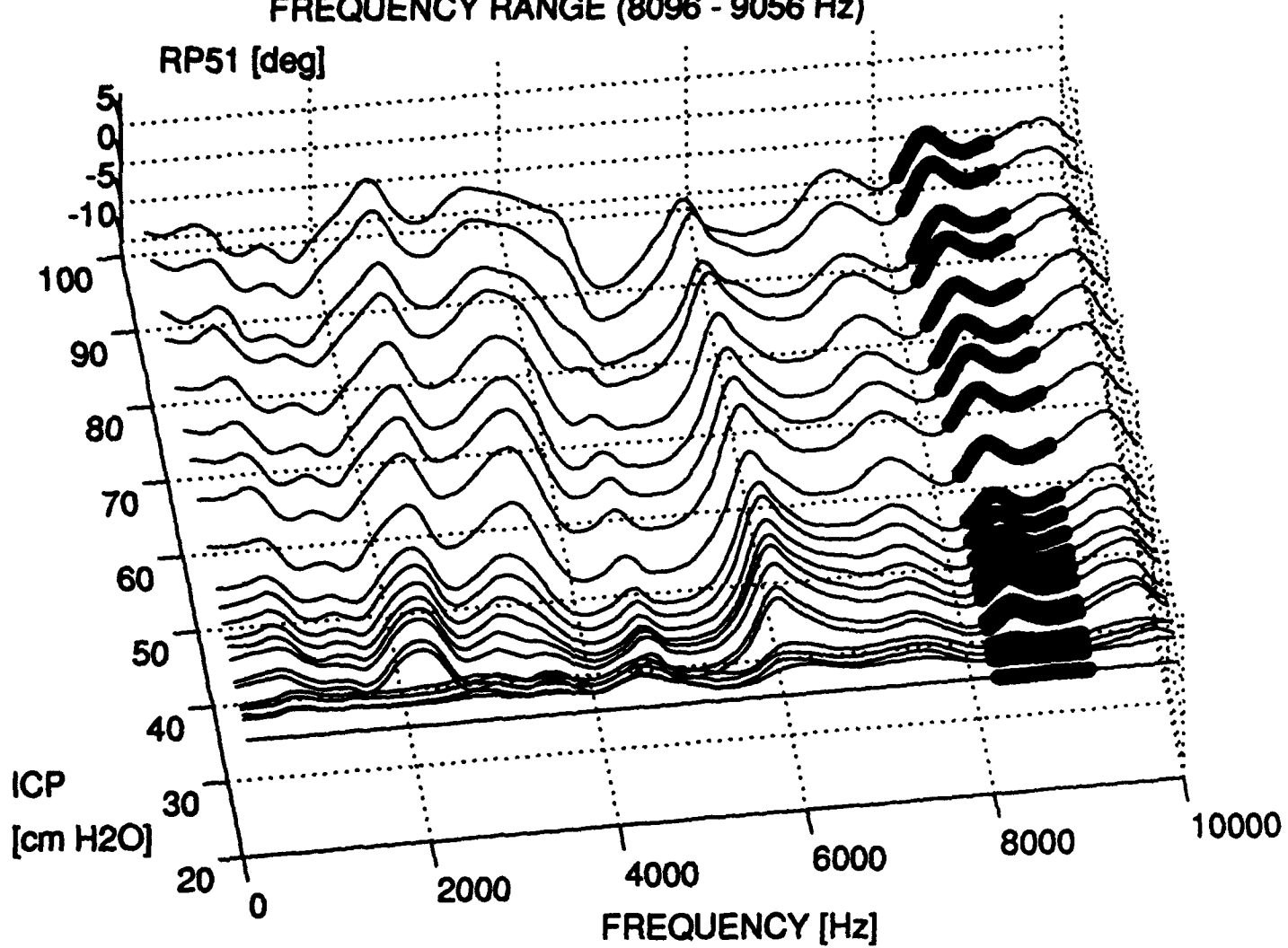
MAGNITUDE OF RELATIVE TRANSFER IMPEDANCE 2, SHEEP4
FREQUENCY RANGE (5696 - 7296 Hz)
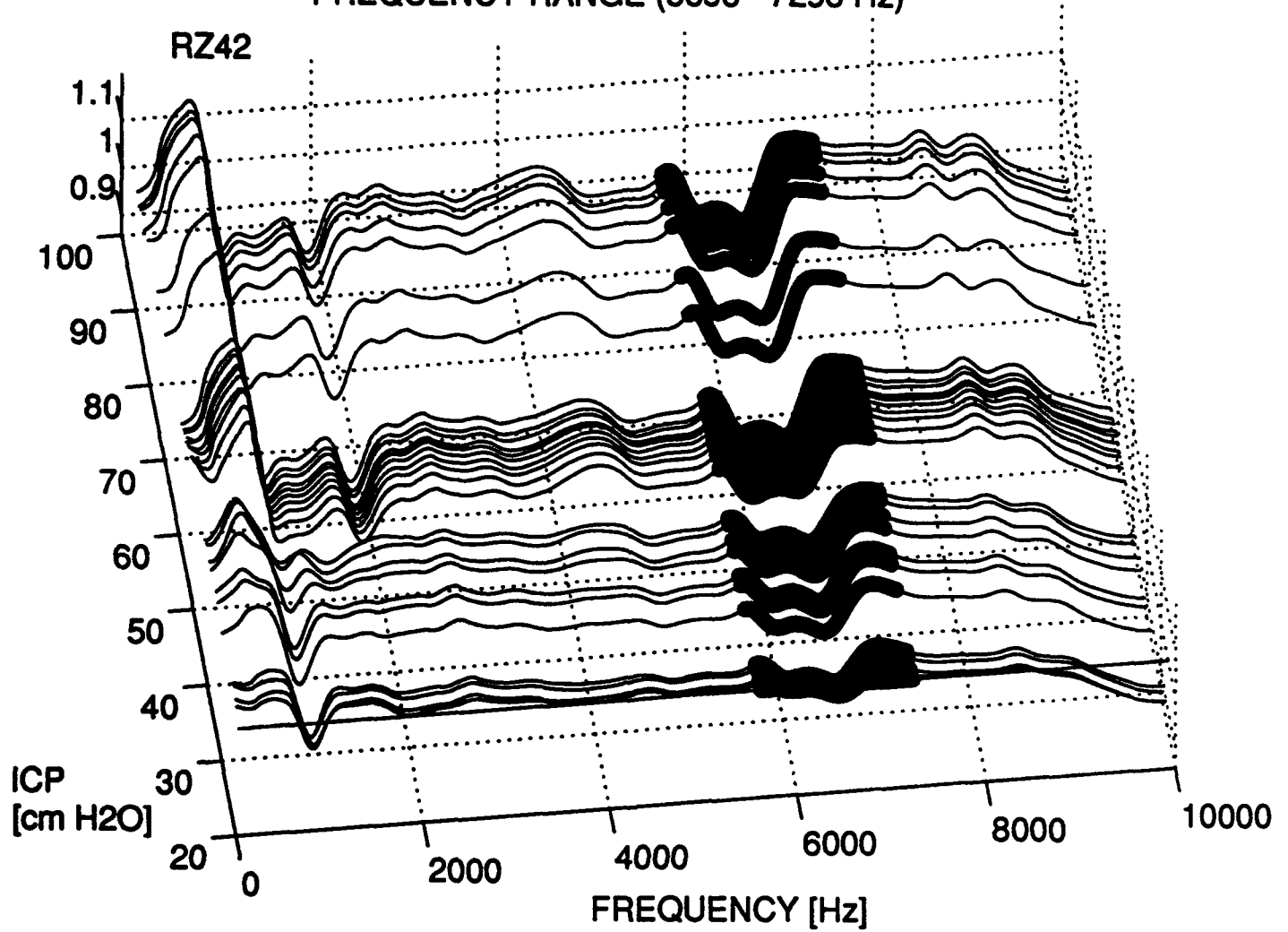
MAGNITUDE STANDARD DEVIATION vs. ICP
SHEEP4: Mag.Rel.T2.   FREQUENCY RANGE (5696 - 7296 Hz)
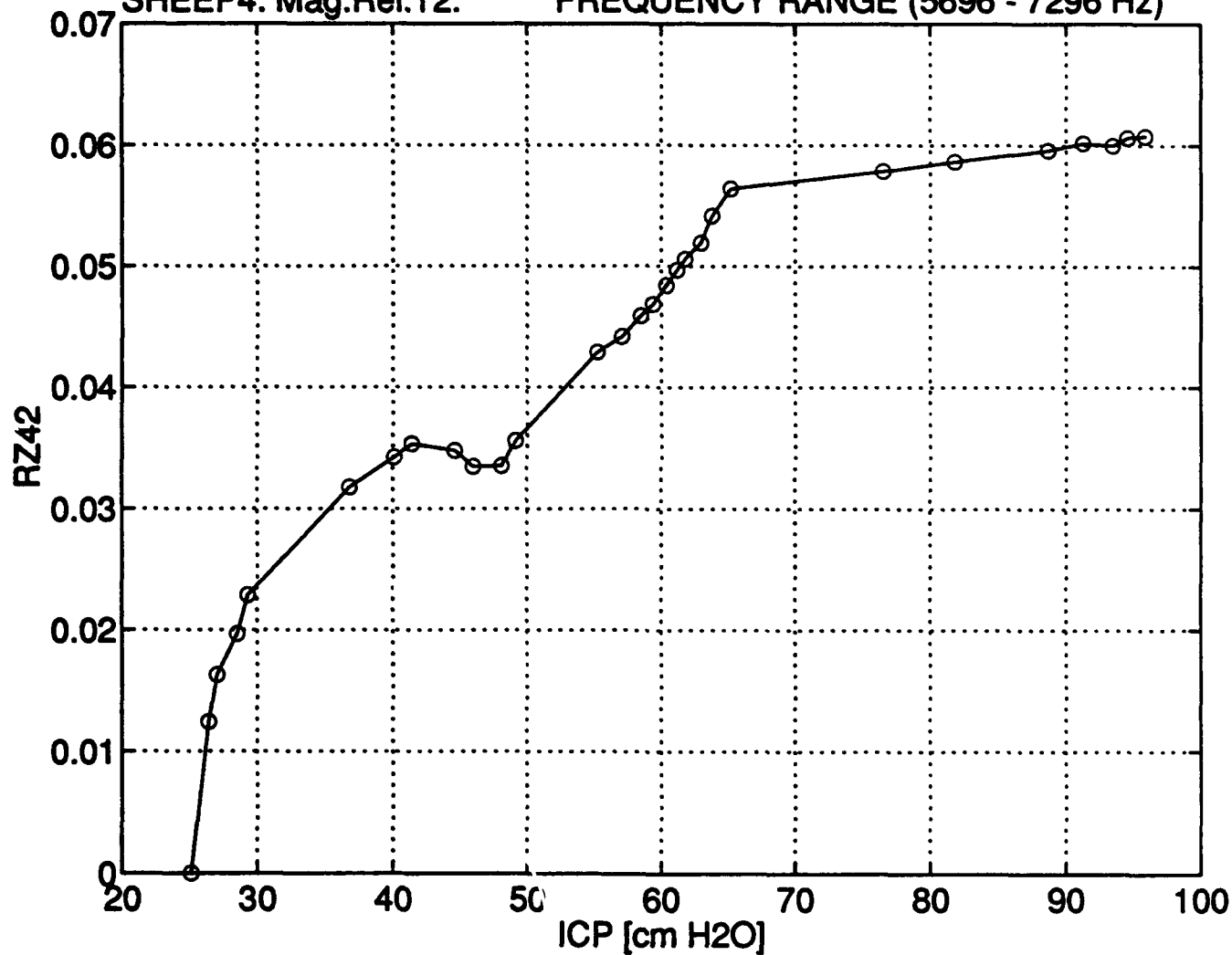
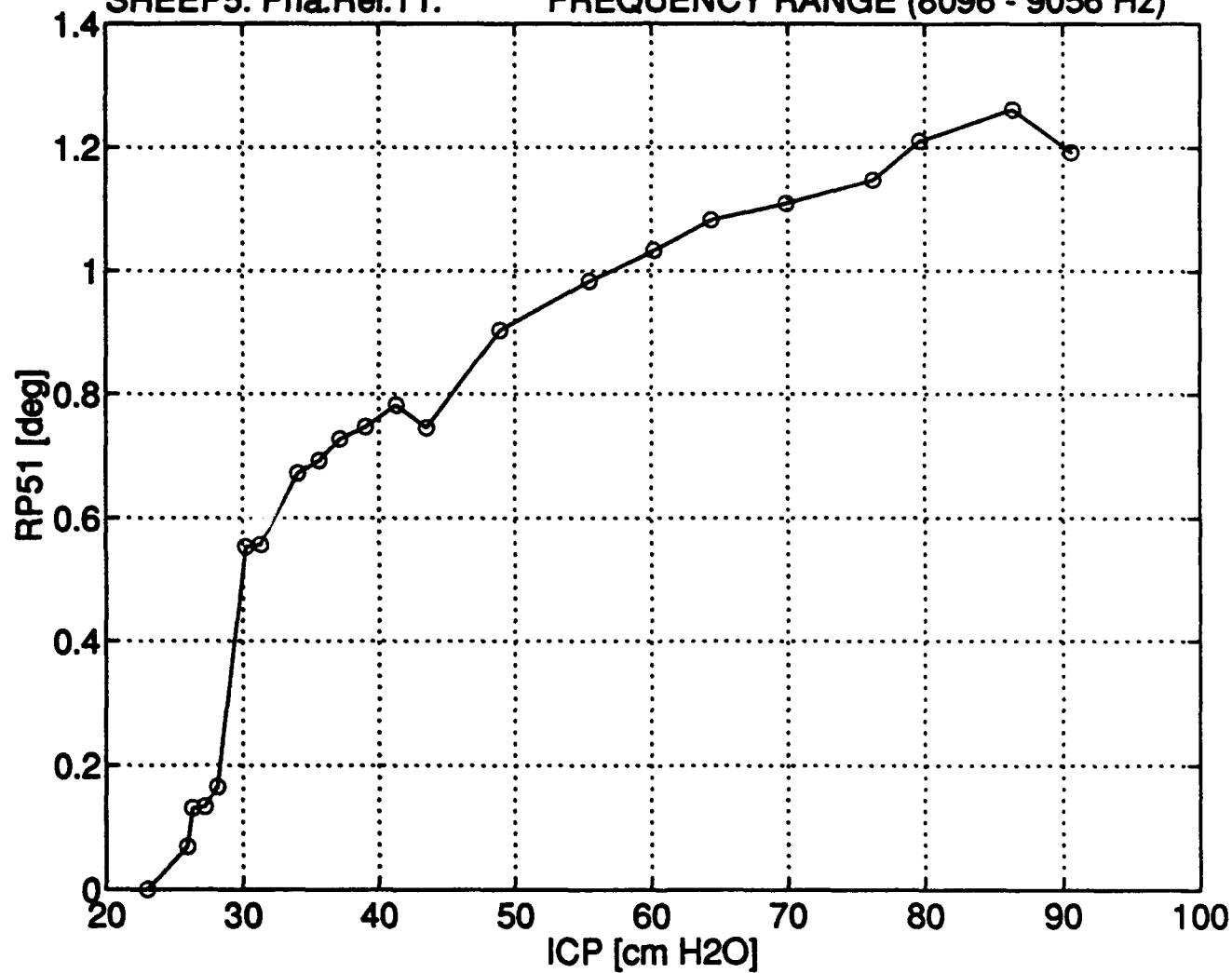MAGNITUDE OF RELATIVE TRANSFER IMPEDANCE 3, SHEEP4

MAGNITUDE OF RELATIVE TRANSFER IMPEDANCE 3, SHEEP4
FREQUENCY RANGE (104 - 1376 Hz)
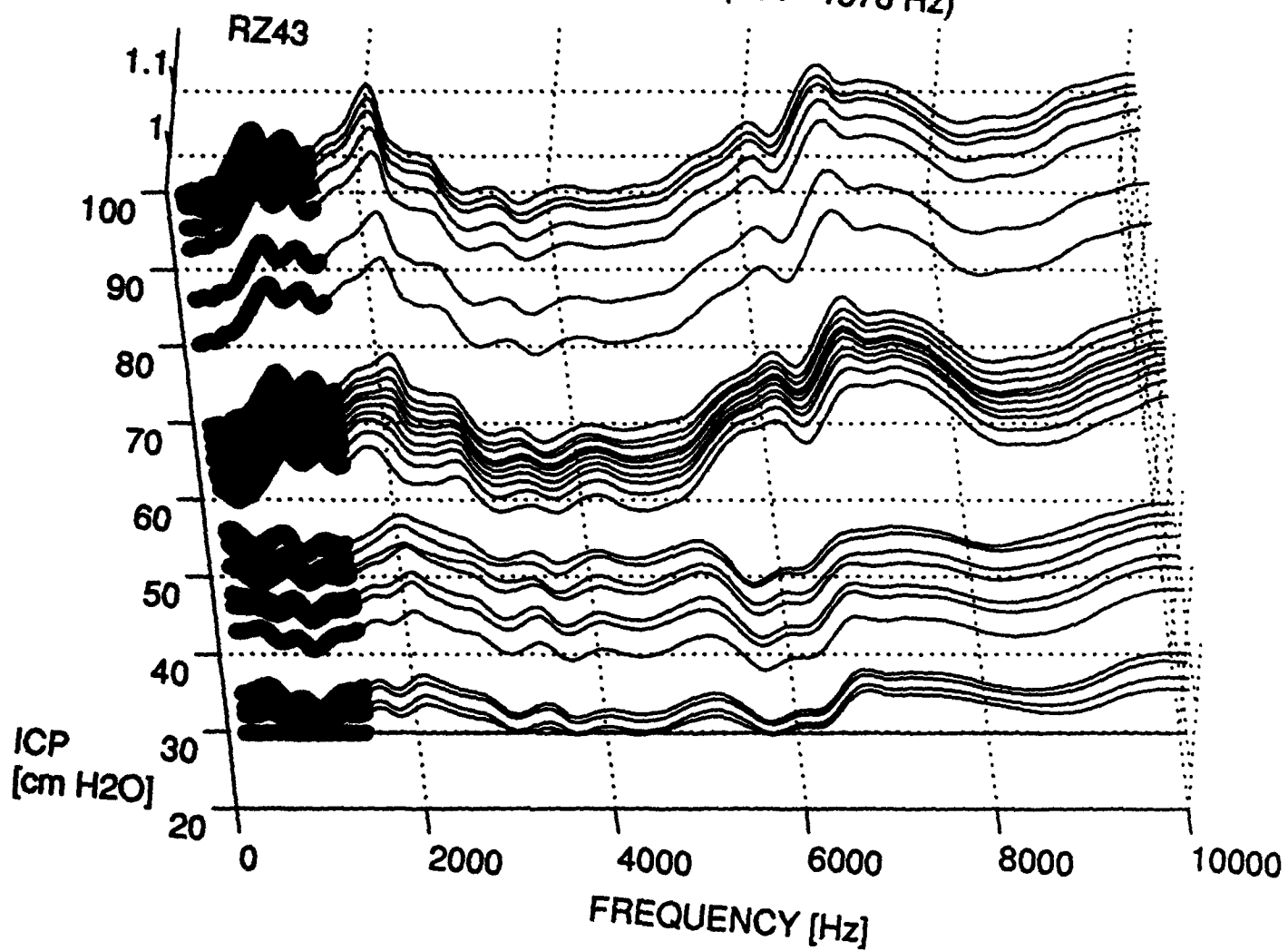
MAGNITUDE STANDARD DEVIATION vs. ICP
SHEEP4: Mag.Rel.T3.   FREQUENCY RANGE (104 - 1376 Hz)

MAGNITUDE OF RELATIVE TRANSFER IMPEDANCE 3, SHEEP4
FREQUENCY RANGE (1696 - 2496 Hz)

RZ43

ICP
[cm H2O]
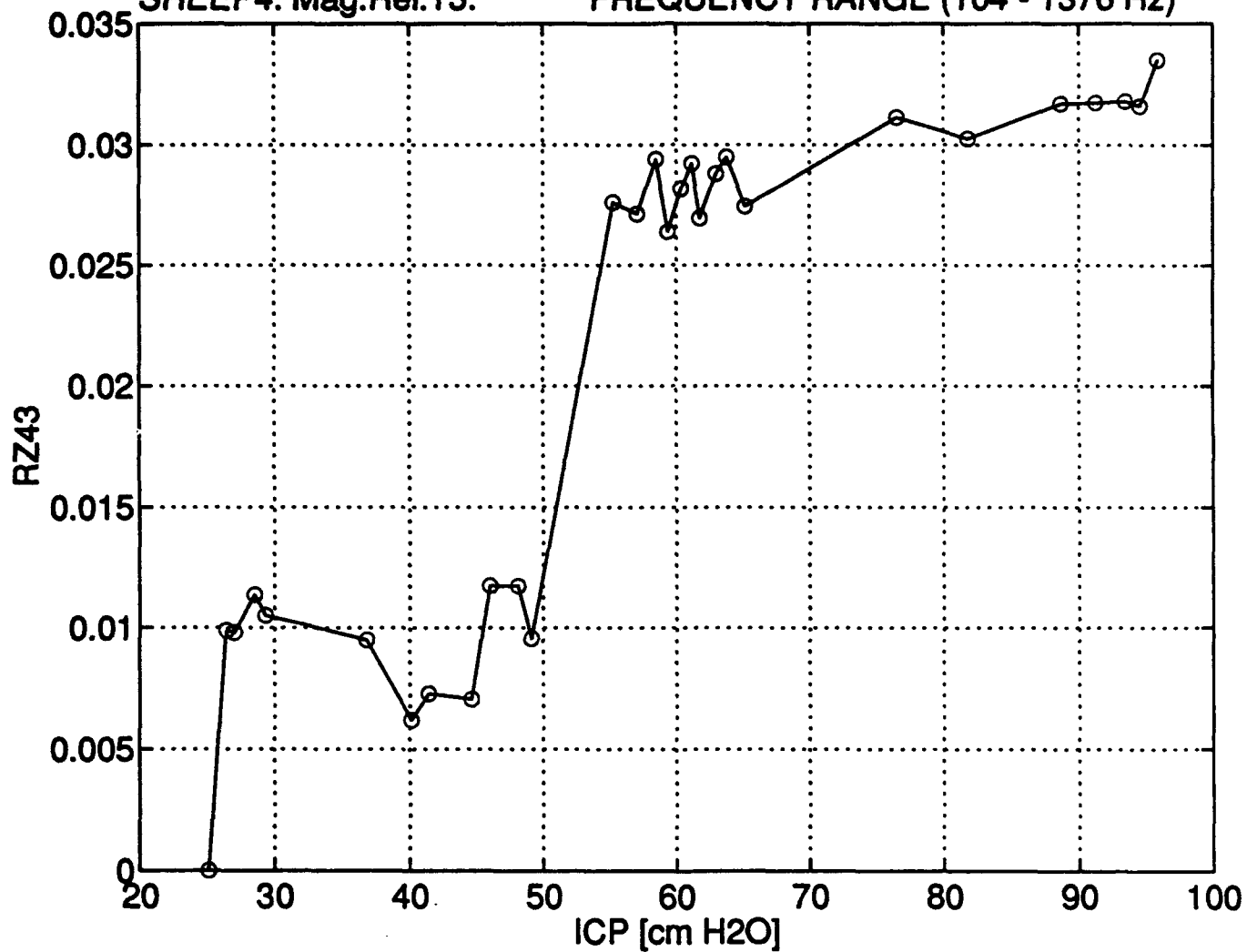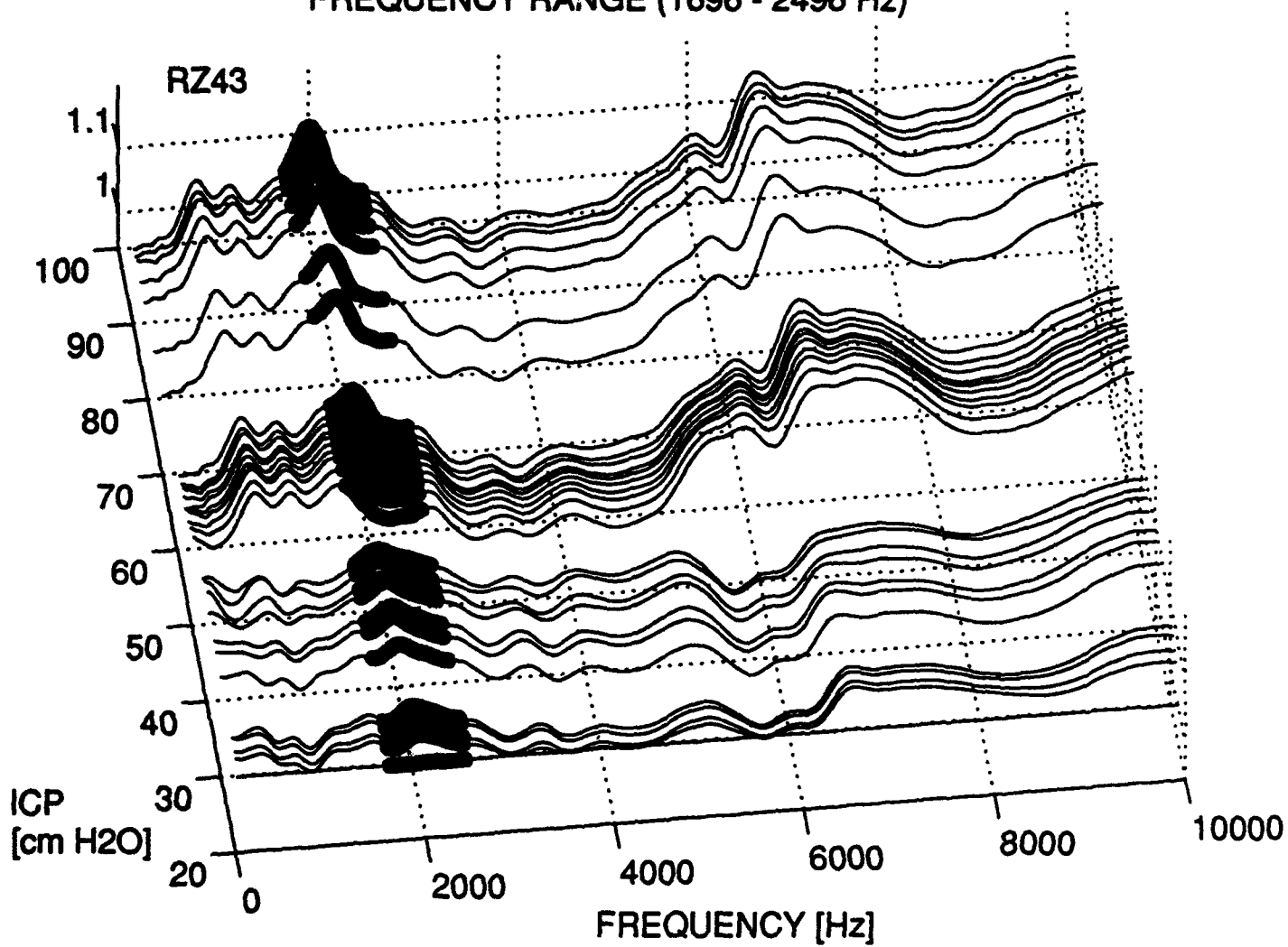
FREQUENCY [Hz]

MAGNITUDE STANDARD DEVIATION vs. ICP
SHEEP4: Mag.Rel.T3.   FREQUENCY RANGE (1696 - 2496 Hz)
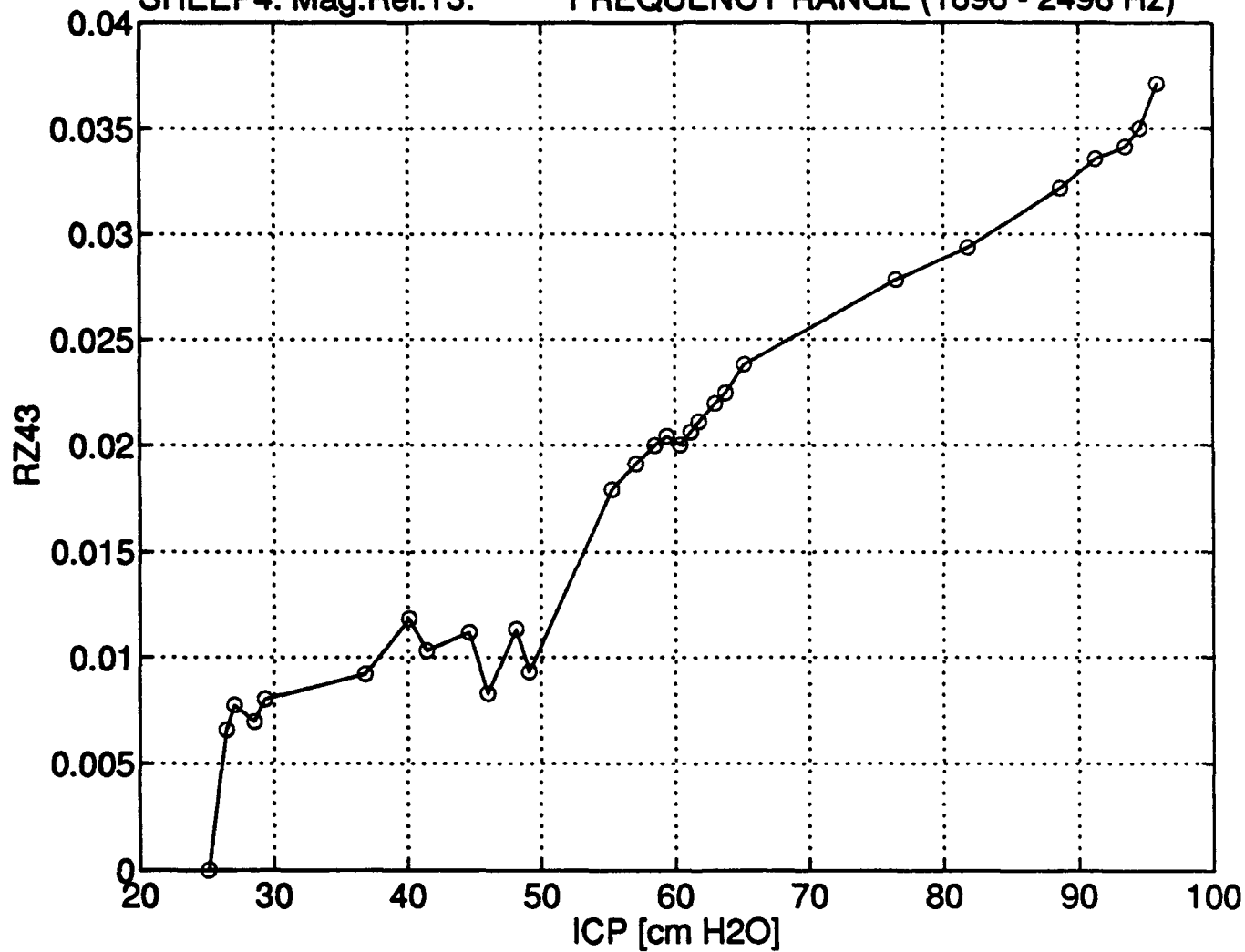
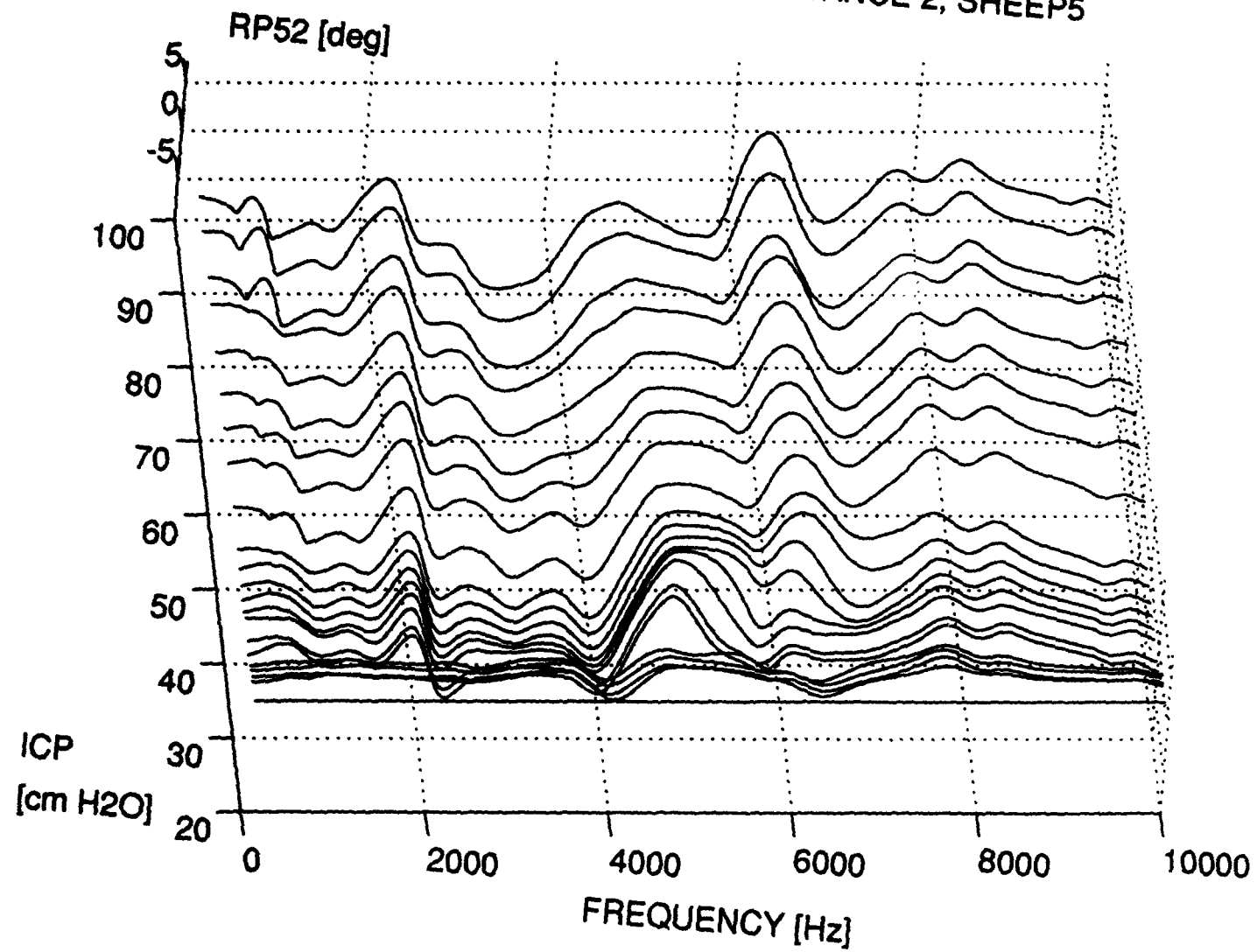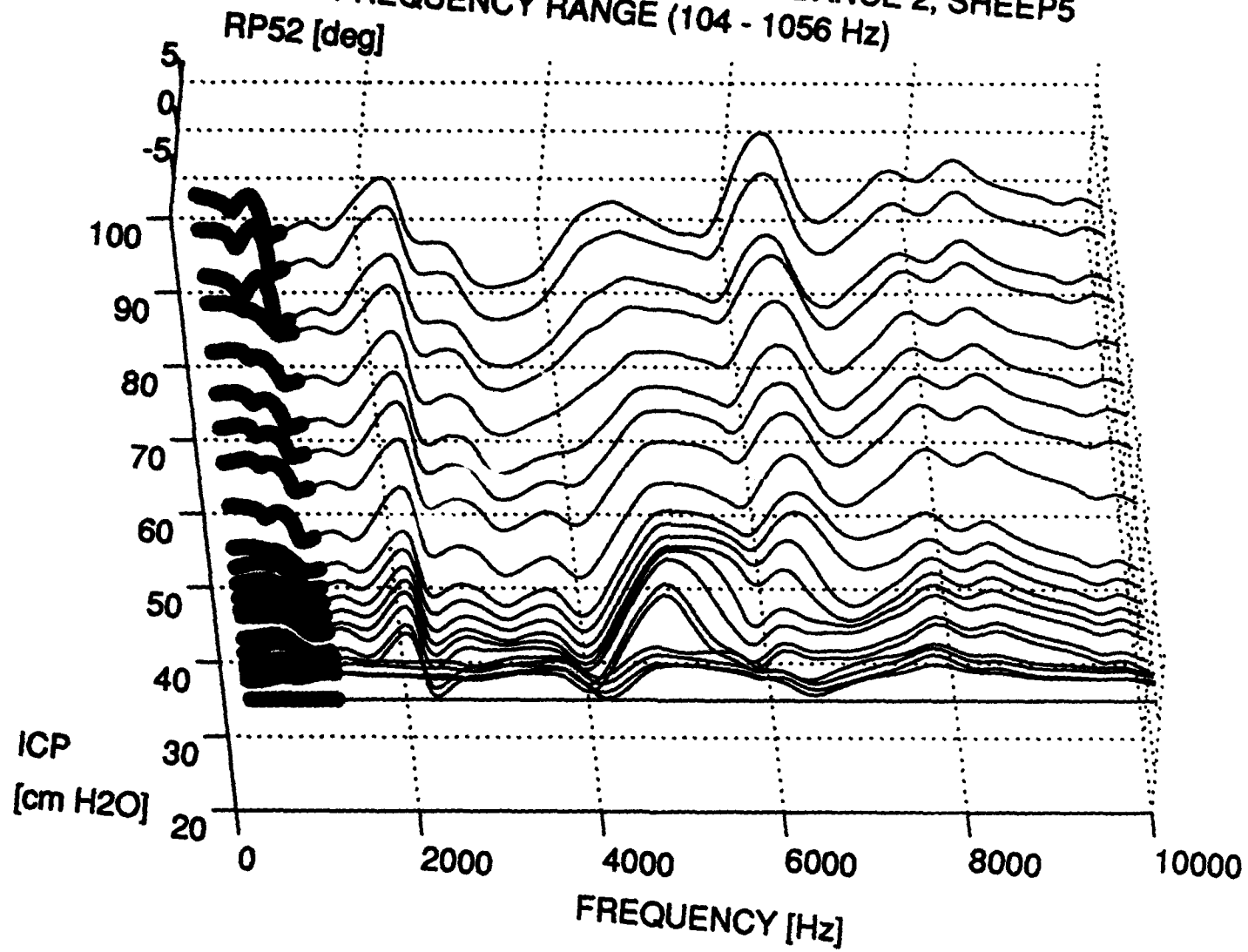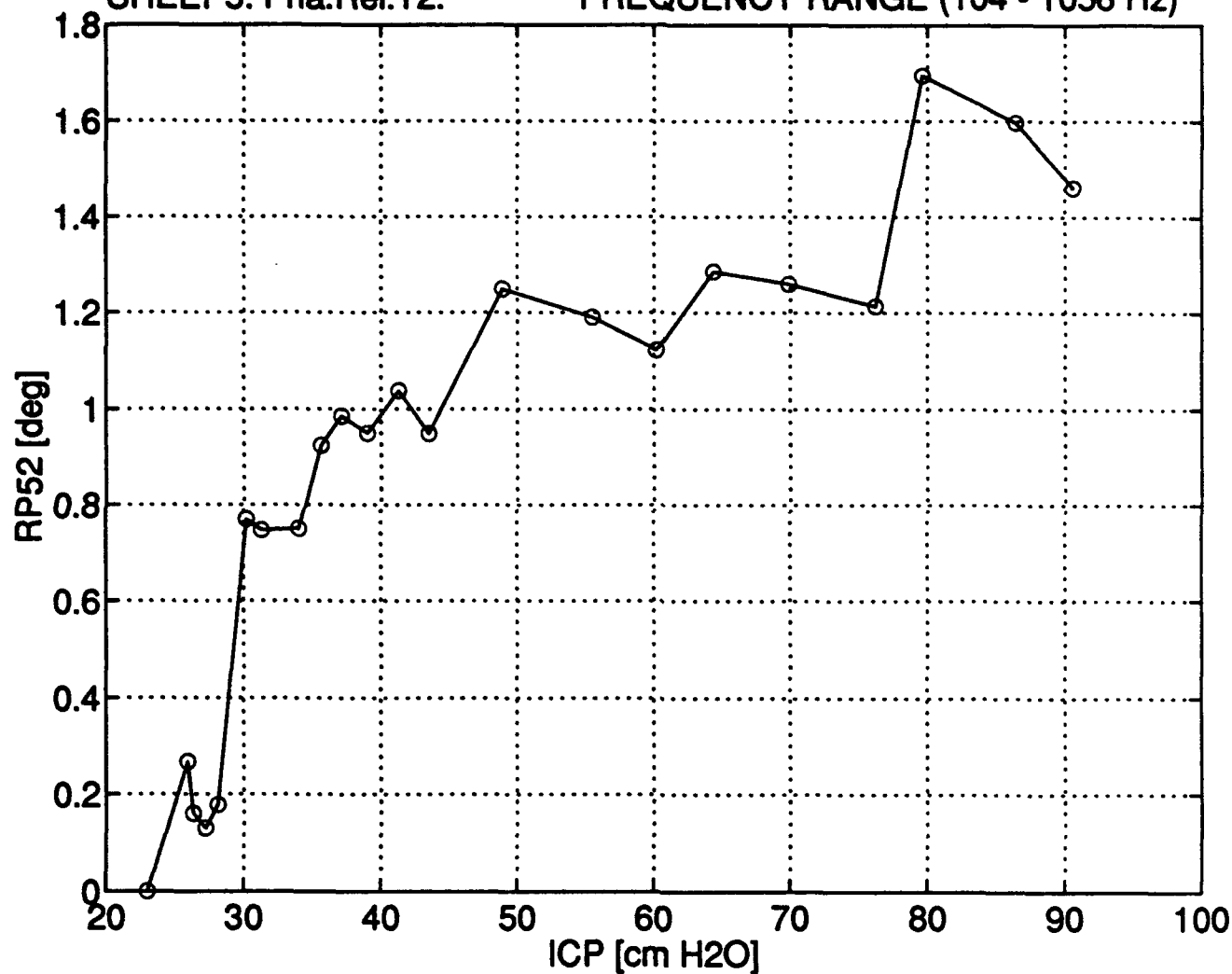MAGNITUDE OF RELATIVE TRANSFER IMPEDANCE 3, SHEEP4
FREQUENCY RANGE (5856 - 6976 Hz)
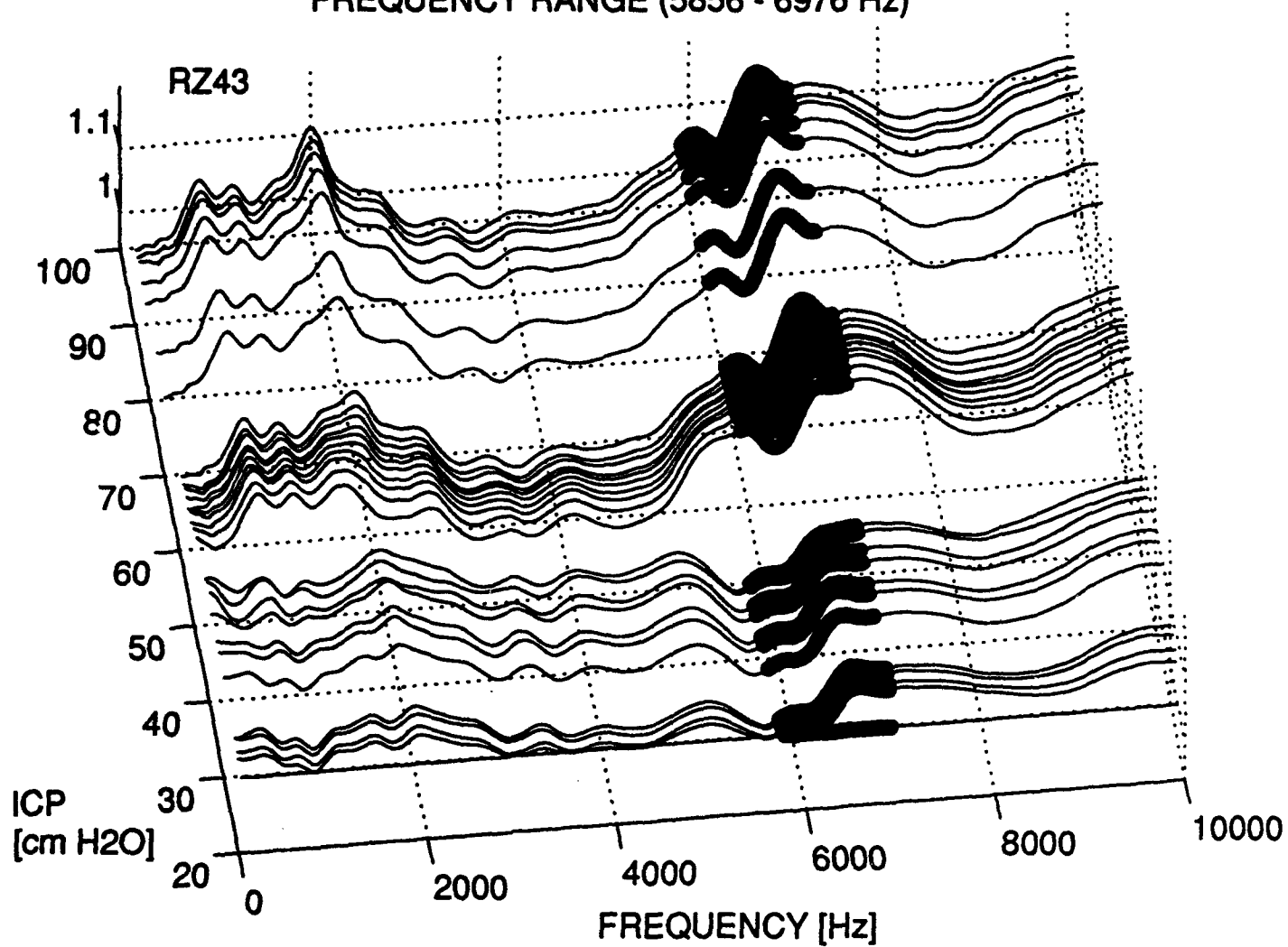
MAGNITUDE STANDARD DEVIATION vs. ICP
SHEEP4: Mag.Rel.T3.   FREQUENCY RANGE (5856 - 6976 Hz)
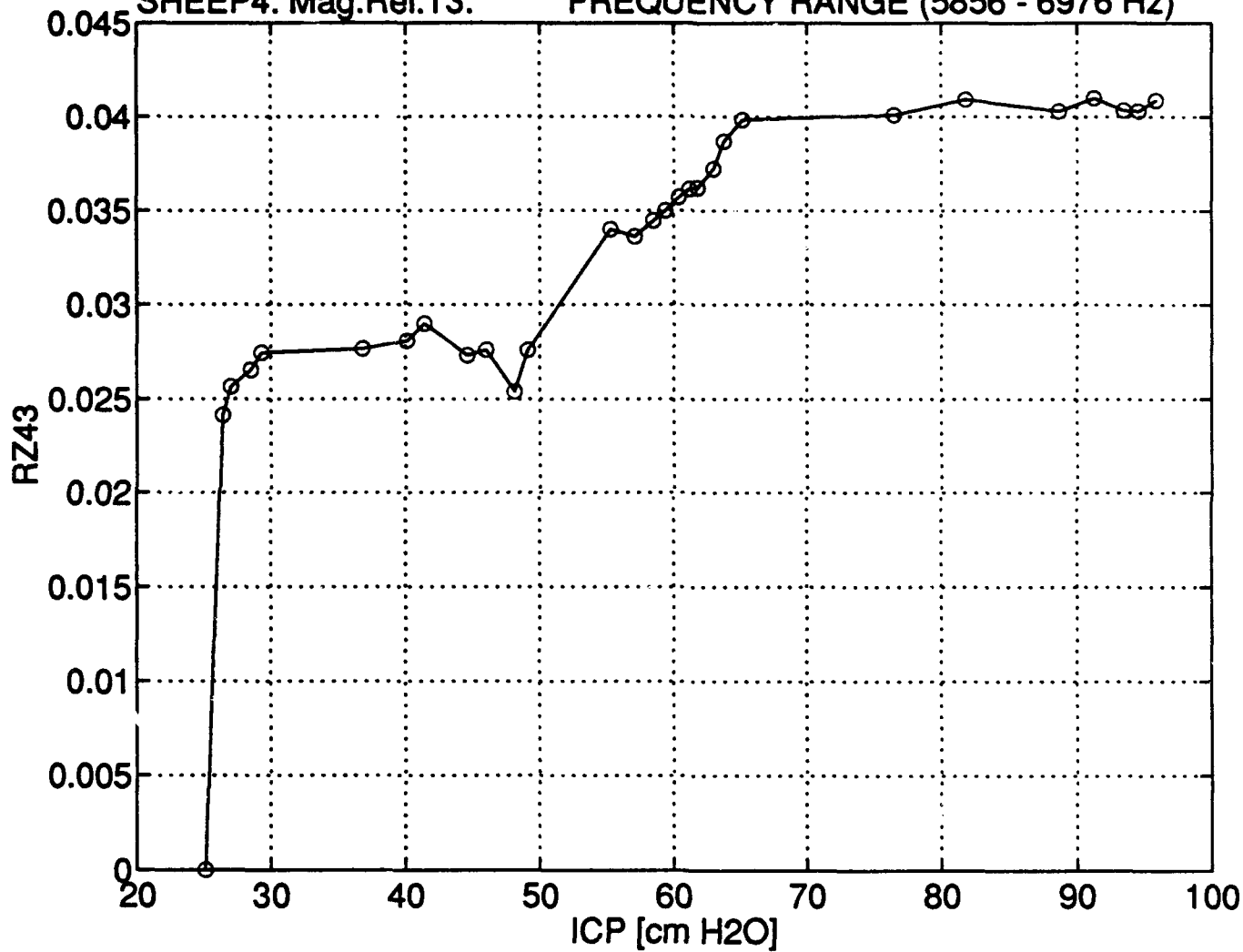
PHASE OF RELATIVE DRIVING POINT IMPEDANCE, SHEEP4
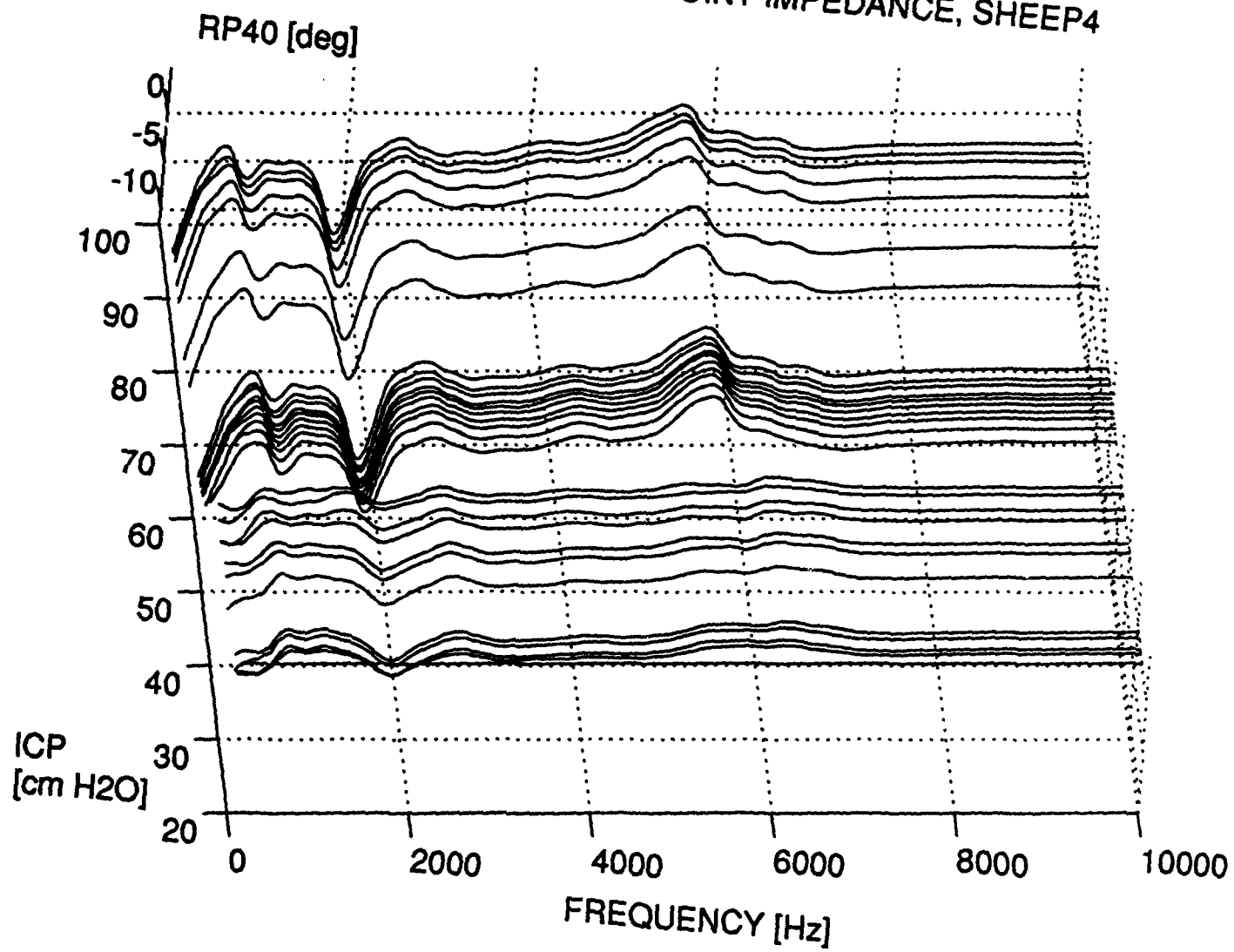
PHASE OF RELATIVE DRIVING POINT IMPEDANCE, SHEEP4
FREQUENCY RANGE (104 - 1856 Hz)
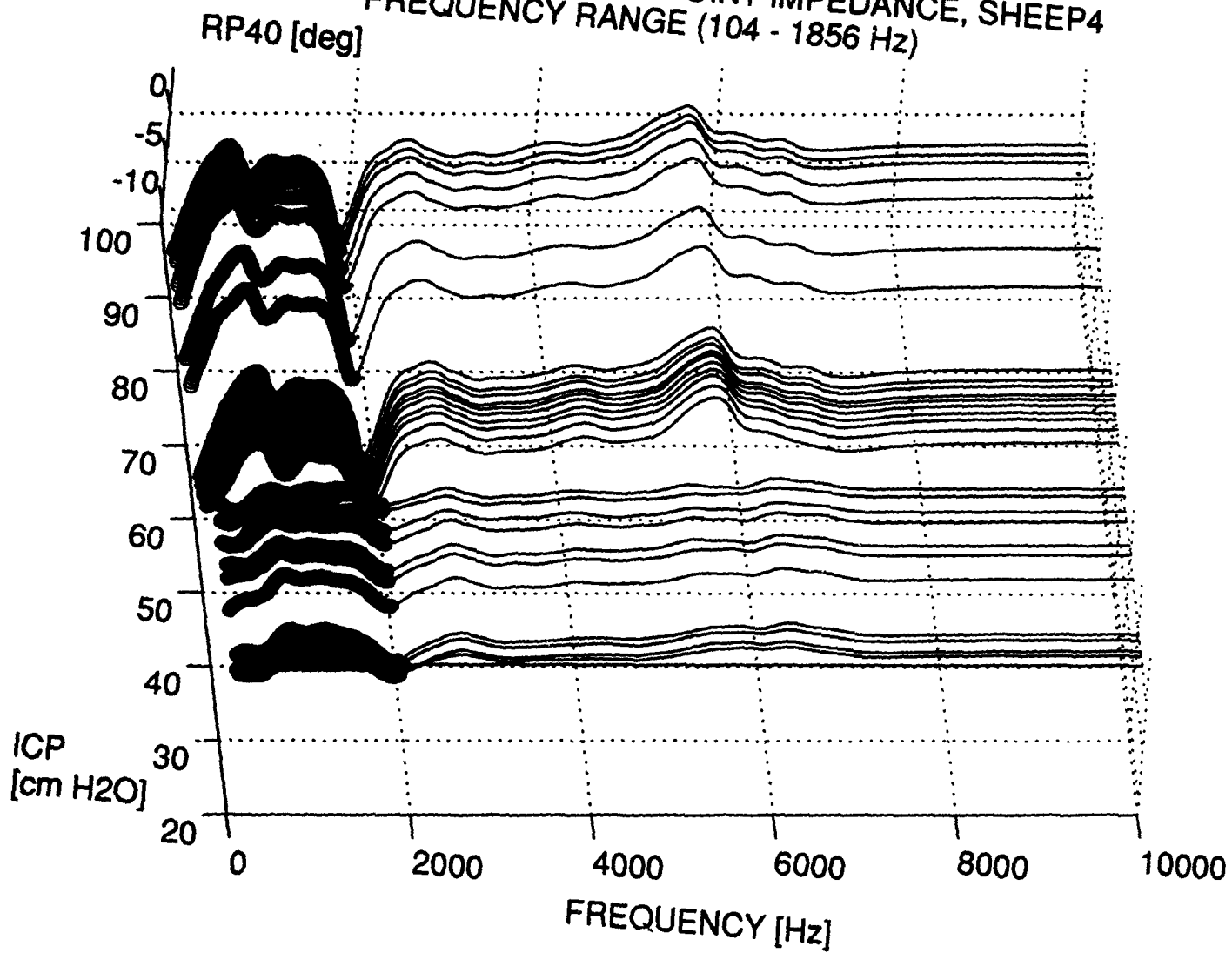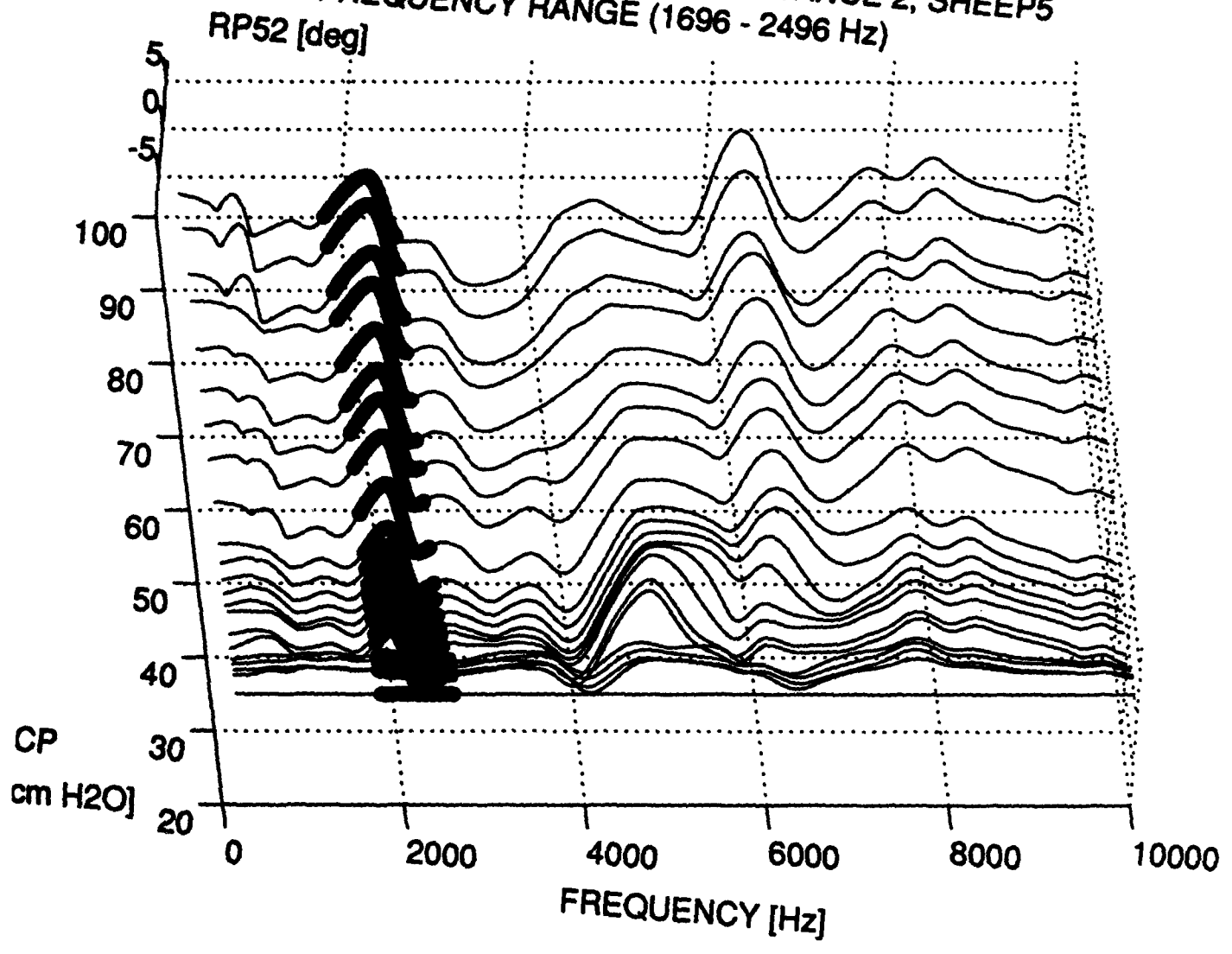
RP40 [deg]

ICP
[cm H2O]

FREQUENCY [Hz]

PHASE STANDARD DEVIATION vs. ICP
SHEEP4: Pha.Rel.DP.   FREQUENCY RANGE (104 - 1856 Hz)
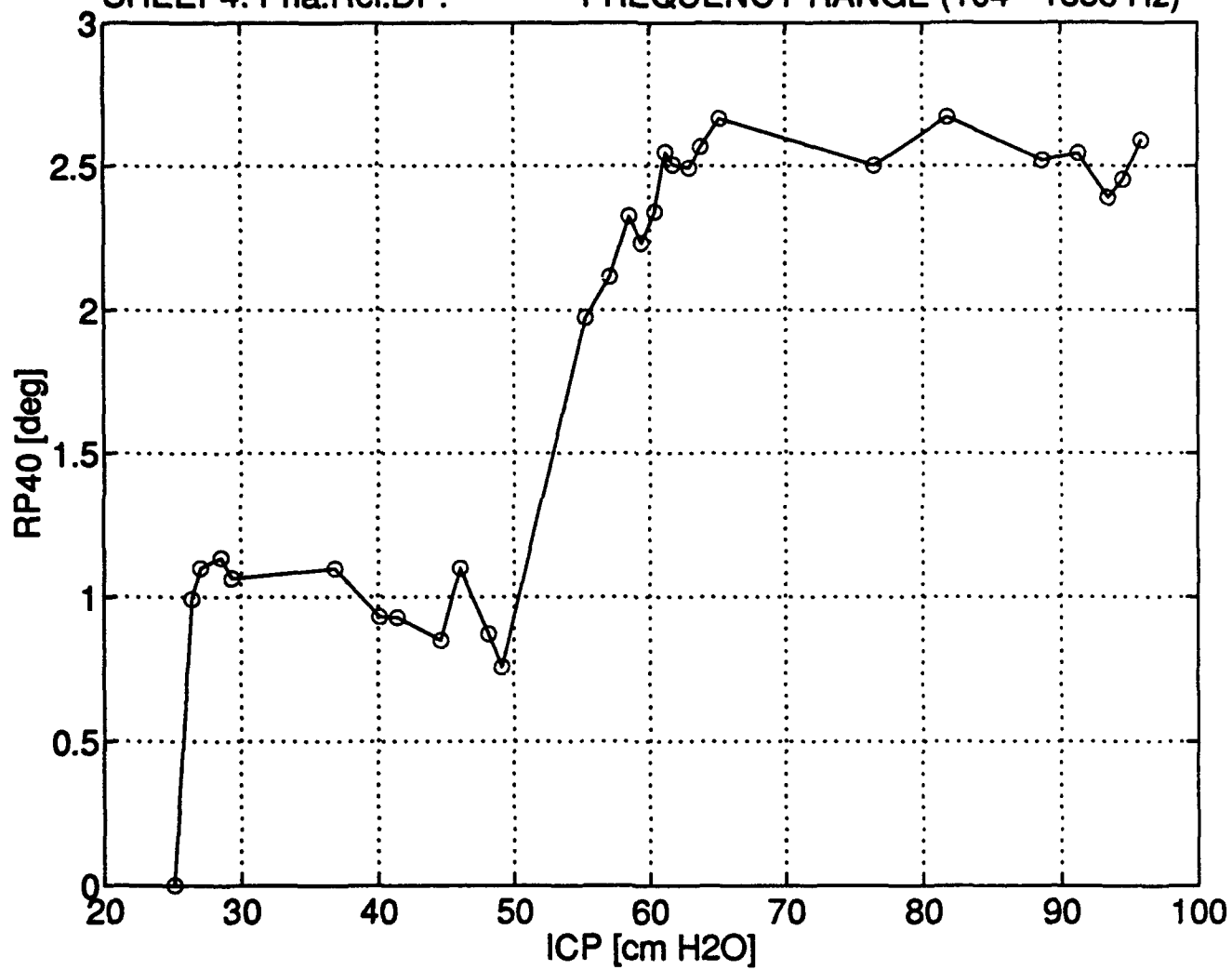
PHASE OF RELATIVE DRIVING POINT IMPEDANCE, SHEEP4
FREQUENCY RANGE (1856 - 2896 Hz)
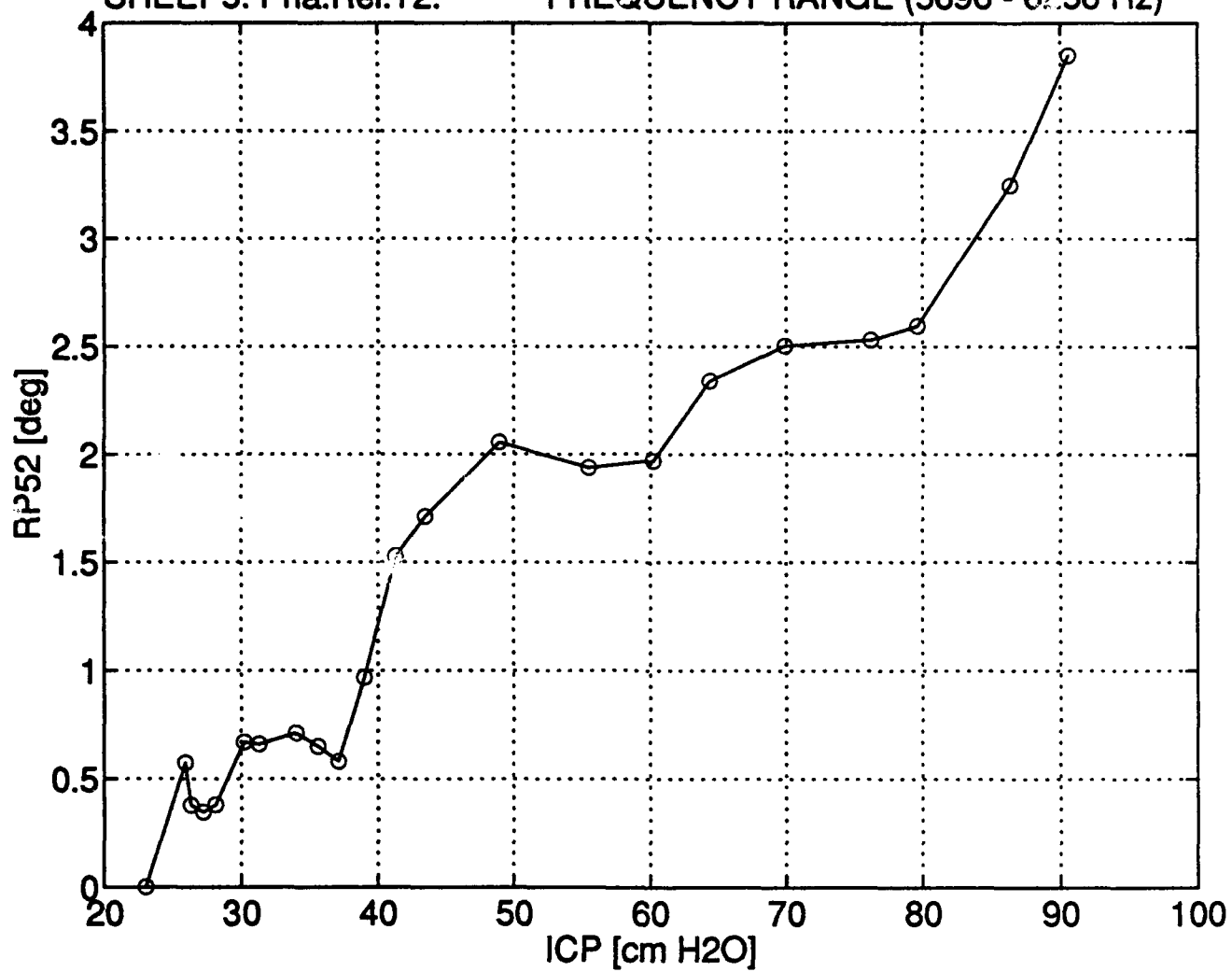
PHASE STANDARD DEVIATION vs. ICP
SHEEP4: Pha.Rel.DP.   FREQUENCY RANGE (1856 - 2896 Hz)

PHASE OF RELATIVE DRIVING POINT IMPEDANCE, SHEEP4
FREQUENCY RANGE (4416 - 6096 Hz)
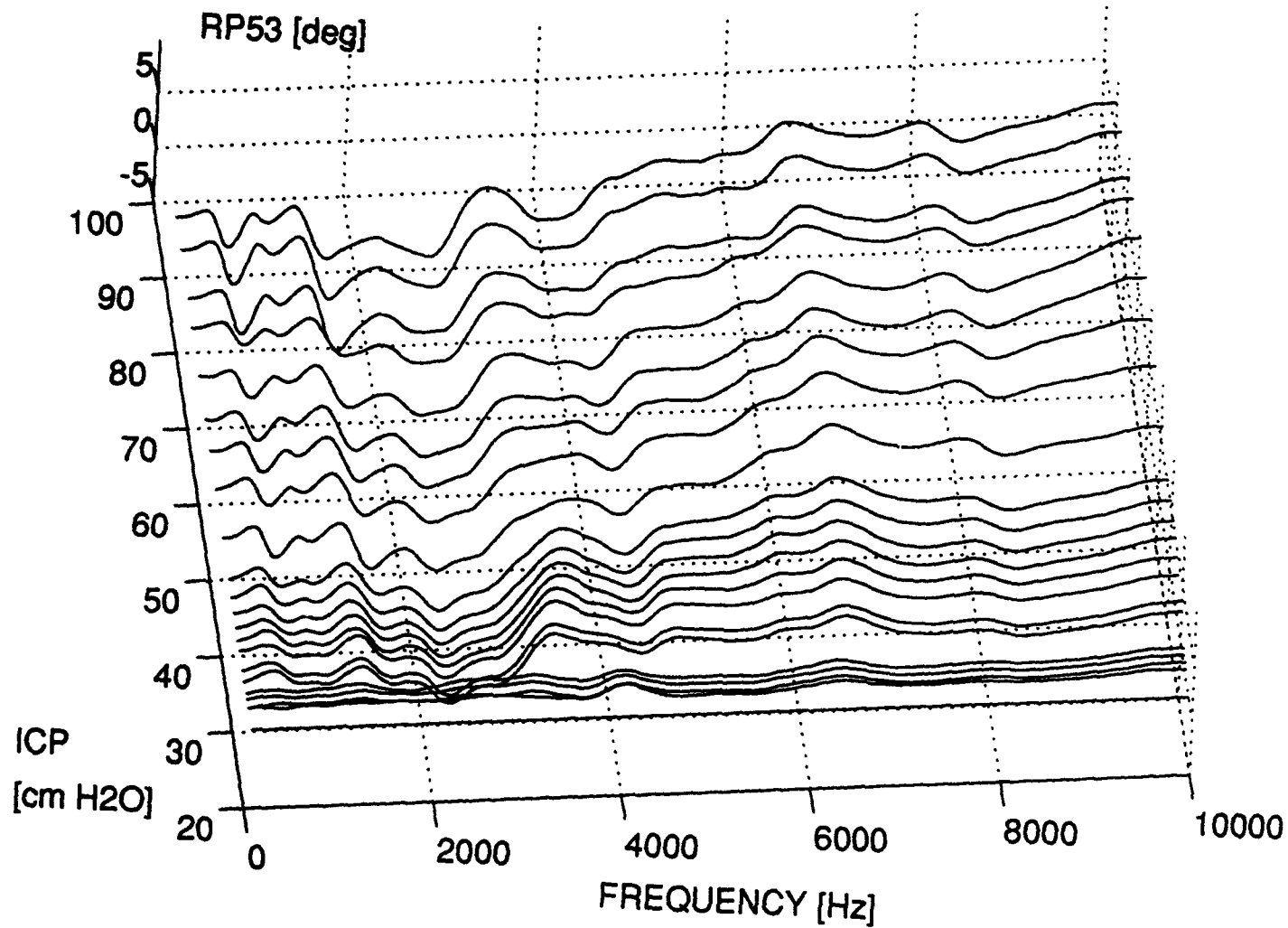
RP40 [deg]

ICP [cm H2O]
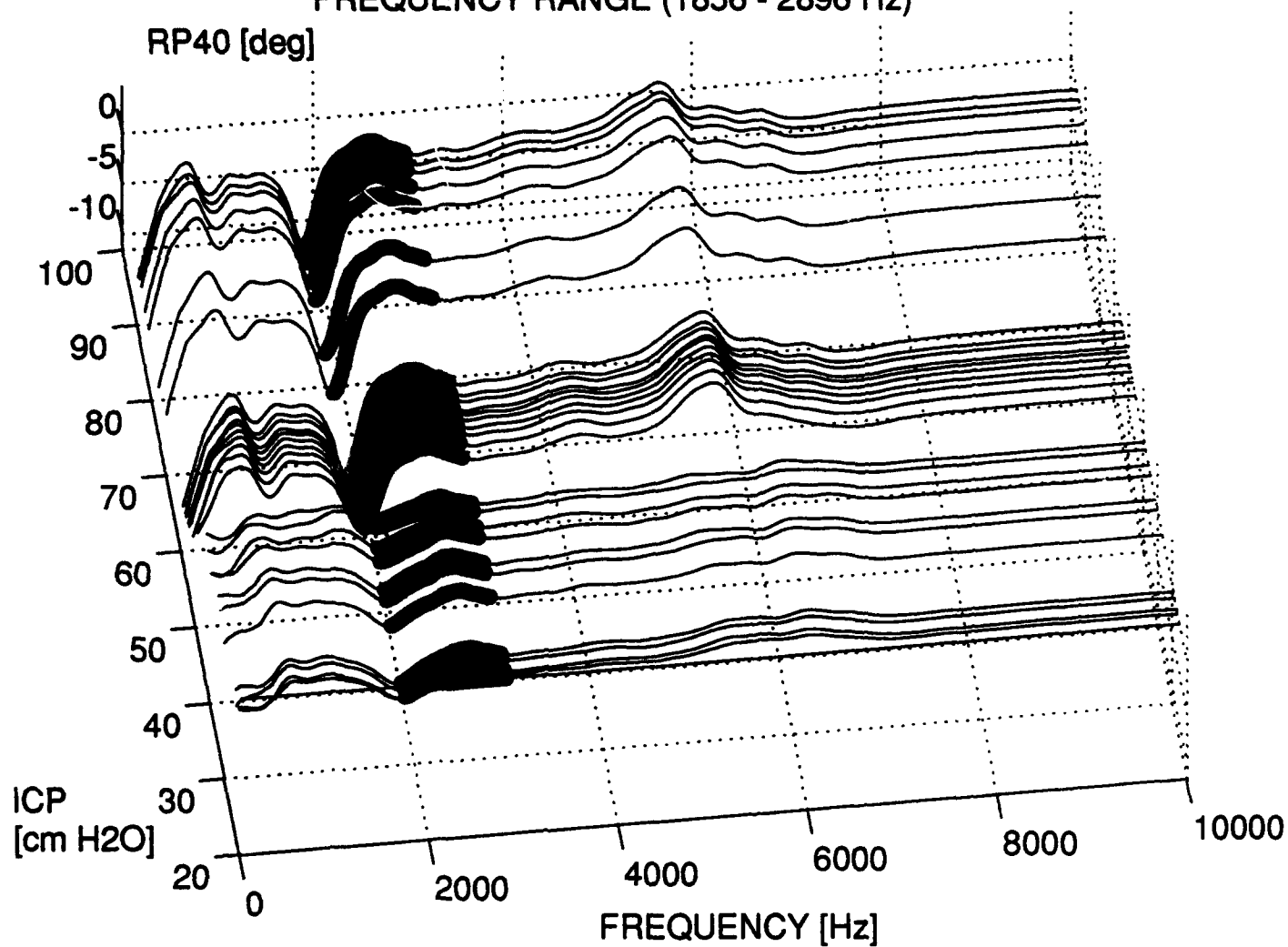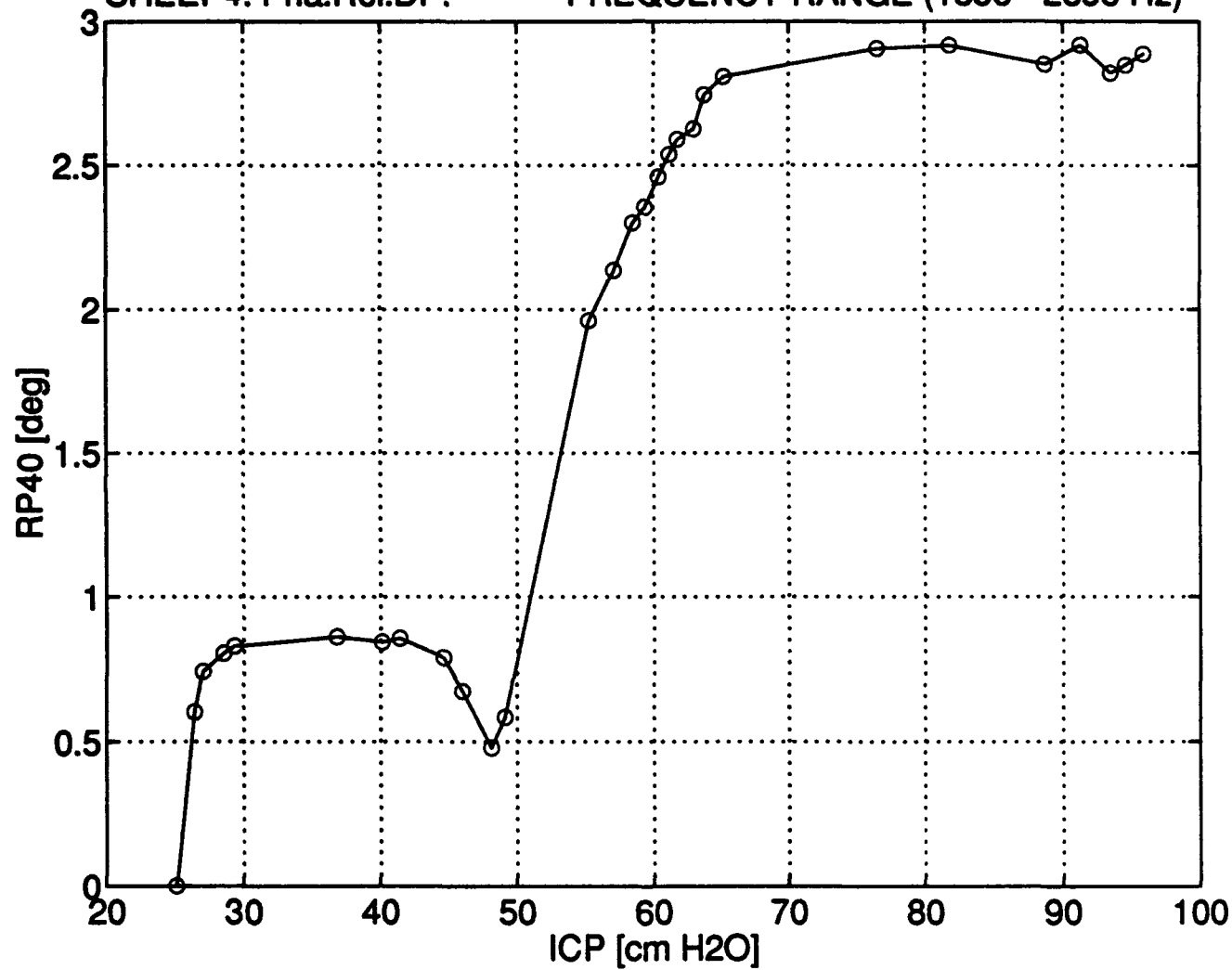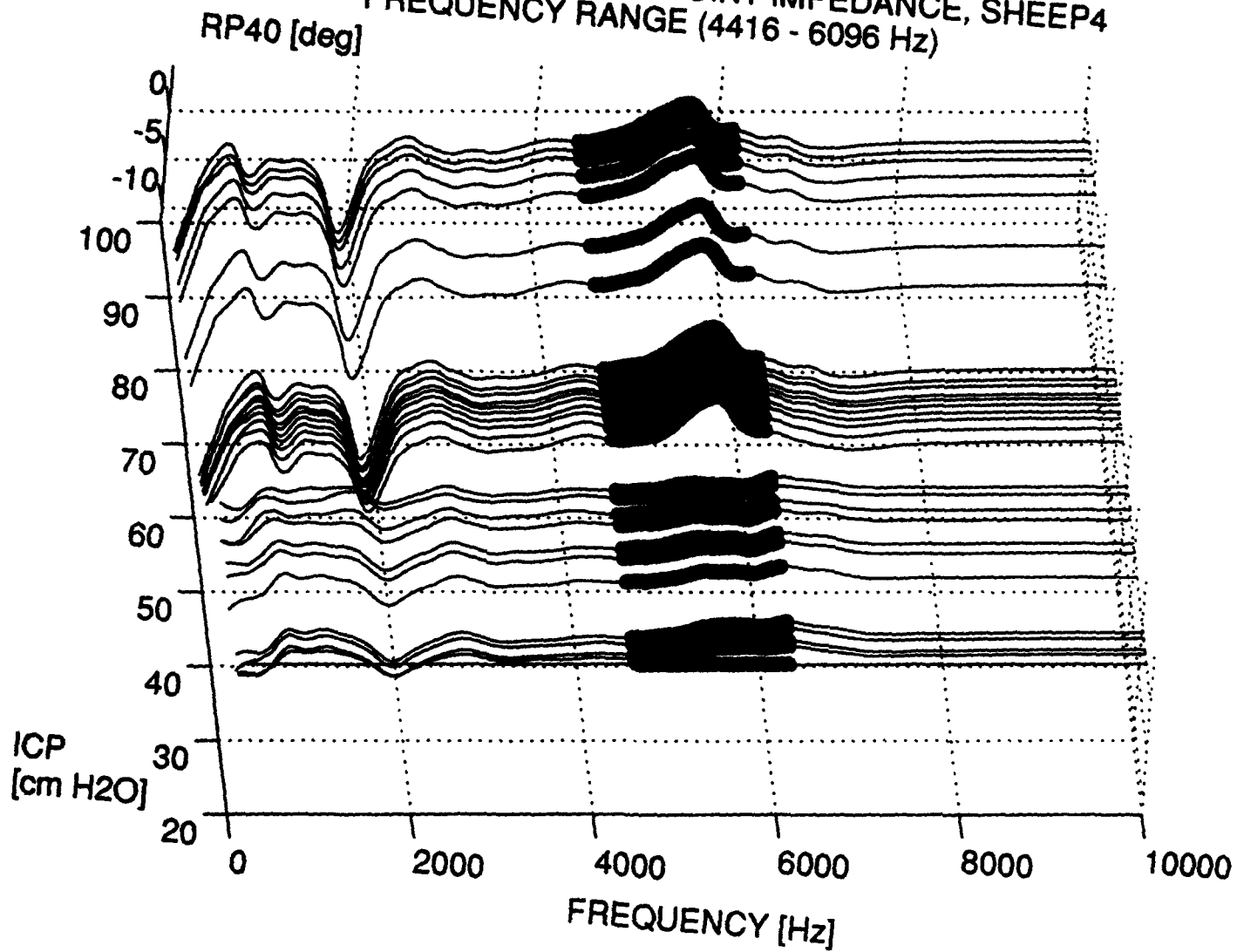
FREQUENCY [Hz]

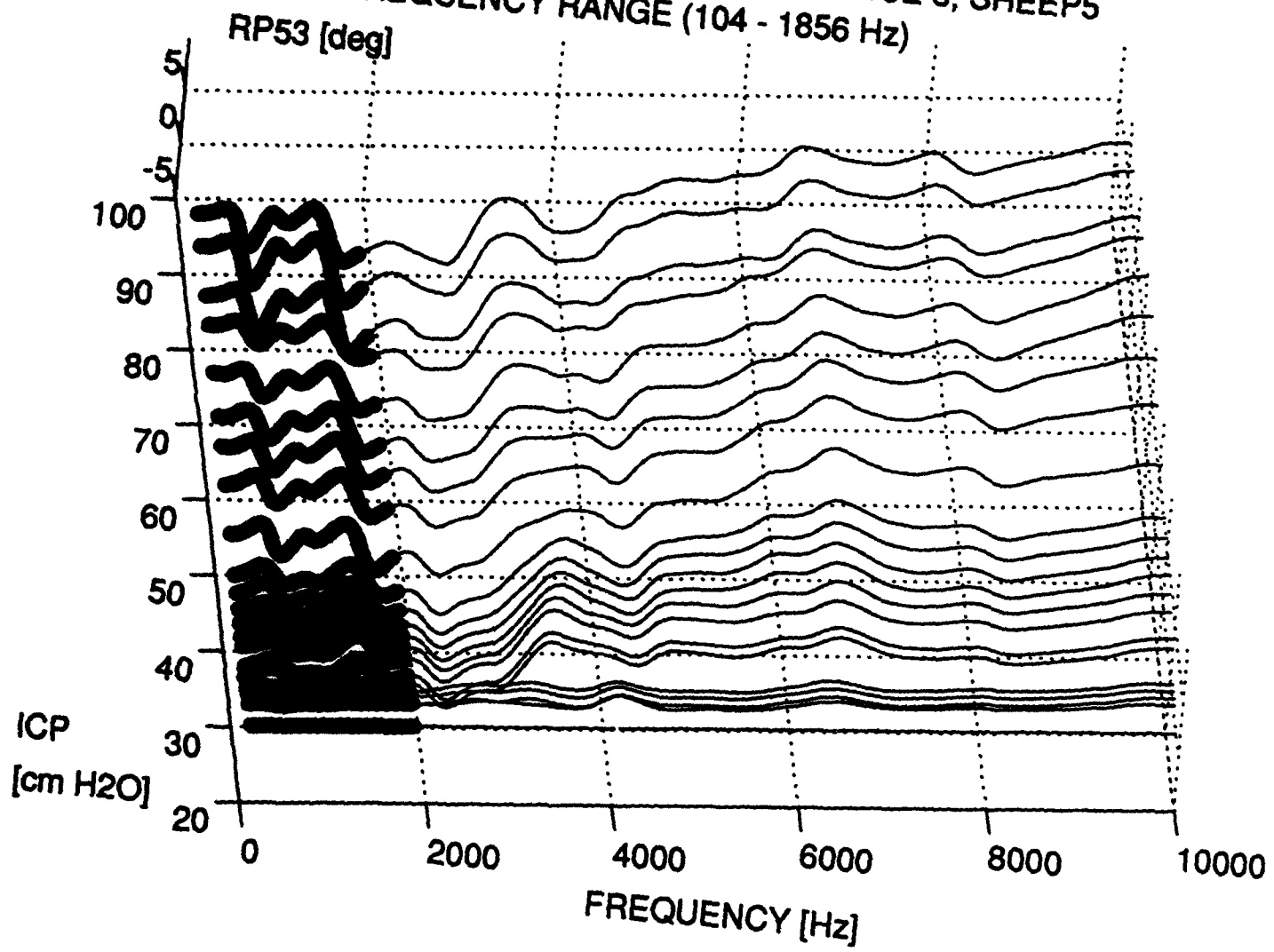PHASE STANDARD DEVIATION vs. ICP
SHEEP4: Pha.Rel.DP.   FREQUENCY RANGE (4416 - 6096 Hz)
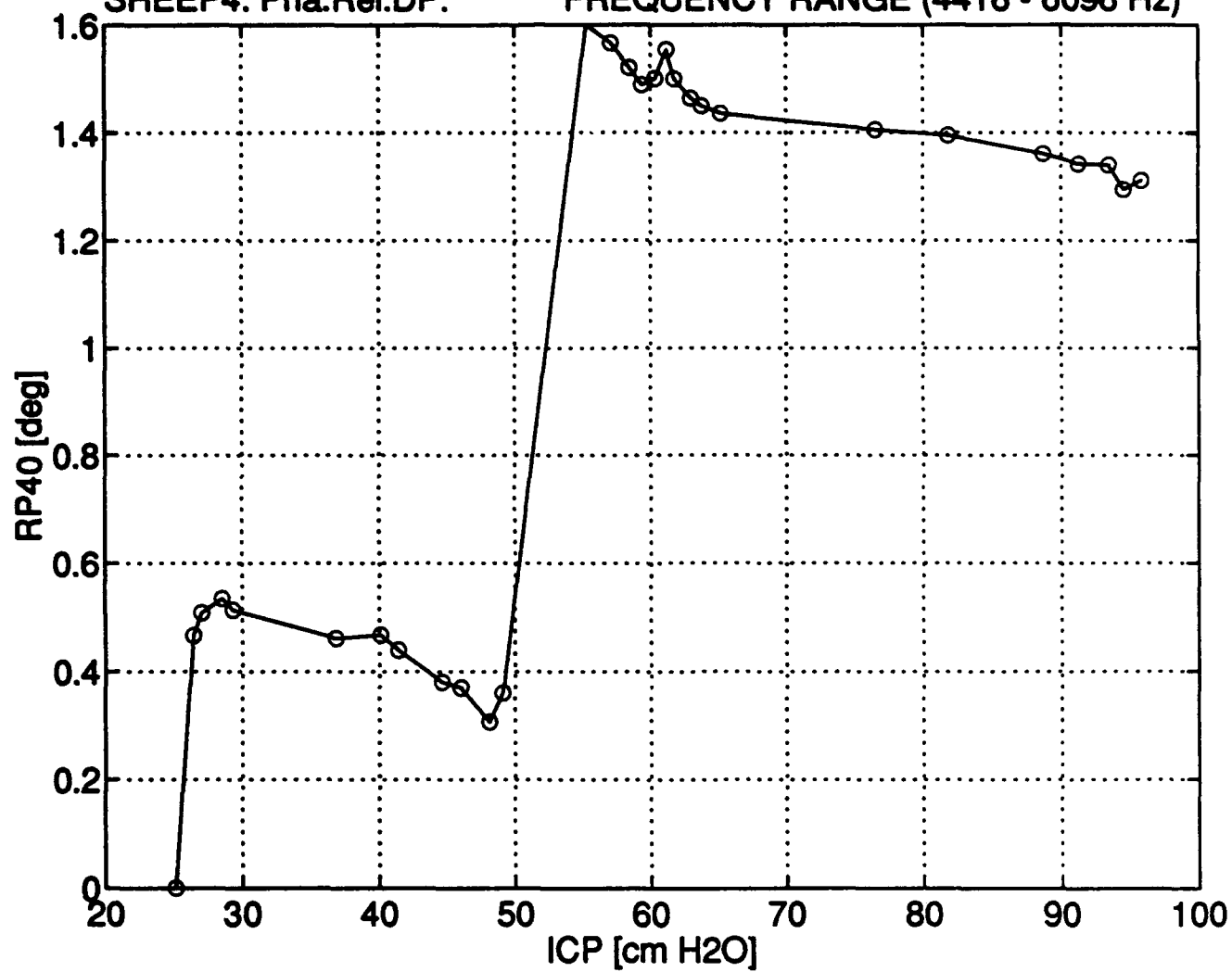
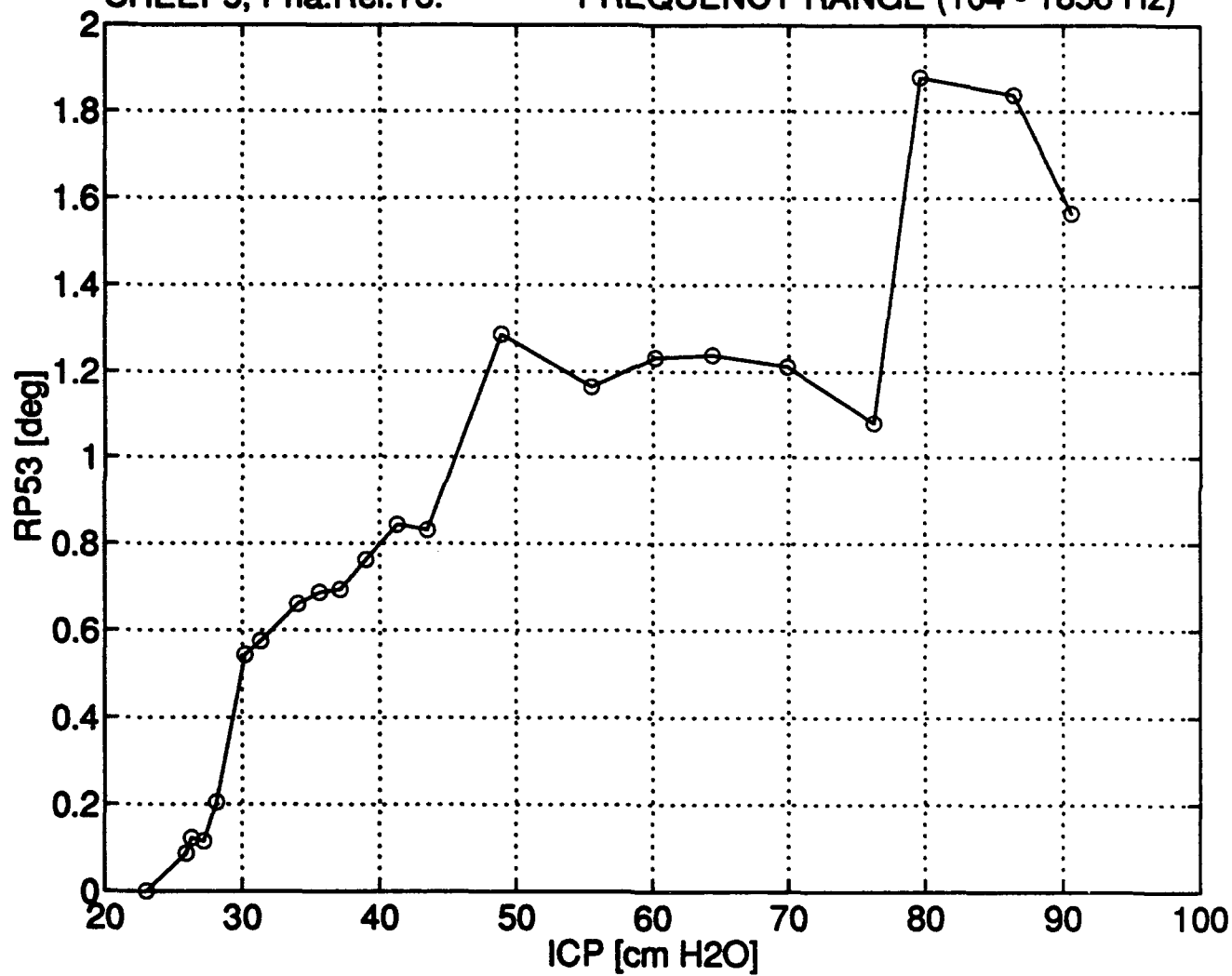PHASE OF RELATIVE TRANSFER IMPEDANCE 1, SHEEP4
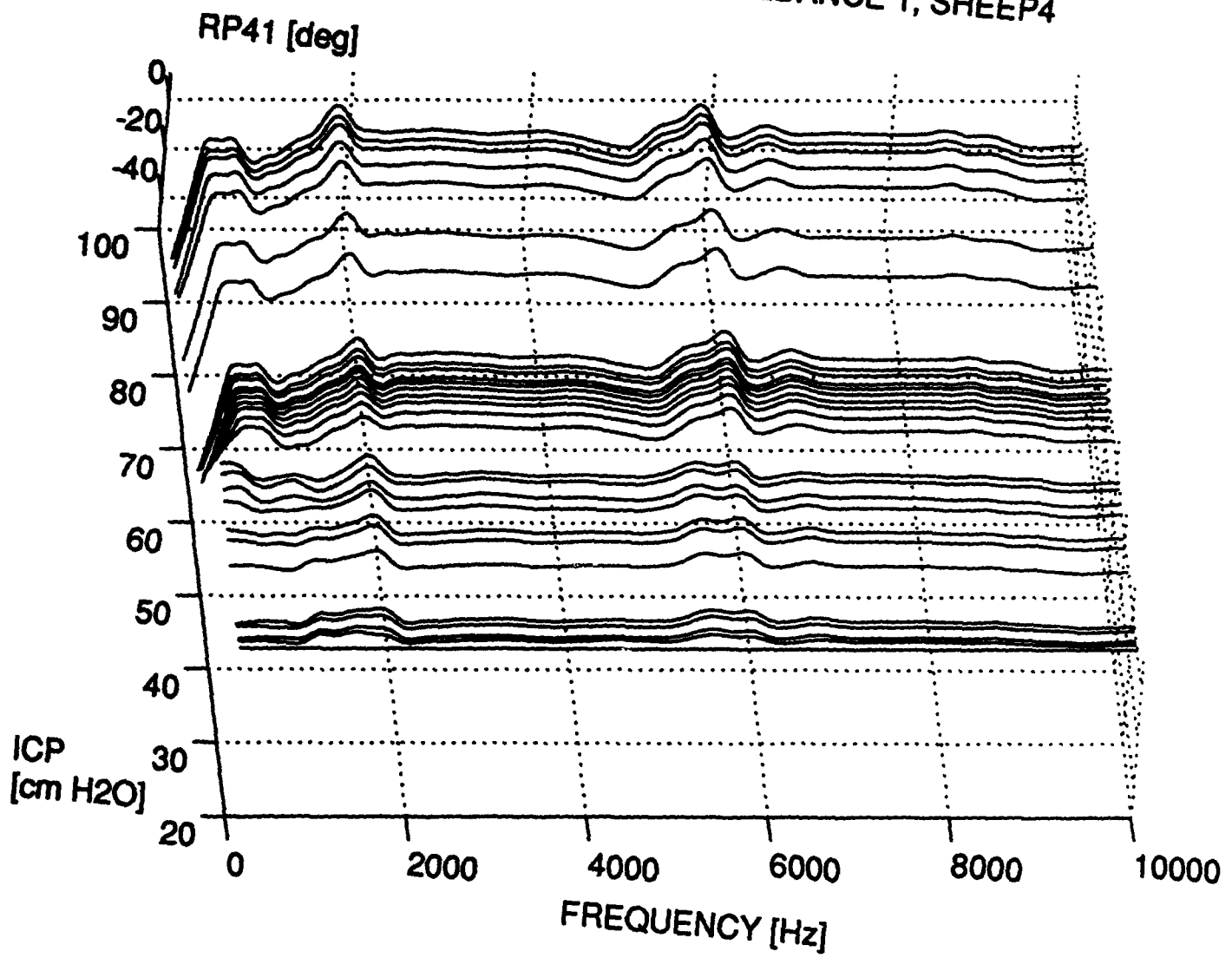
PHASE OF RELATIVE TRANSFER IMPEDANCE 1, SHEEP4
FREQUENCY RANGE (104 - 2096 Hz)
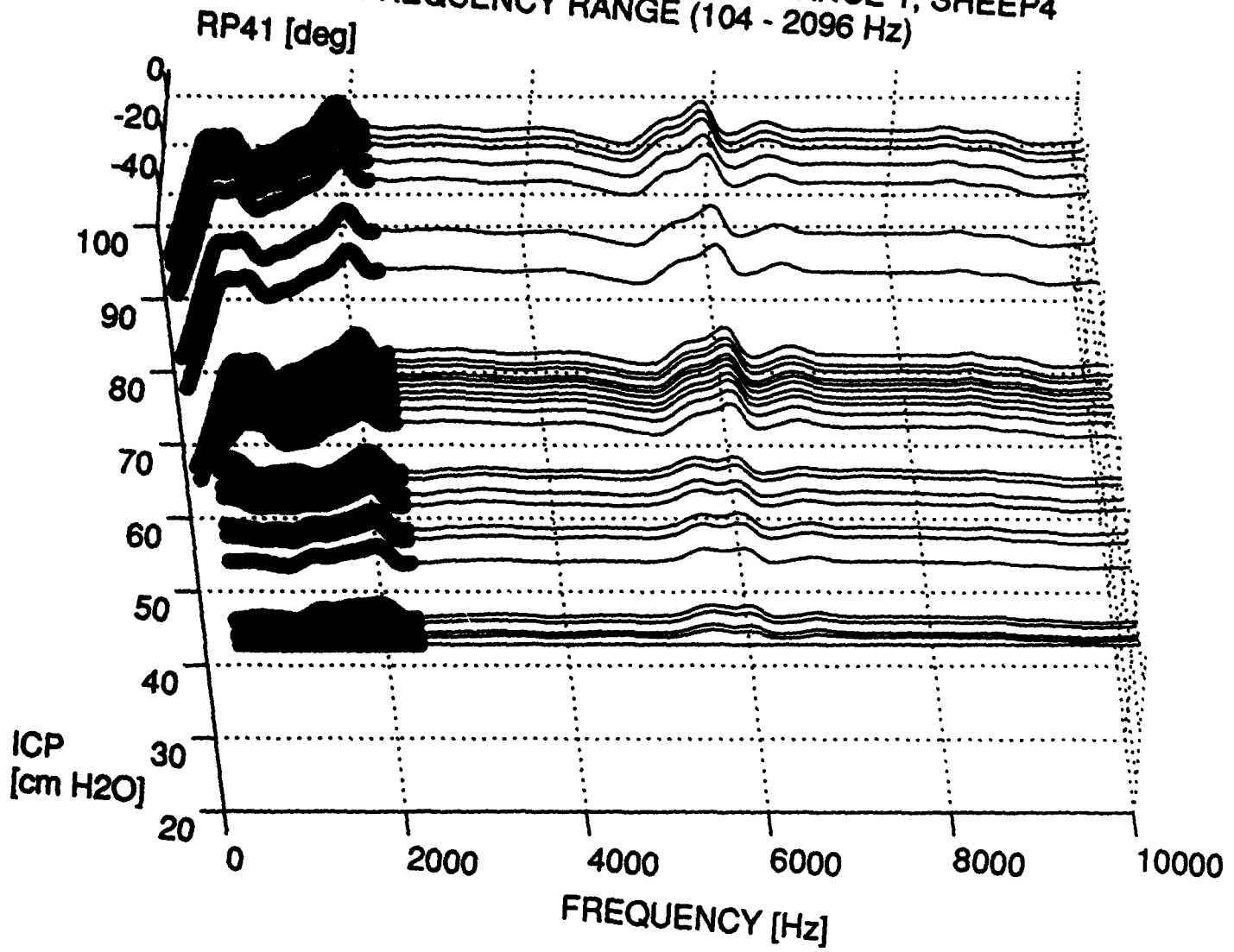
PHASE STANDARD DEVIATION vs. ICP
SHEEP4: Pha.Rel.T1.   FREQUENCY RANGE (104 - 2096 Hz)
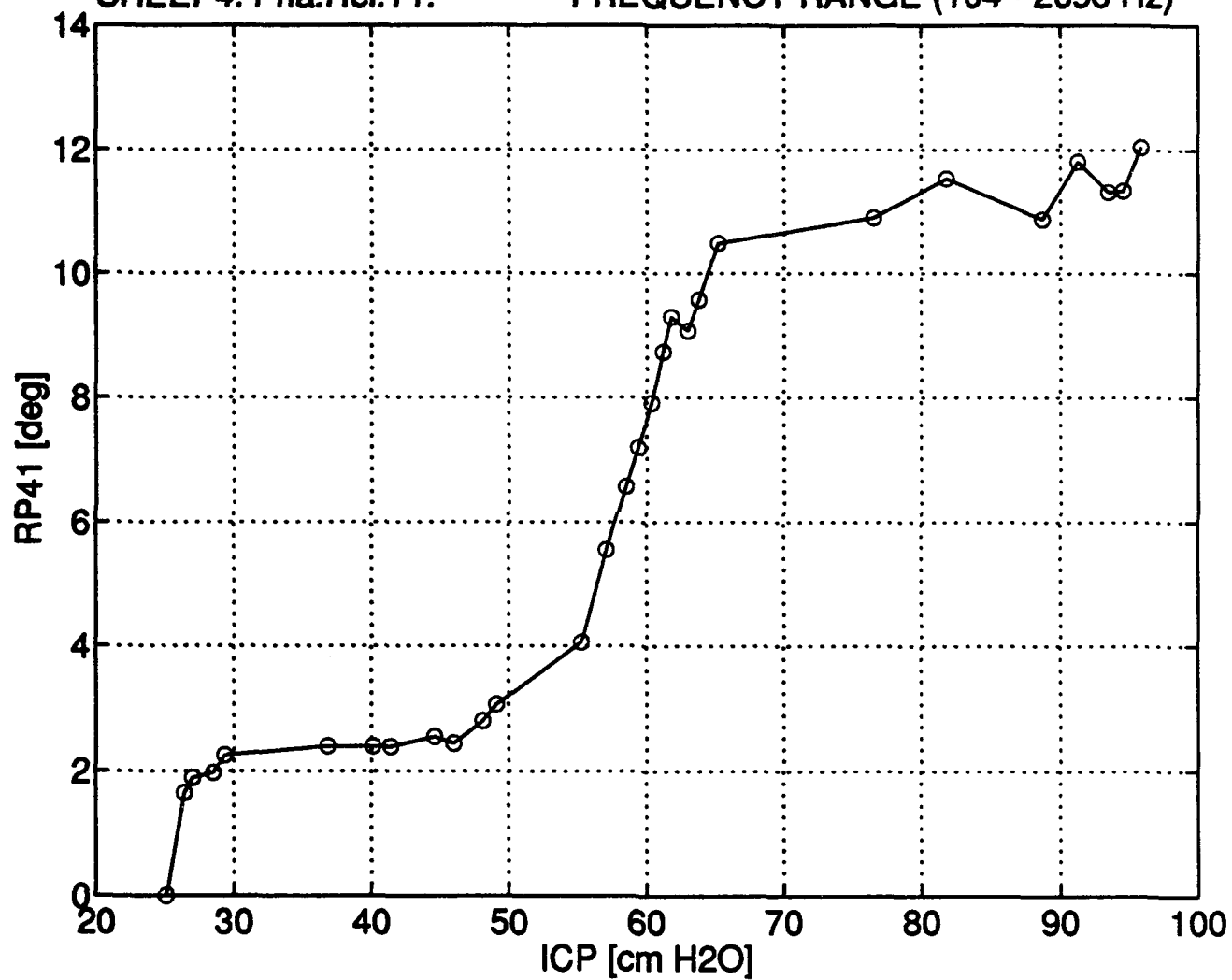
PHASE OF RELATIVE TRANSFER IMPEDANCE 1, SHEEP4
FREQUENCY RANGE (4896 - 6896 Hz)
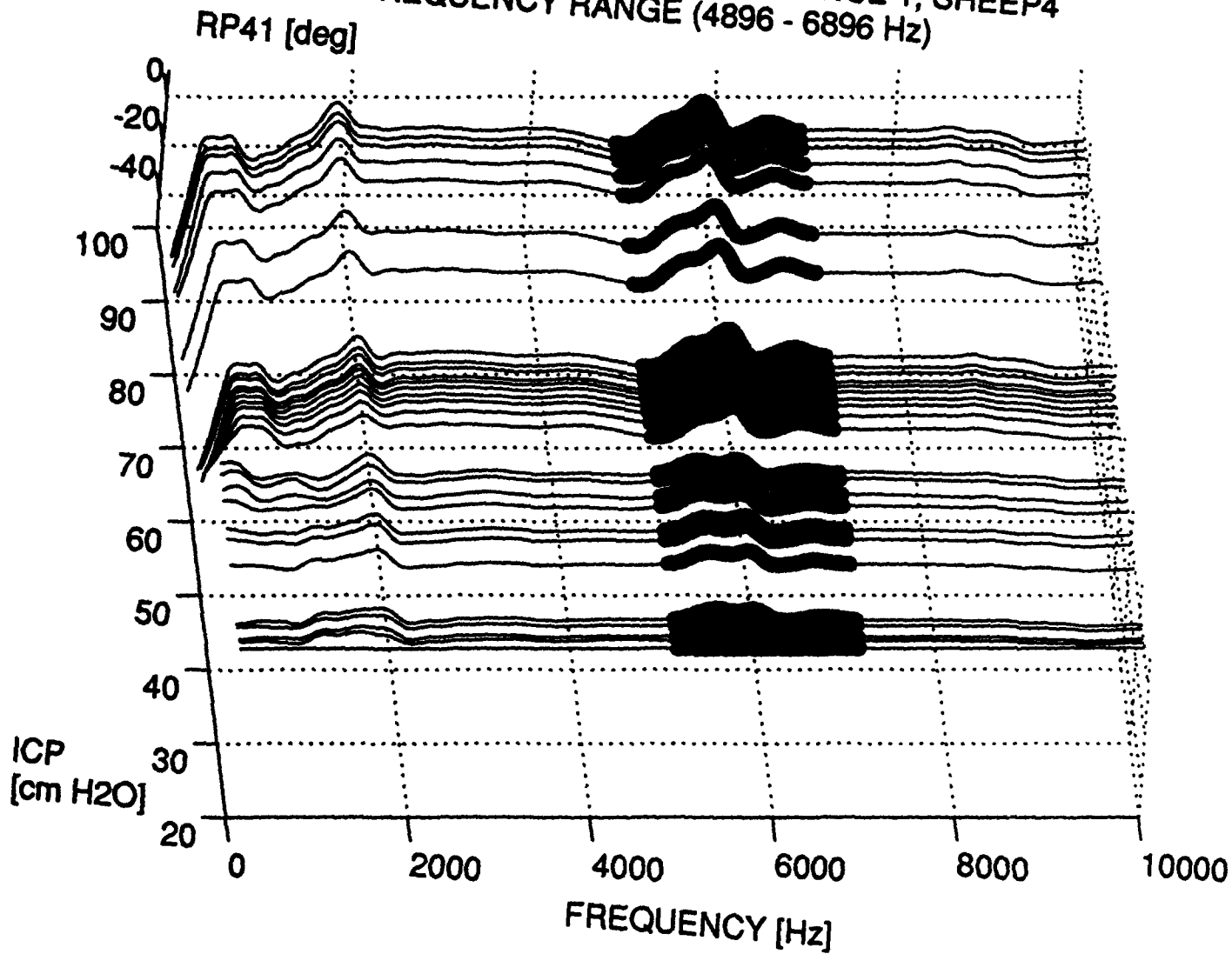
PHASE STANDARD DEVIATION vs. ICP
SHEEP4: Pha.Rel.T1.   FREQUENCY RANGE (4896 - 6896 Hz)
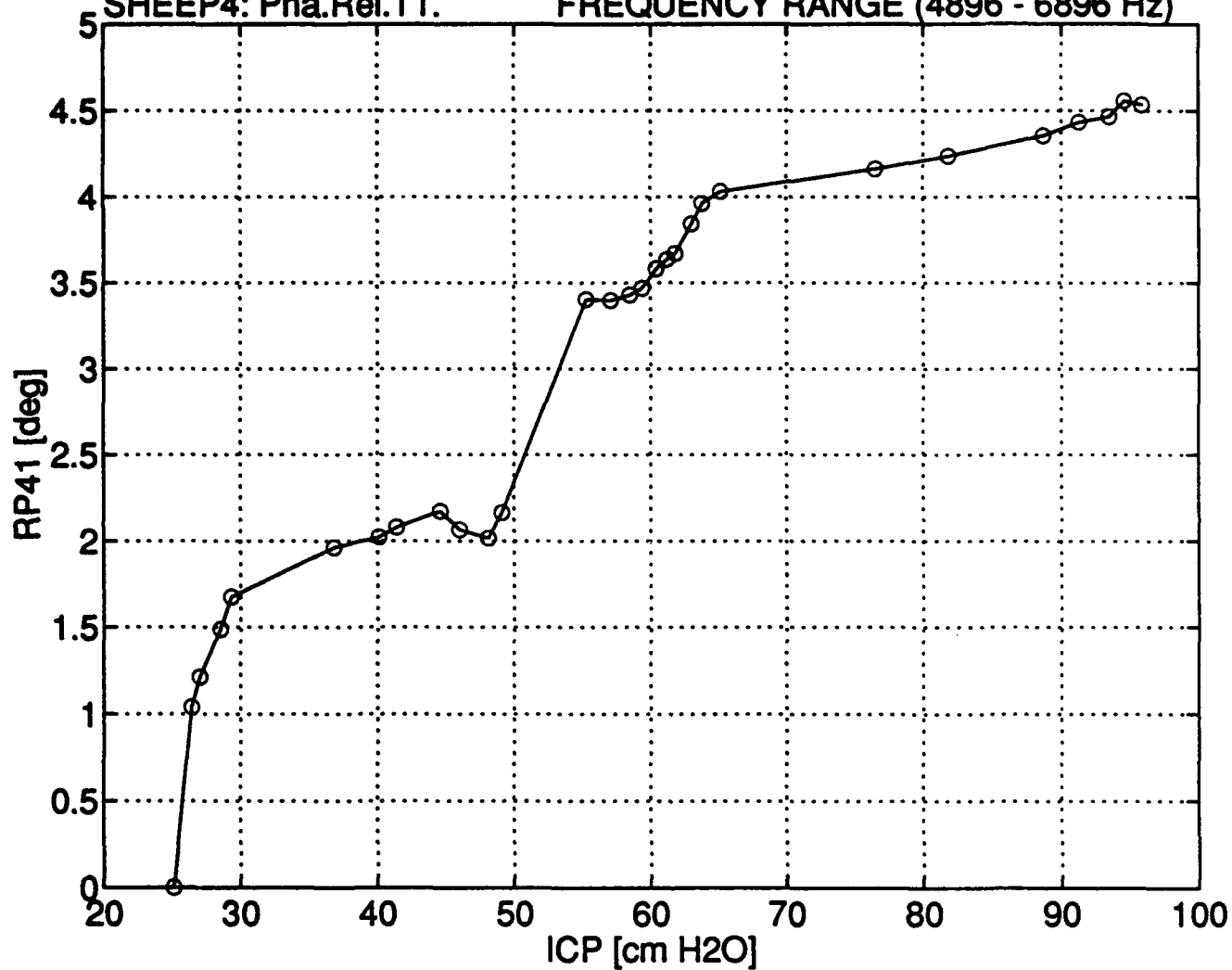
PHASE OF RELATIVE TRANSFER IMPEDANCE 2, SHEEP4
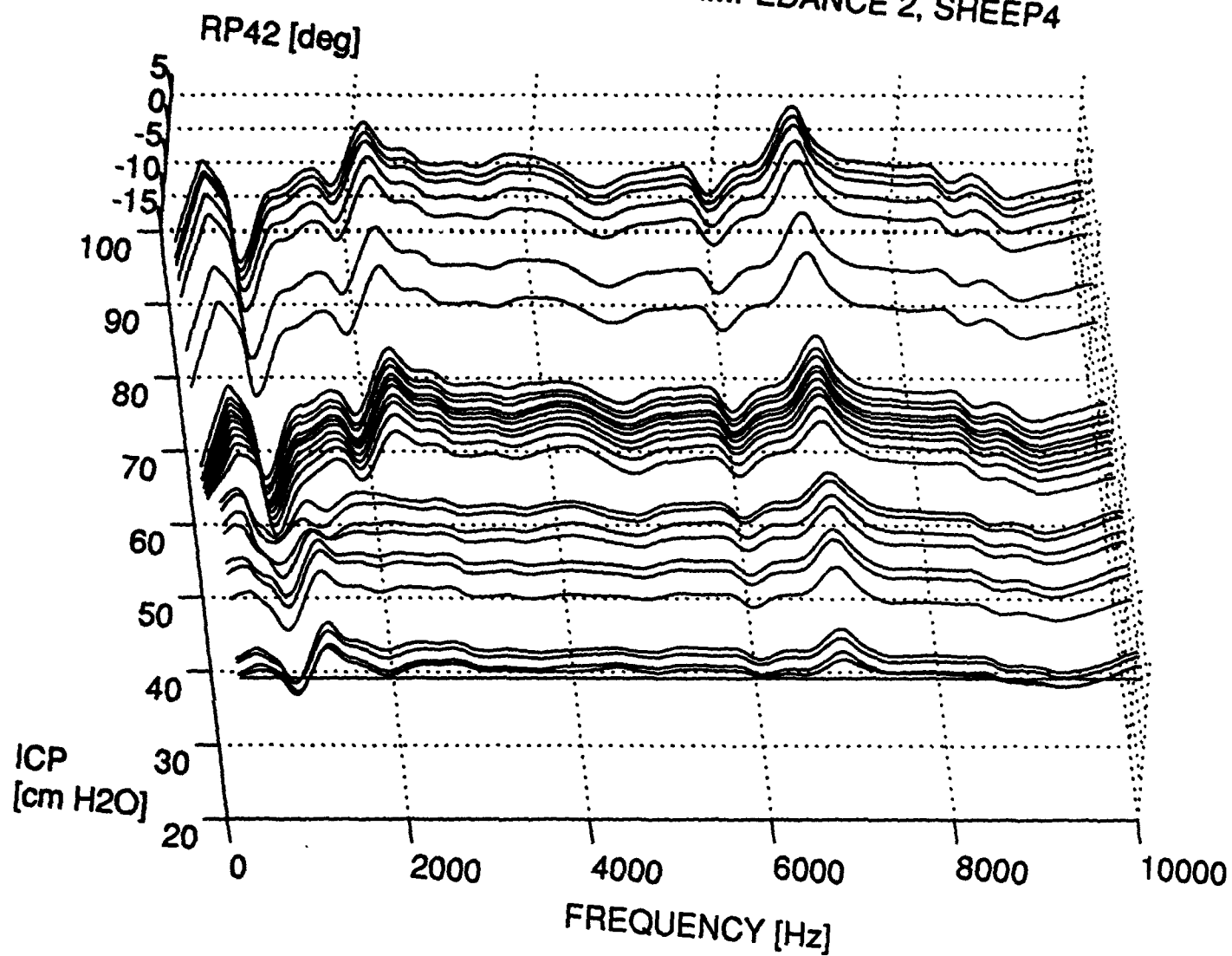
PHASE OF RELATIVE TRANSFER IMPEDANCE 2, SHEEP4
FREQUENCY RANGE (104 - 816 Hz)
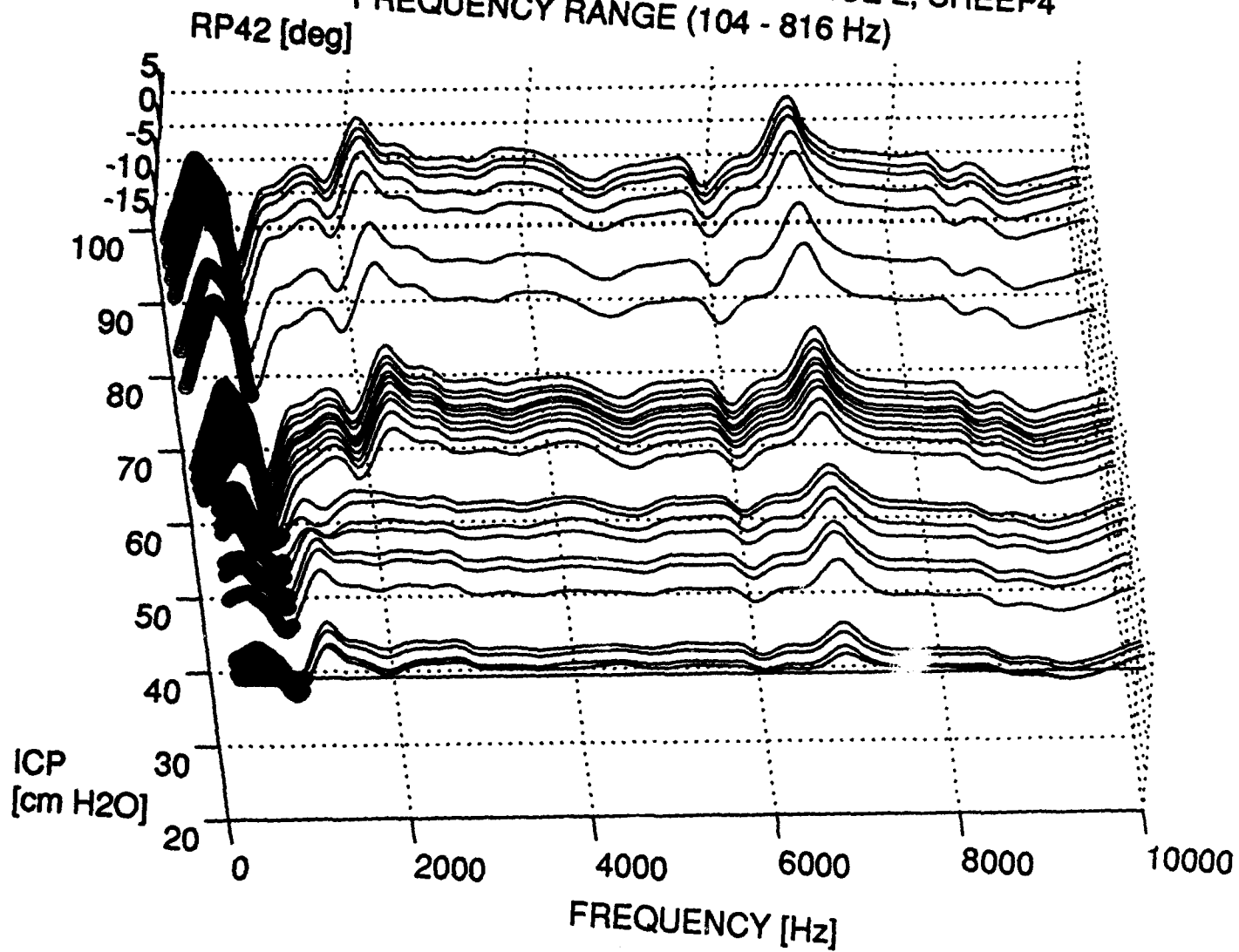
PHASE STANDARD DEVIATION vs. ICP
SHEEP4: Pha.Rel.T2.   FREQUENCY RANGE (104 - 816 Hz)
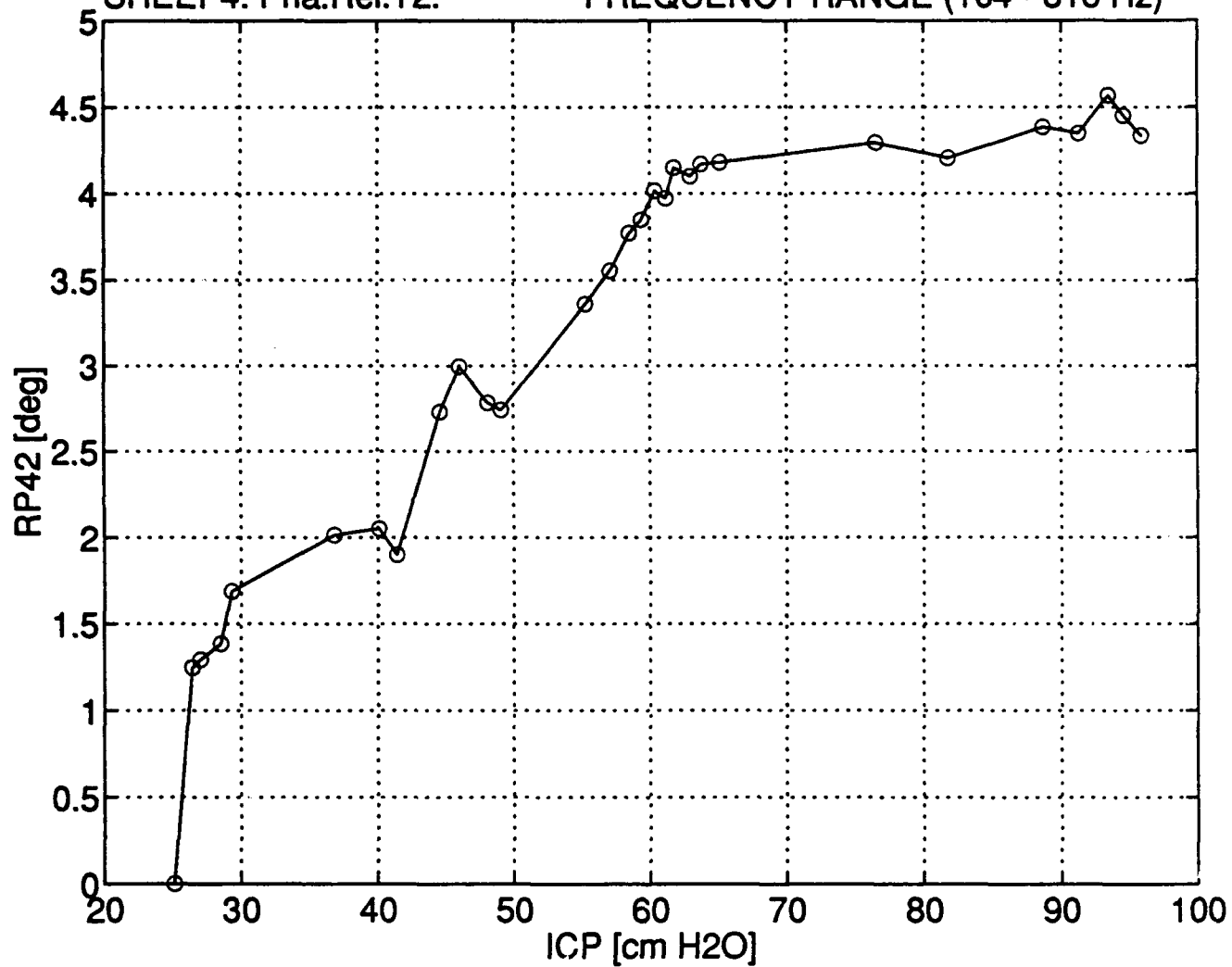
PHASE OF RELATIVE TRANSFER IMPEDANCE 2, SHEEP4
FREQUENCY RANGE (816 - 1776 Hz)
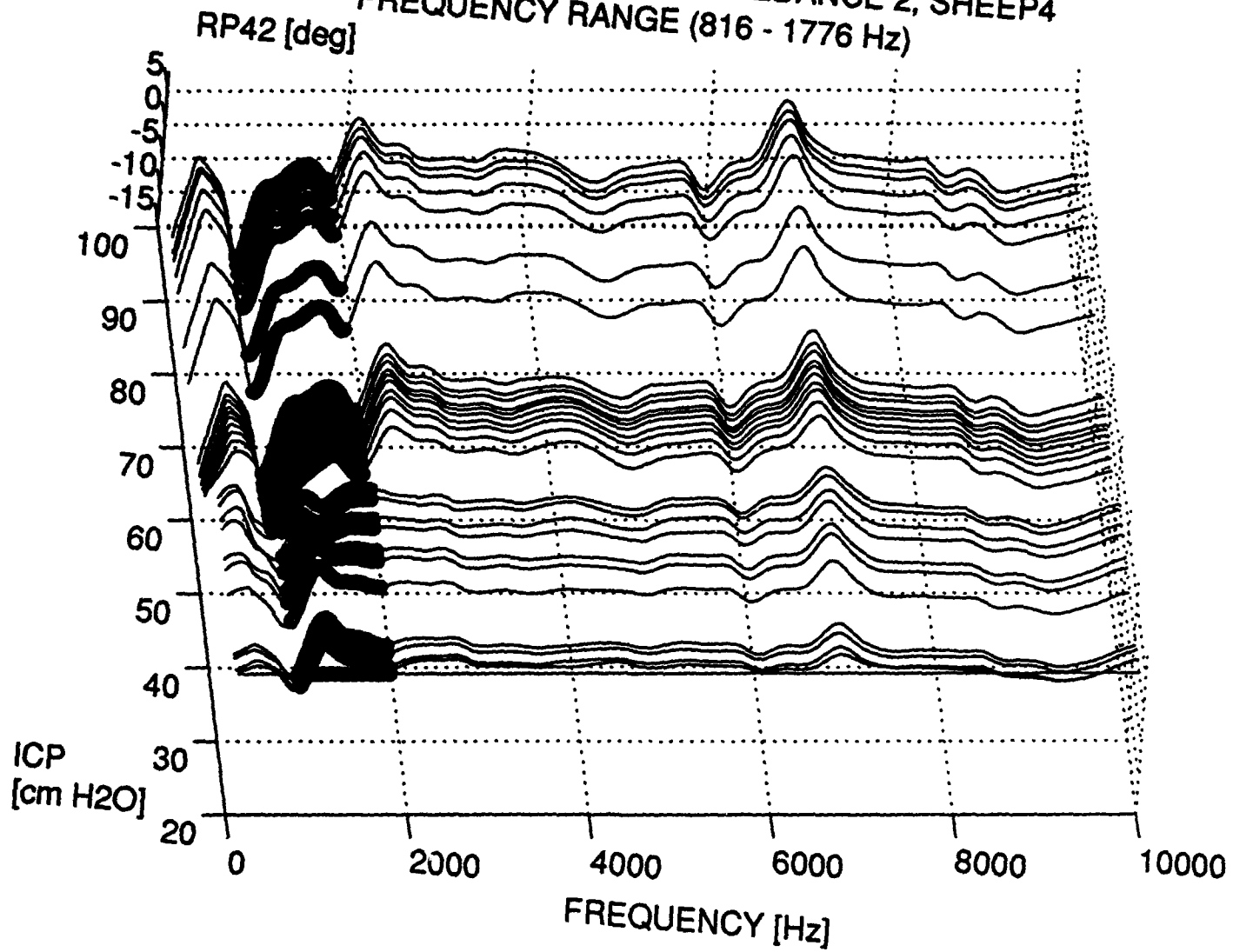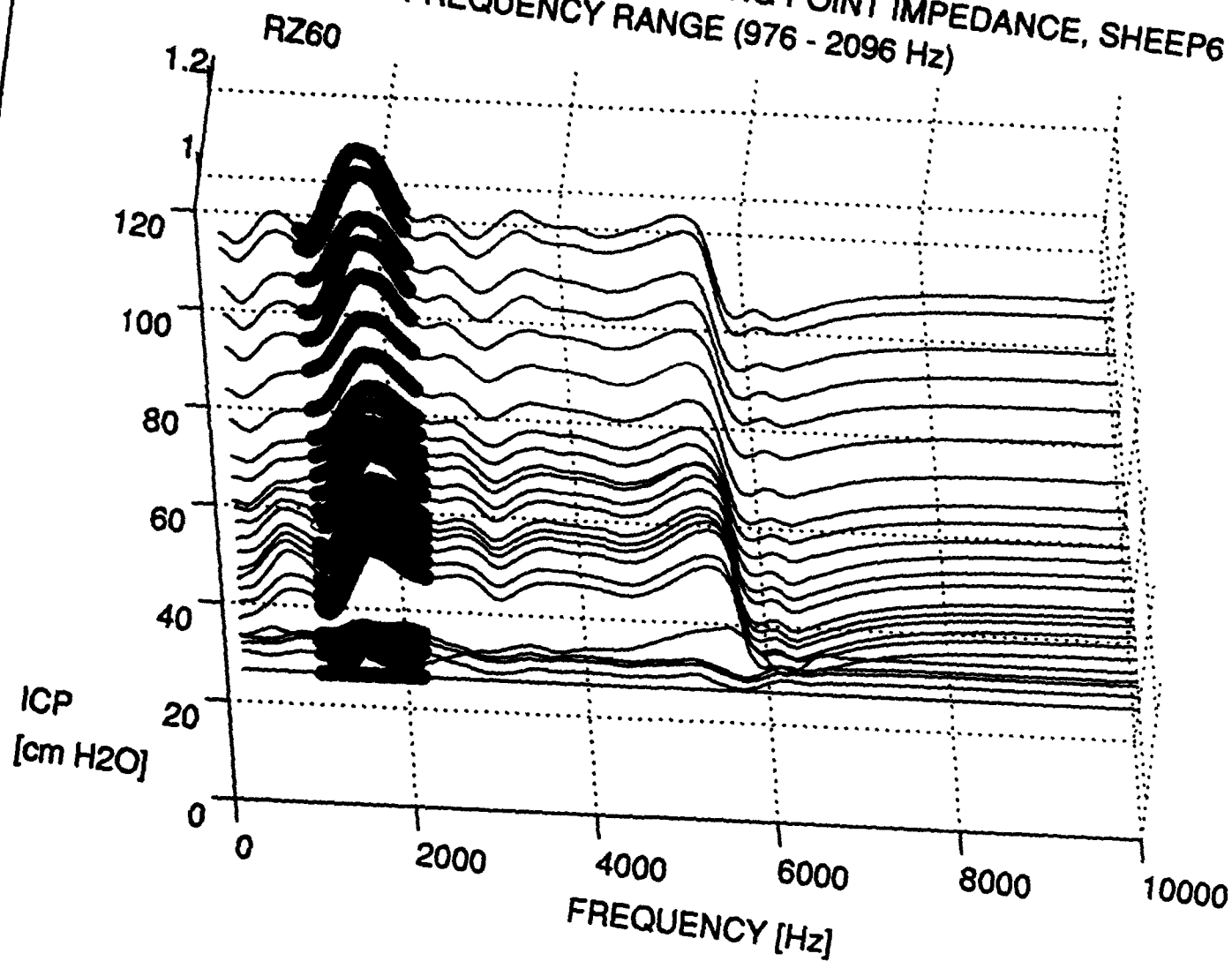
PHASE STANDARD DEVIATION vs. ICP
SHEEP4: Pha.Rel.T2.   FREQUENCY RANGE (816 - 1776 Hz)
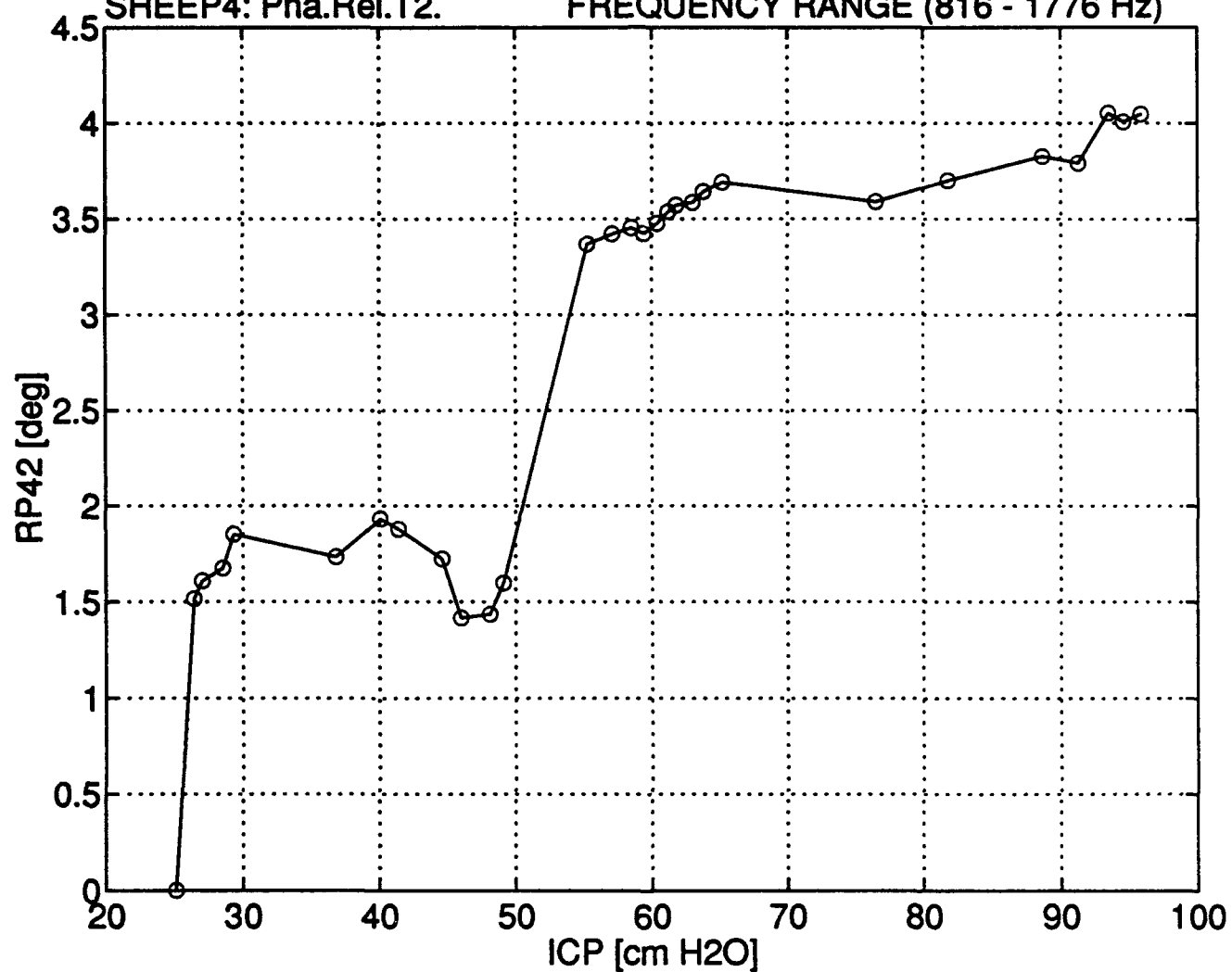
PHASE OF RELATIVE TRANSFER IMPEDANCE 2, SHEEP4
FREQUENCY RANGE (1776 - 2896 Hz)
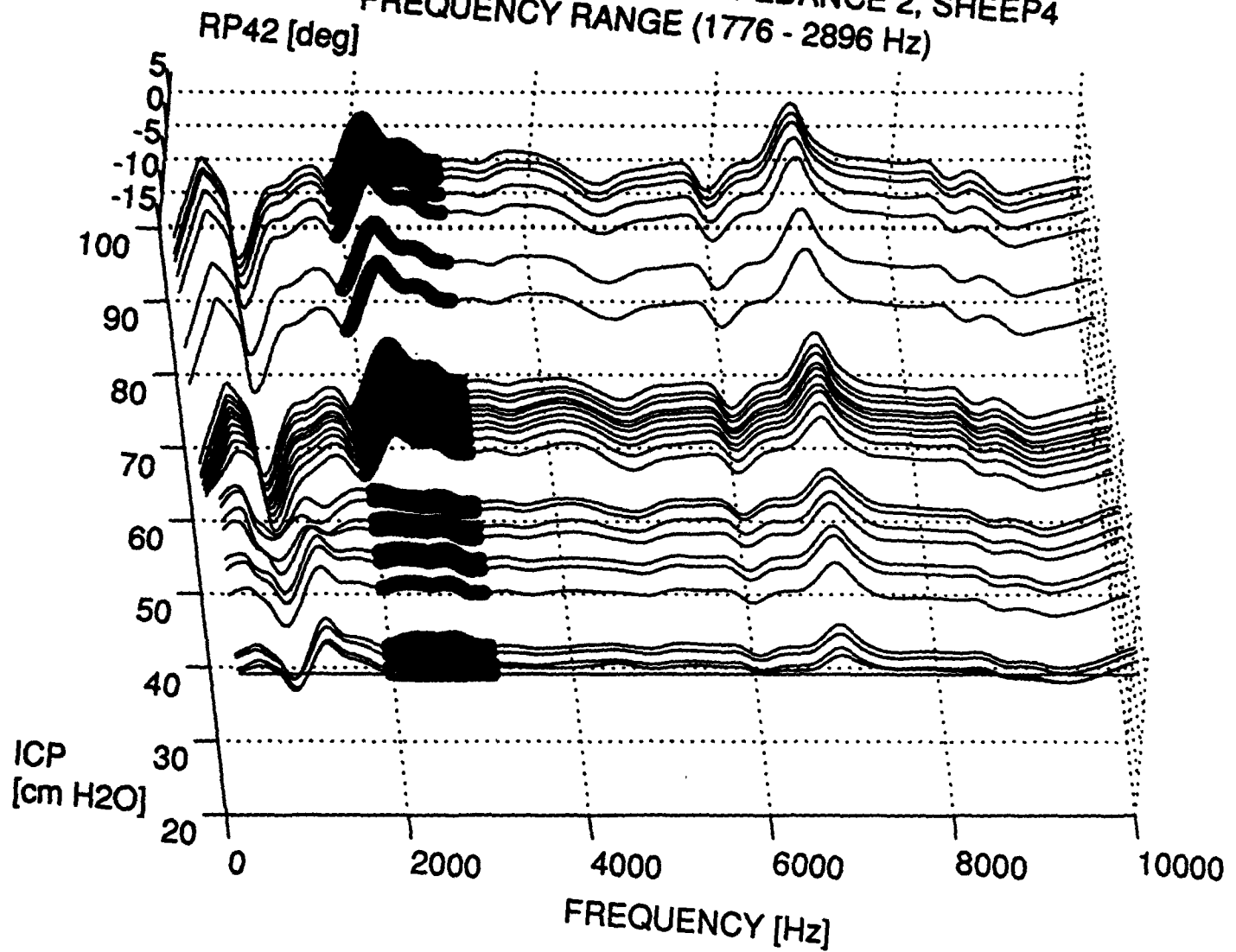
PHASE STANDARD DEVIATION vs. ICP
SHEEP4: Pha.Rel.T2.   FREQUENCY RANGE (1776 - 2896 Hz)
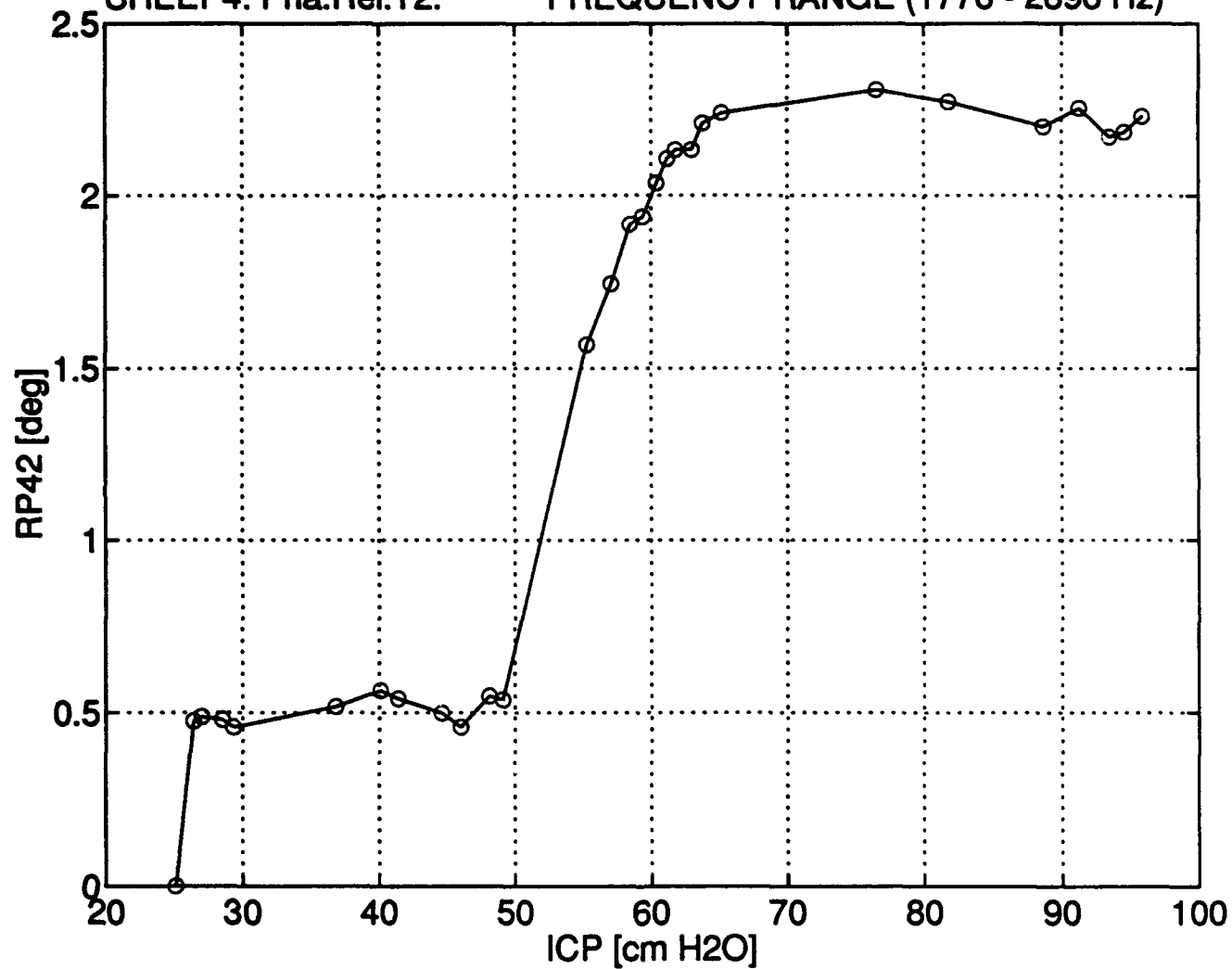
PHASE OF RELATIVE TRANSFER IMPEDANCE 2, SHEEP4
FREQUENCY RANGE (5536 - 7696 Hz)

RP42 [deg]

ICP
[cm H2O]
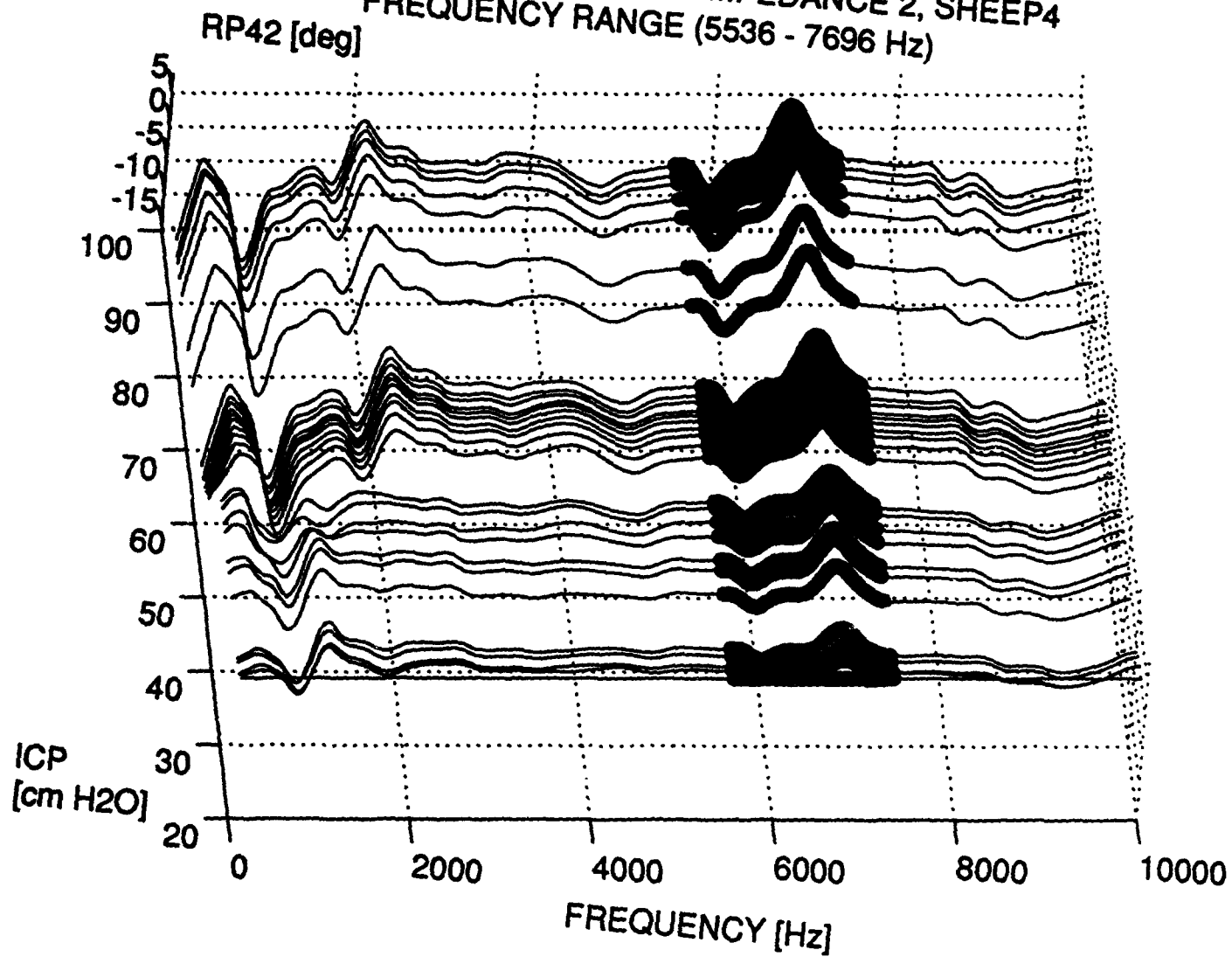
FREQUENCY [Hz]

PHASE STANDARD DEVIATION vs. ICP
SHEEP4: Pha.Rel.T2.   FREQUENCY RANGE (5536 - 7696 Hz)
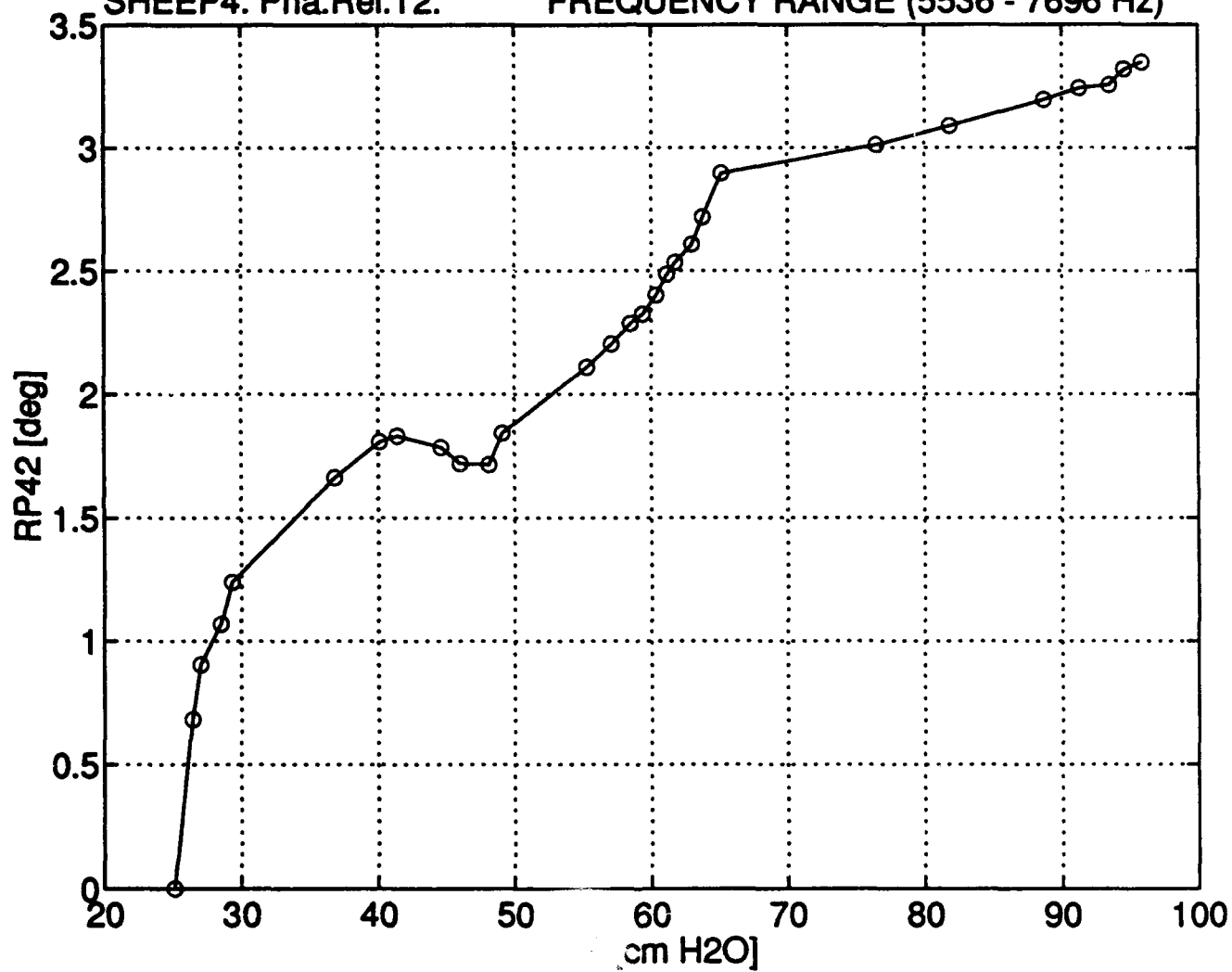
PHASE OF RELATIVE TRANSFER IMPEDANCE 3, SHEEP4
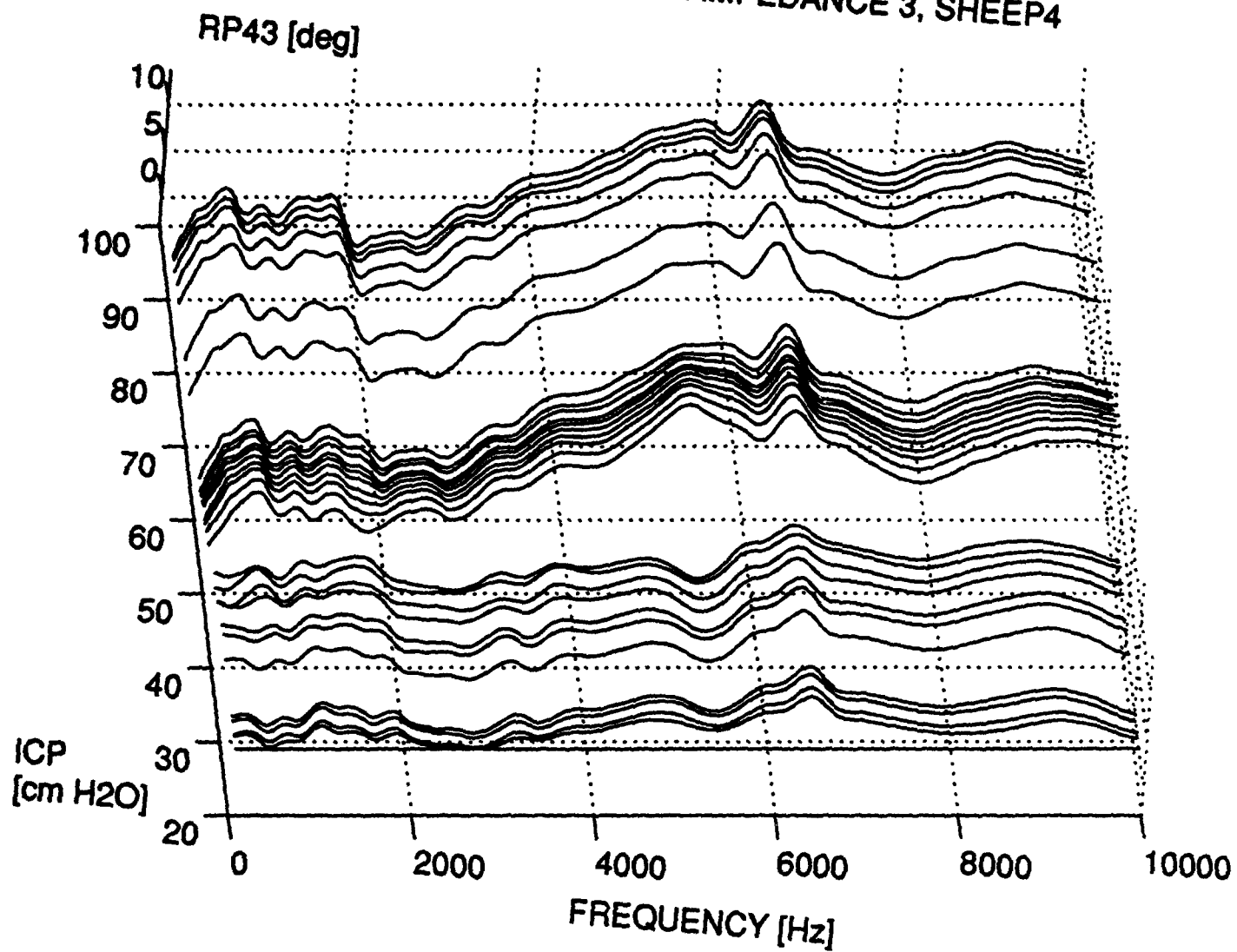
PHASE OF RELATIVE TRANSFER IMPEDANCE 3, SHEEP4
FREQUENCY RANGE (104 - 2096 Hz)
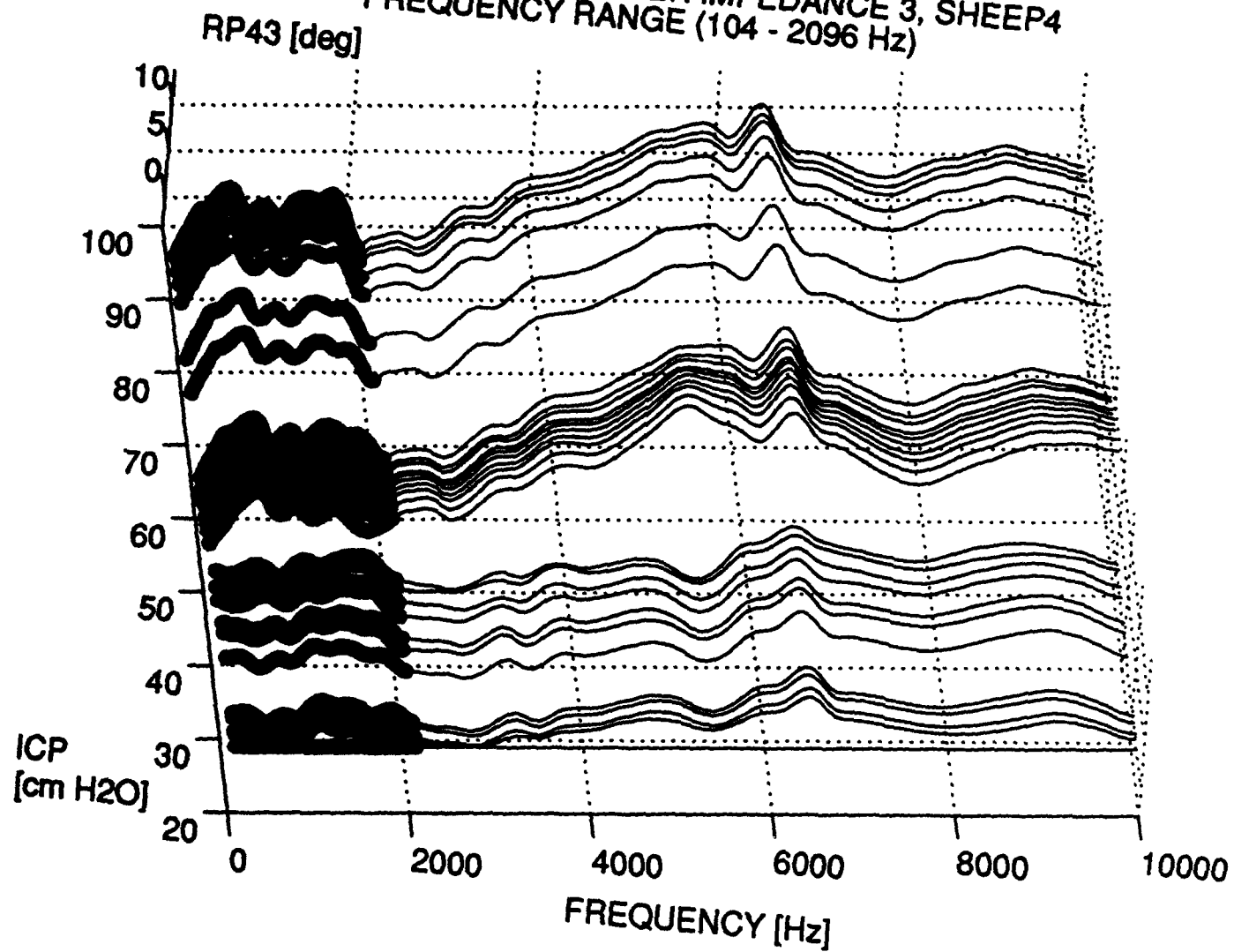
PHASE STANDARD DEVIATION vs. ICP
SHEEP4: Pha.Rel.T3.   FREQUENCY RANGE (104 - 2096 Hz)

PHASE OF RELATIVE TRANSFER IMPEDANCE 3, SHEEP4
FREQUENCY RANGE (4096 - 6896 Hz)

RP43 [deg]

ICP
[cm H2O]
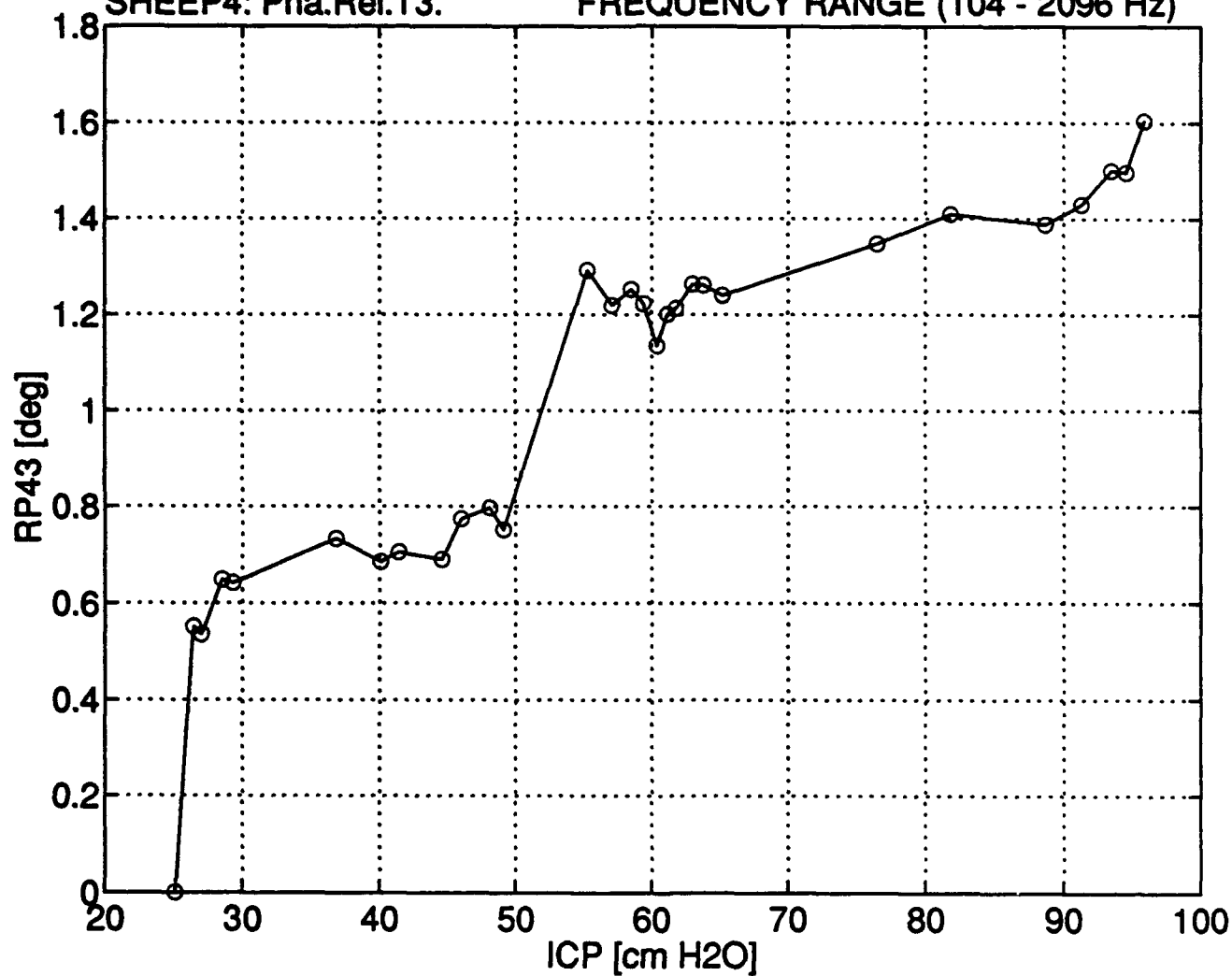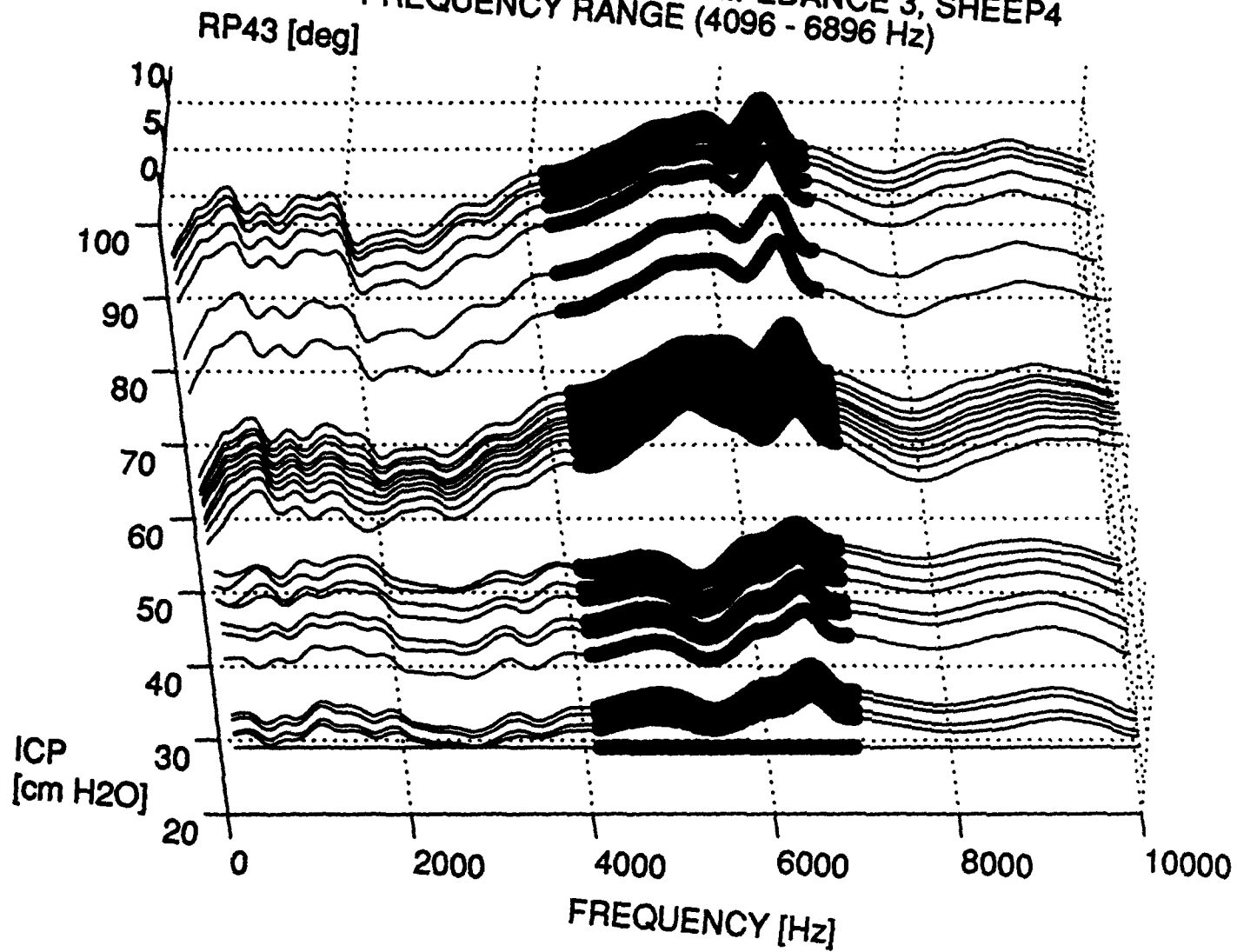
FREQUENCY [Hz]

PHASE STANDARD DEVIATION vs. ICP

SHEEP4: Pha.Rel.T3.   FREQUENCY RANGE (4096 - 6896 Hz)
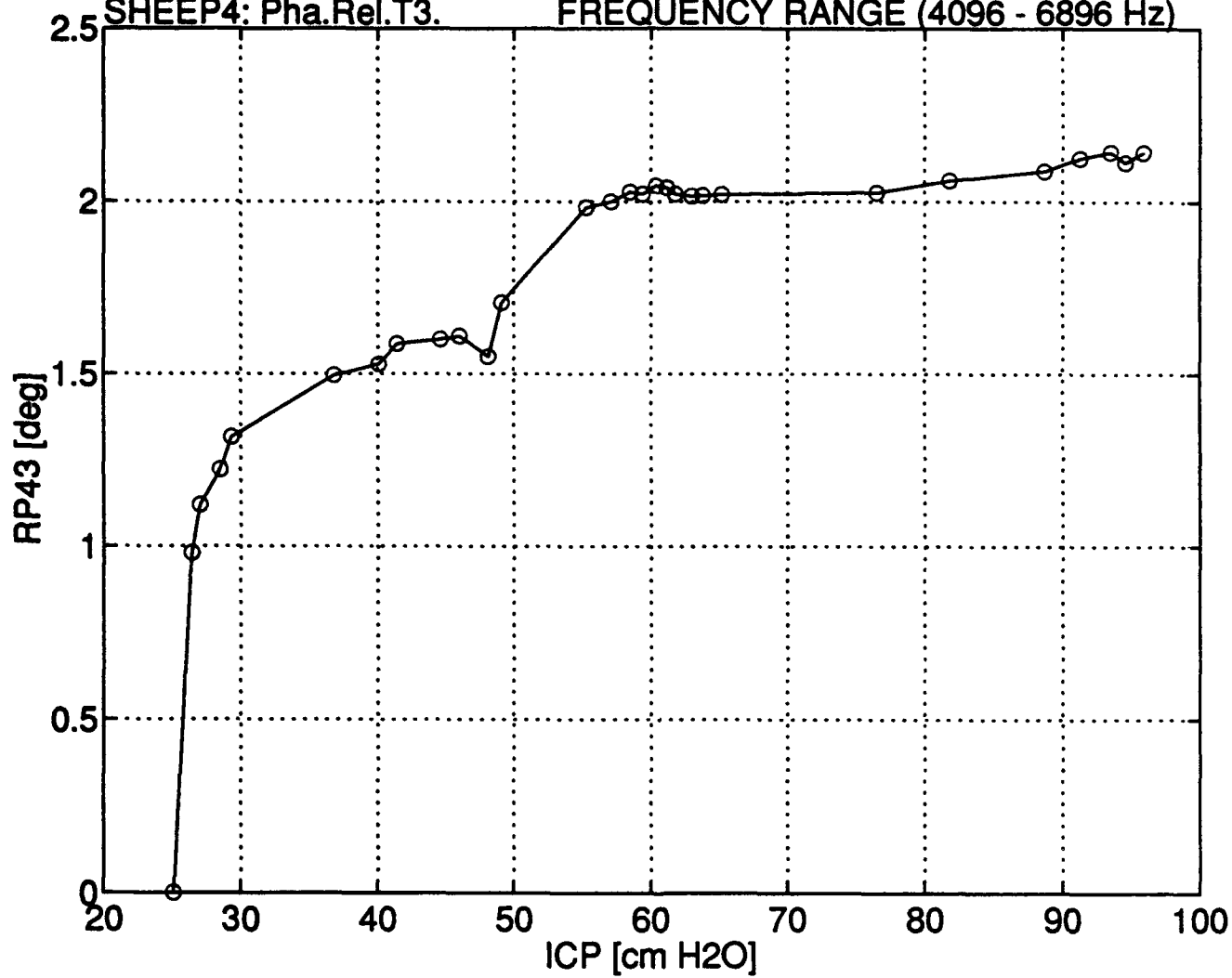
MAGNITUDE OF RELATIVE DRIVING POINT IMPEDANCE, SHEEP5
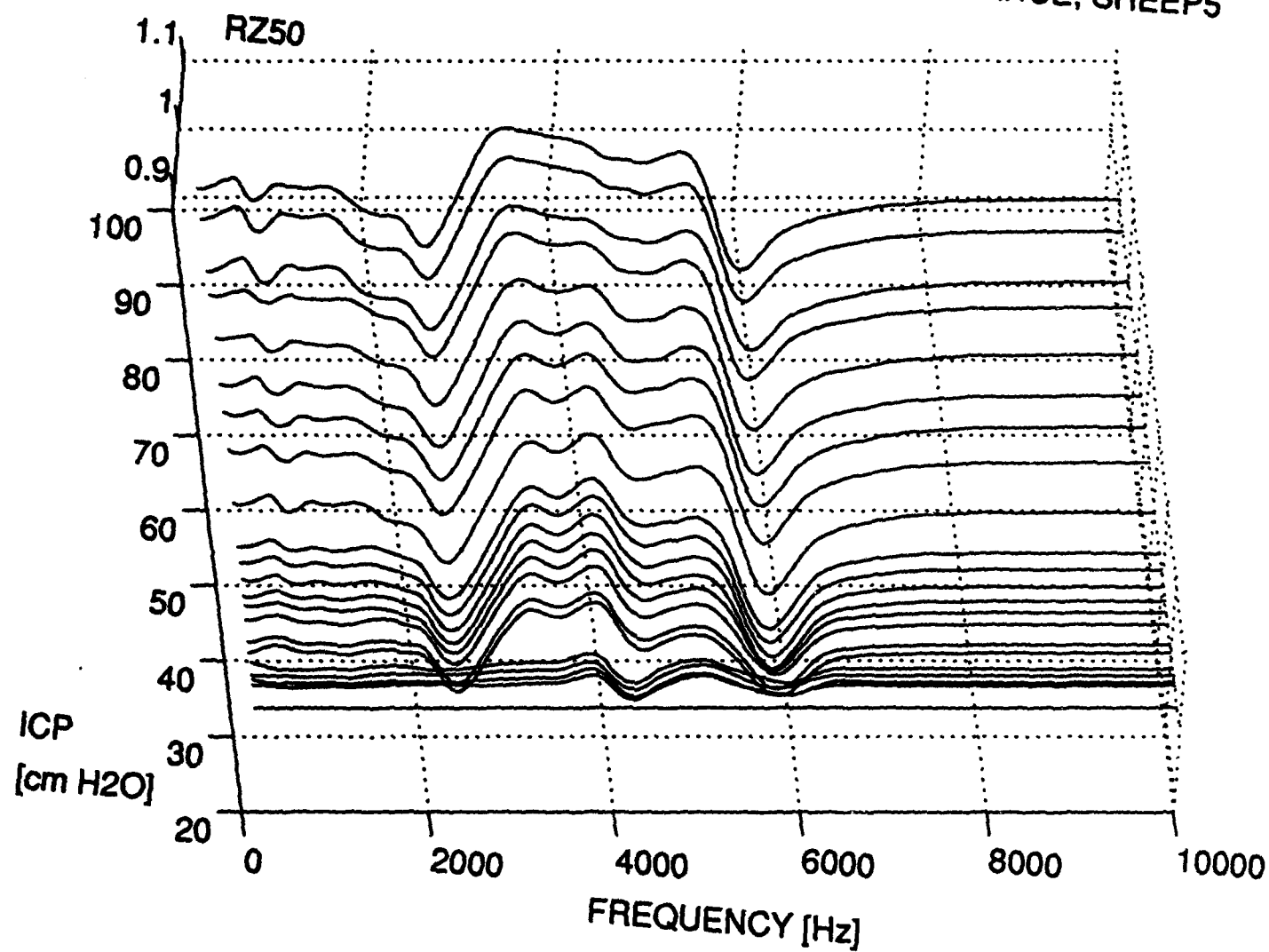
MAGNITUDE OF RELATIVE DRIVING POINT IMPEDANCE, SHEEP5
FREQUENCY RANGE (104 - 896 Hz)
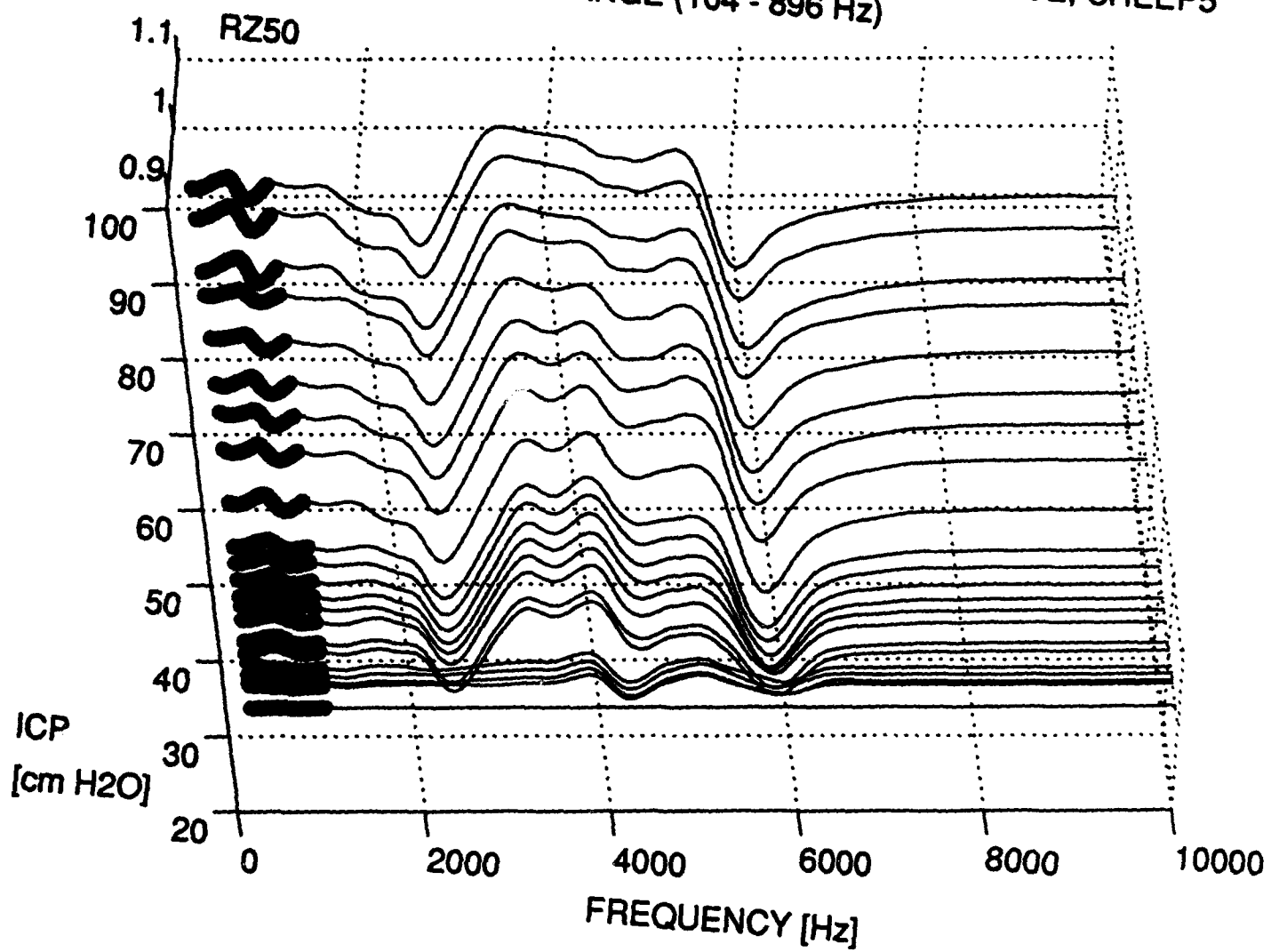
MAGNITUDE STANDARD DEVIATION vs. ICP
SHEEP5, Mag.Rel.DP.   FREQUENCY RANGE (104 - 896 Hz)
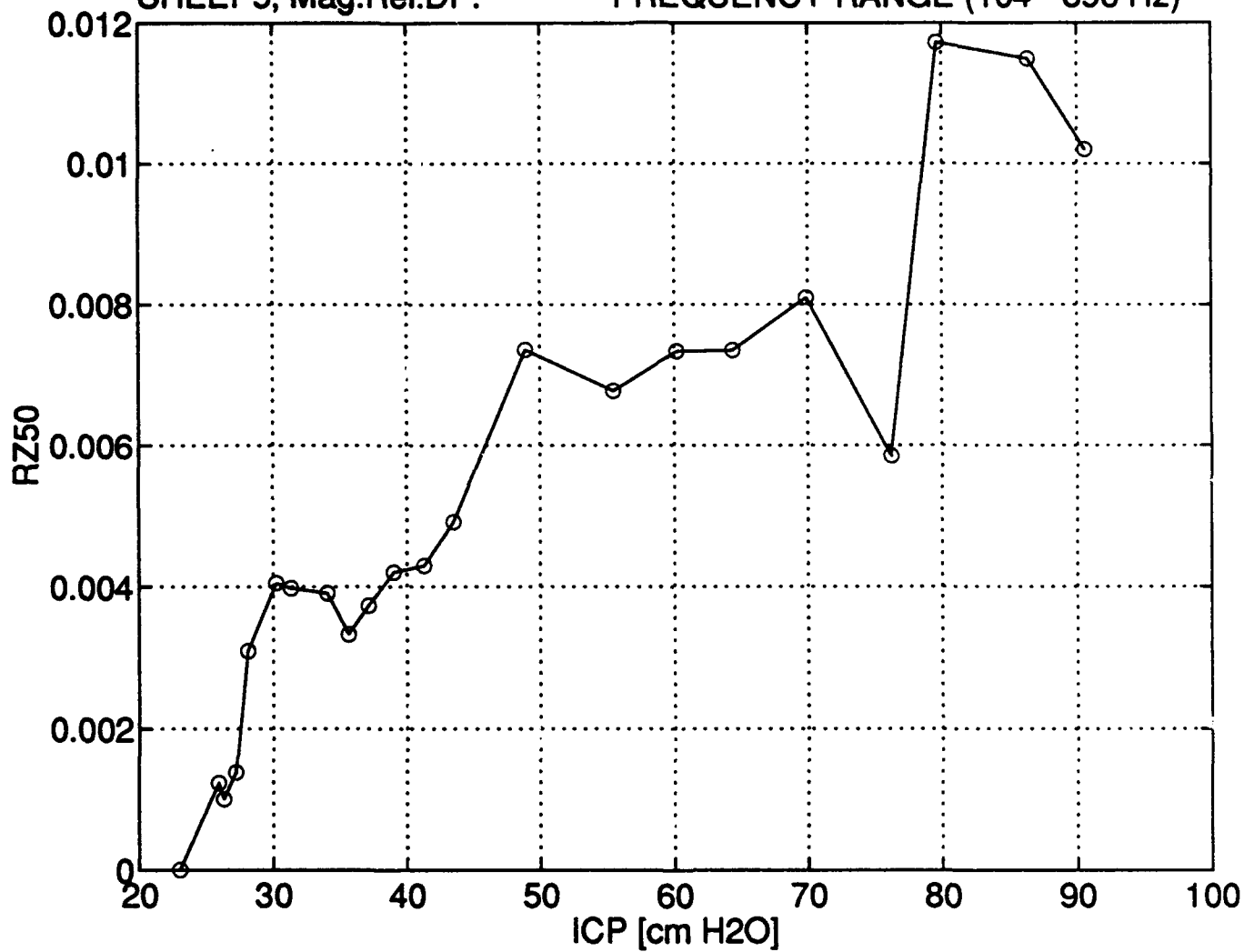
MAGNITUDE OF RELATIVE DRIVING POINT IMPEDANCE, SHEEP5
FREQUENCY RANGE (2096 - 3456 Hz)
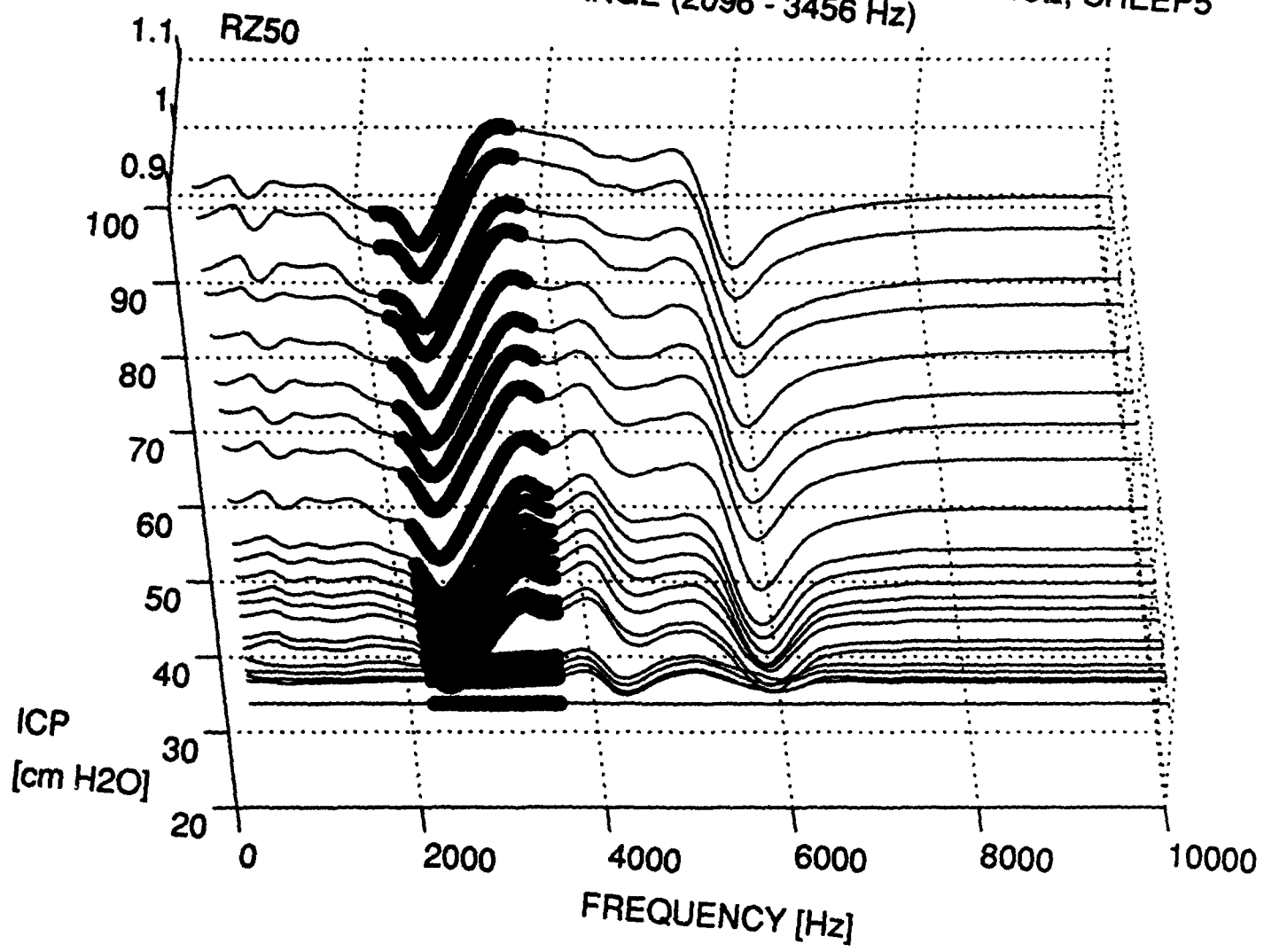
MAGNITUDE STANDARD DEVIATION vs. ICP
SHEEP5, Mag.Rel.DP.   FREQUENCY RANGE (2096 - 3456 Hz)
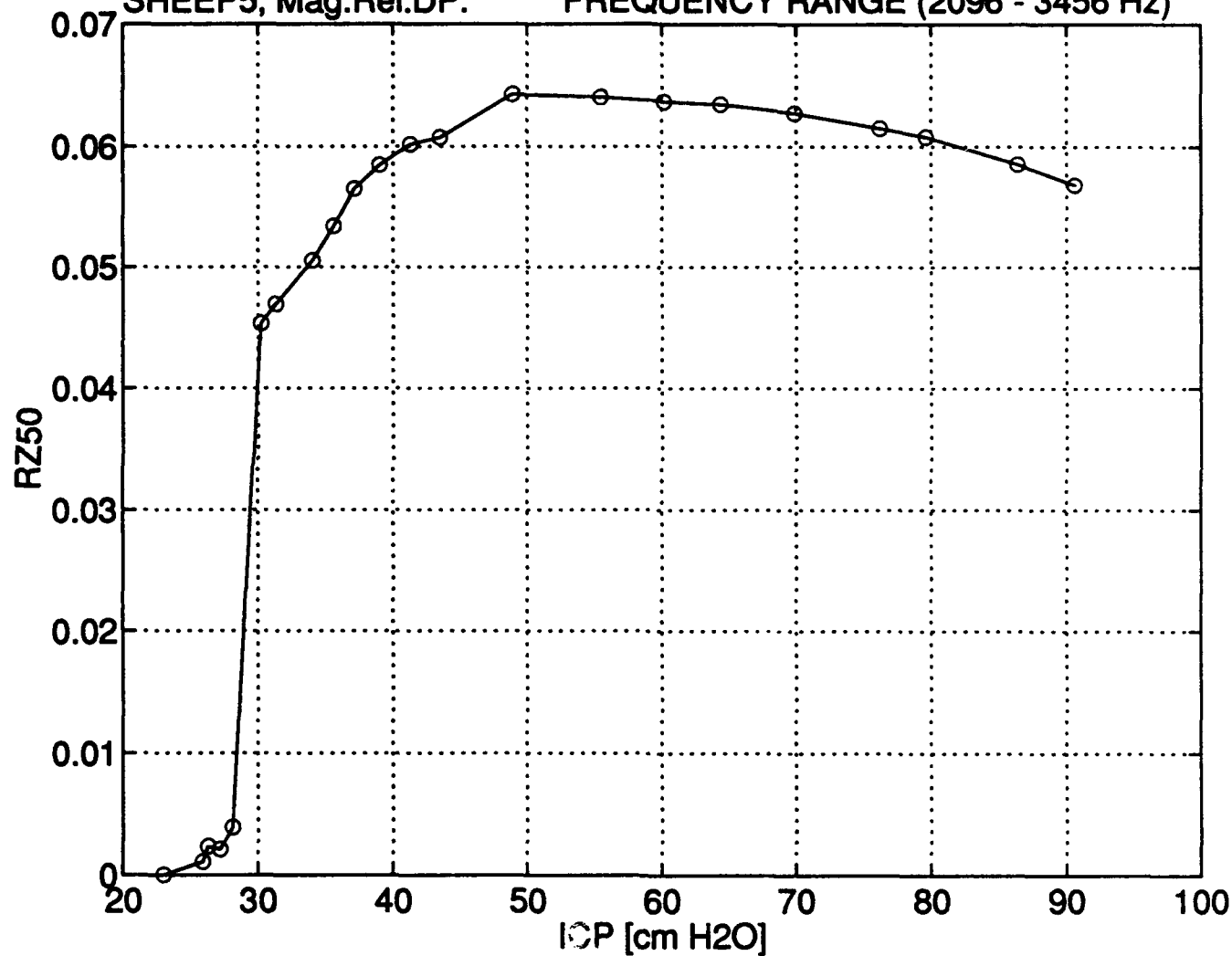
MAGNITUDE OF RELATIVE DRIVING POINT IMPEDANCE, SHEEP5
FREQUENCY RANGE (5000 - 6256 Hz)
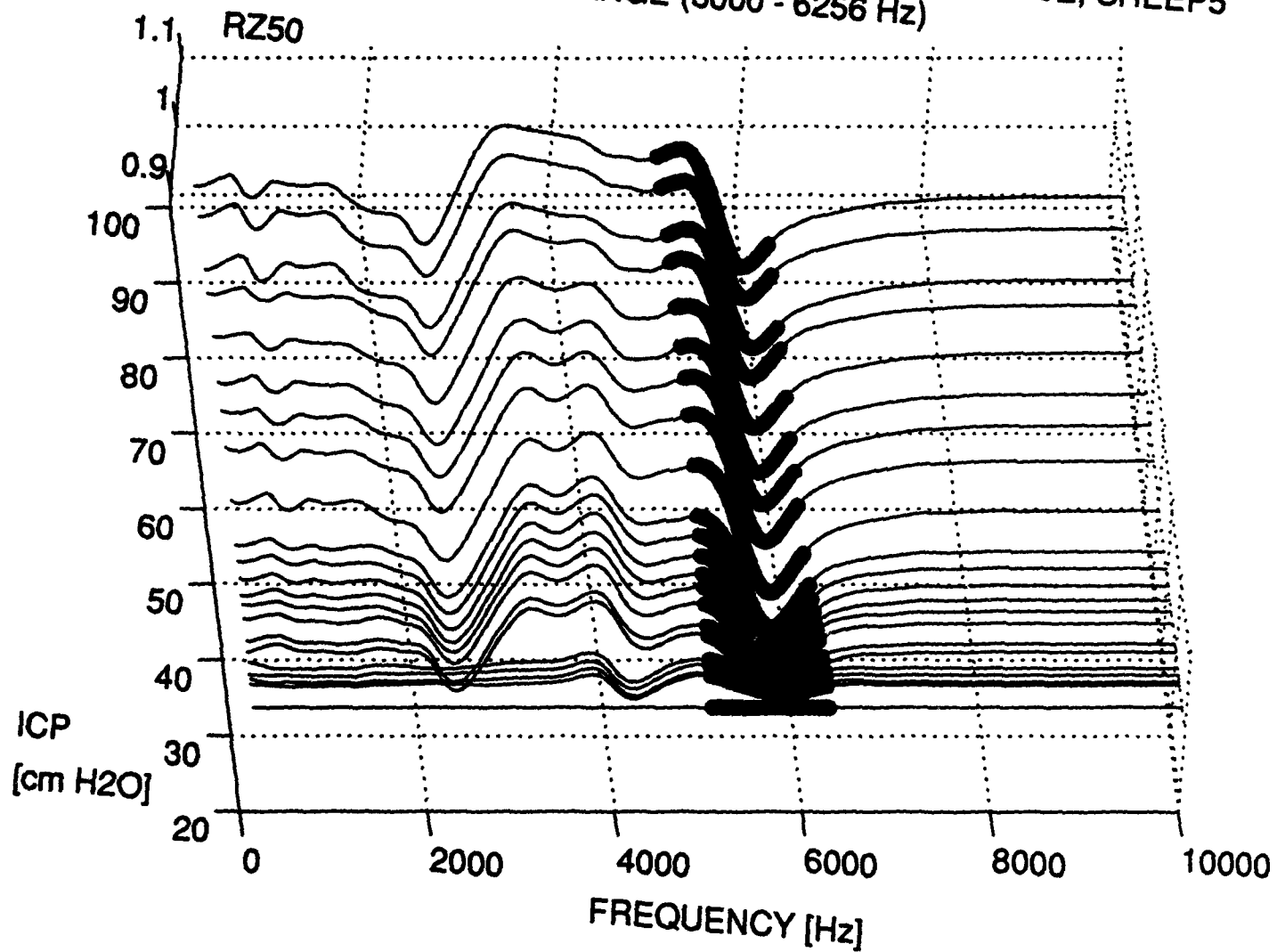
MAGNITUDE STANDARD DEVIATION vs. ICP
SHEEP5, Mag.Rel.DP.   FREQUENCY RANGE (5000 - 6256 Hz)
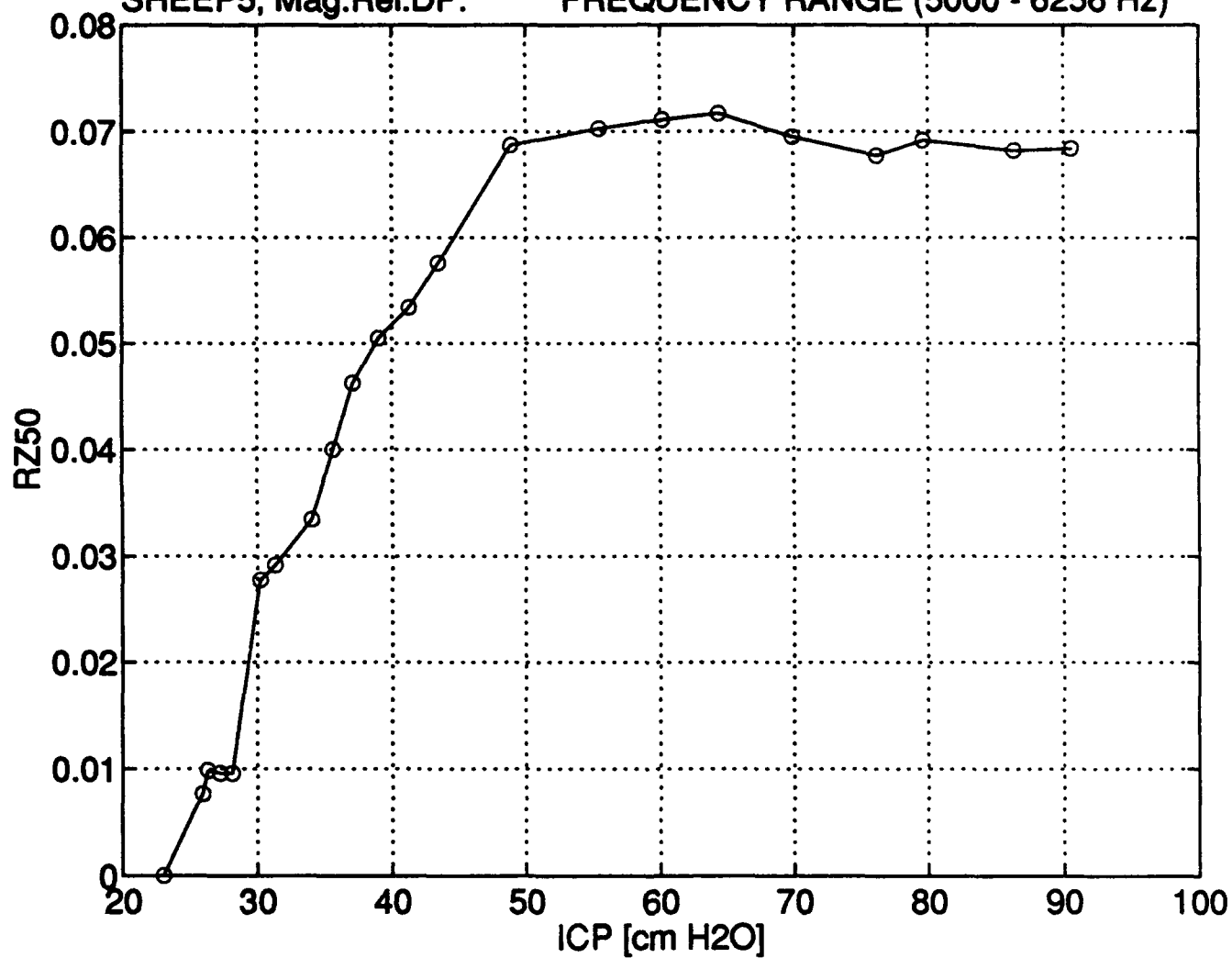
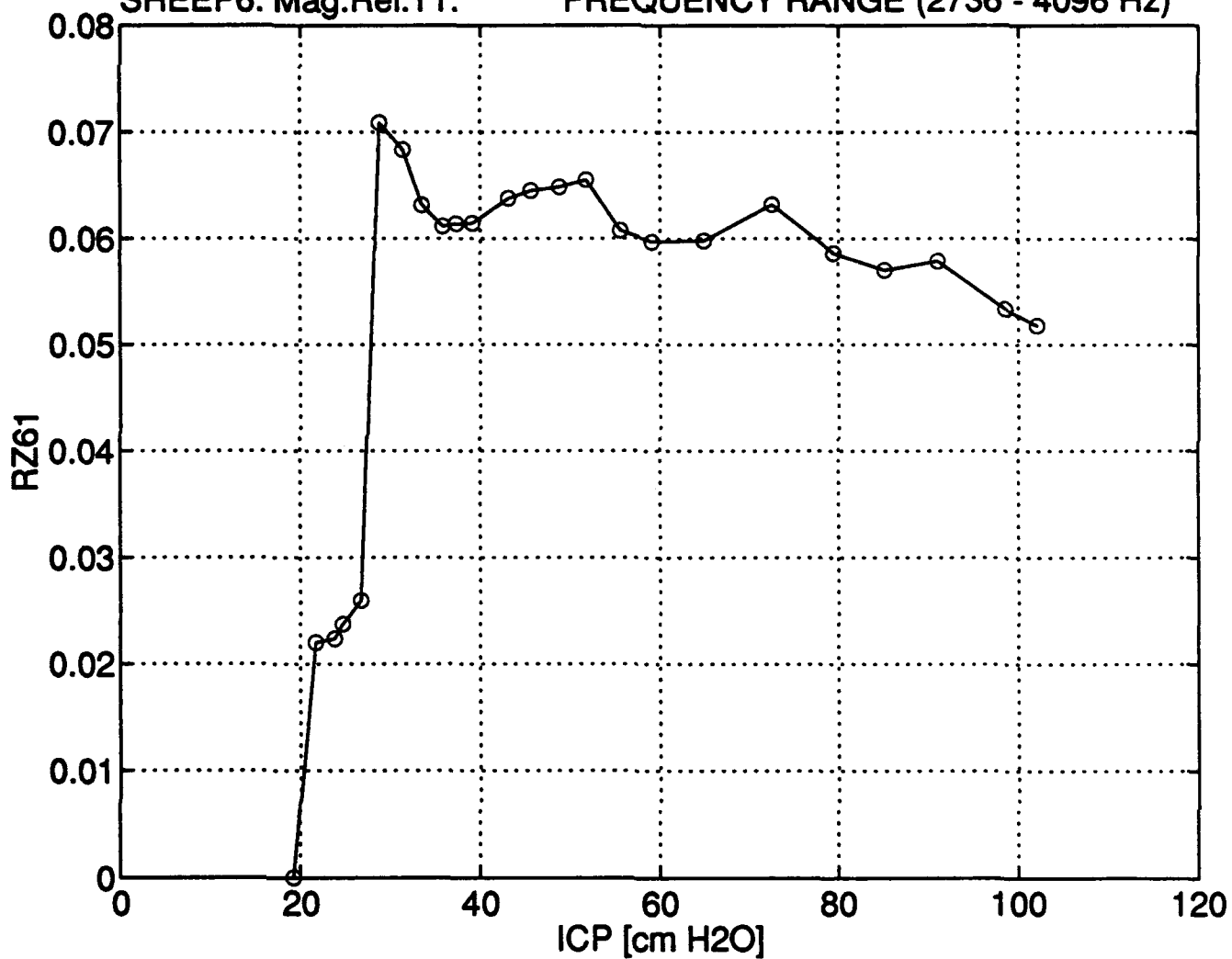MAGNITUDE OF THE RELATIVE TRANSFER IMPEDANCE 1, SHEEP 5

MAGNITUDE OF THE RELATIVE TRANSFER IMPEDANCE 1, SHEEP 5
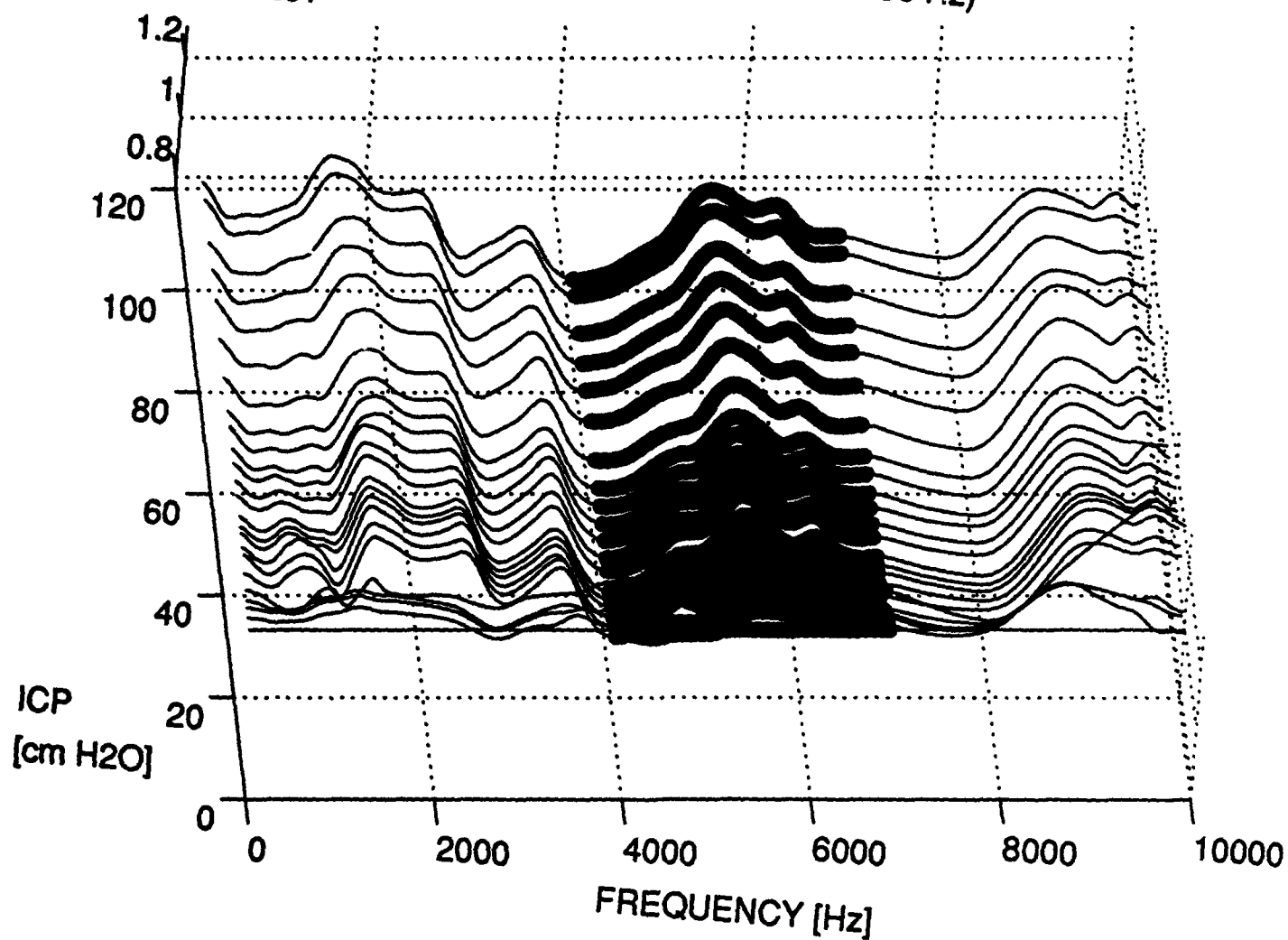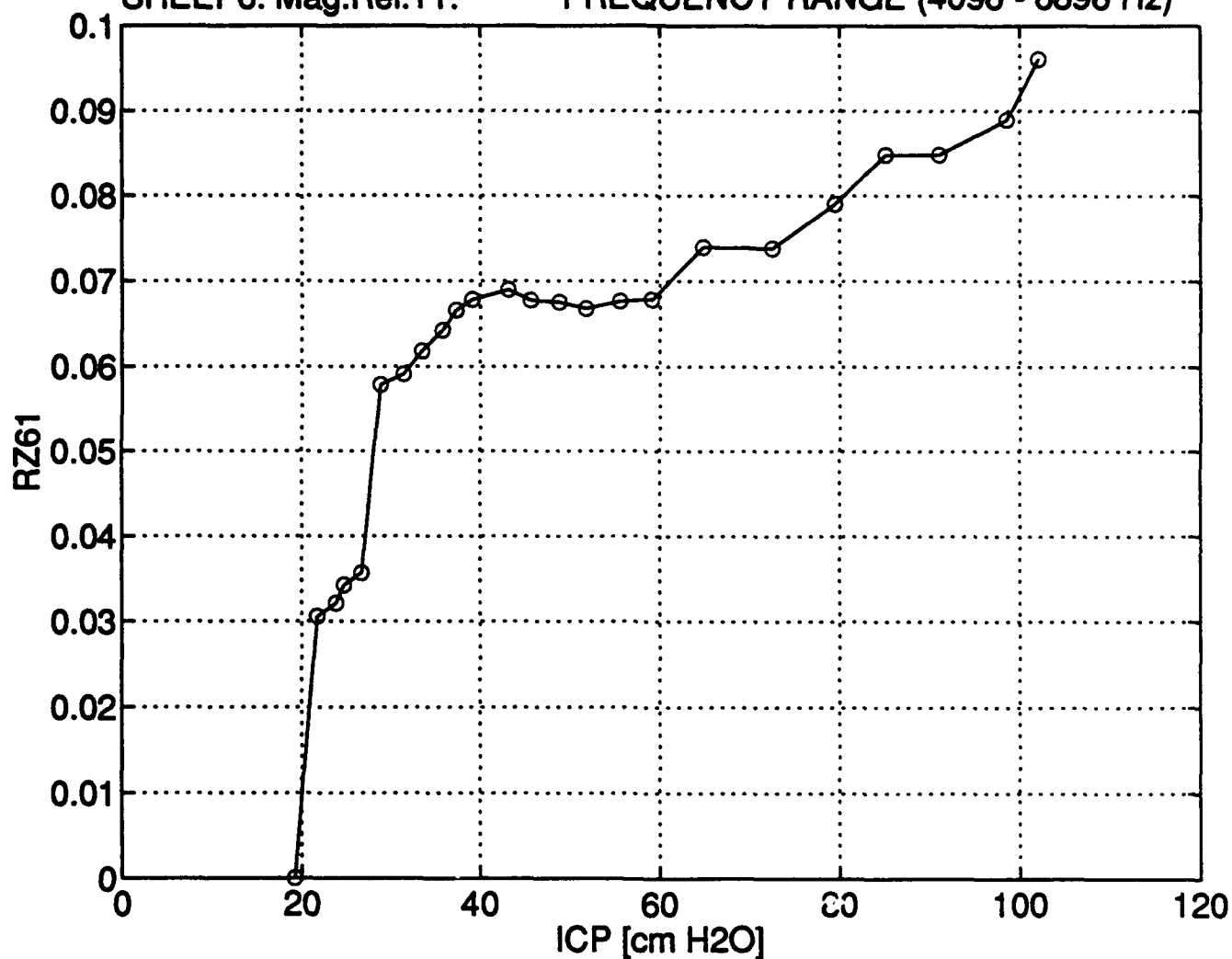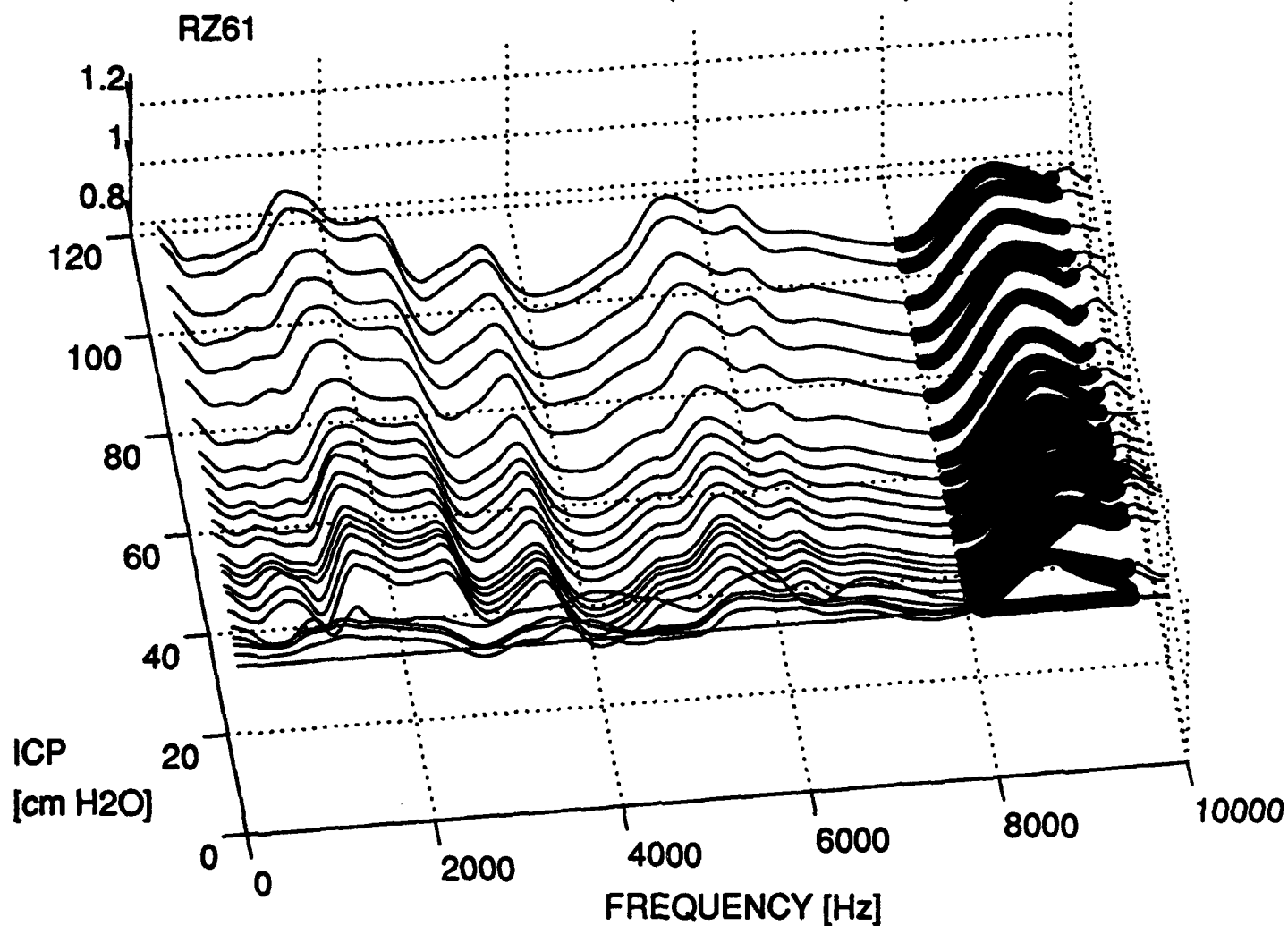FREQUENCY RANGE (104 - 1296 Hz)

MAGNITUDE STANDARD DEVIATION vs. ICP
SHEEP5, Mag.Rel.T1.   FREQUENCY RANGE (104 - 1296 Hz)

MAGNITUDE OF THE RELATIVE TRANSFER IMPEDANCE 1, SHEEP 5
FREQUENCY RANGE (2248 - 3296 Hz)
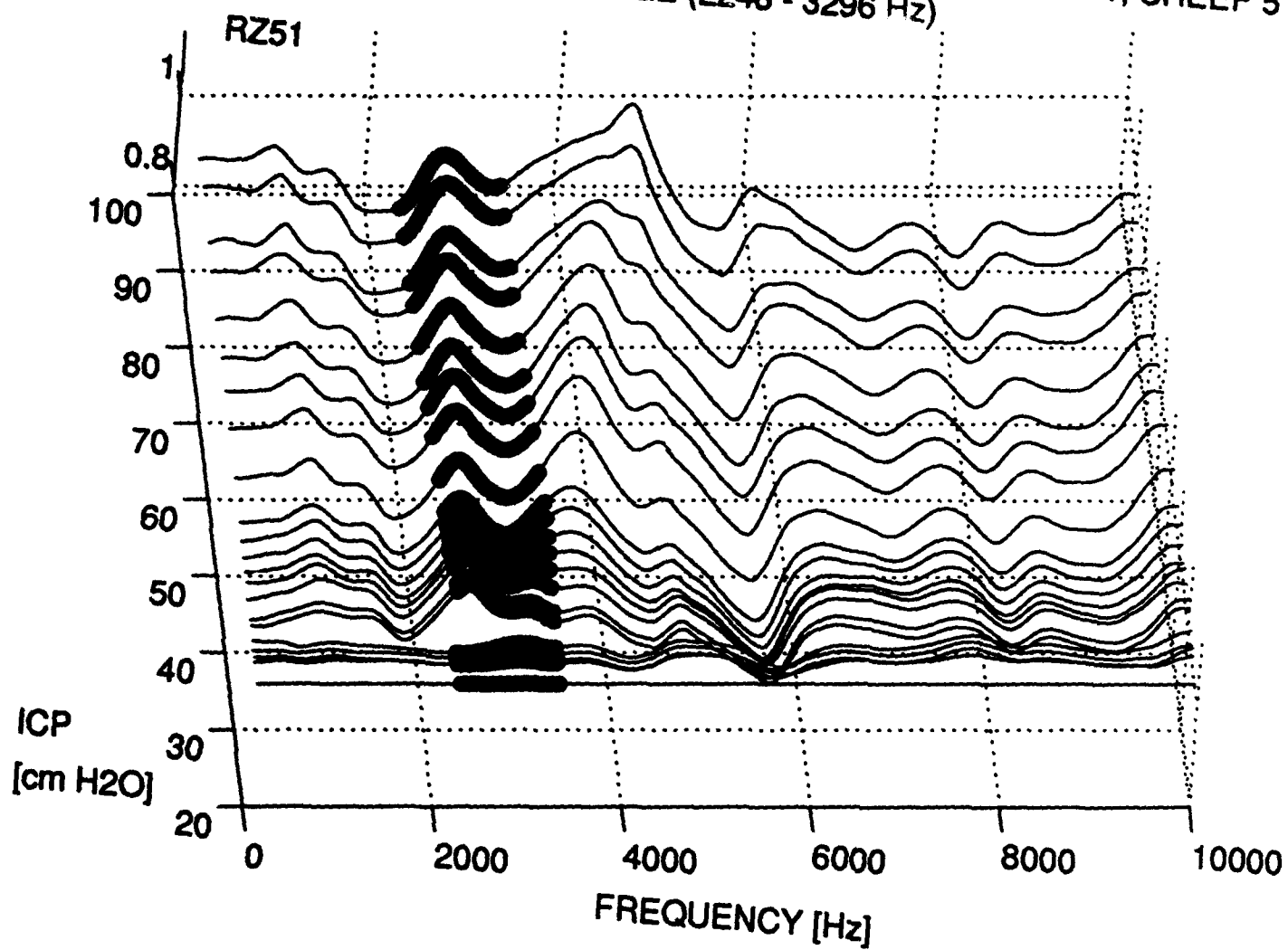
MAGNITUDE STANDARD DEVIATION vs. ICP
SHEEP5, Mag.Rel.T1.   FREQUENCY RANGE (2248 - 3296 Hz)
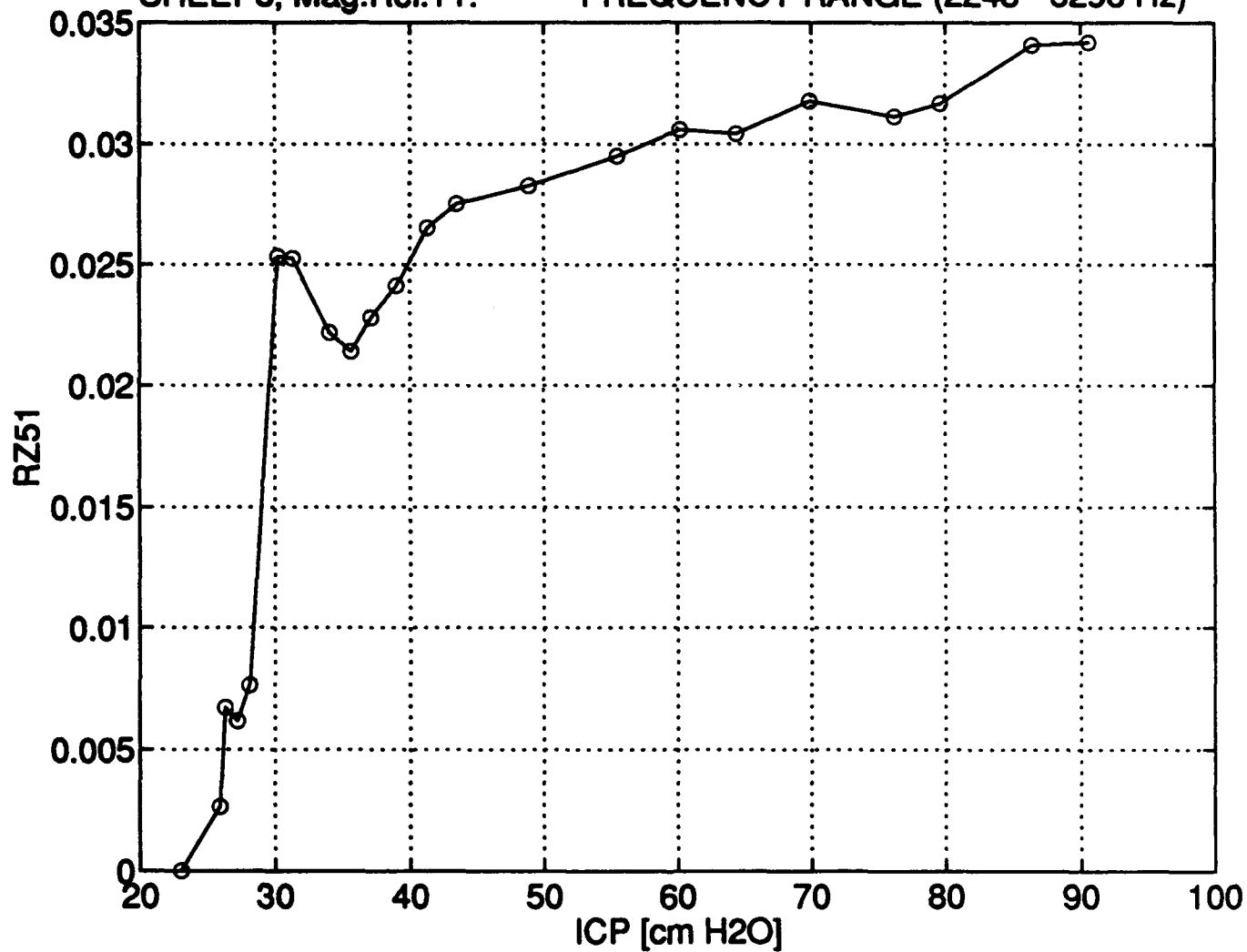
MAGNITUDE OF THE RELATIVE TRANSFER IMPEDANCE 1, SHEEP 5
FREQUENCY RANGE (4296 - 6256 Hz)
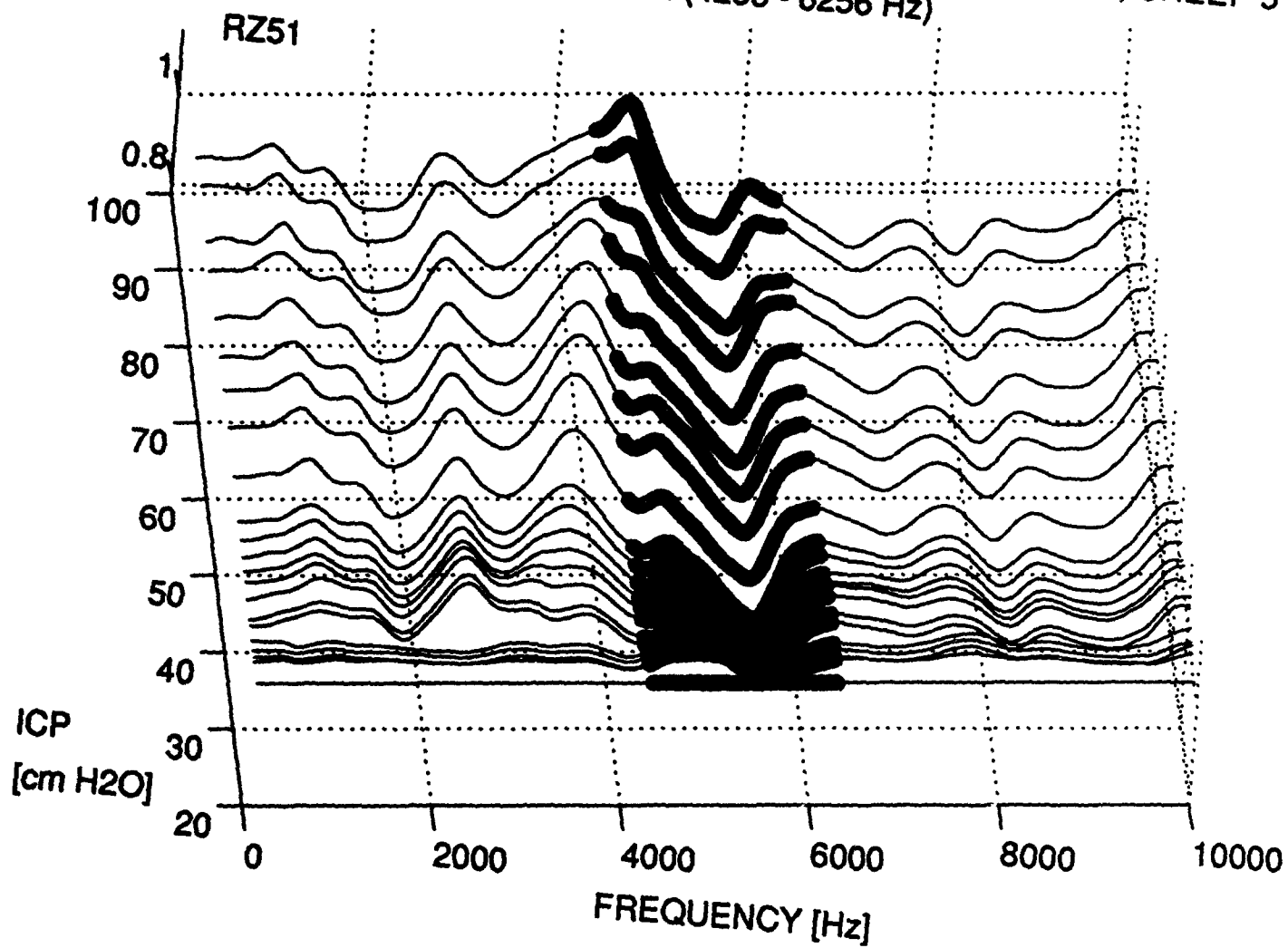
MAGNITUDE STANDARD DEVIATION vs. ICP
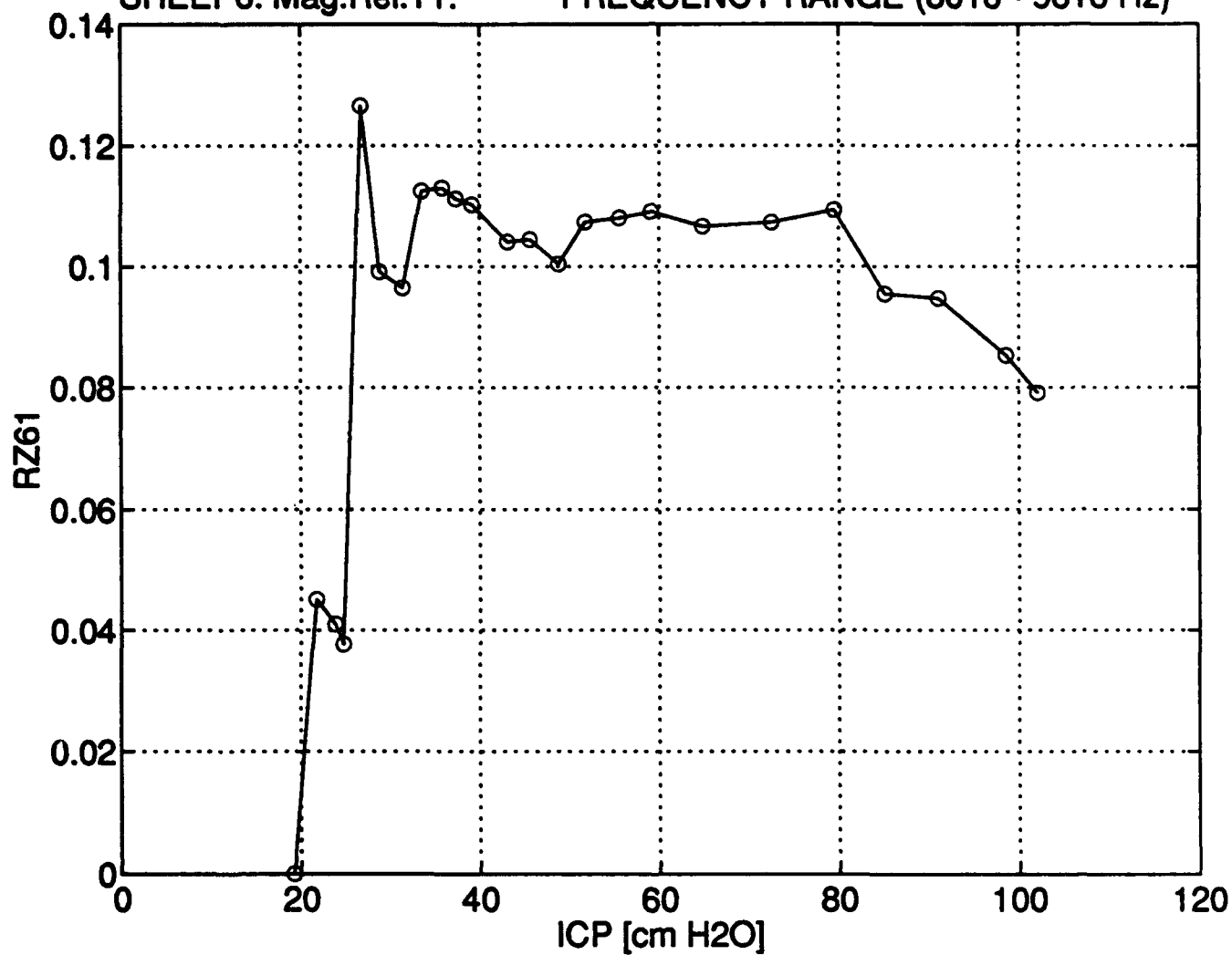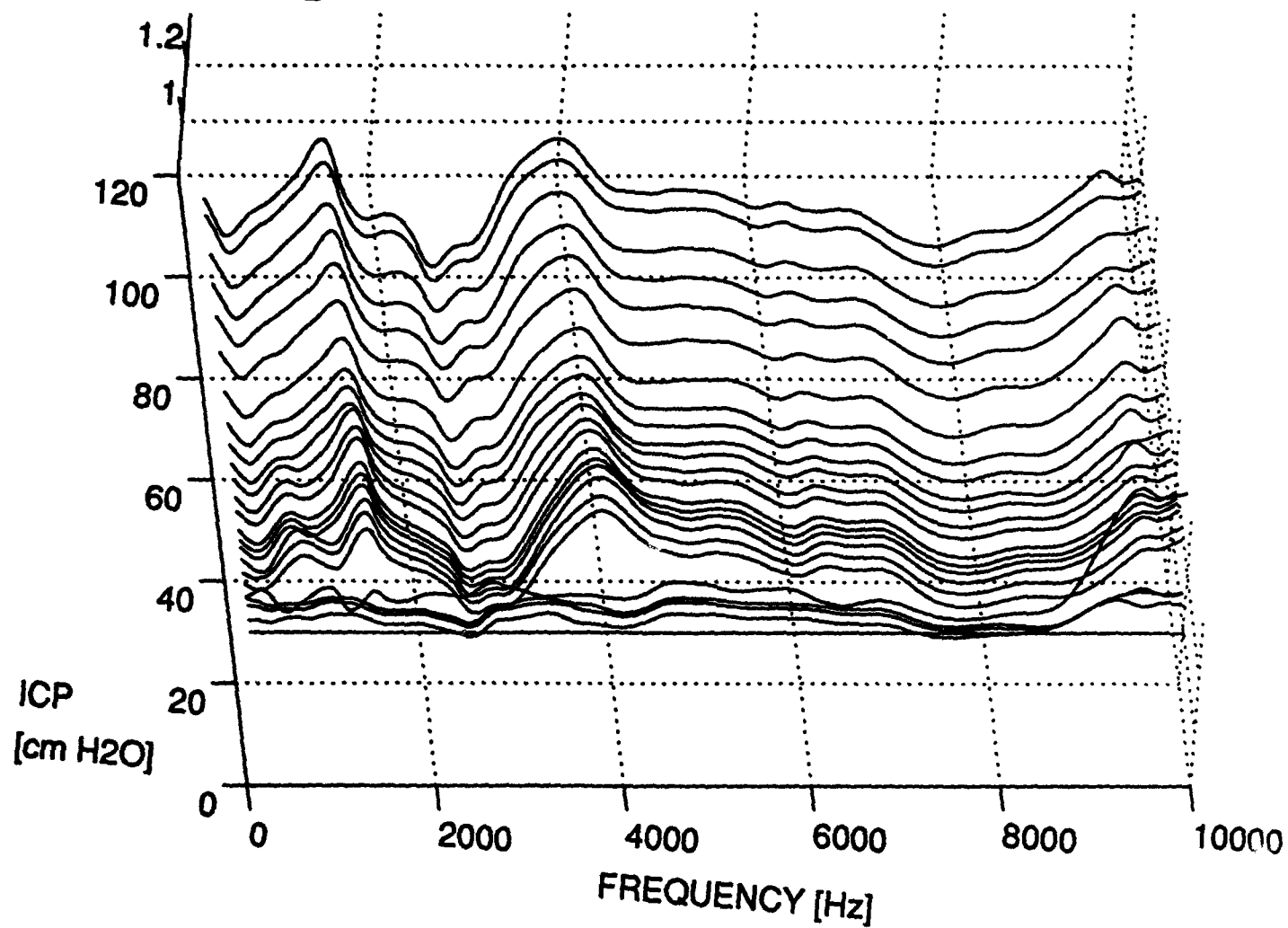SHEEP5, Mag.Rel.T1.   FREQUENCY RANGE (4296 - 6256 Hz)
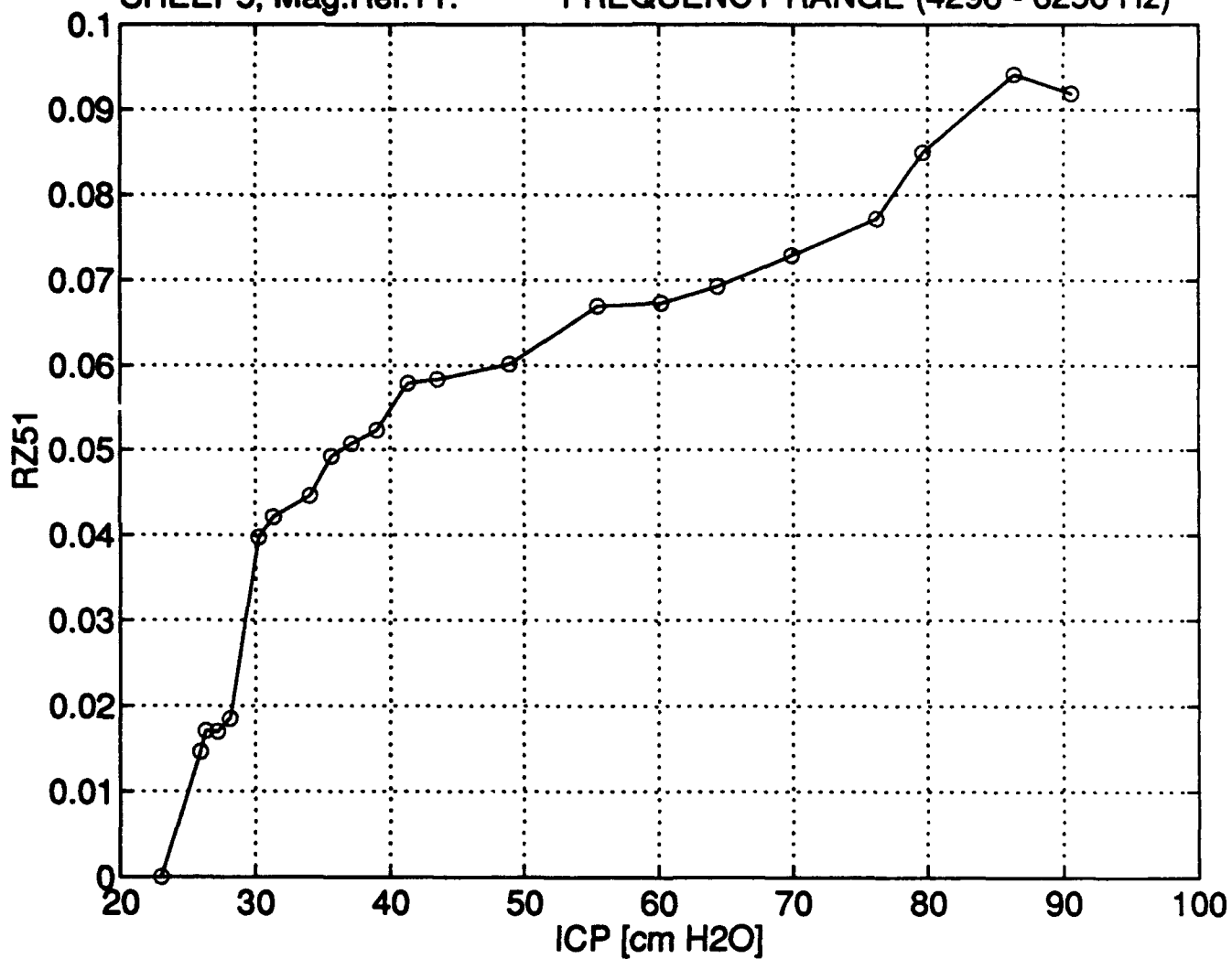
MAGNITUDE OF THE RELATIVE TRANSFER IMPEDANCE 1, SHEEP 5
FREQUENCY RANGE (5936 - 7296 Hz)
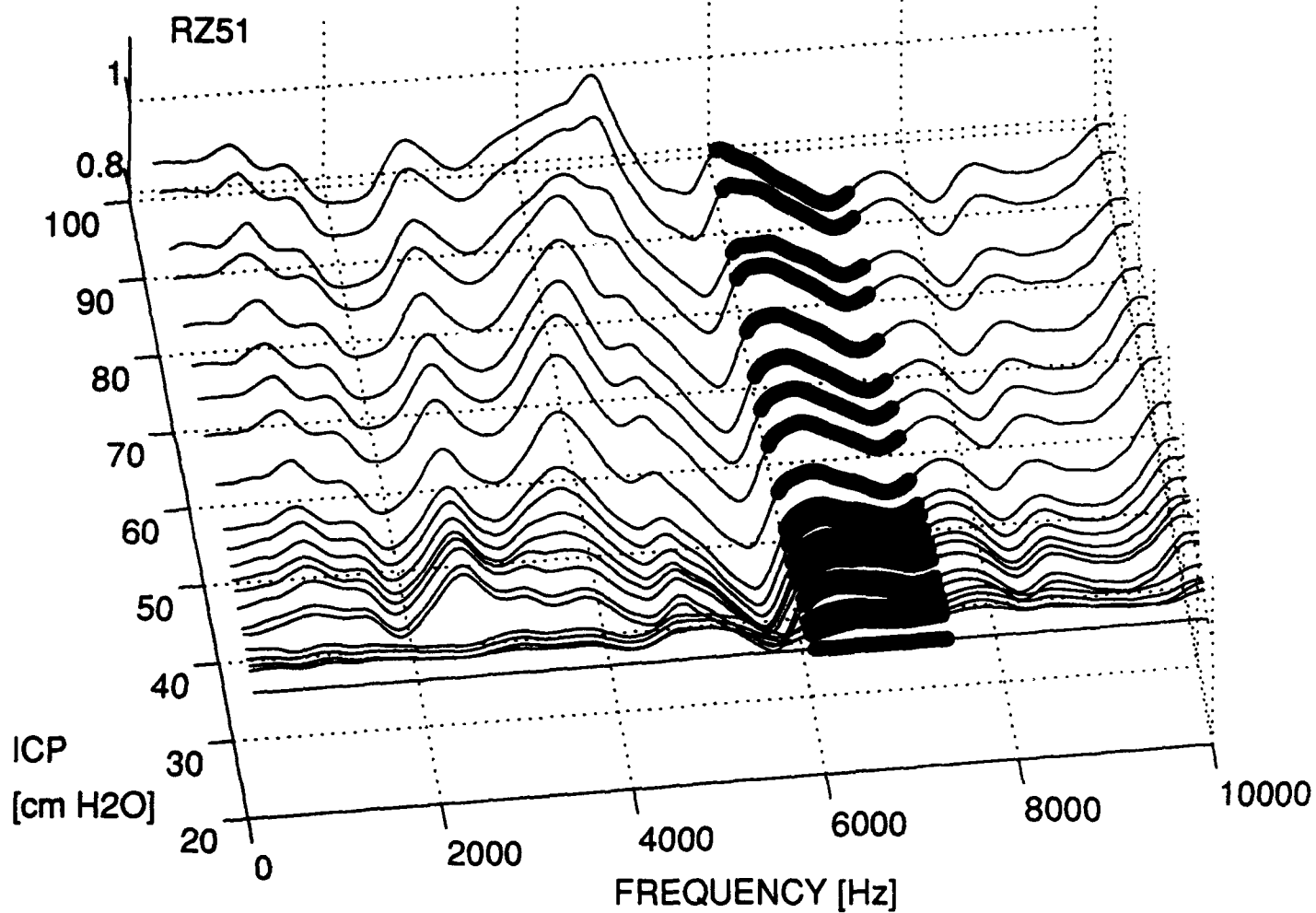
MAGNITUDE STANDARD DEVIATION vs. ICP
SHEEP5, Mag.Rel.T1.   FREQUENCY RANGE (5936 - 7296 Hz)
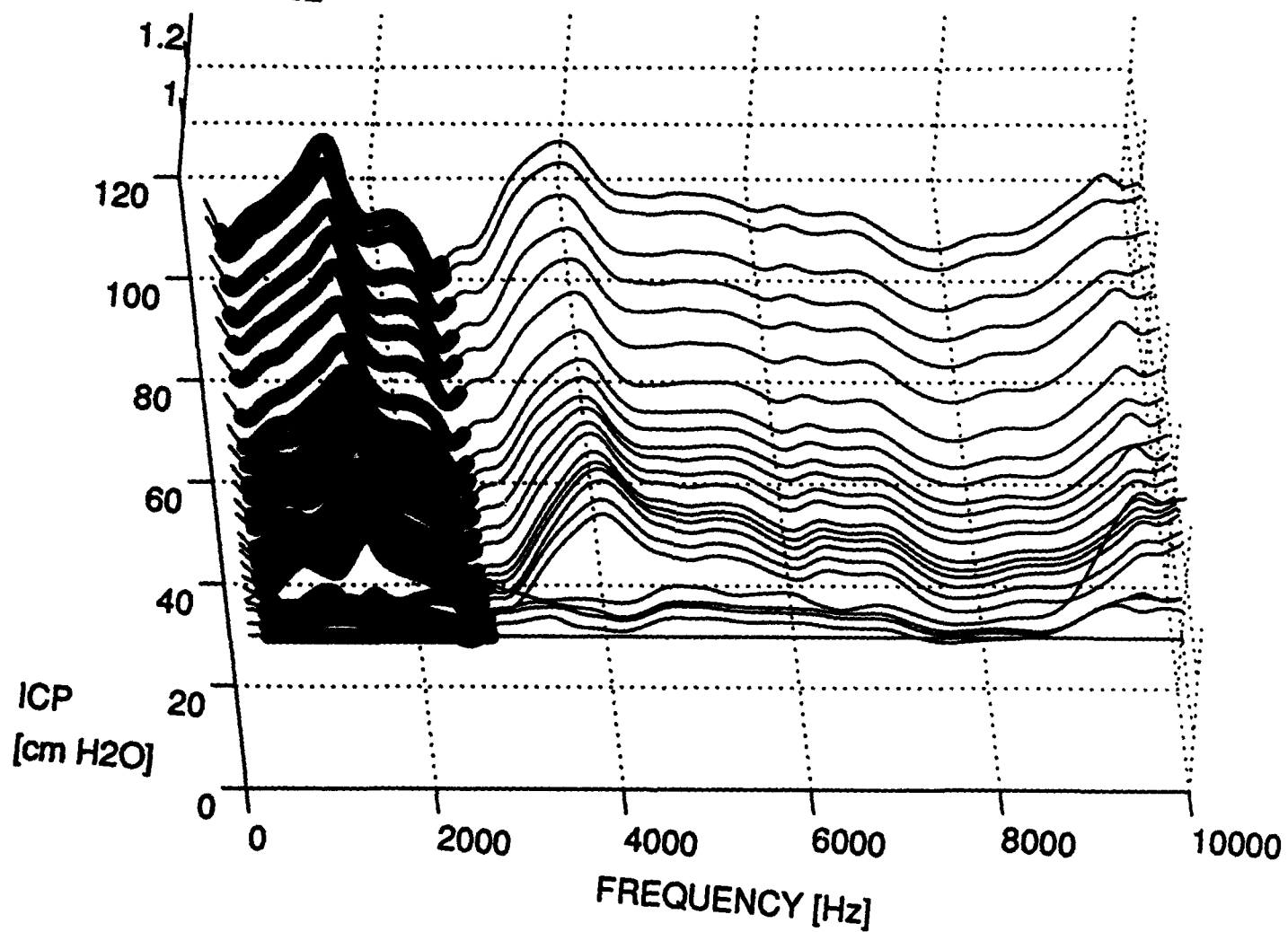
MAGNITUDE OF THE RELATIVE TRANSFER IMPEDANCE 1, SHEEP 5
FREQUENCY RANGE (7376 - 8416 Hz)

MAGNITUDE STANDARD DEVIATION vs. ICP

SHEEP5, Mag.Rel.T1.   FREQUENCY RANGE (7376 - 8416 Hz)
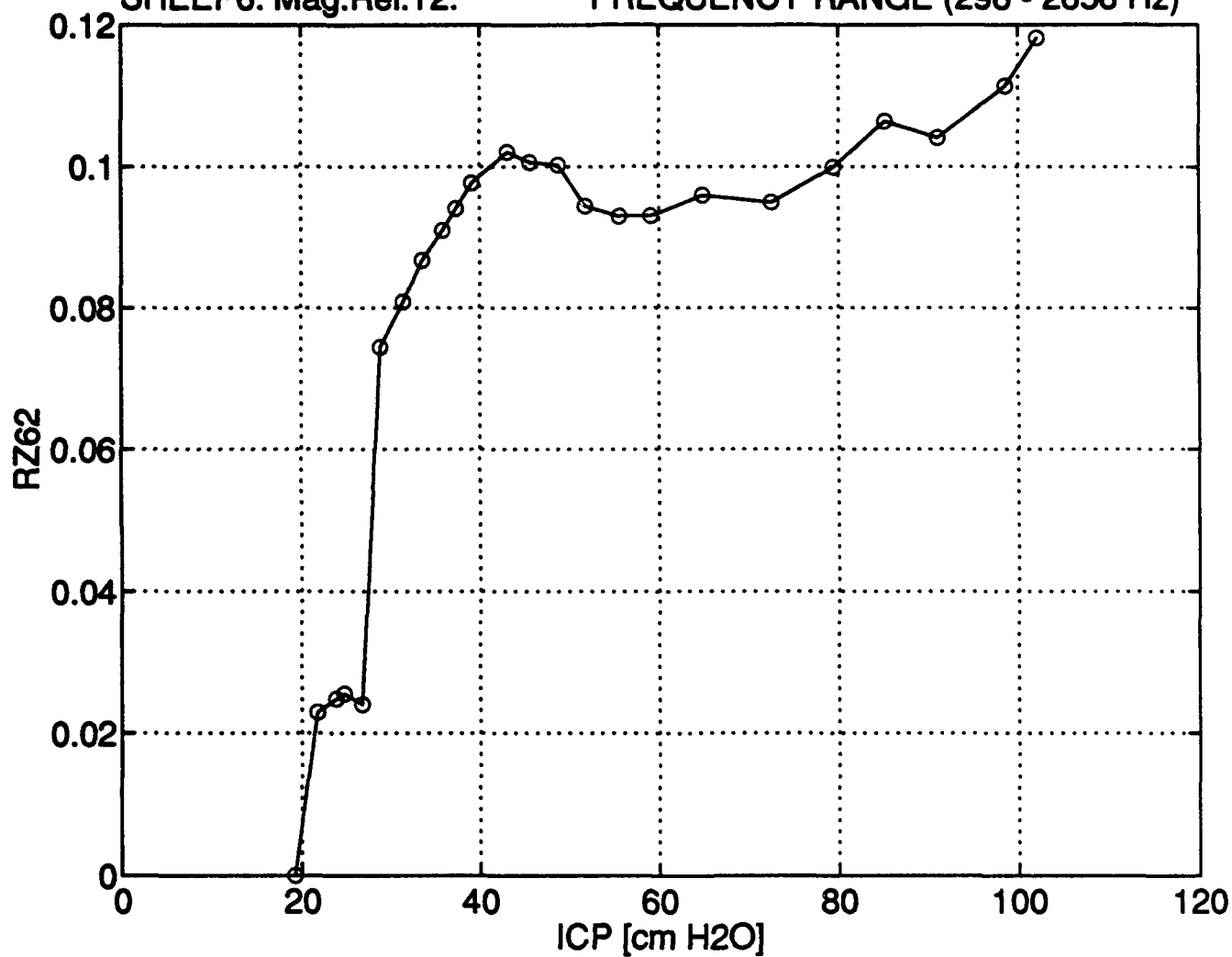
MAGNITUDE OF RELATIVE TRANSFER IMPEDANCE 2, SHEEP5
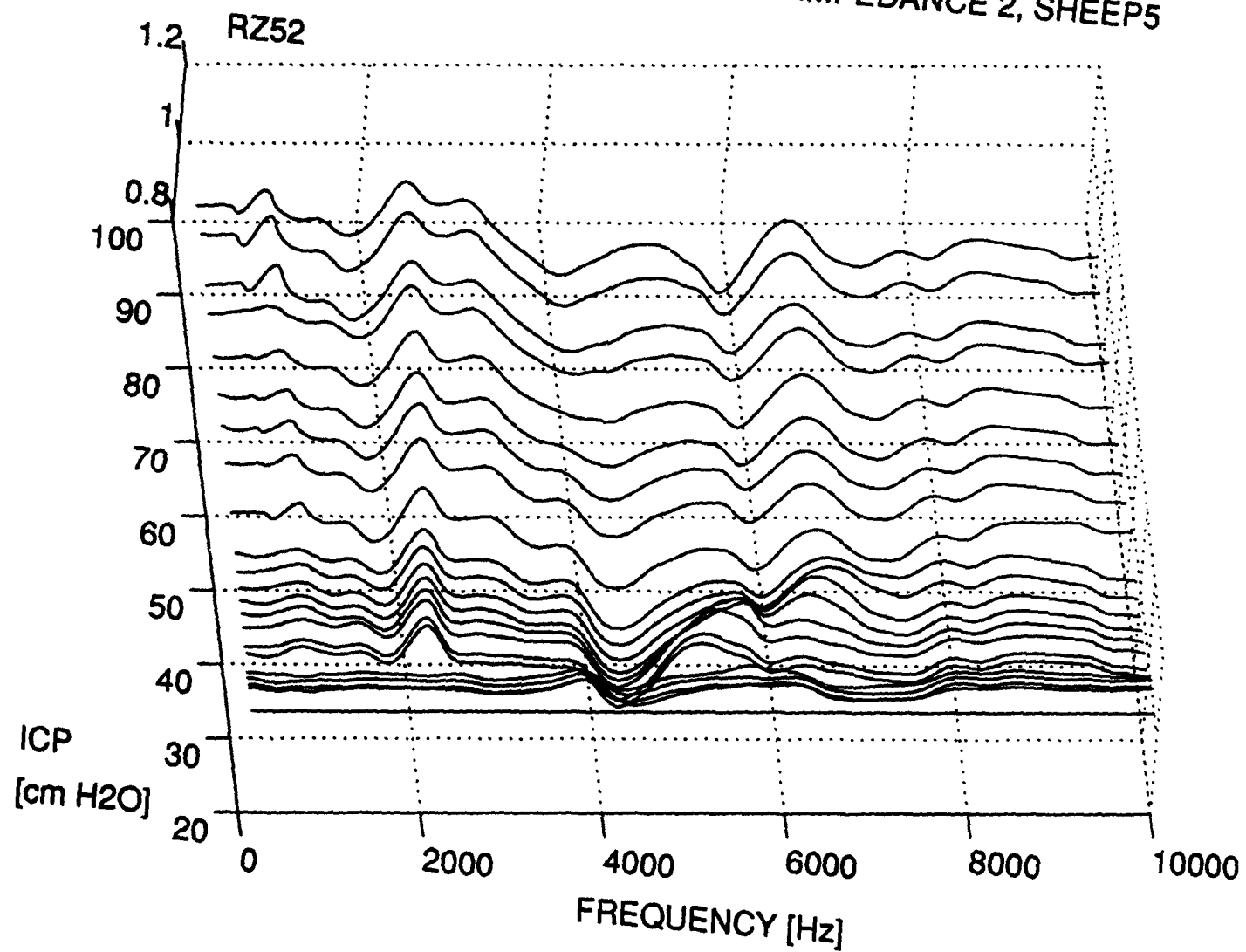
MAGNITUDE OF RELATIVE TRANSFER IMPEDANCE 2, SHEEP5
FREQUENCY RANGE (104 - 976 Hz)
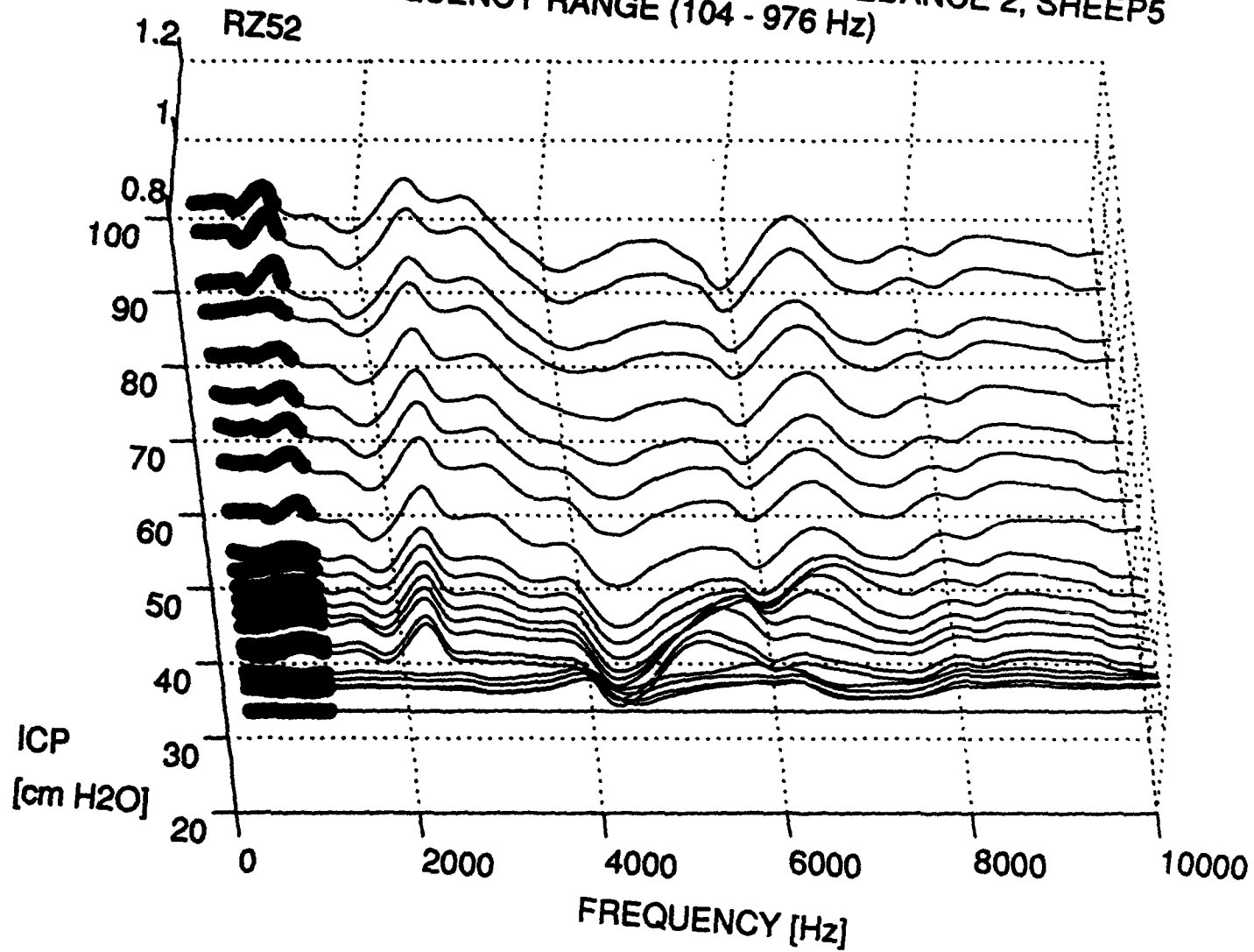
RZ52

ICP [cm H2O]

FREQUENCY [Hz]

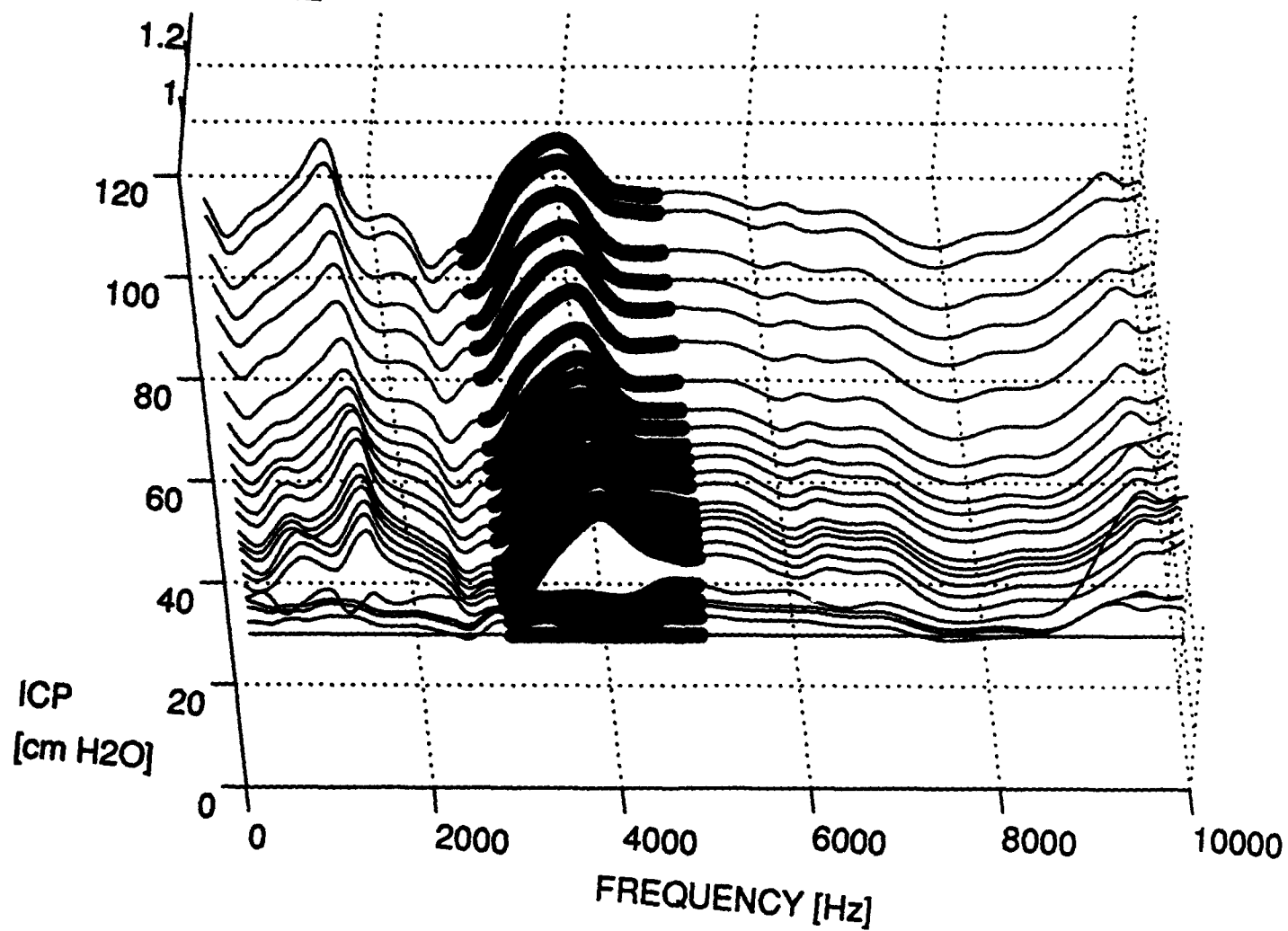MAGNITUDE STANDARD DEVIATION vs. ICP
SHEEP5, Mag.Rel.T2.   FREQUENCY RANGE (104 - 976 Hz)
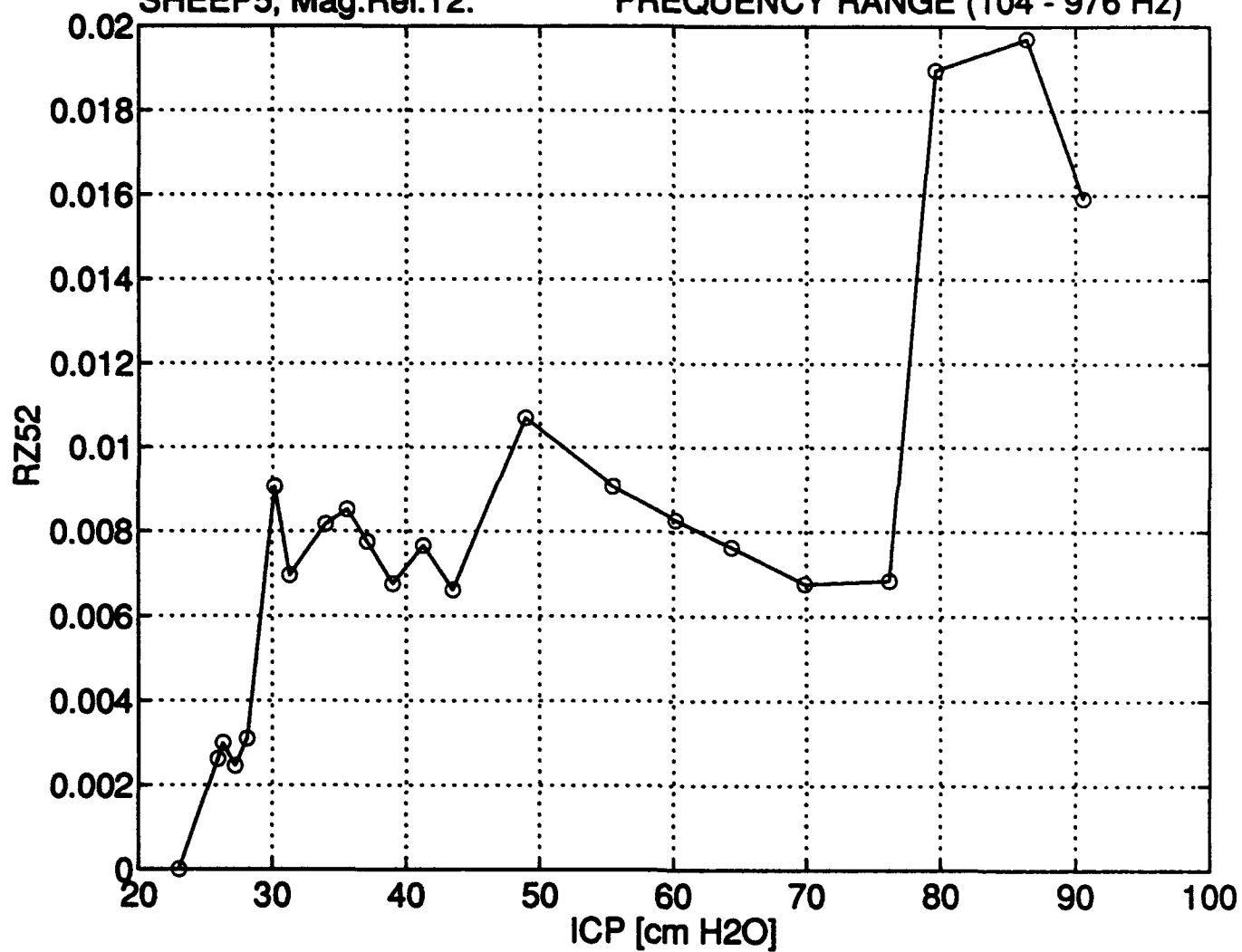
MAGNITUDE OF RELATIVE TRANSFER IMPEDANCE 2, SHEEP5
FREQUENCY RANGE (1456 - 2496 Hz)
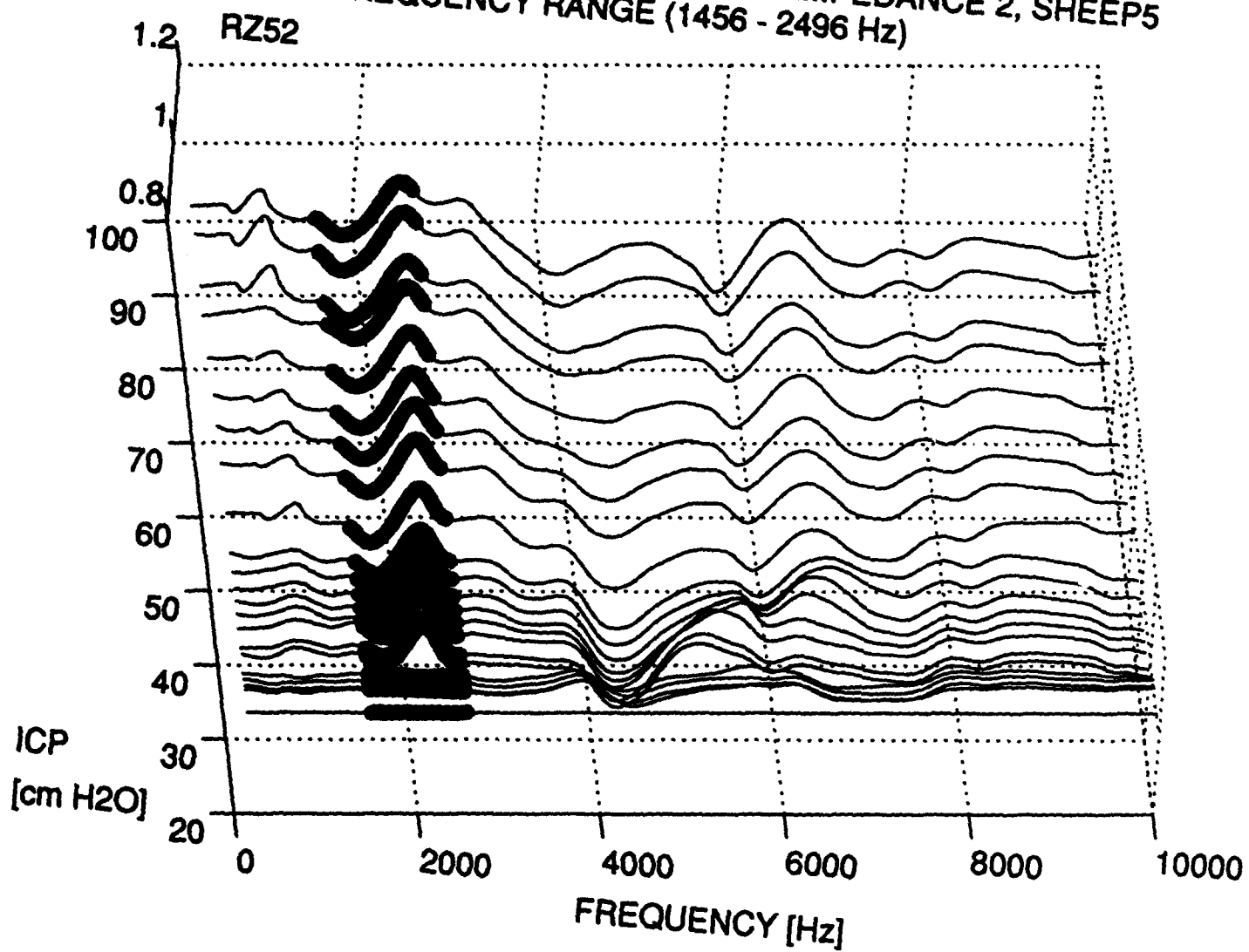
MAGNITUDE STANDARD DEVIATION vs. ICP
SHEEP5, Mag.Rel.T2.   FREQUENCY RANGE (1456 -2496 Hz)
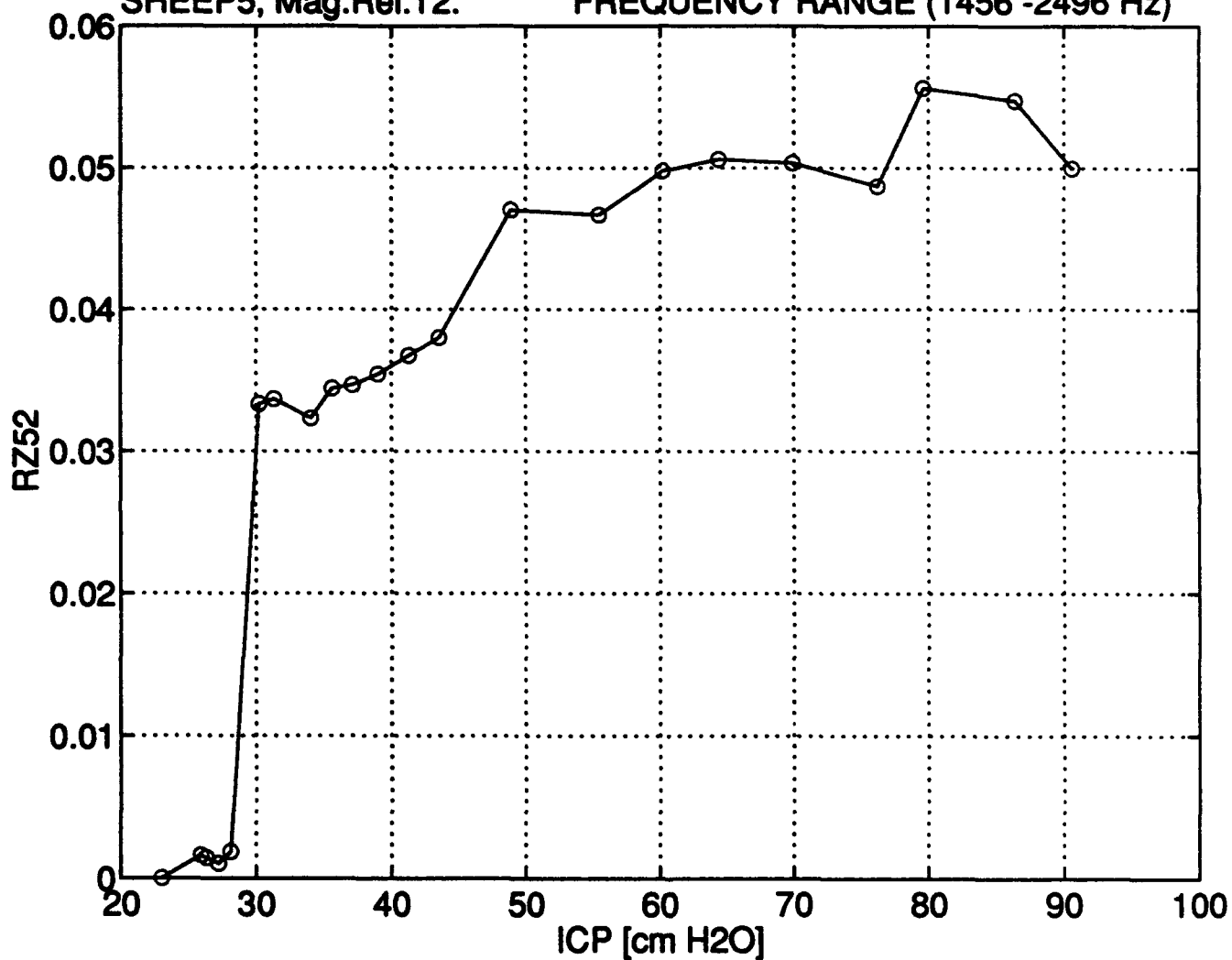
MAGNITUDE OF RELATIVE TRANSFER IMPEDANCE 2, SHEEP5
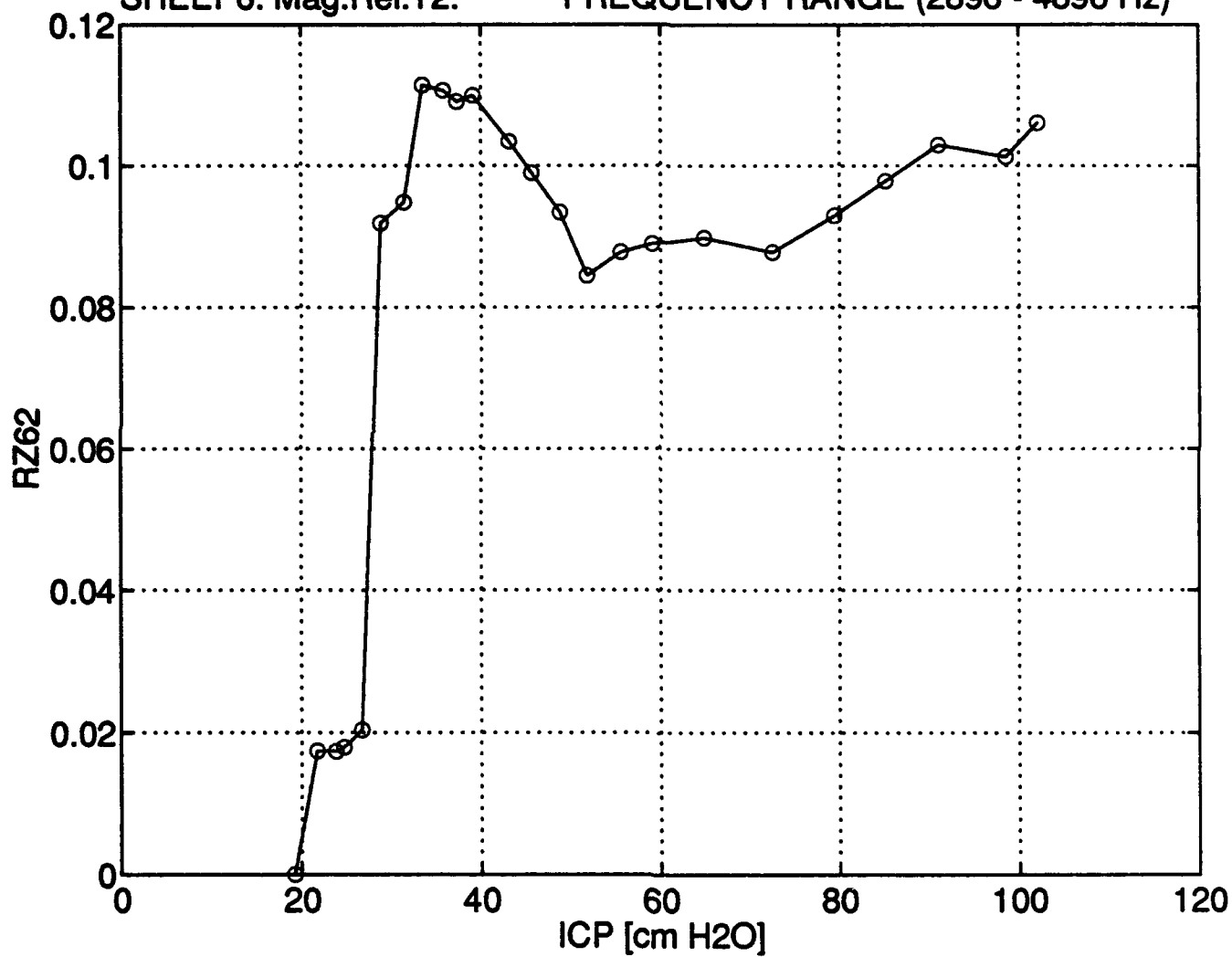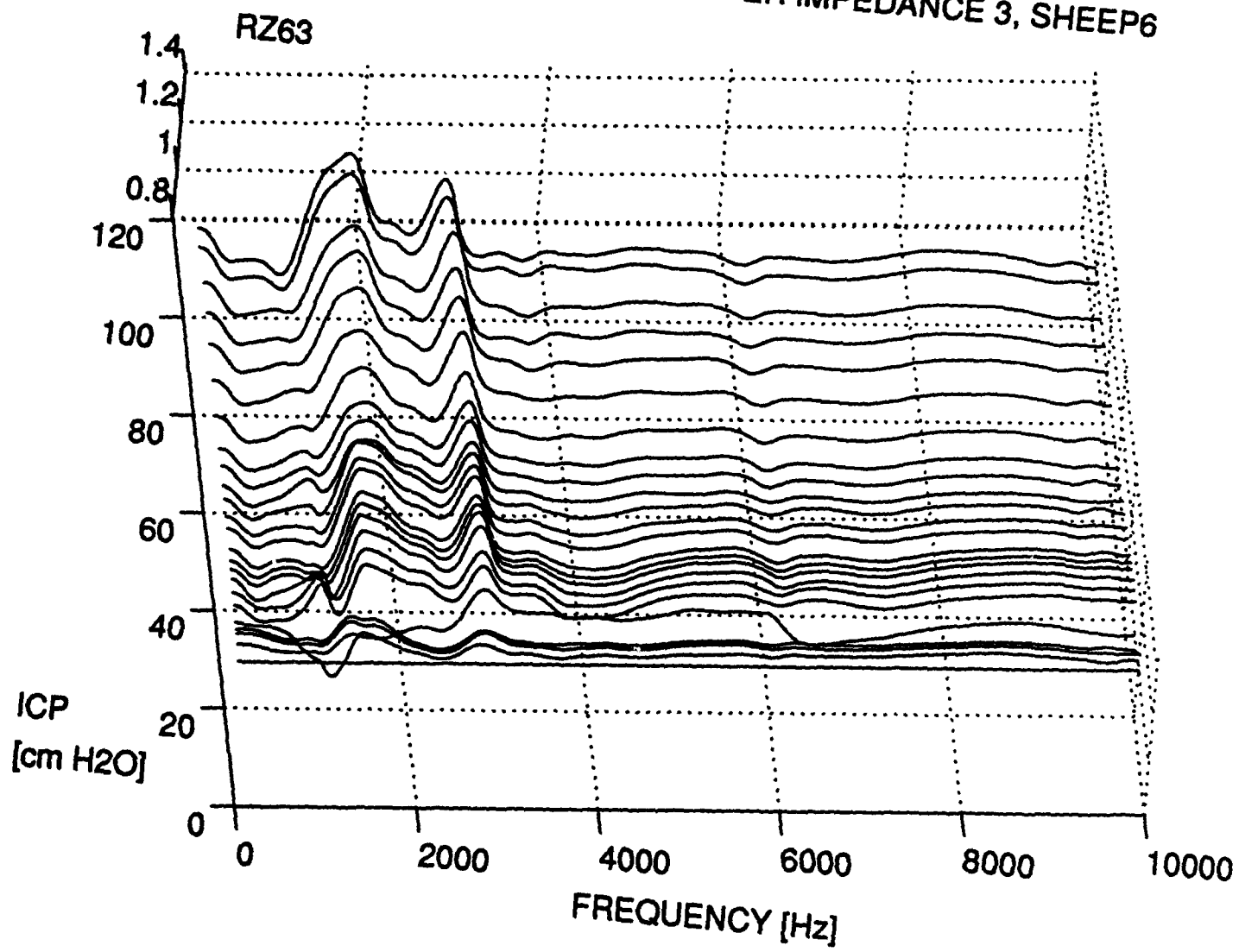FREQUENCY RANGE (5696 - 7776 Hz)

MAGNITUDE STANDARD DEVIATION vs. ICP
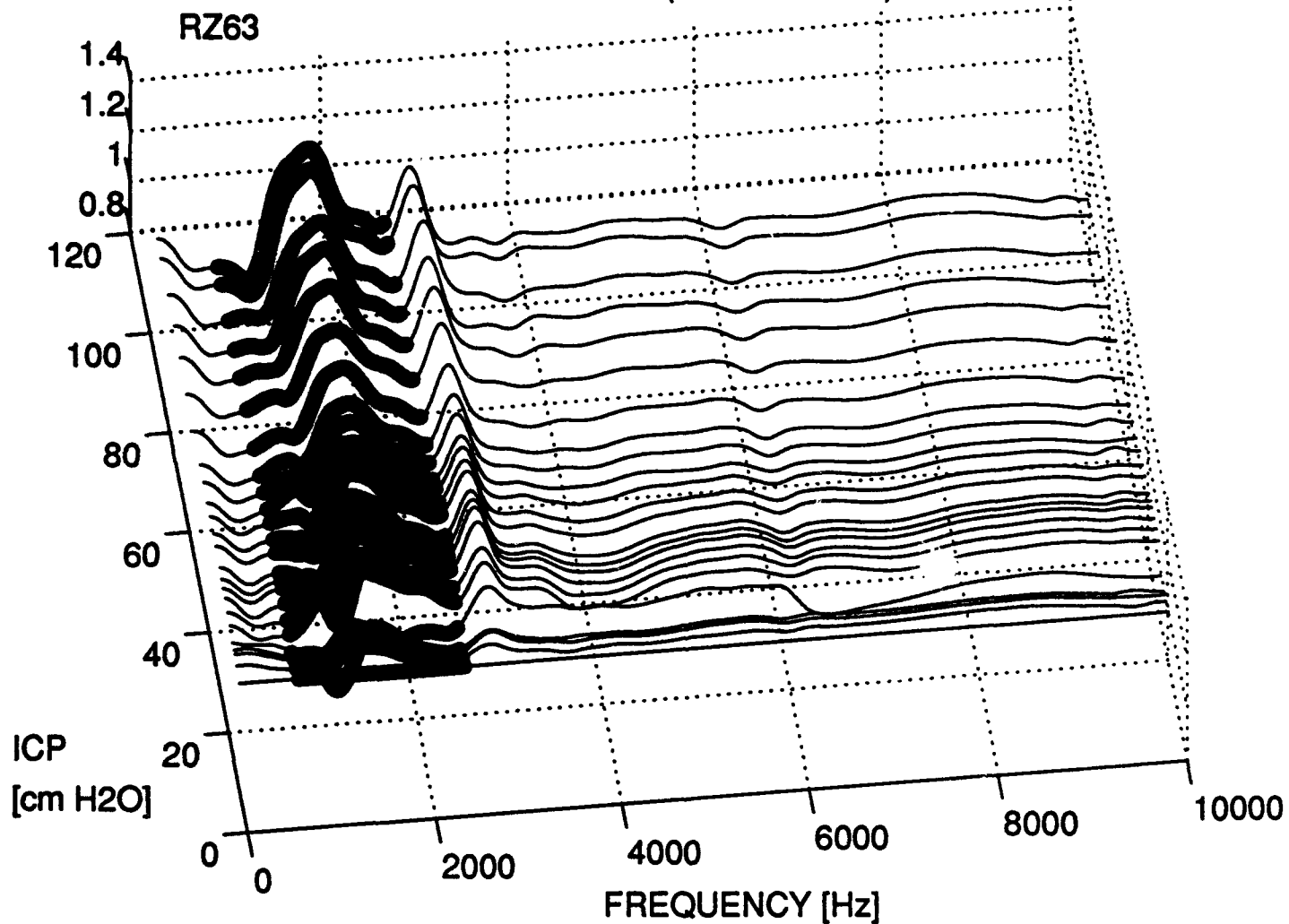SHEEP5, Mag.Rel.T2.   FREQUENCY RANGE (5696 - 7776 Hz)
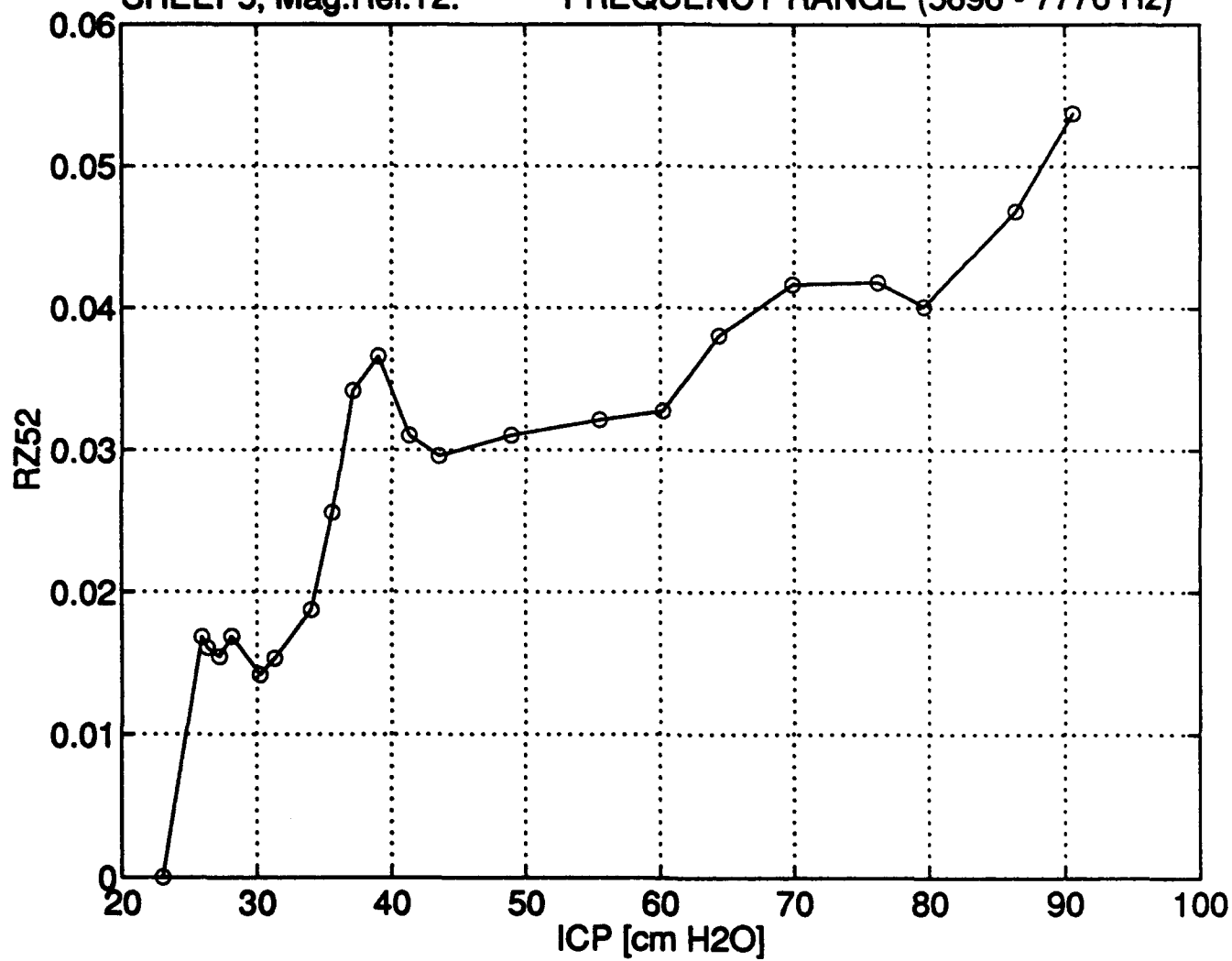
MAGNITUDE OF RELATIVE TRANSFER IMPEDANCE 3, SHEEP5
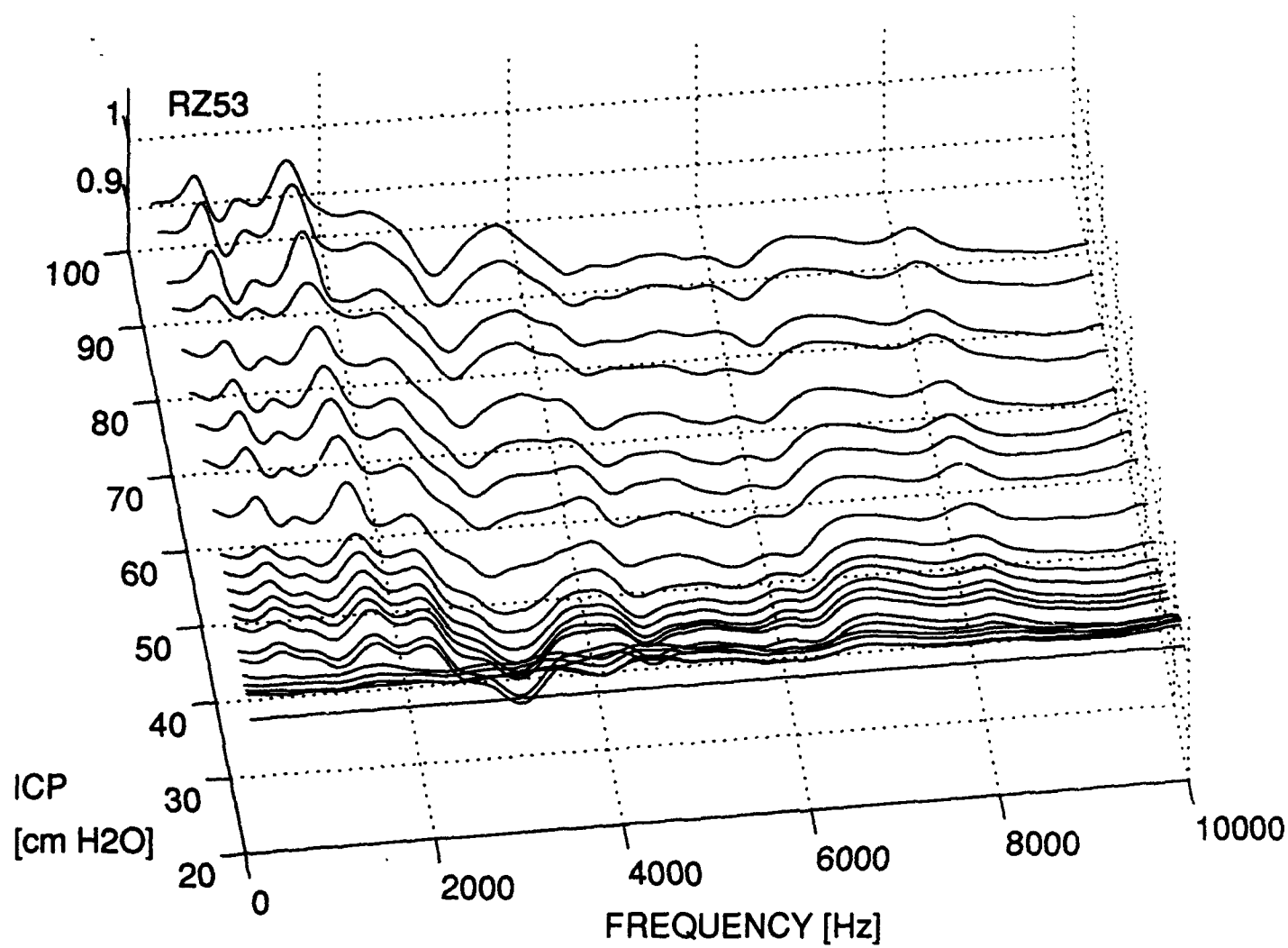
MAGNITUDE OF RELATIVE TRANSFER IMPEDANCE 3, SHEEP5
FREQUENCY RANGE (104 - 816 Hz)
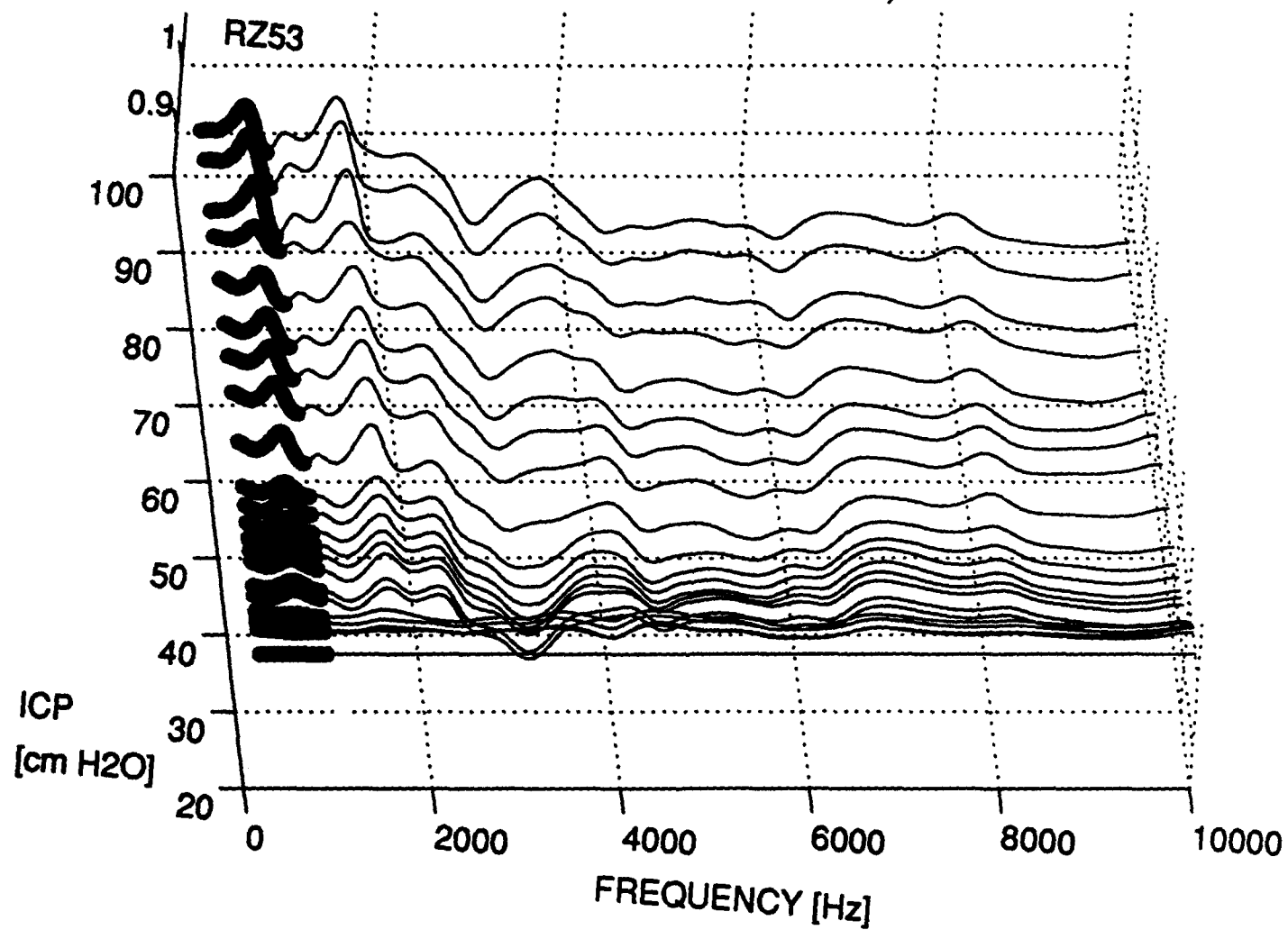
MAGNITUDE STANDARD DEVIATION vs. ICP
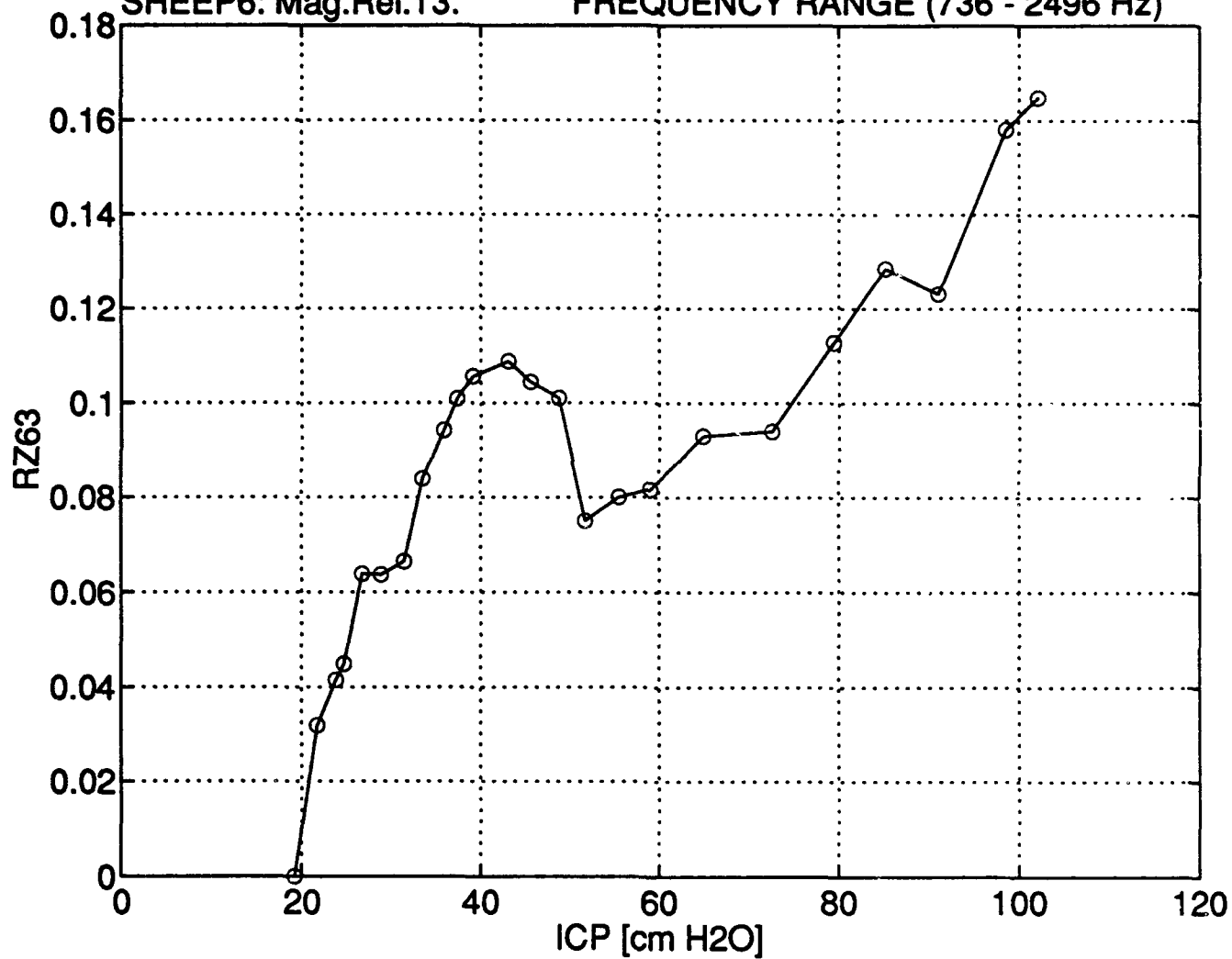SHEEP5, Mag.Rel.T3.   FREQUENCY RANGE (104 - 816 Hz)
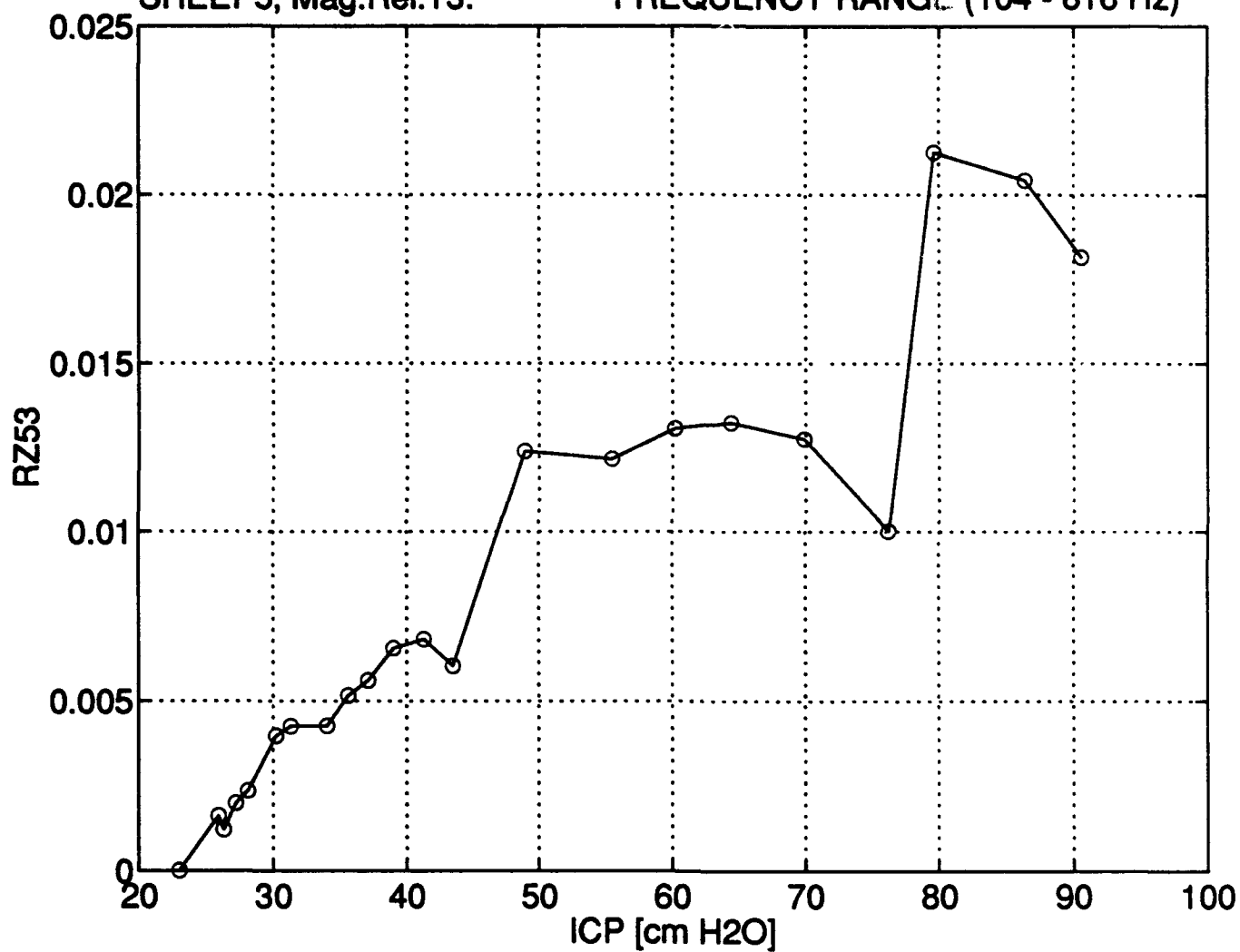
MAGNITUDE OF RELATIVE TRANSFER IMPEDANCE 3, SHEEP5
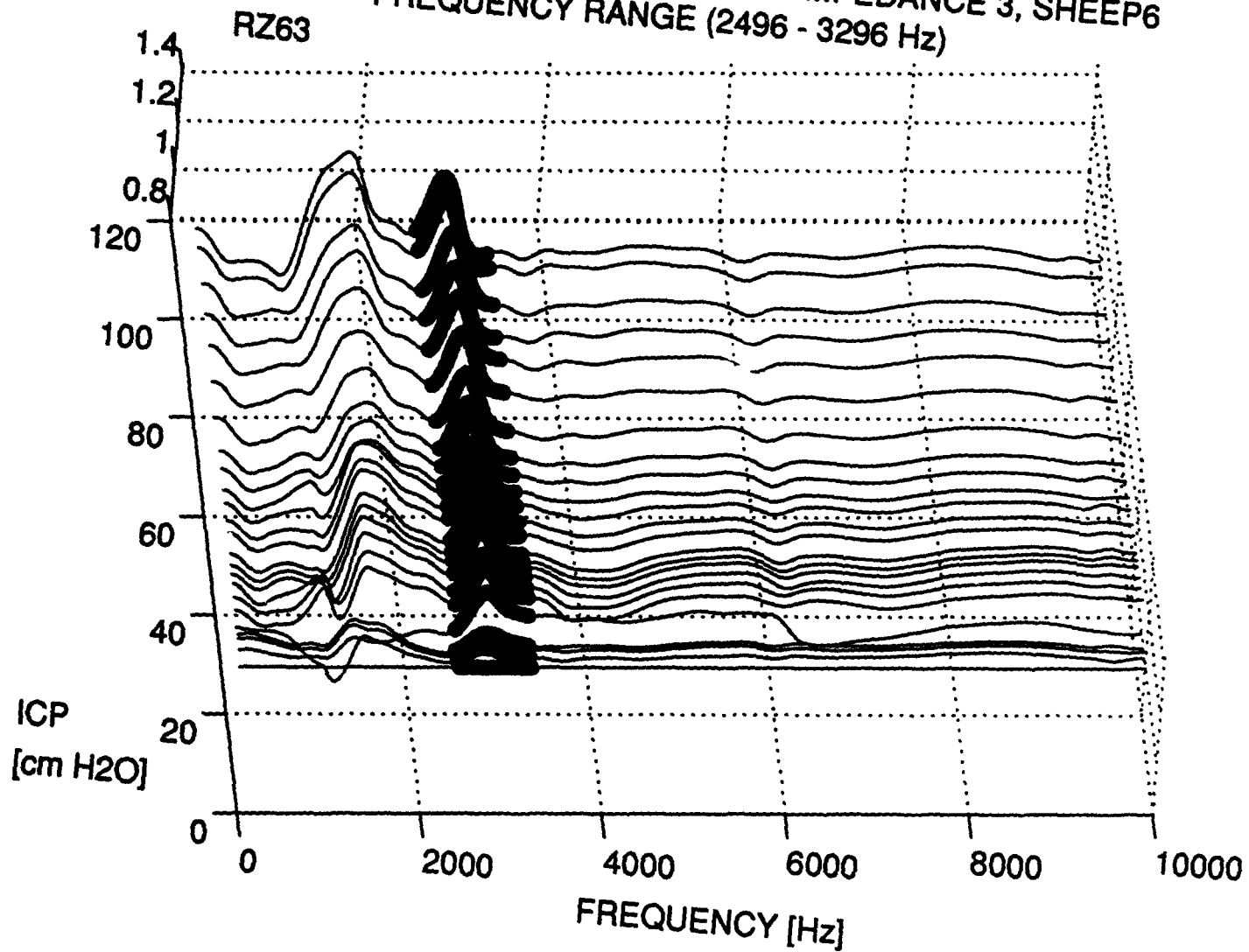FREQUENCY RANGE (1056 - 2946 Hz)
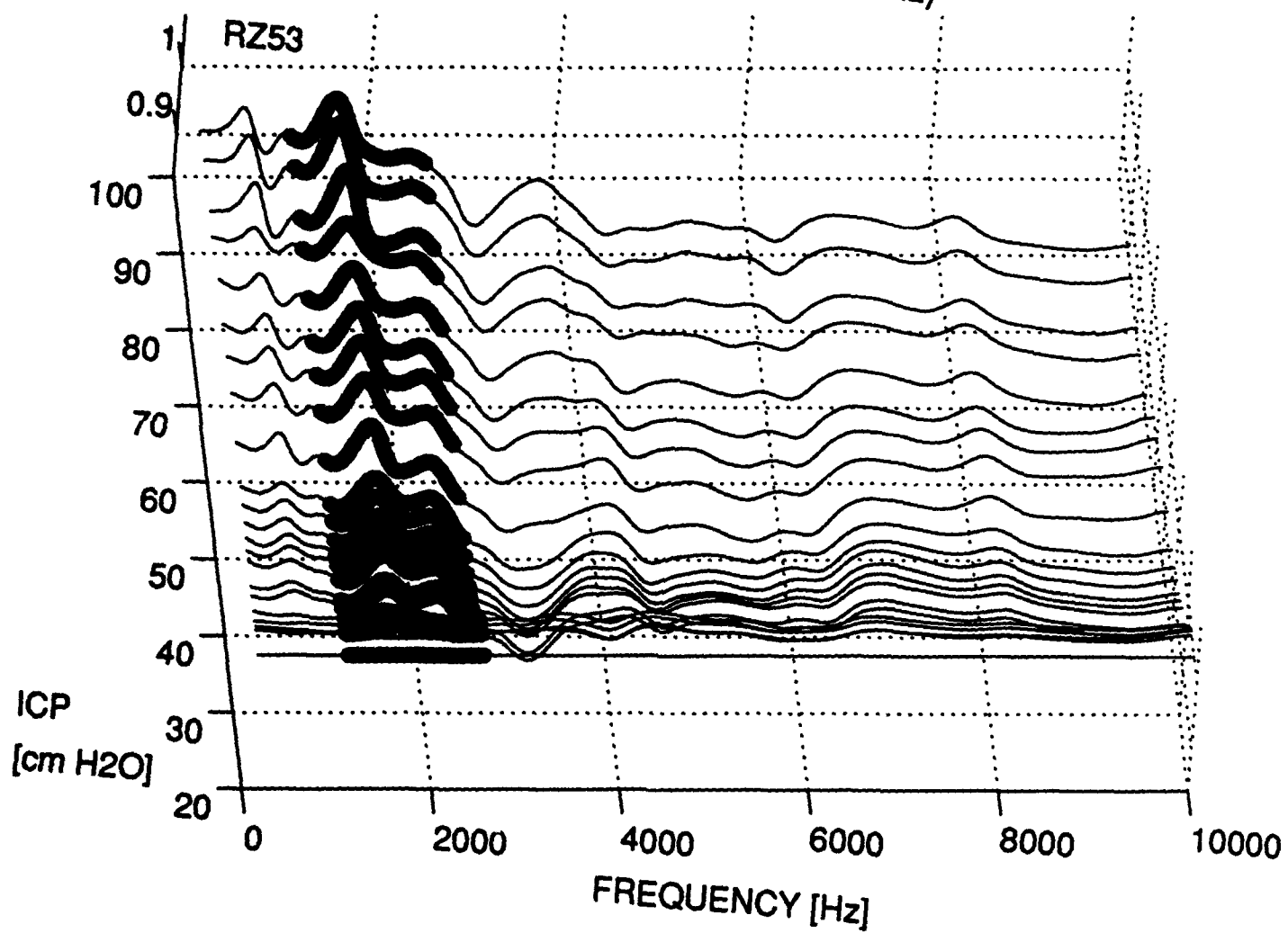
MAGNITUDE STANDARD DEVIATION vs. ICP
SHEEP5, Mag.Rel.T3.   FREQUENCY RANGE (1056 - 2946 Hz)
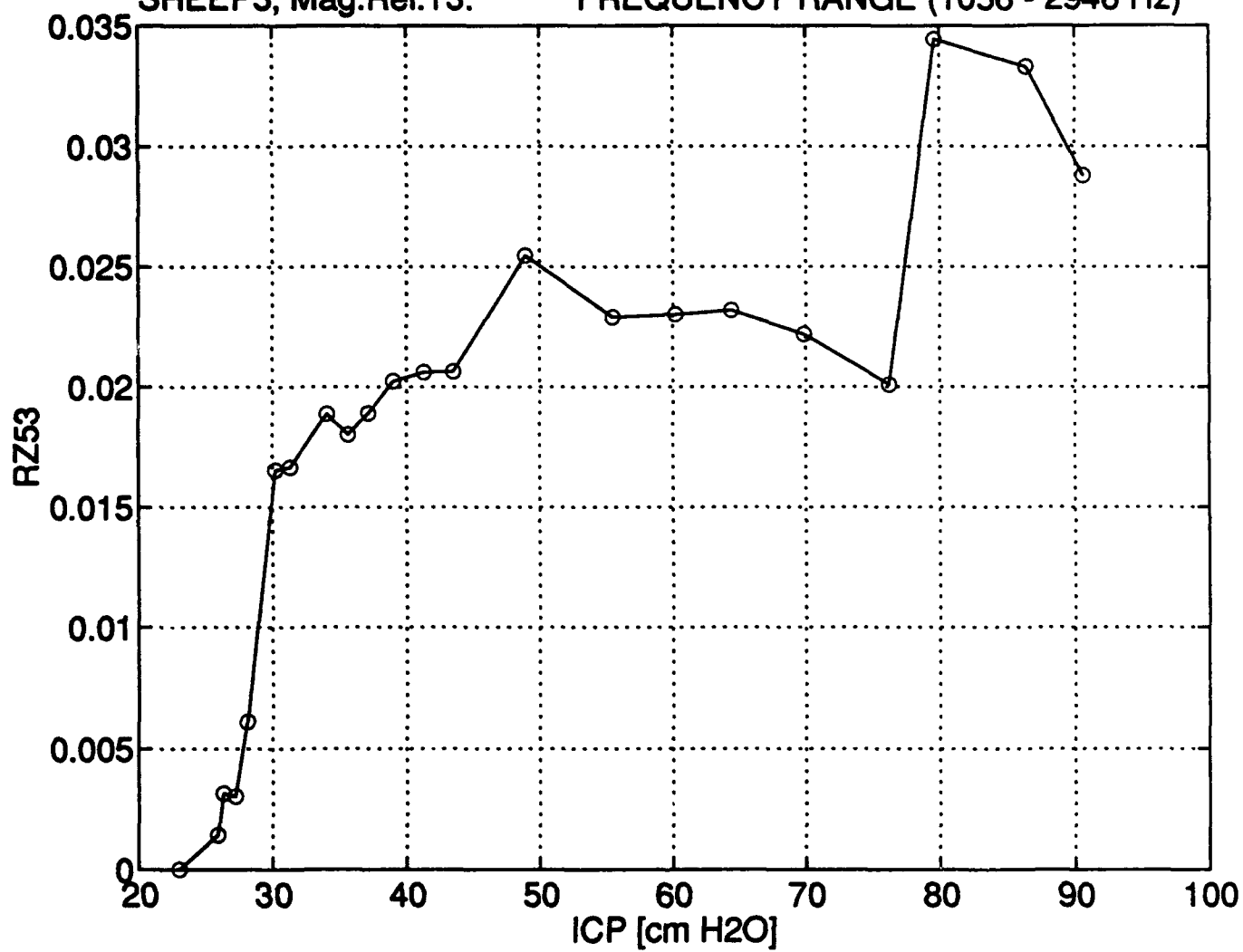
MAGNITUDE OF RELATIVE TRANSFER IMPEDANCE 3, SHEEP5
FREQUENCY RANGE (2496 - 3296 Hz)
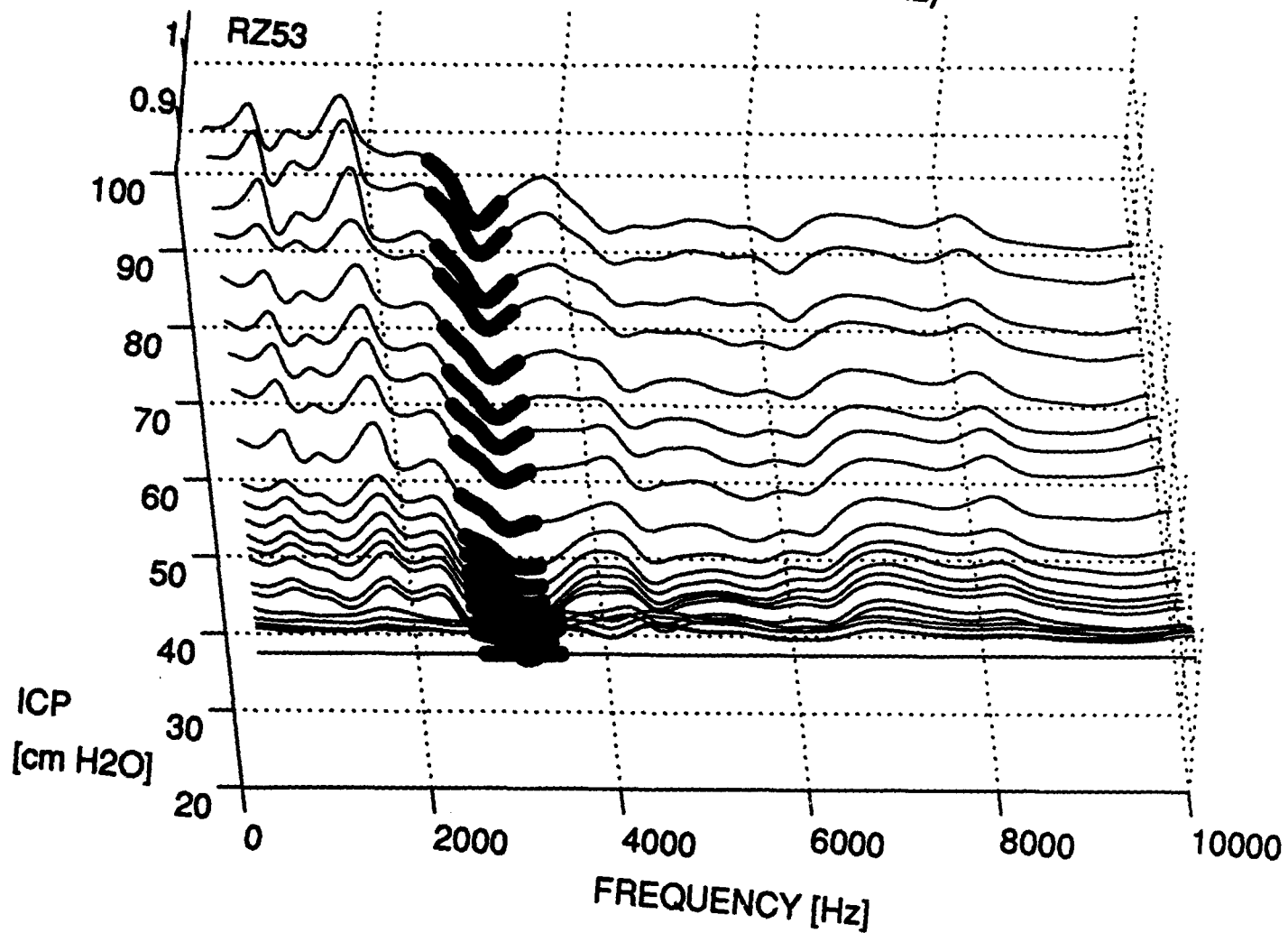
MAGNITUDE STANDARD DEVIATION vs. ICP
SHEEP5, Mag.Rel.T3.   FREQUENCY RANGE (2496 - 3296 Hz)
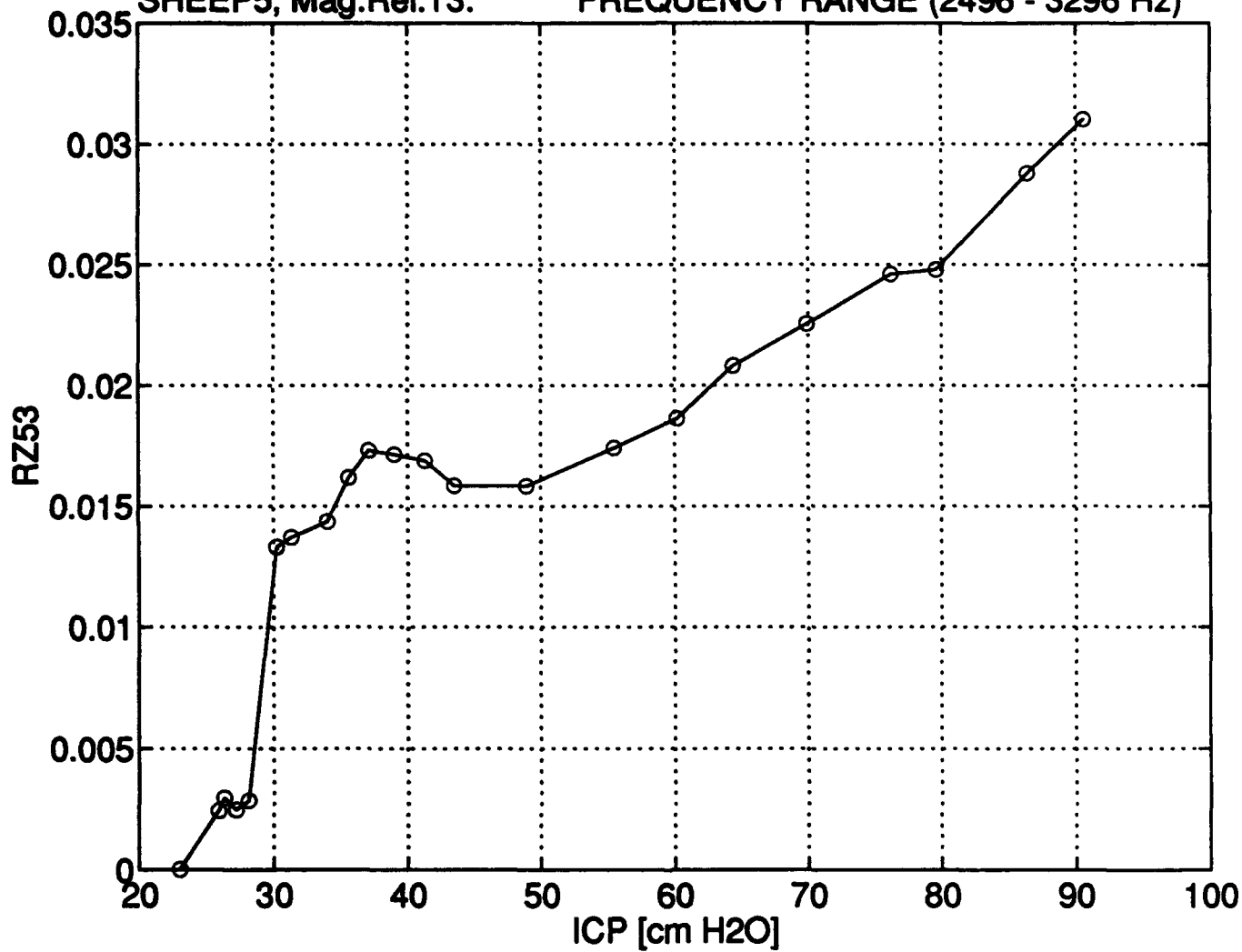
MAGNITUDE OF RELATIVE TRANSFER IMPEDANCE 3, SHEEP5
FREQUENCY RANGE (3536 - 4896 Hz)
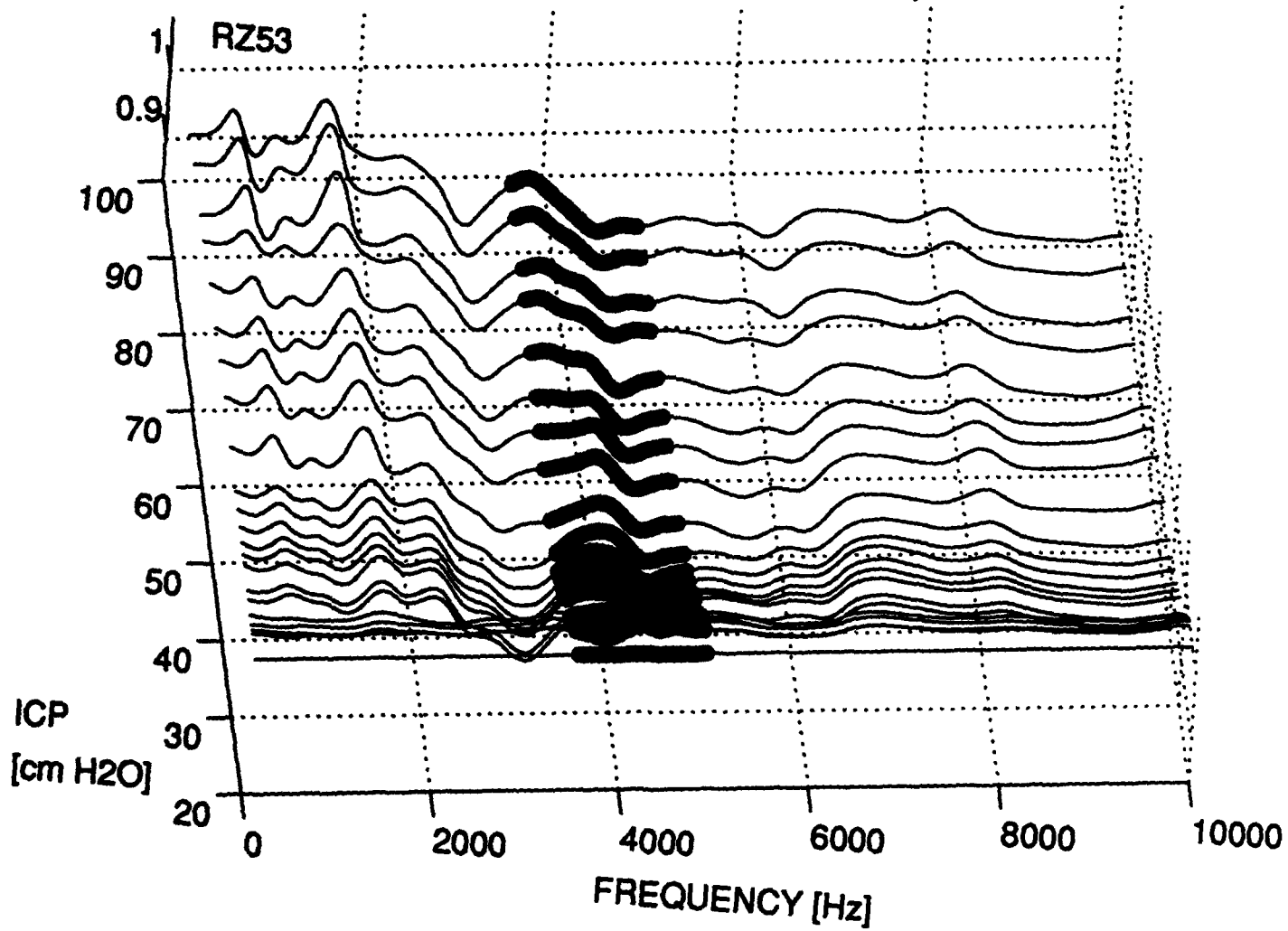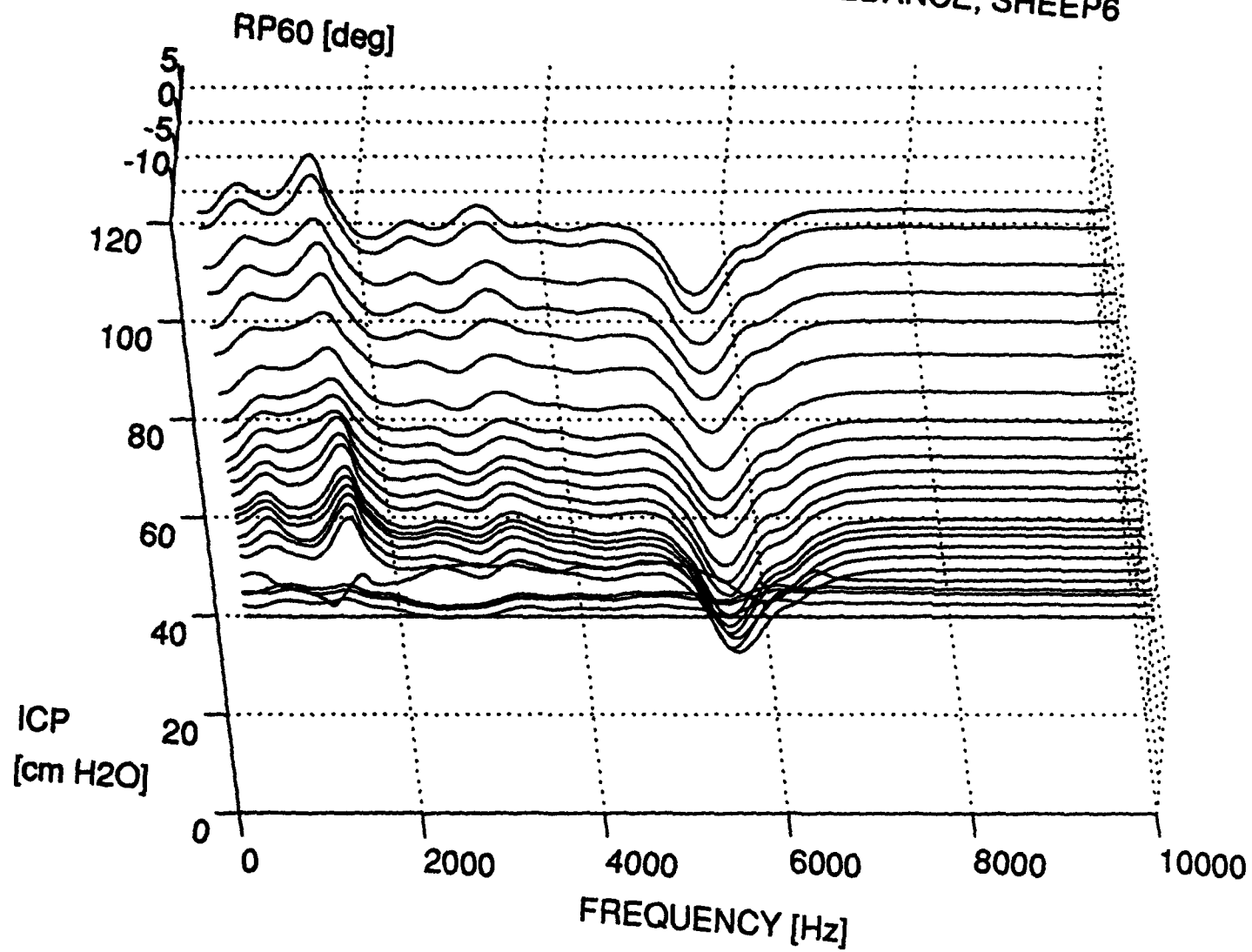
MAGNITUDE STANDARD DEVIATION vs. ICP
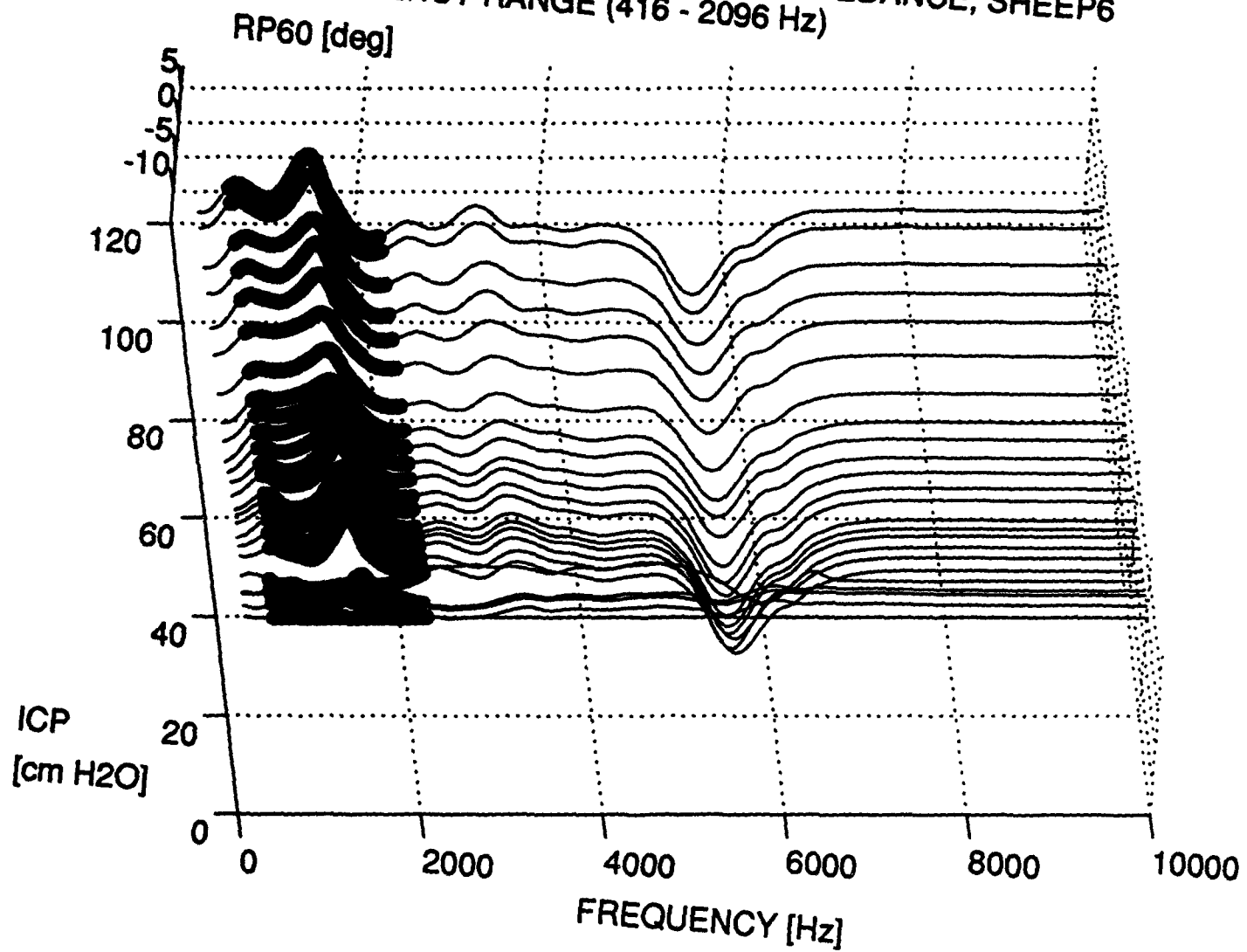SHEEP5, Mag.Rel.T3.   FREQUENCY RANGE (3536 - 4896 Hz)
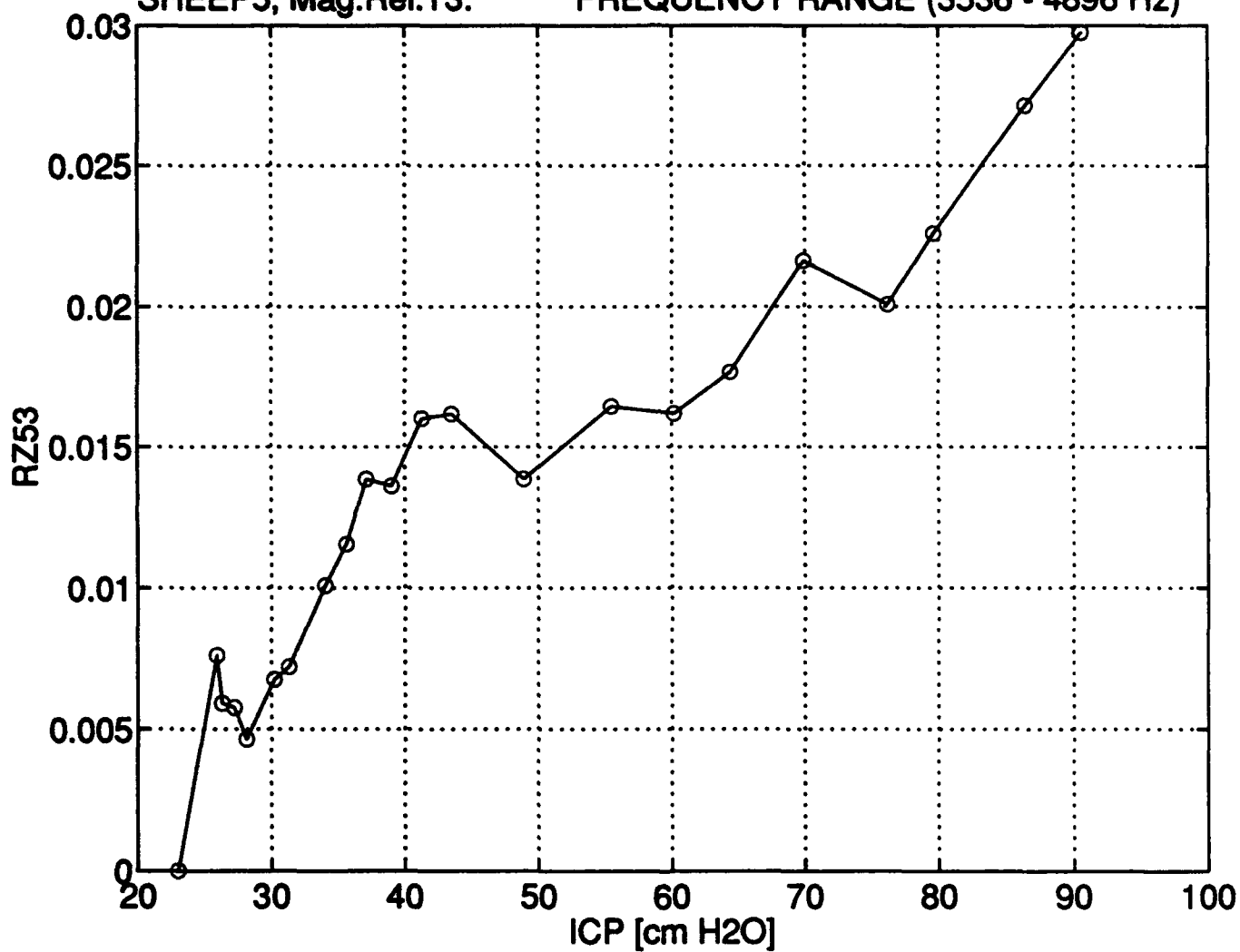
PHASE OF RELATIVE DRIVING POINT IMPEDANCE, SHEEP5
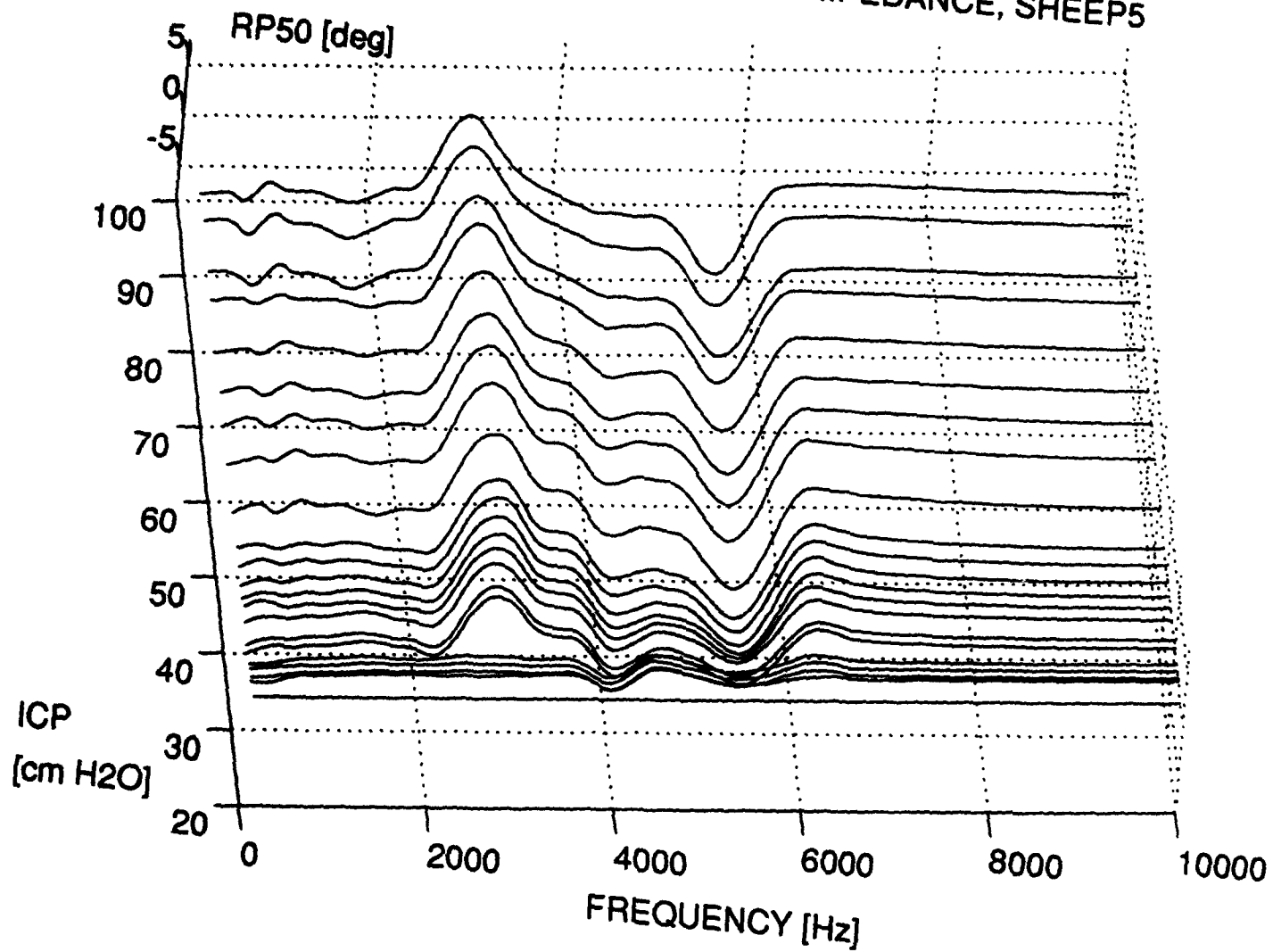
LATIVE DRIVING POINT IMPEDANCE, SHEEP5
QUENCY RANGE (104 - 1136 Hz)

: (104 - 1136 Hz)

FREQUENCY [Hz]

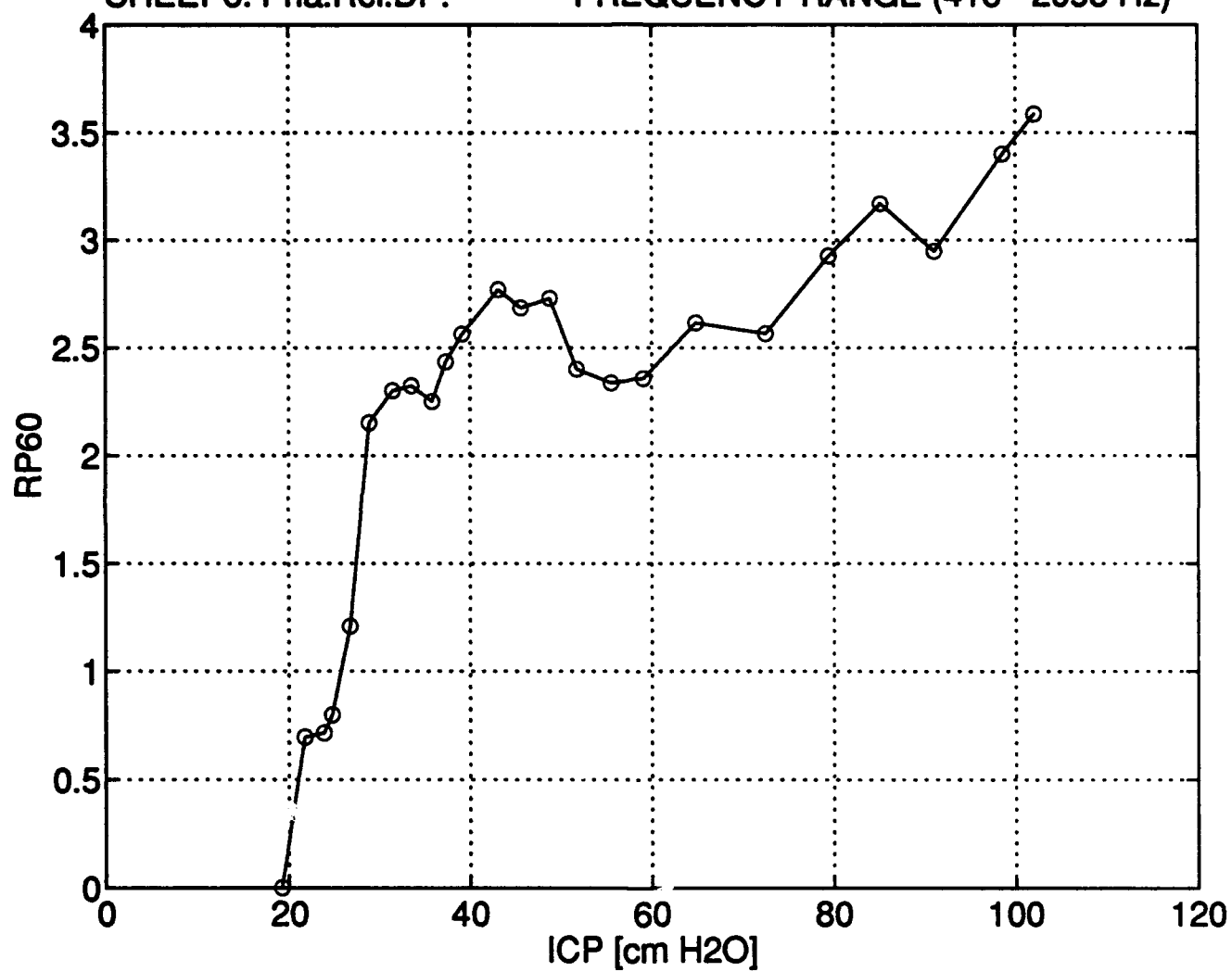2000   4000   6000   8000   10000

80   90   100

PHASE OF RELATIVE DRIVING POINT IMPEDANCE, SHEEP5
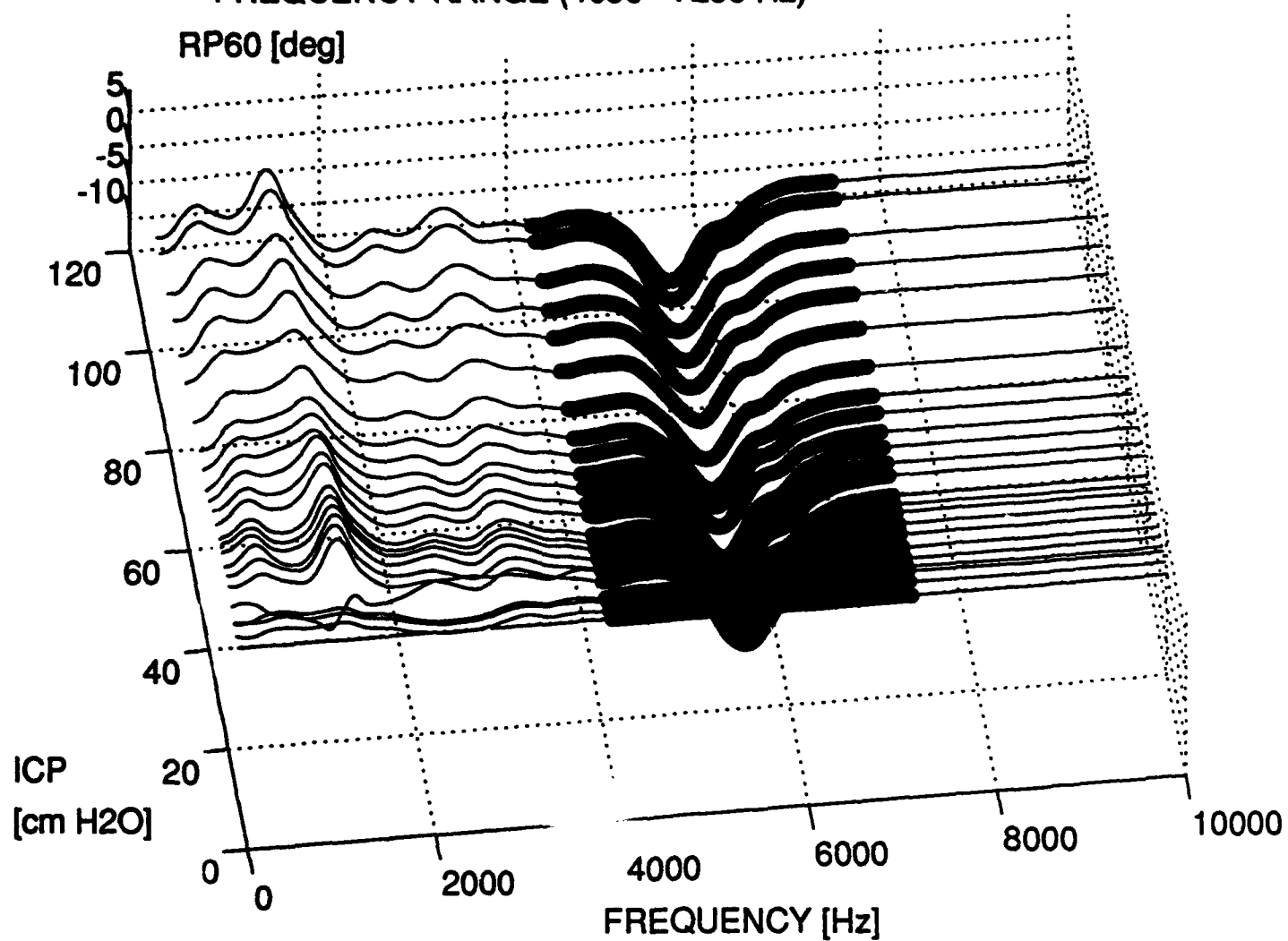FREQUENCY RANGE (2000 - 3296 Hz)

PHASE STANDARD DEVIATION vs. ICP
SHEEP5: Pha.Rel.DP.   FREQUENCY RANGE (2000 - 3296 Hz)

PHASE OF RELATIVE DRIVING POINT IMPEDANCE, SHEEP5
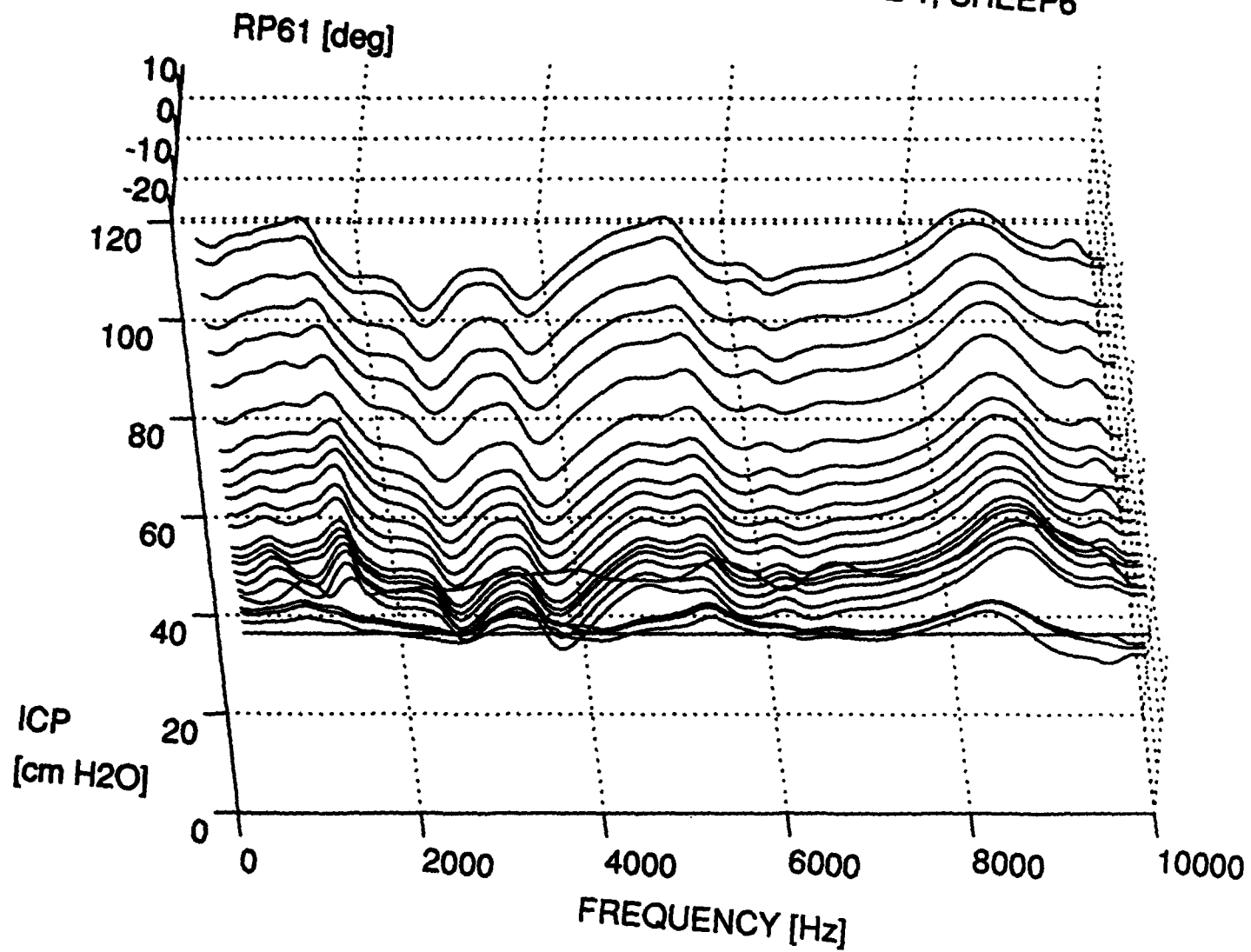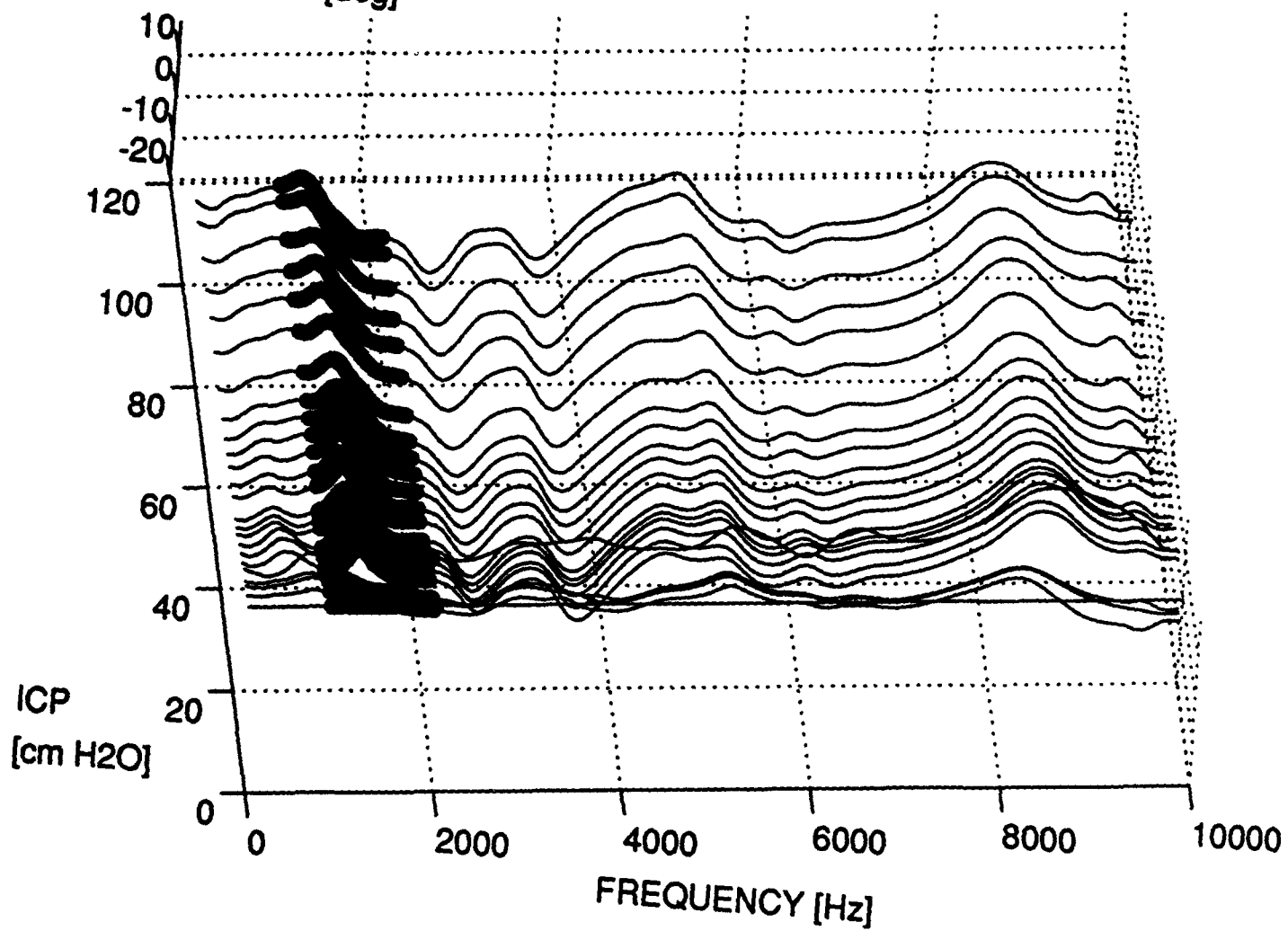FREQUENCY RANGE (5000 - 6496 Hz)

PHASE STANDARD DEVIATION vs. ICP
SHEEP5: Pha.Rel.DP.   FREQUENCY RANGE (5000 - 6496 Hz)

PHASE OF RELATIVE TRANSFER IMPEDANCE 1, SHEEP5

PHASE OF RELATiVE TRANSFER IMPEDANCE 1, SHEEP5
FREQUENCY RANGE (104 - 1216 Hz)

RP51 [deg]

ICP
[cm H2O]

FREQUENCY [Hz]

PHASE STANDARD DEVIATION vs. ICP
SHEEP5: Pha.Rel.T1.   FREQUENCY RANGE (104 - 1216 Hz)

PHASE OF RELATIVE TRANSFER IMPEDANCE 1, SHEEP5
FREQUENCY RANGE (1456 - 2496 Hz)
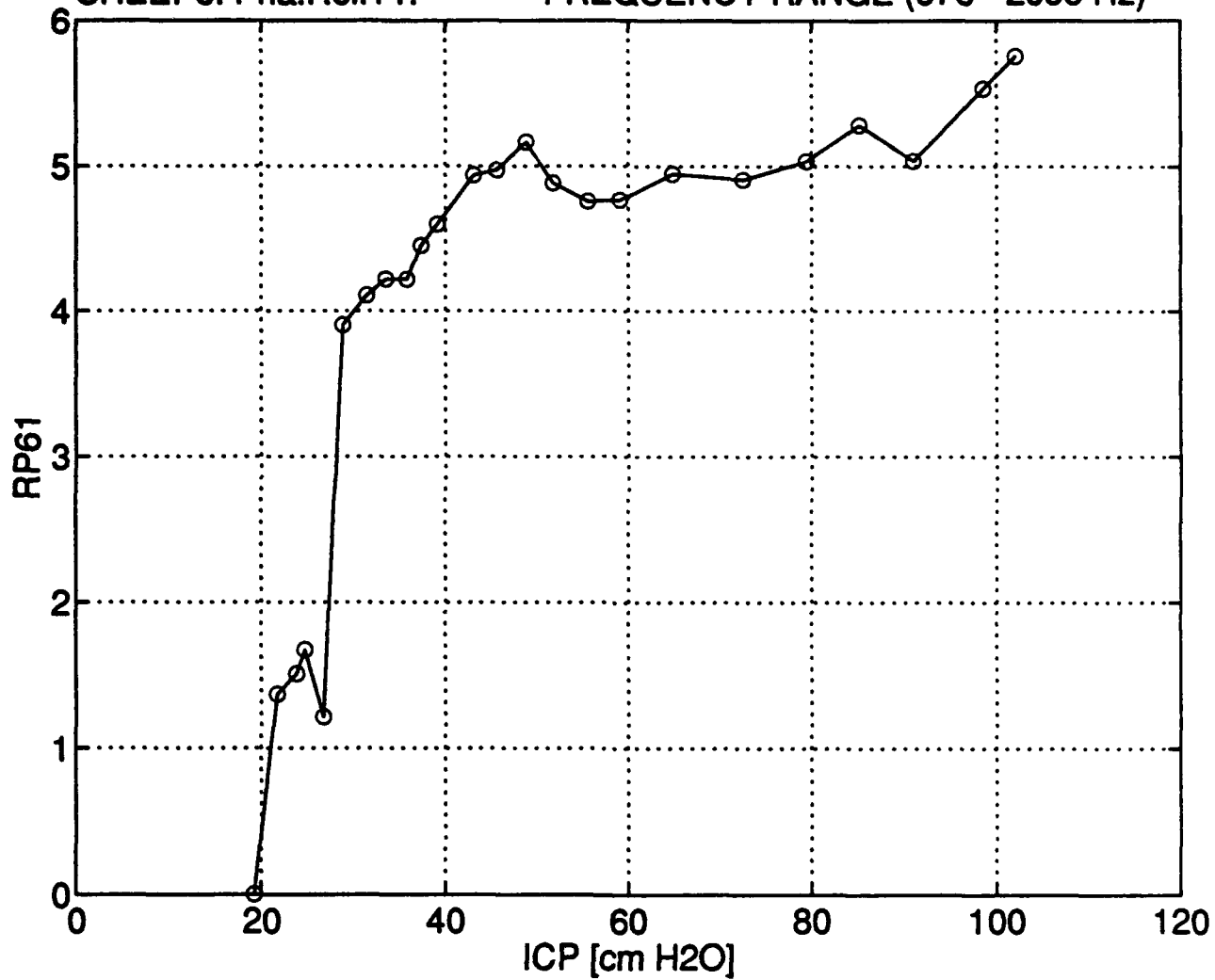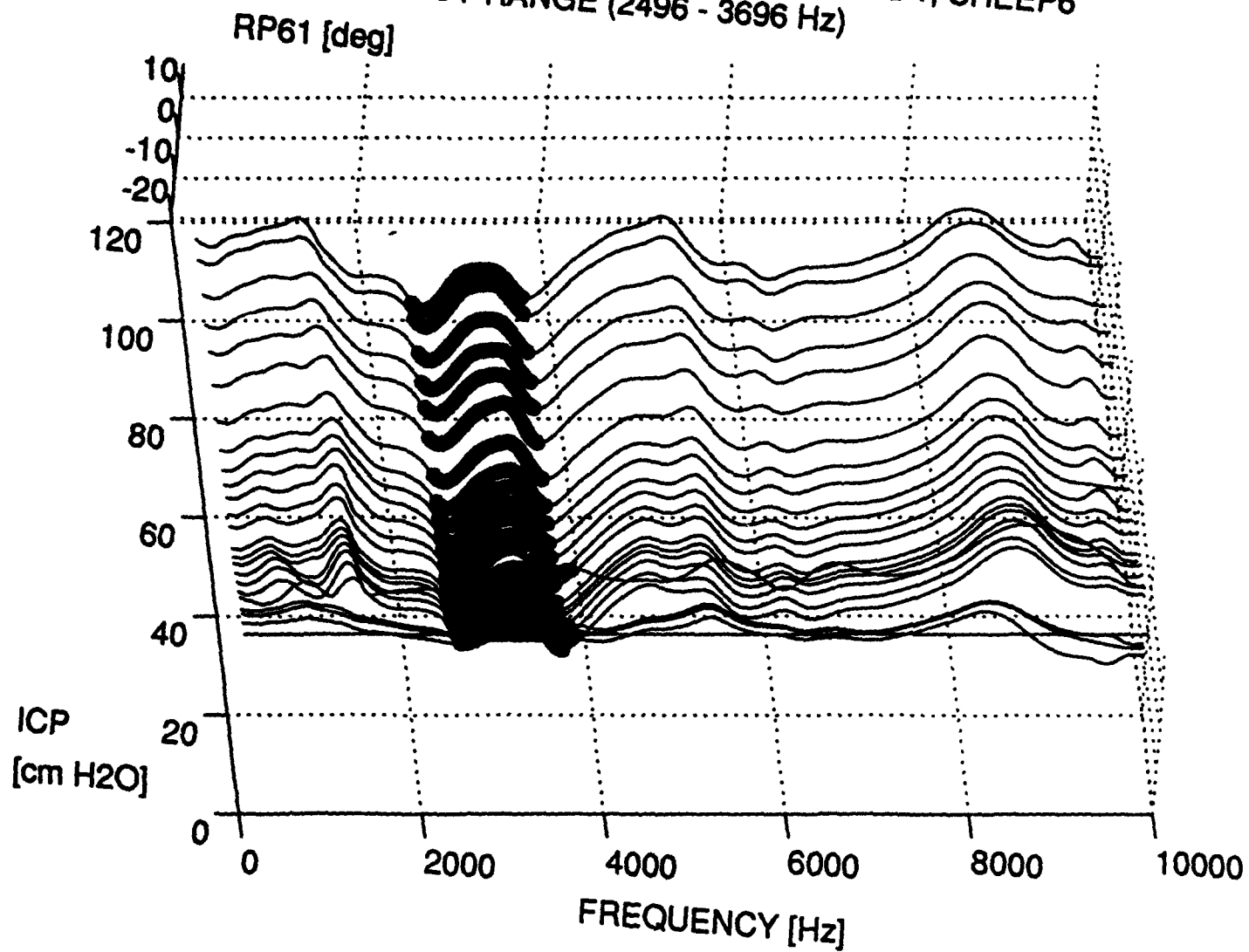
PHASE STANDARD DEVIATION vs. ICP
SHEEP5: Pha.Rel.T1.   FREQUENCY RANGE (1456 - 2496 Hz)

PHASE OF RELATIVE TRANSFER IMPEDANCE 1, SHEEP5
FREQUENCY RANGE (4336 - 4896 Hz)

PHASE STANDARD DEVIATION vs. ICP
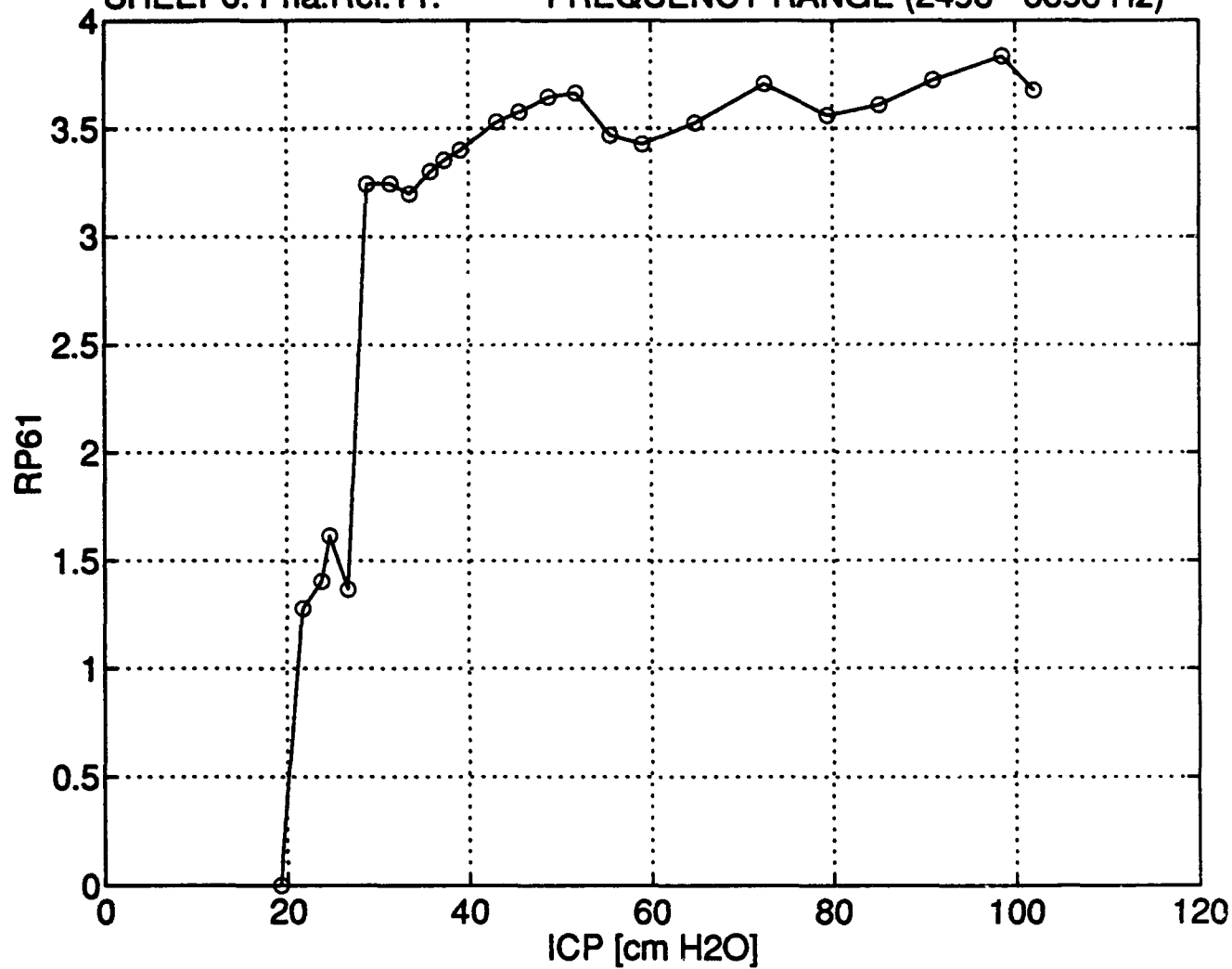SHEEP5: Pha.Rel.T1.   FREQUENCY RANGE (4336 - 4896 Hz)

PHASE OF RELATIVE TRANSFER IMPEDANCE 1, SHEEP5
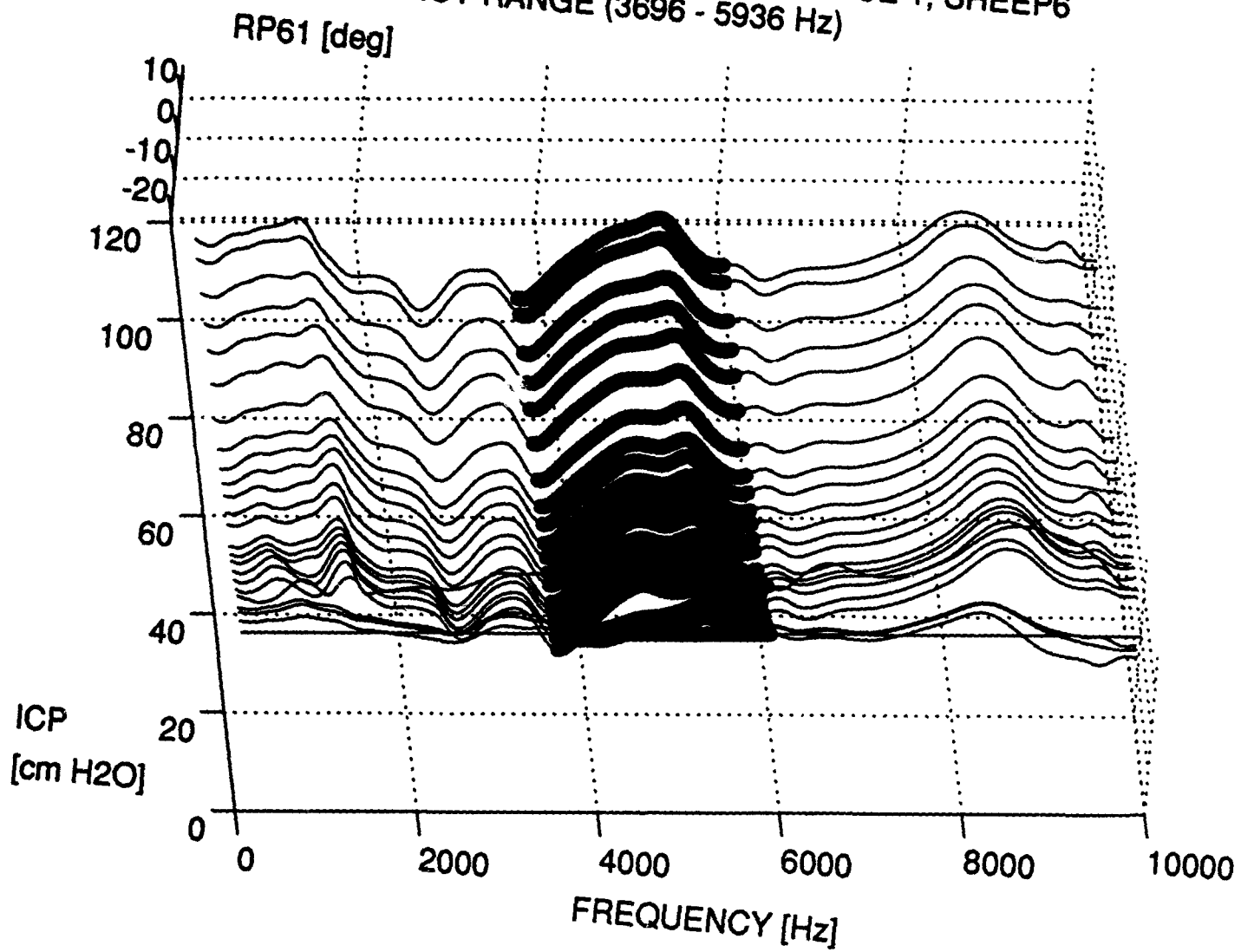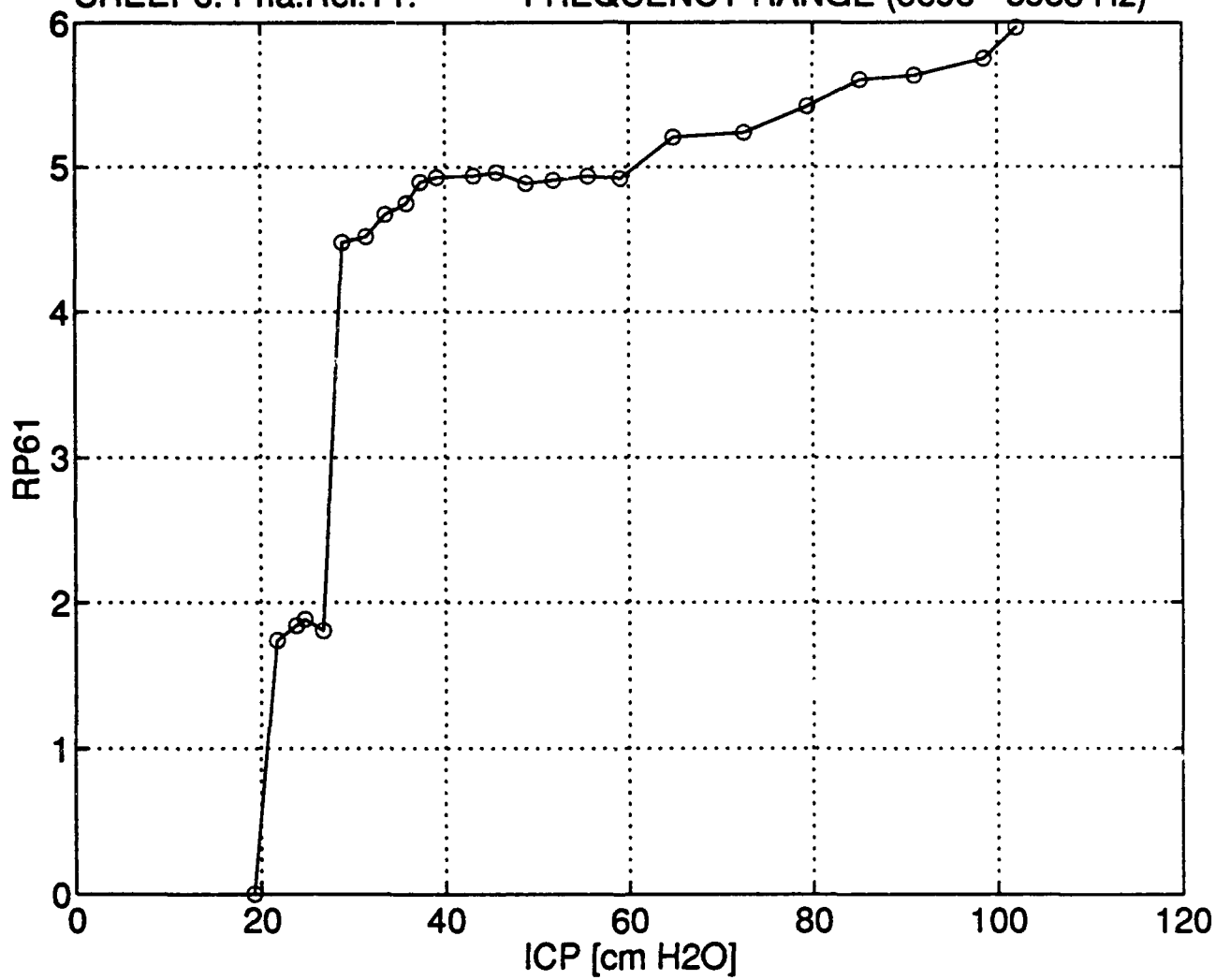FREQUENCY RANGE (4896 - 6496 Hz)

PHASE STANDARD DEVIATION vs. ICP
SHEEP5: Pha.Rel.T1.   FREQUENCY RANGE (4896 - 6496 Hz)
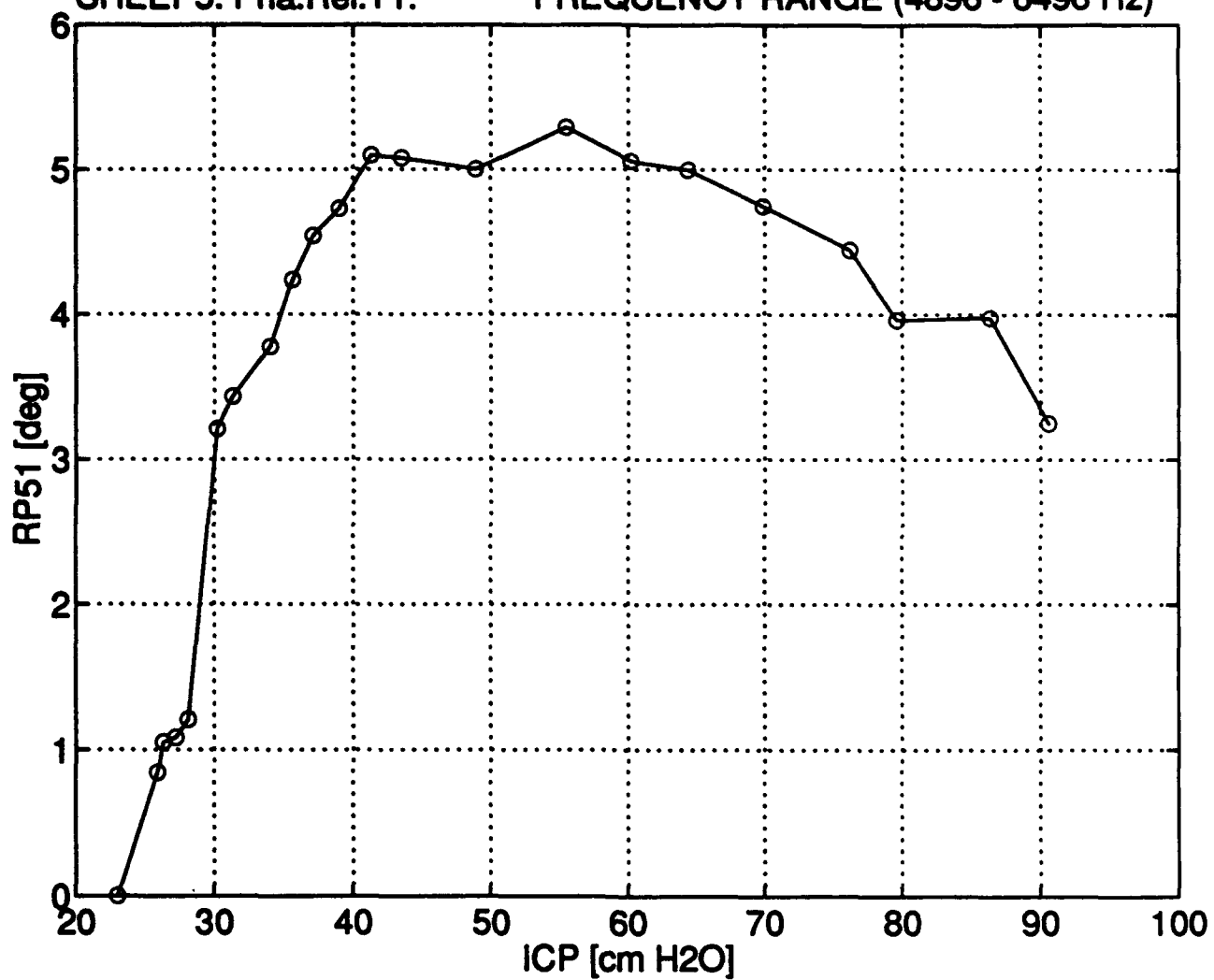
PHASE OF RELATIVE TRANSFER IMPEDANCE 1, SHEEP5
FREQUENCY RANGE (8096 - 9056 Hz)

PHASE STANDARD DEVIATION vs. ICP
SHEEP5: Pha.Rel.T1.   FREQUENCY RANGE (8096 - 9056 Hz)

PHASE OF RELATIVE TRANSFER IMPEDANCE 2, SHEEP5

PHASE OF RELATIVE TRANSFER IMPEDANCE 2, SHEEP5
FREQUENCY RANGE (104 - 1056 Hz)

RP52 [deg]

ICP
[cm H2O]

FREQUENCY [Hz]

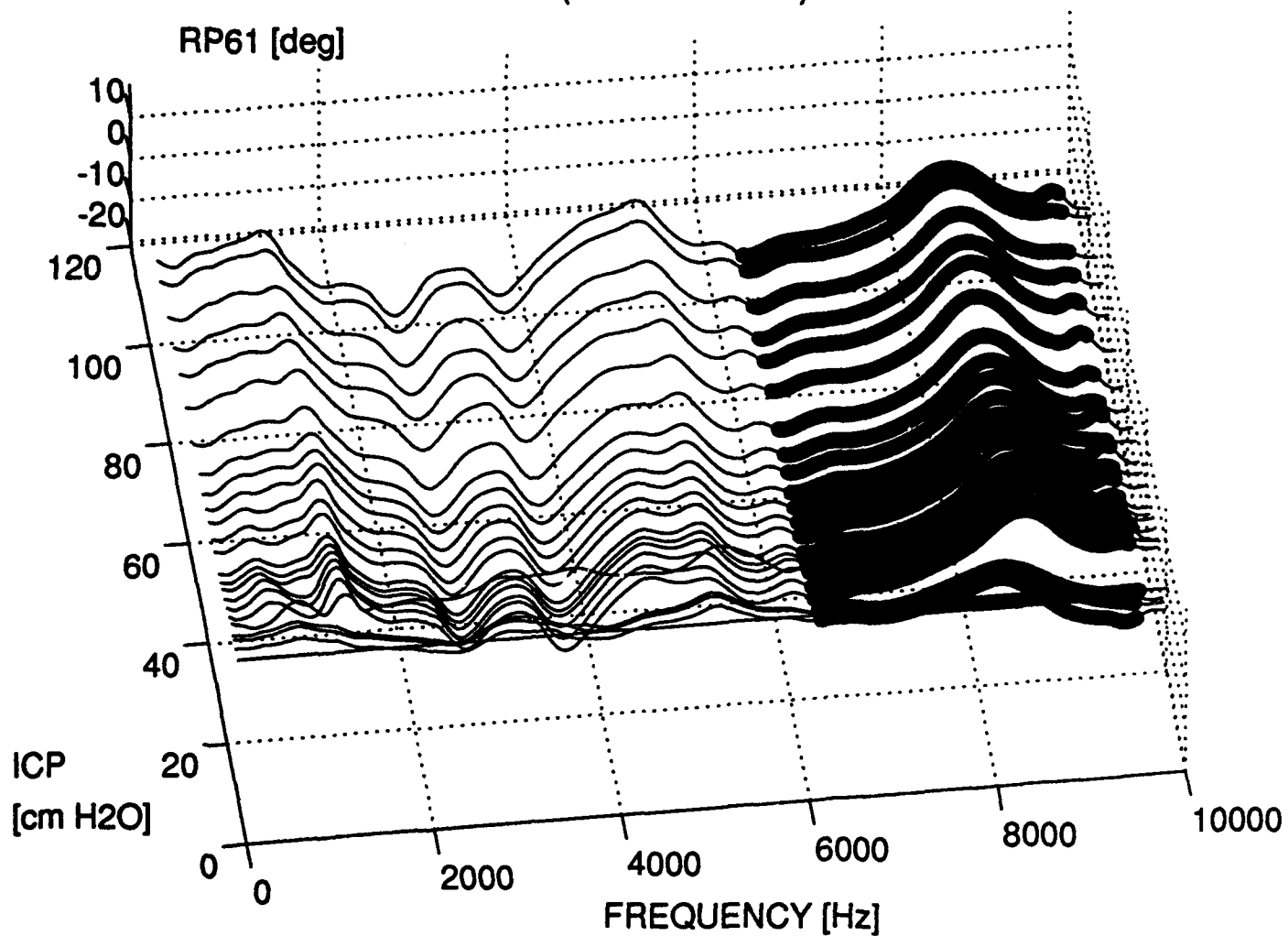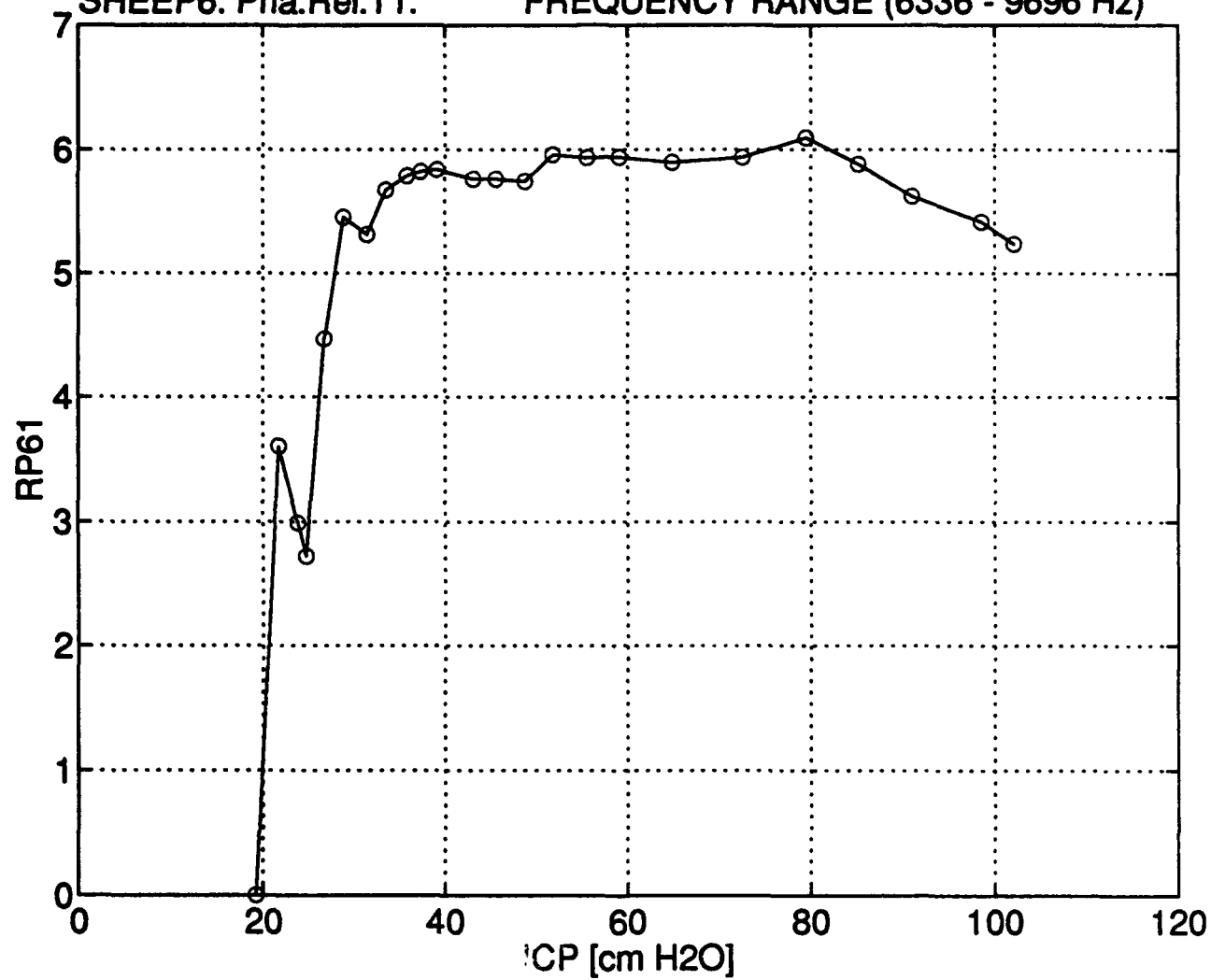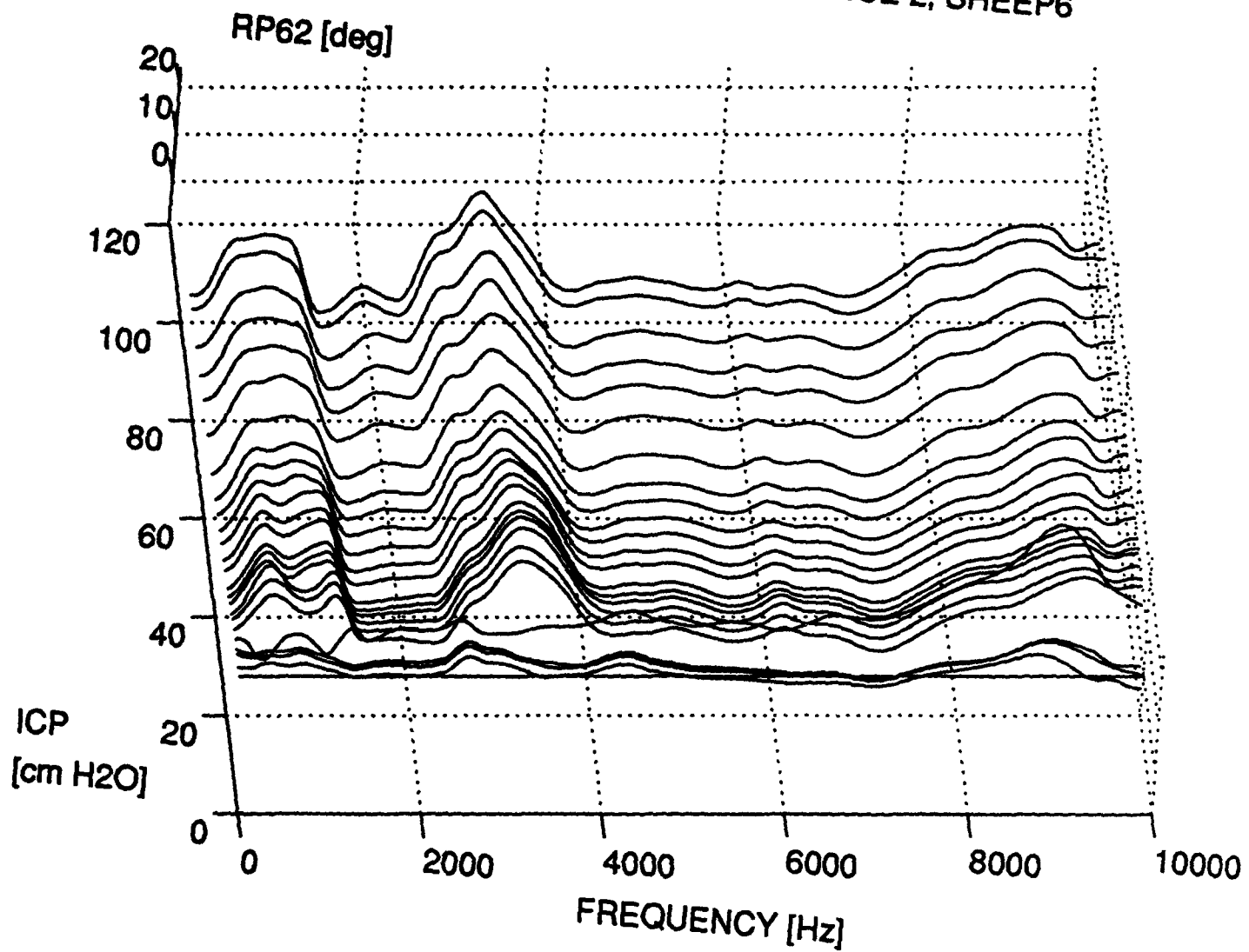PHASE STANDARD DEVIATION vs. ICP
SHEEP5: Pha.Rel.T2.   FREQUENCY RANGE (104 - 1056 Hz)

PHASE OF RELATIVE TRANSFER IMPEDANCE 2, SHEEP5
FREQUENCY RANGE (1696 - 2496 Hz)

PHASE OF RELATIVE TRANSFER IMPEDANCE 2, SHEEP5
FREQUENCY RANGE (5696 - 6256 Hz)
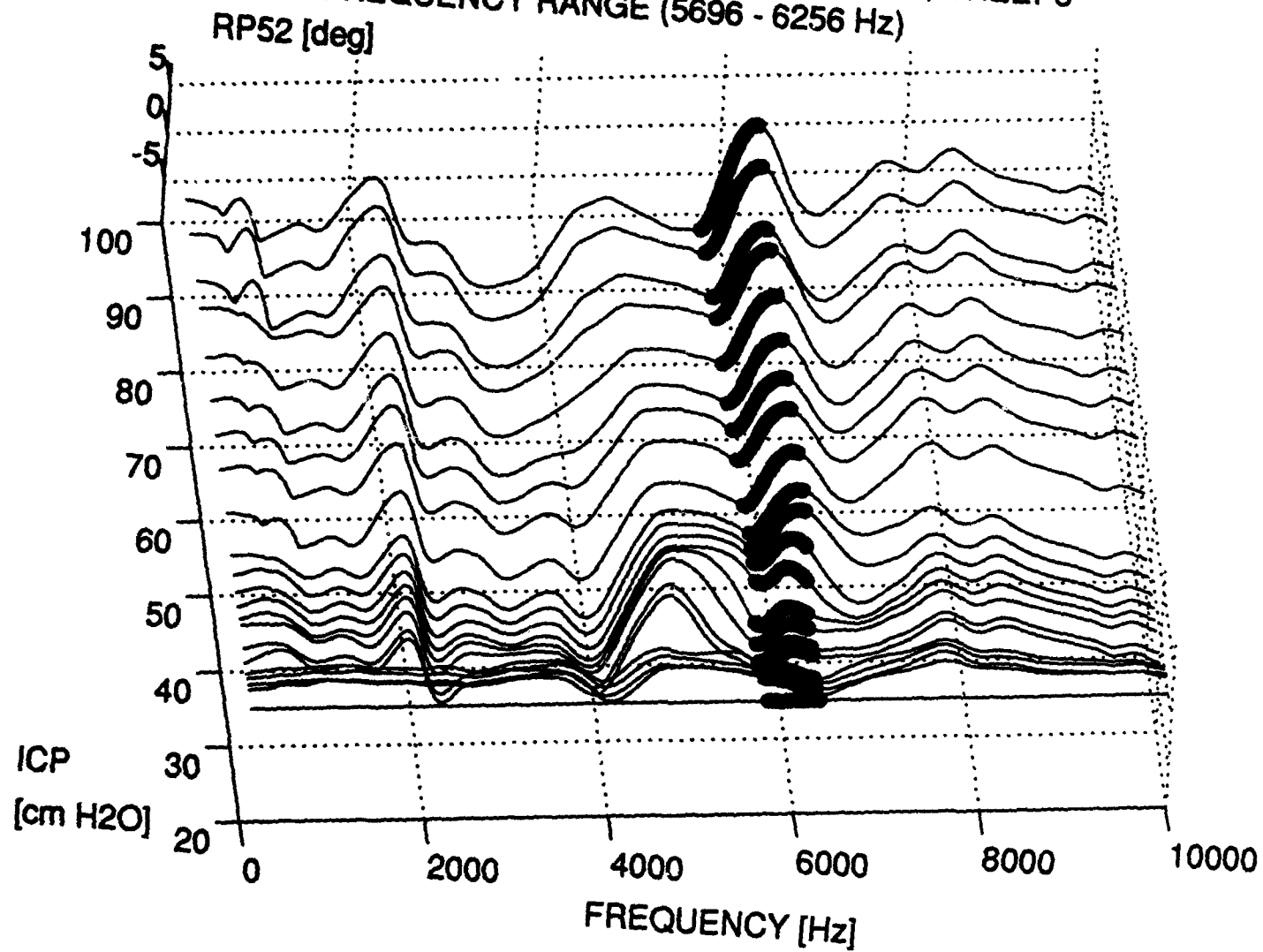
PHASE STANDARD DEVIATION vs. ICP
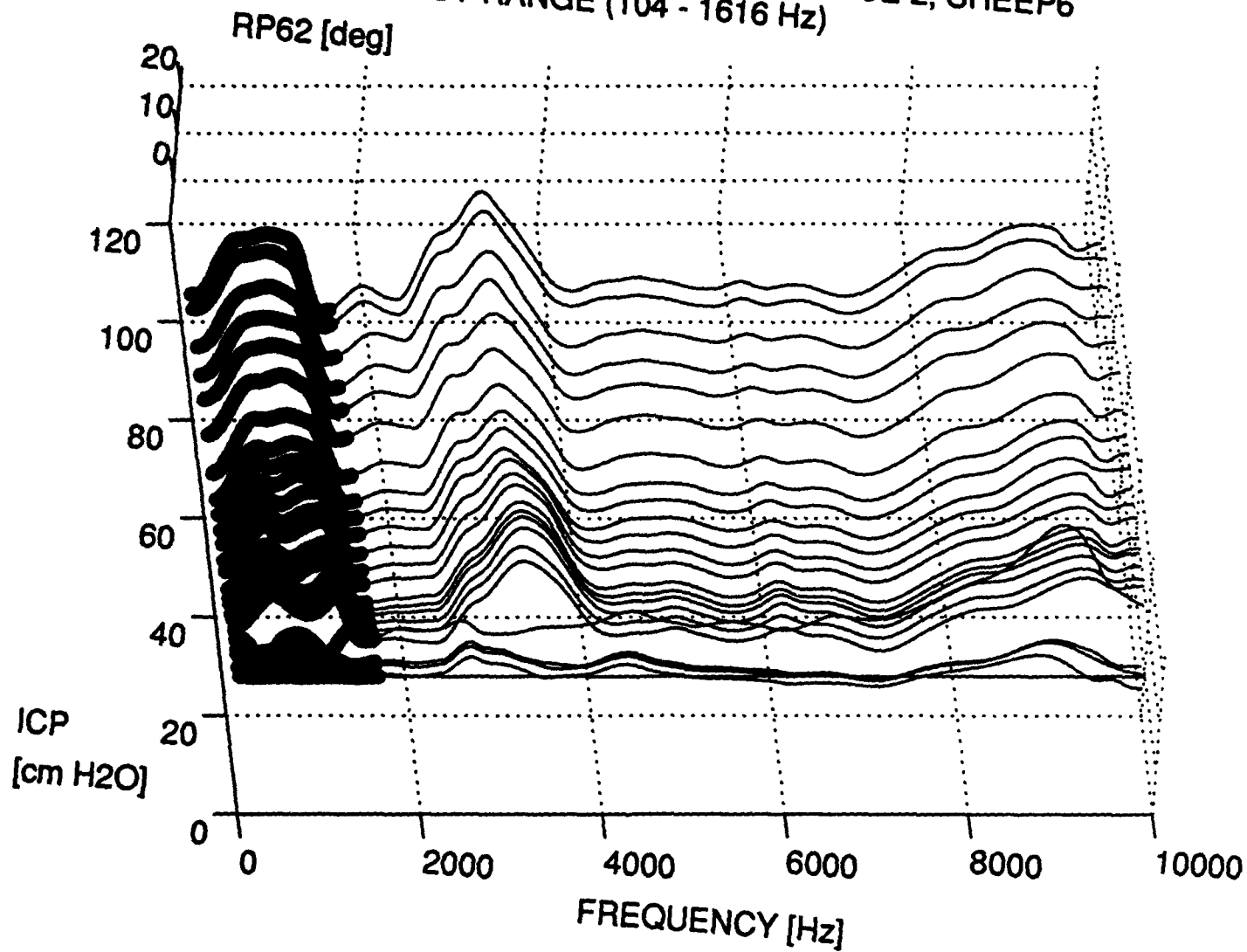SHEEP5: Pha.Rel.T2.   FREQUENCY RANGE (5696 - 6256 Hz)

PHASE OF RELATIVE TRANSFER IMPEDANCE 3, SHEEP5

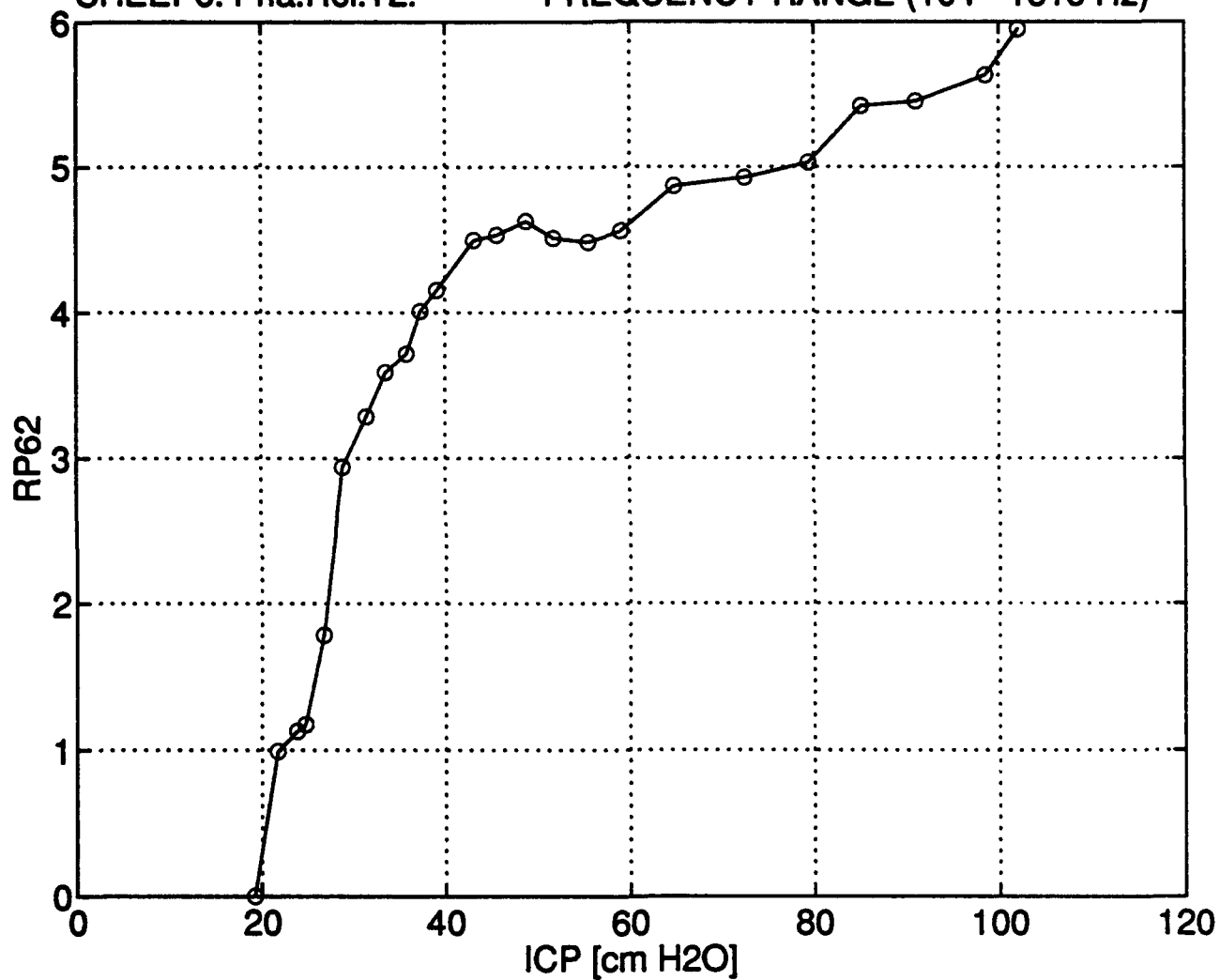RP53 [deg]

ICP
[cm H2O]

FREQUENCY [Hz]

PHASE OF RELATIVE TRANSFER IMPEDANCE 3, SHEEP5
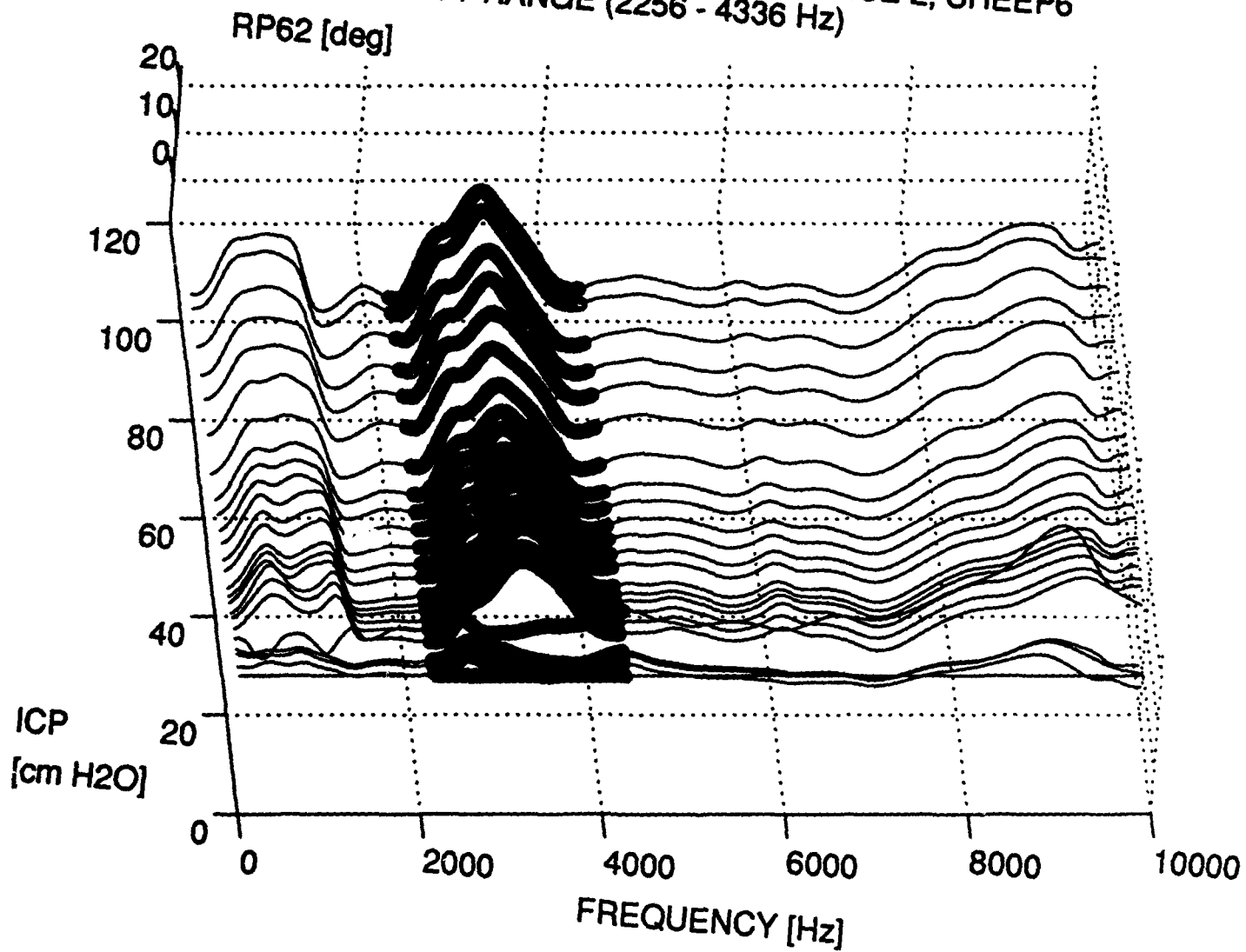FREQUENCY RANGE (104 - 1856 Hz)

PHASE STANDARD DEVIATION vs. ICP
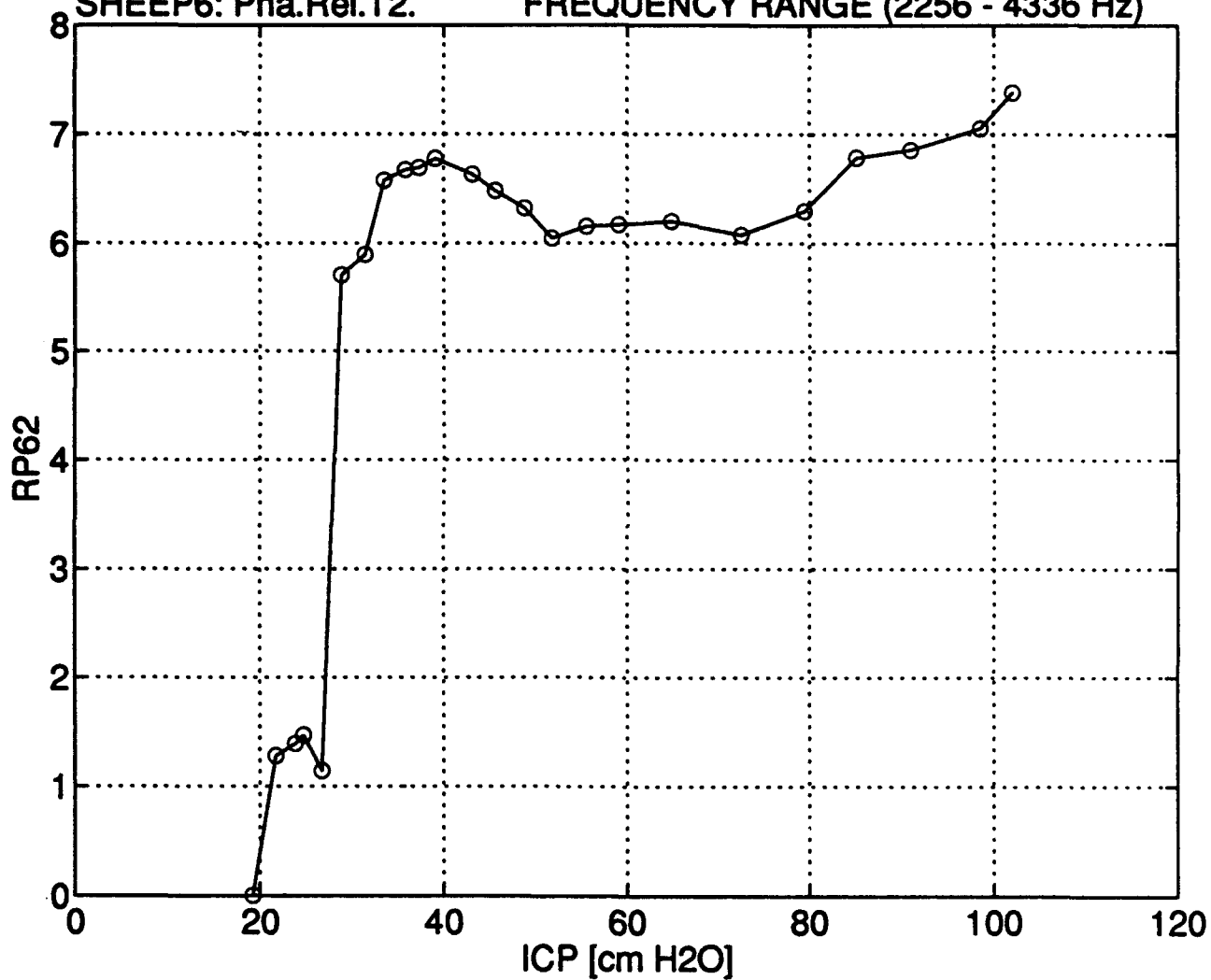SHEEP5, Pha.Rel.T3.   FREQUENCY RANGE (104 - 1856 Hz)

PHASE OF RELATIVE TRANSFER IMPEDANCE 3, SHEEP5
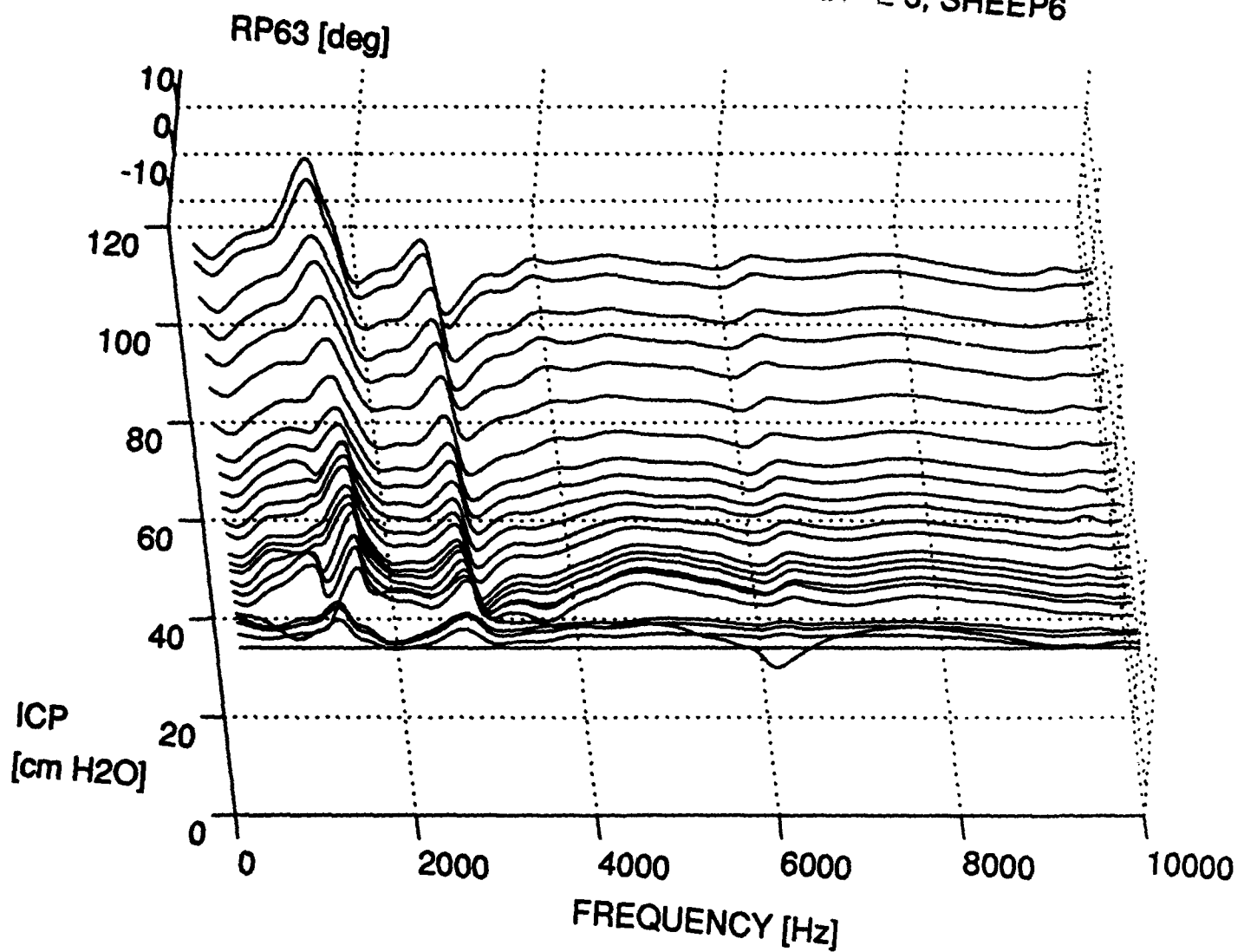FREQUENCY RANGE (2896 - 3296 Hz)
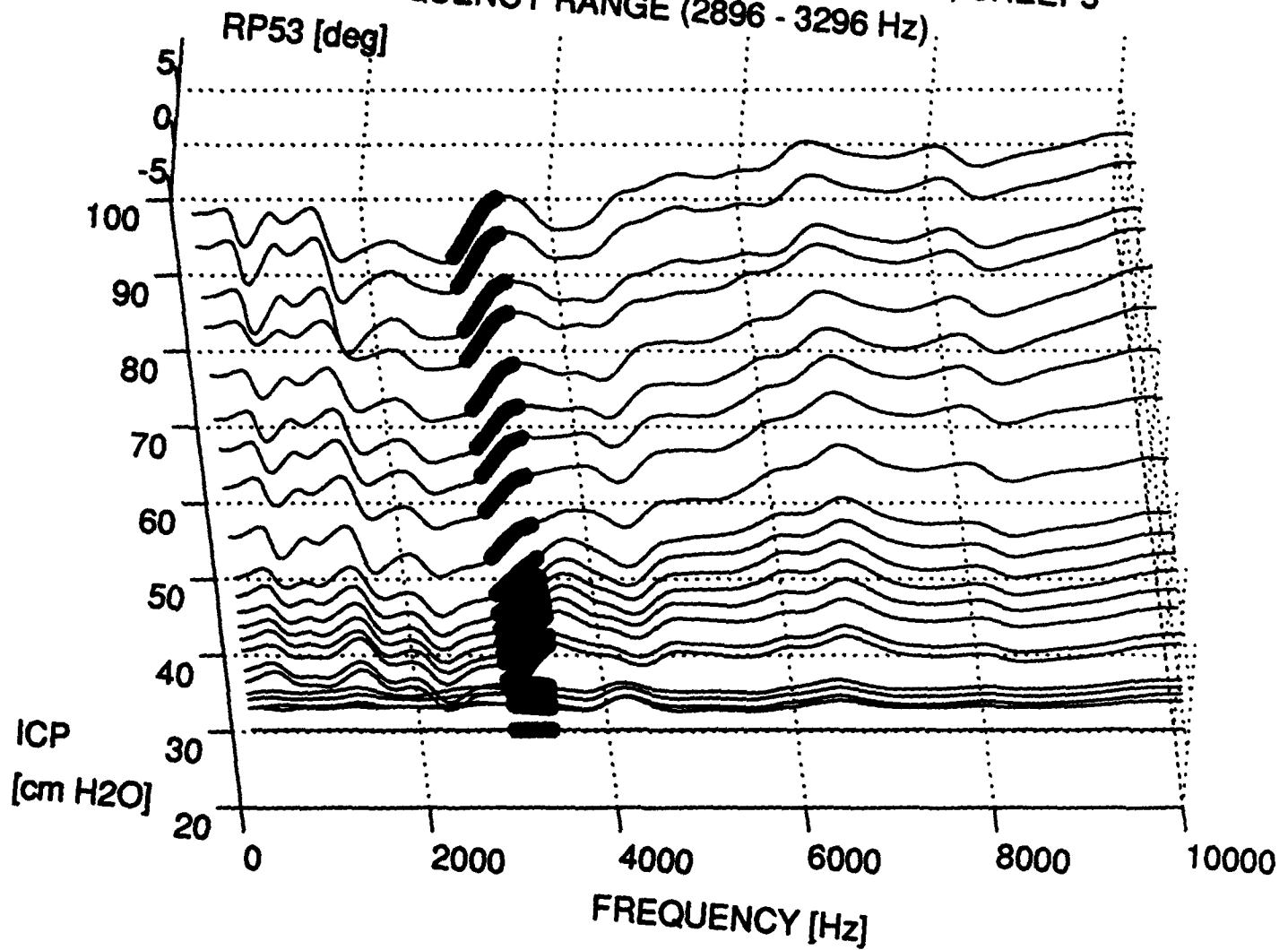
PHASE STANDARD DEVIATION vs. ICP
SHEEP5, Pha.Rel.T3.   FREQUENCY RANGE (2896 - 3296 Hz)
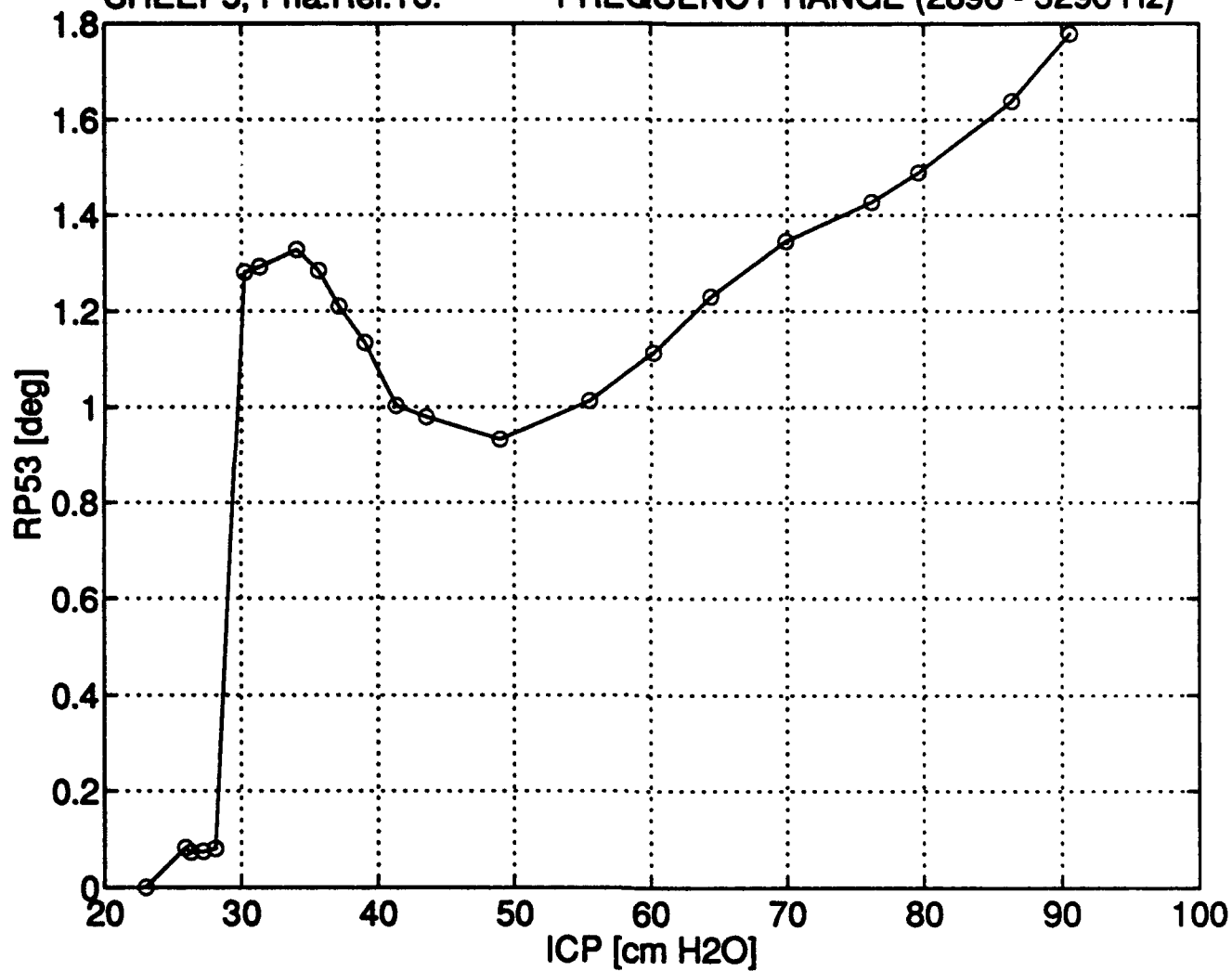
MAGNITUDE OF RELATIVE DRIVING POINT IMPEDANCE, SHEEP6
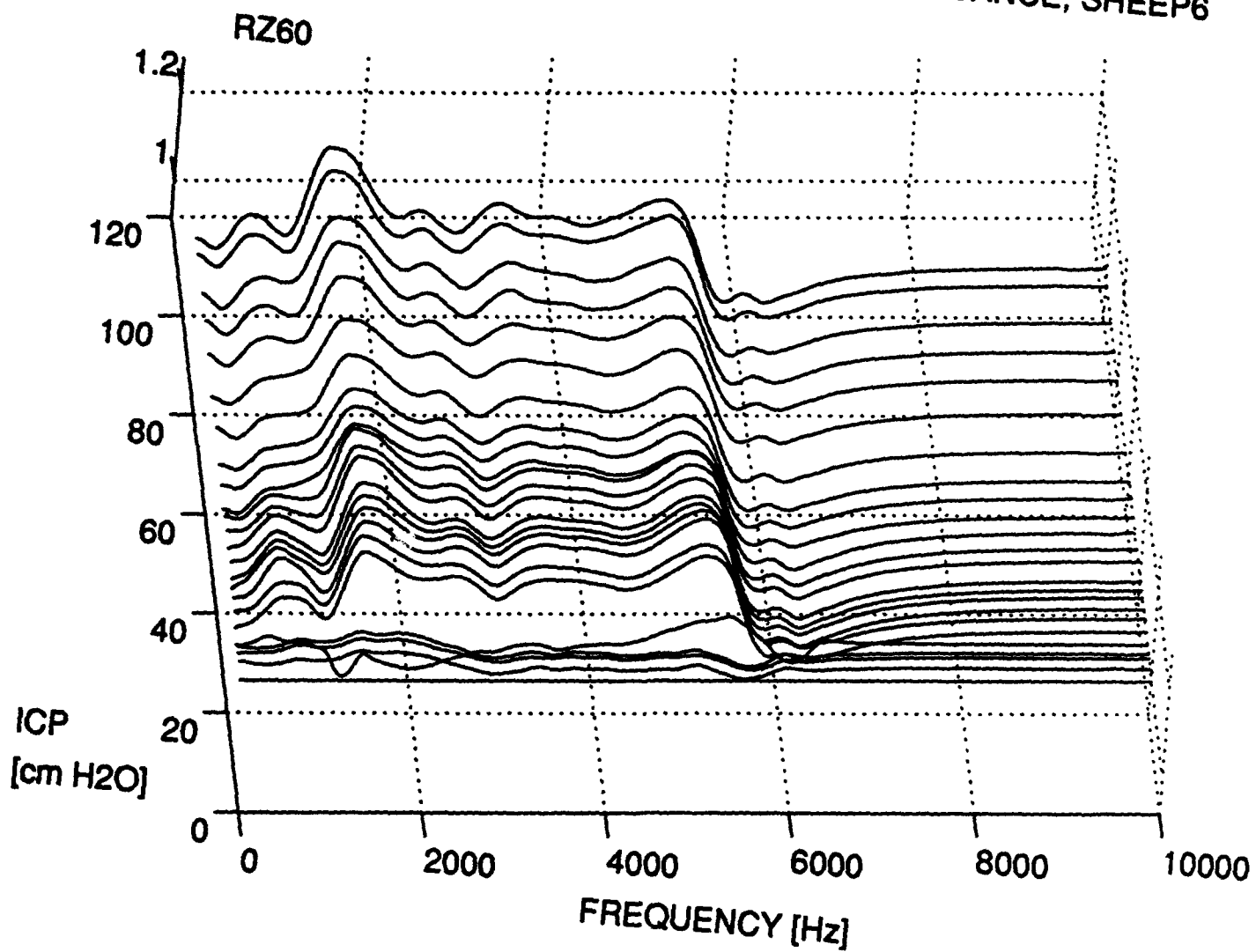
MAGNITUDE OF RELATIVE DRIVING POINT IMPEDANCE, SHEEP6
FREQUENCY RANGE (976 - 2096 Hz)

MAGNITUDE STANDARD DEVIATION vs. ICP
SHEEP6: Mag.Rel.DP.   FREQUENCY RANGE (976 - 2096 Hz)
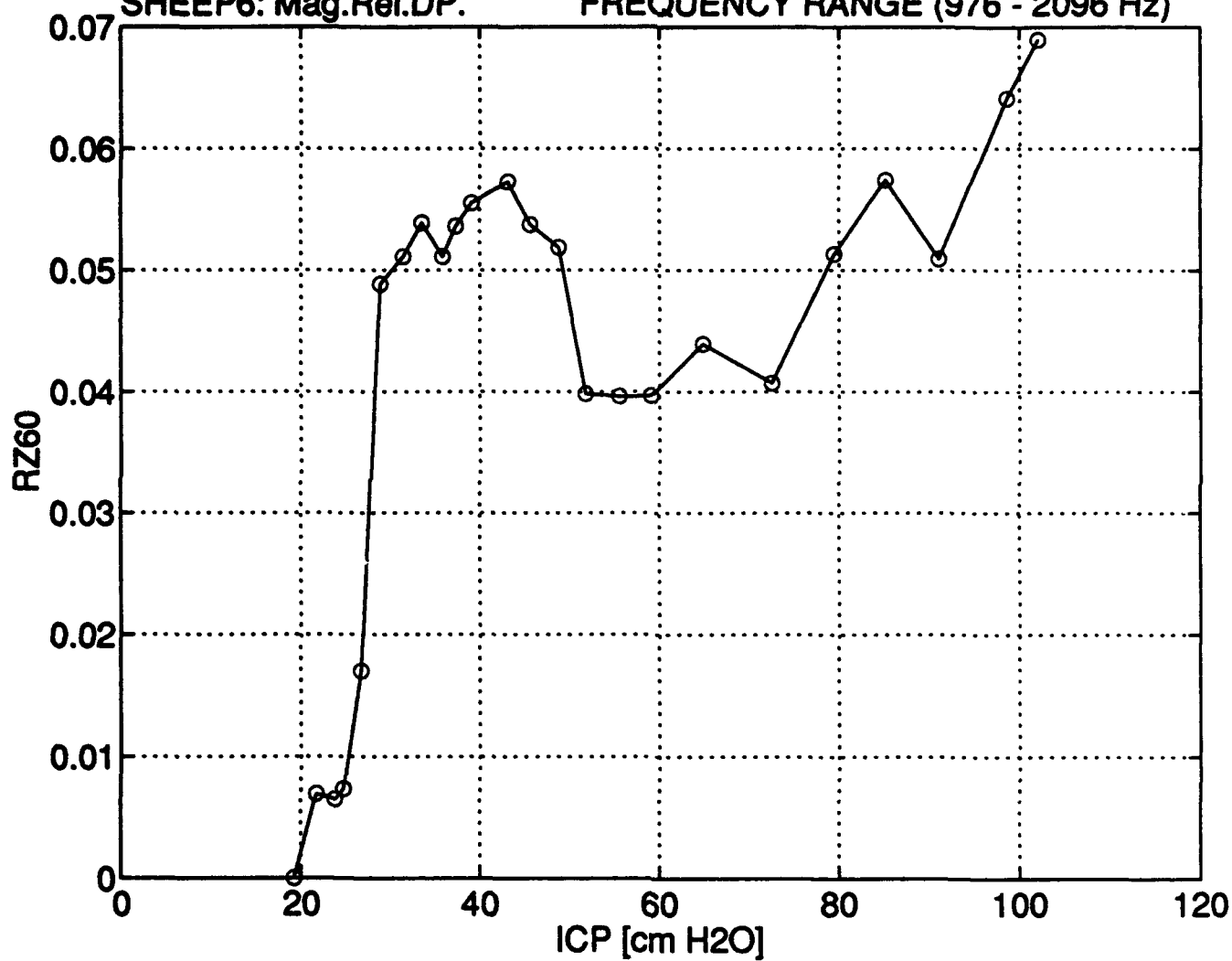
MAGNITUDE OF RELATIVE DRIVING POINT IMPEDANCE, SHEEP6
FREQUENCY RANGE (2896 - 3696 Hz)
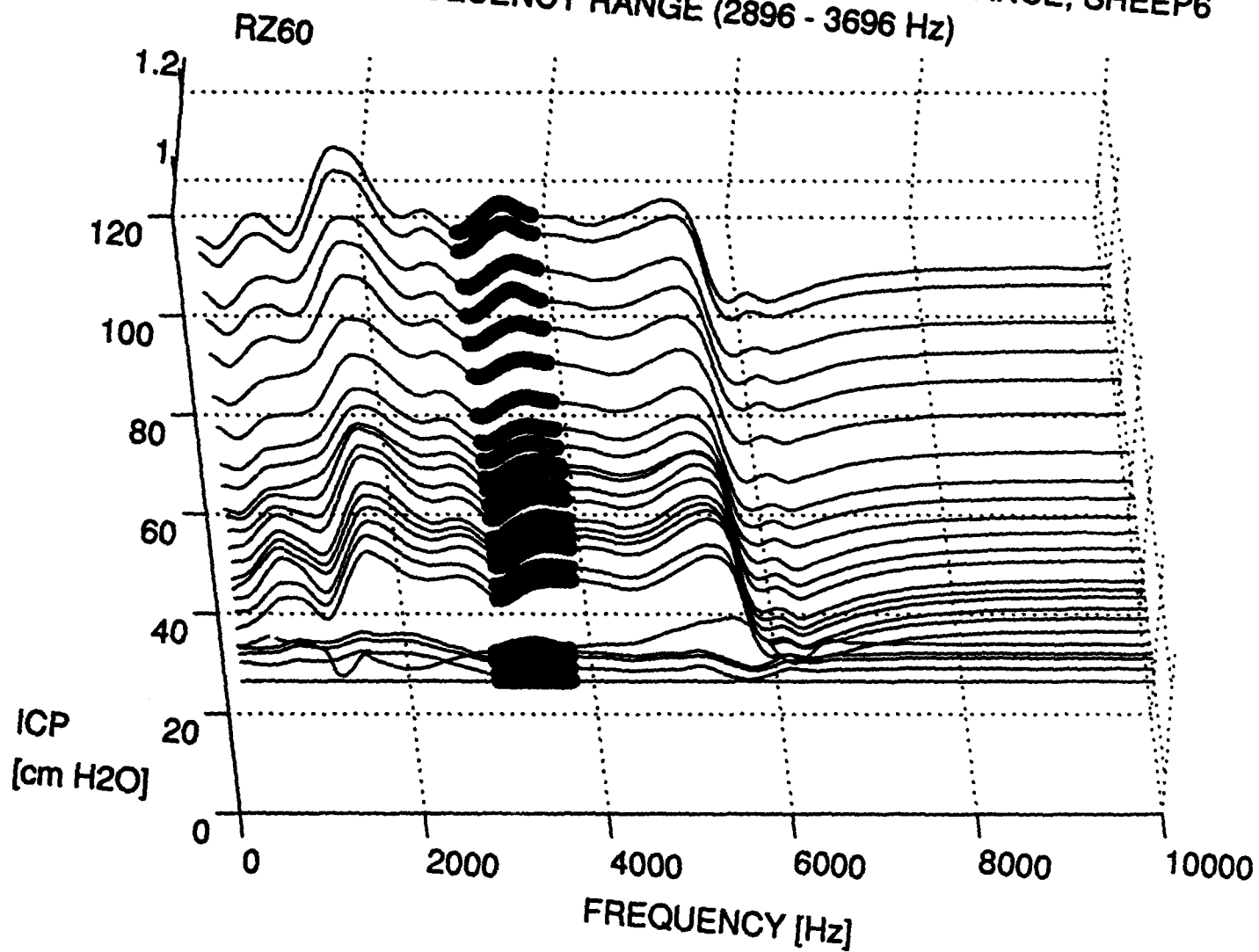
MAGNITUDE STANDARD DEVIATION vs. ICP
SHEEP6: Mag.Rel.DP.   FREQUENCY RANGE (2896 - 3696 Hz)
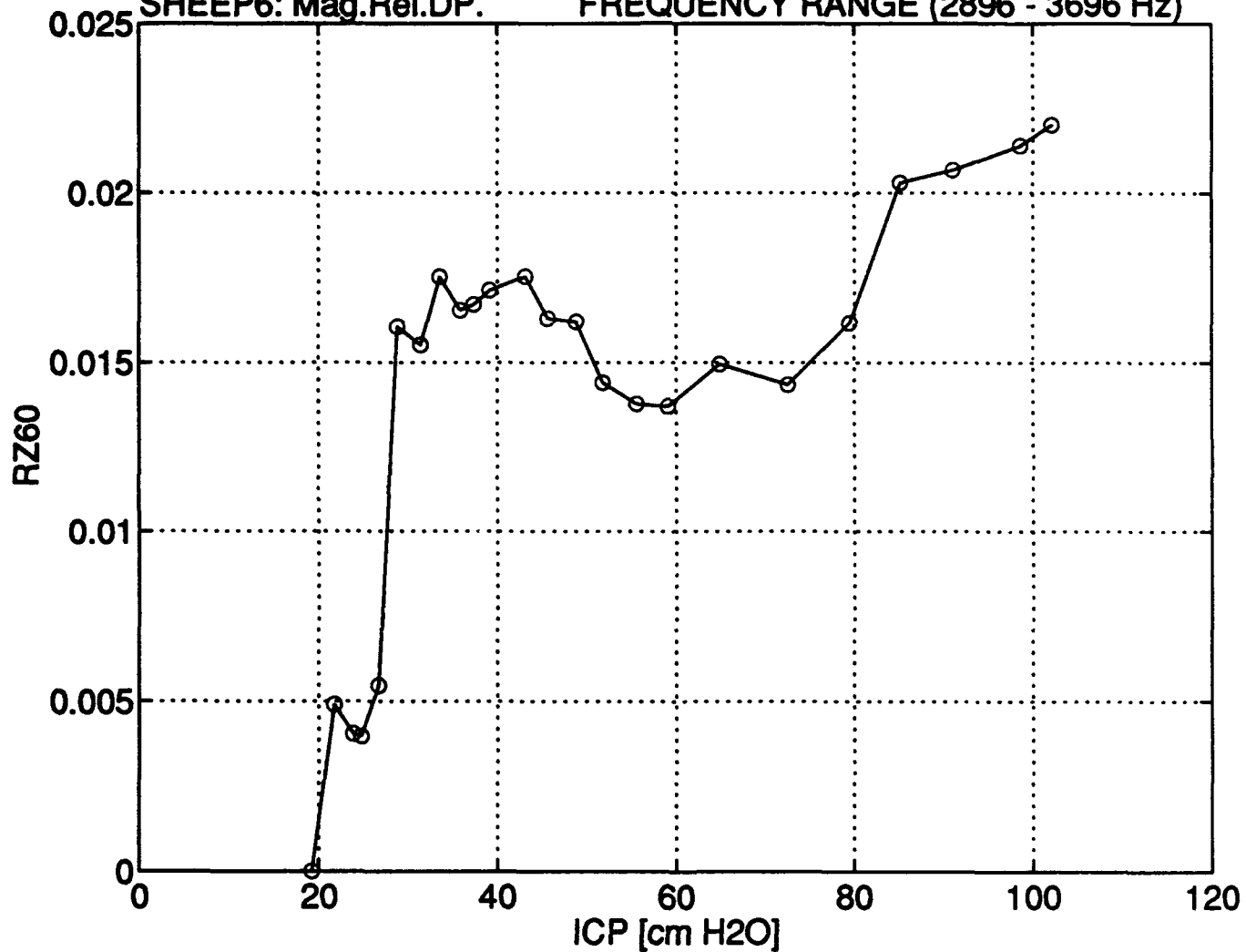
MAGNITUDE STANDARD DEVIATION vs. ICP
SHEEP6: Mag.Rel.DP.   FREQUENCY RANGE (4096 - 6096 Hz)
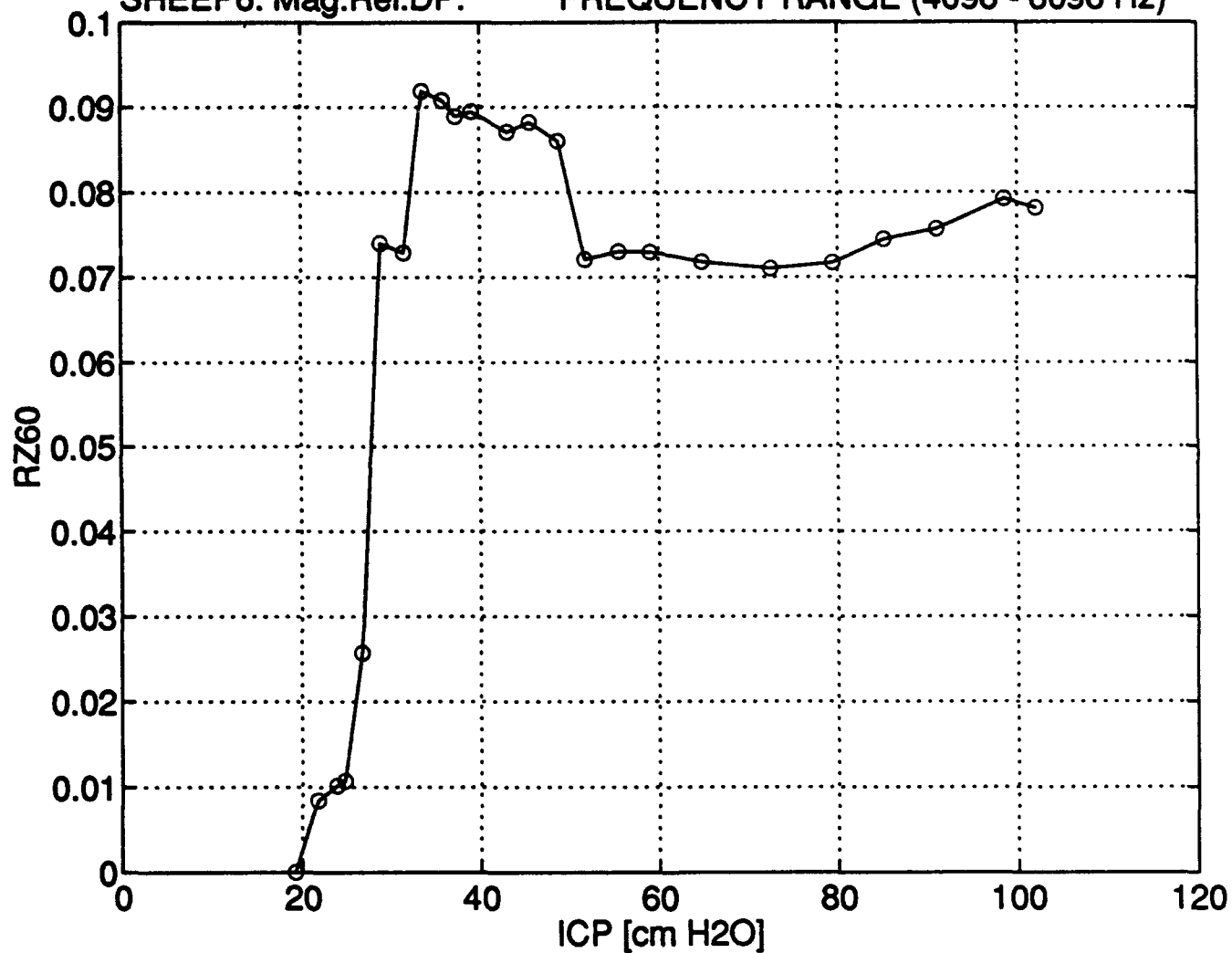
MAGNITUDE OF RELATIVE TRANSFER IMPEDANCE 1, SHEEP6
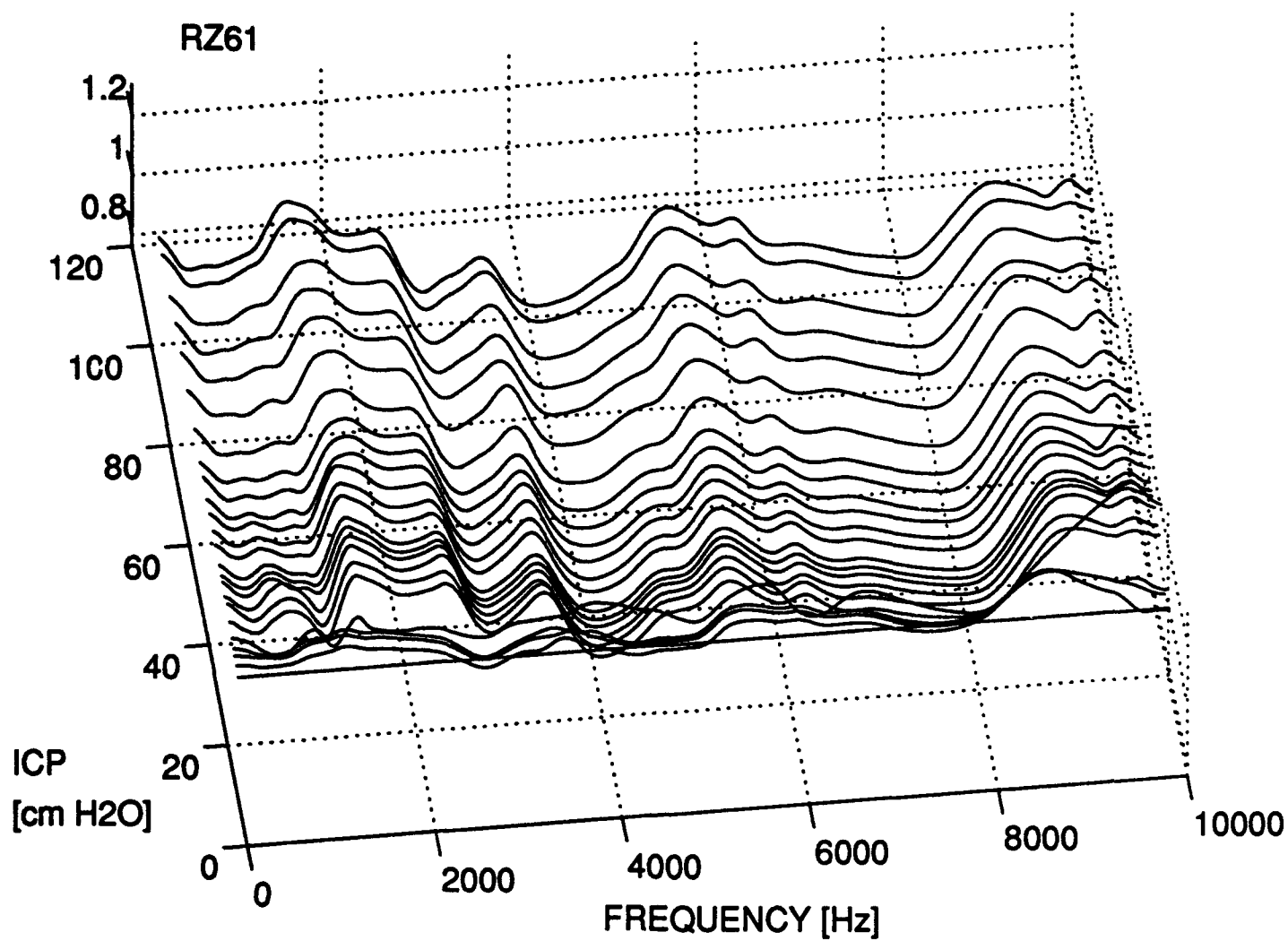
MAGNITUDE OF RELATIVE TRANSFER IMPEDANCE 1, SHEEP6
FREQUENCY RANGE (336 - 2976 Hz)

RZ61

FREQUENCY [Hz]
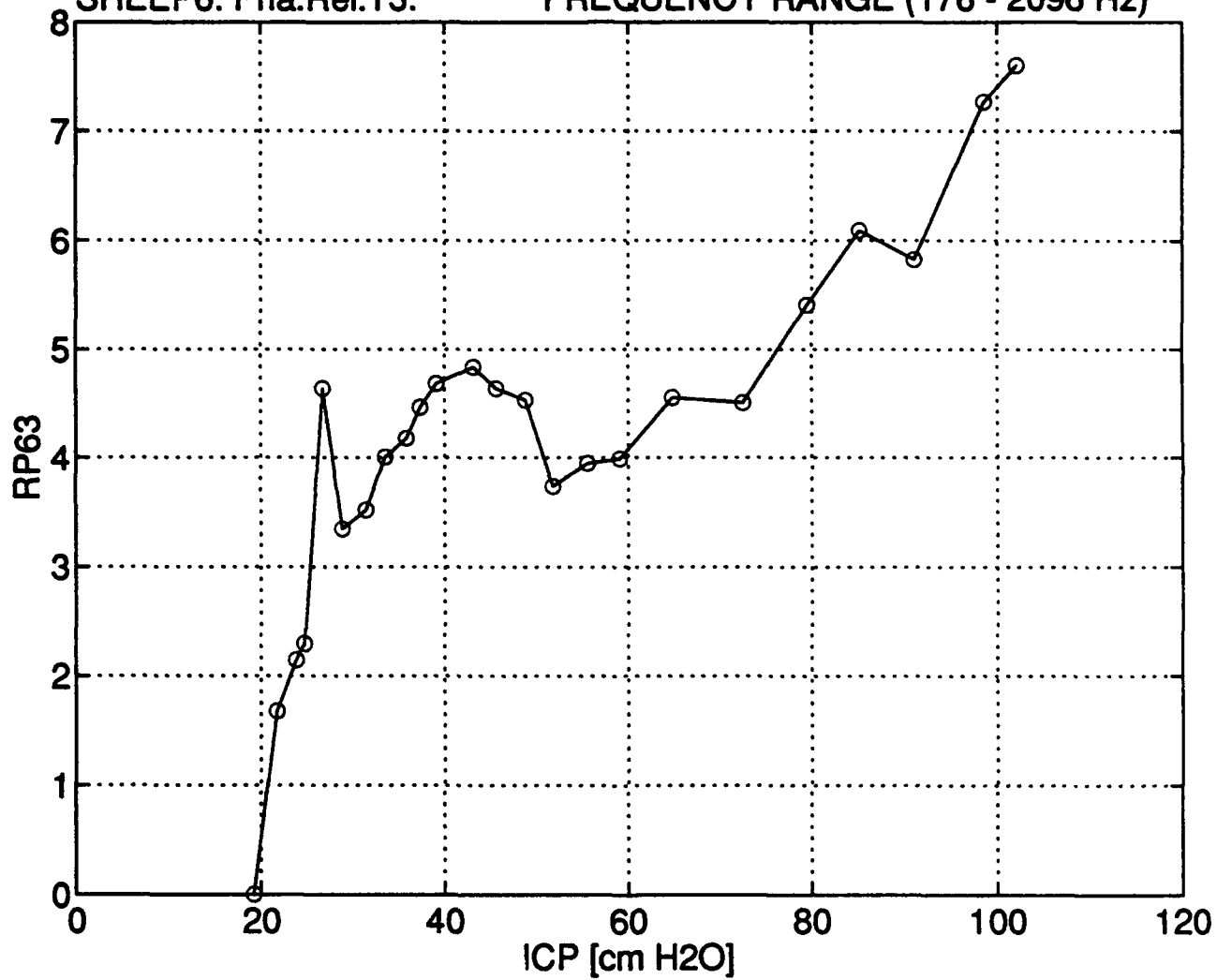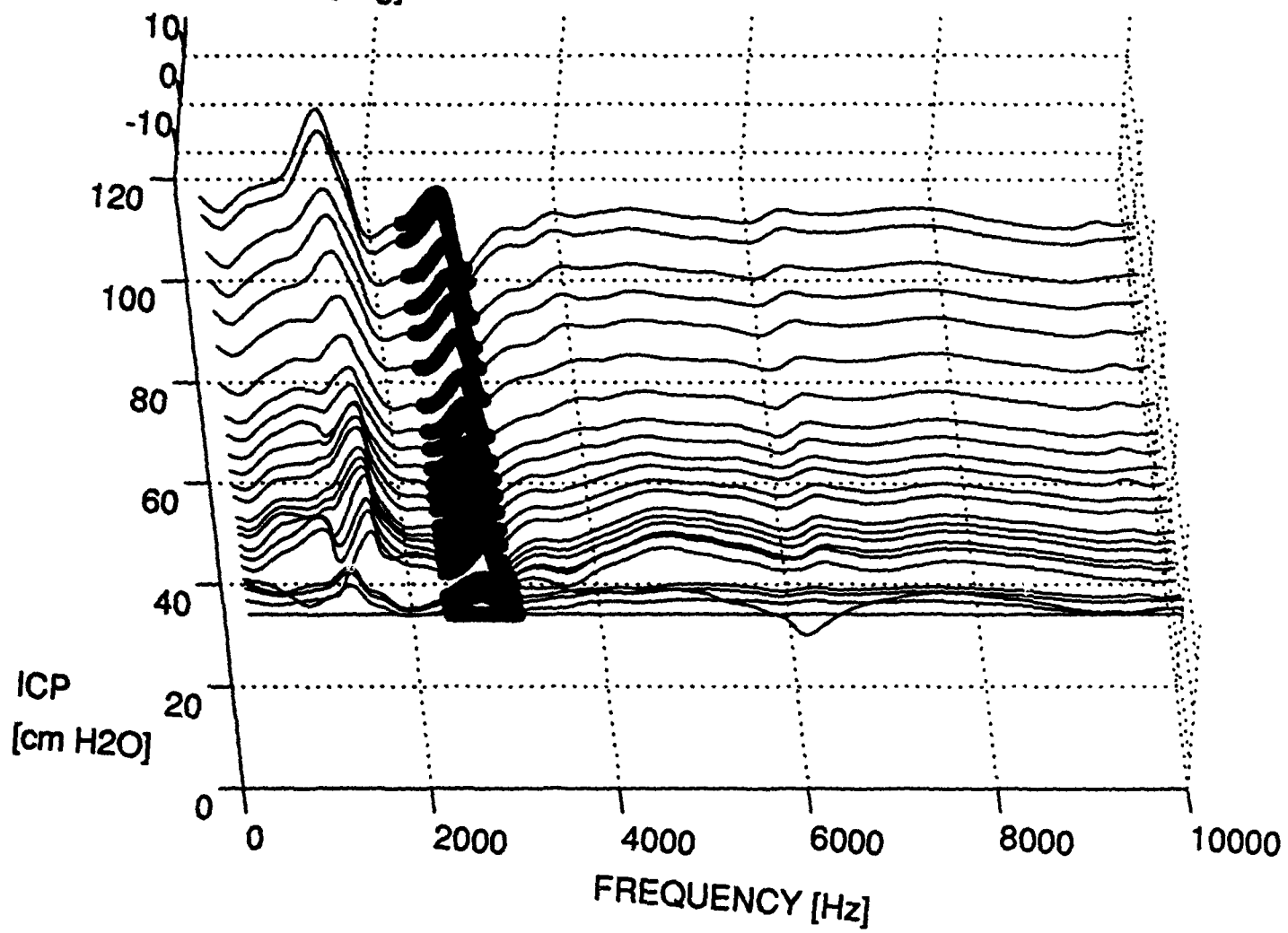
ICP
[cm H2O]
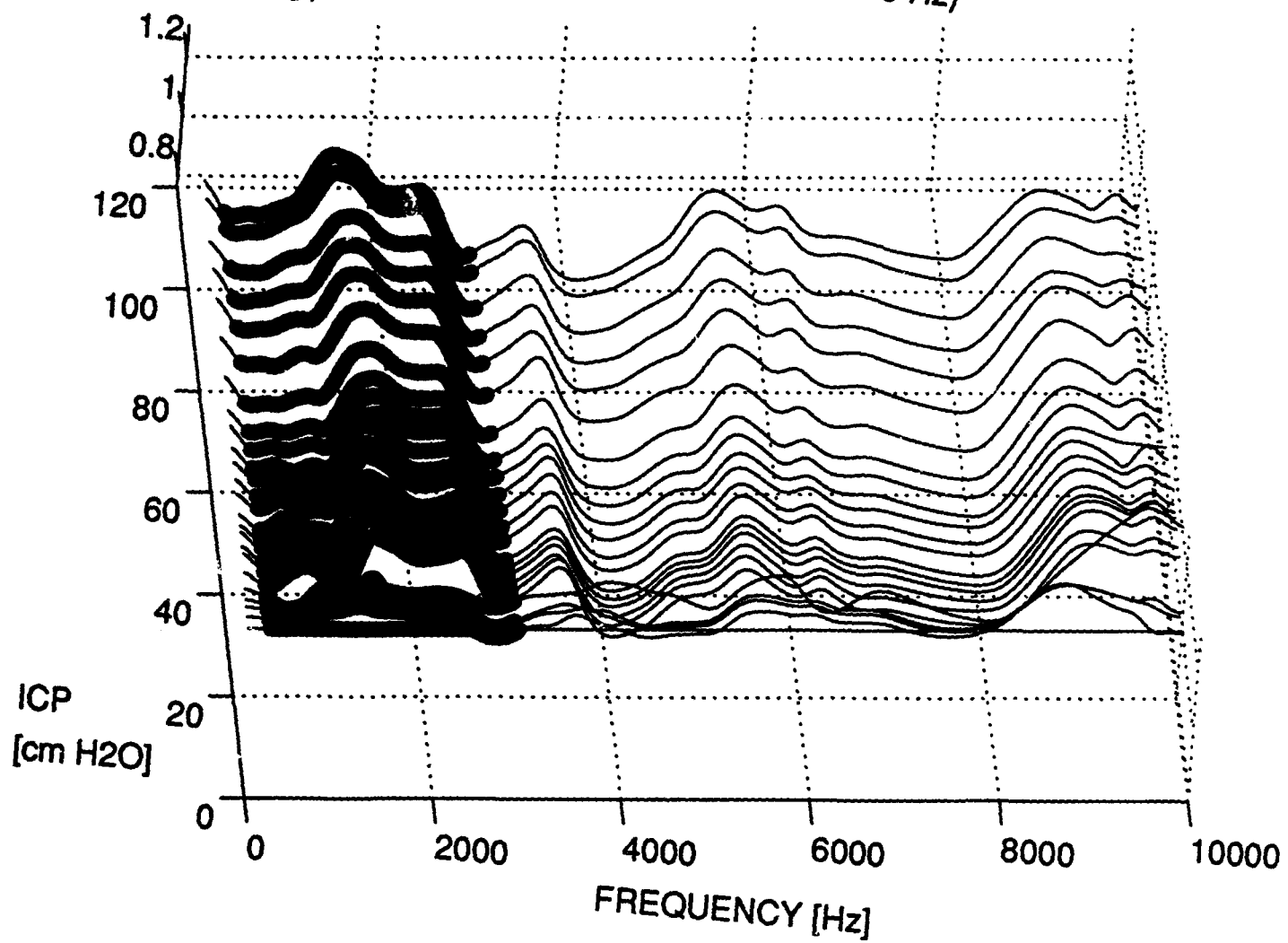
MAGNITUDE STANDARD DEVIATION vs. ICP
SHEEP6: Mag.Rel.T1.   FREQUENCY RANGE (336 - 2976 Hz)
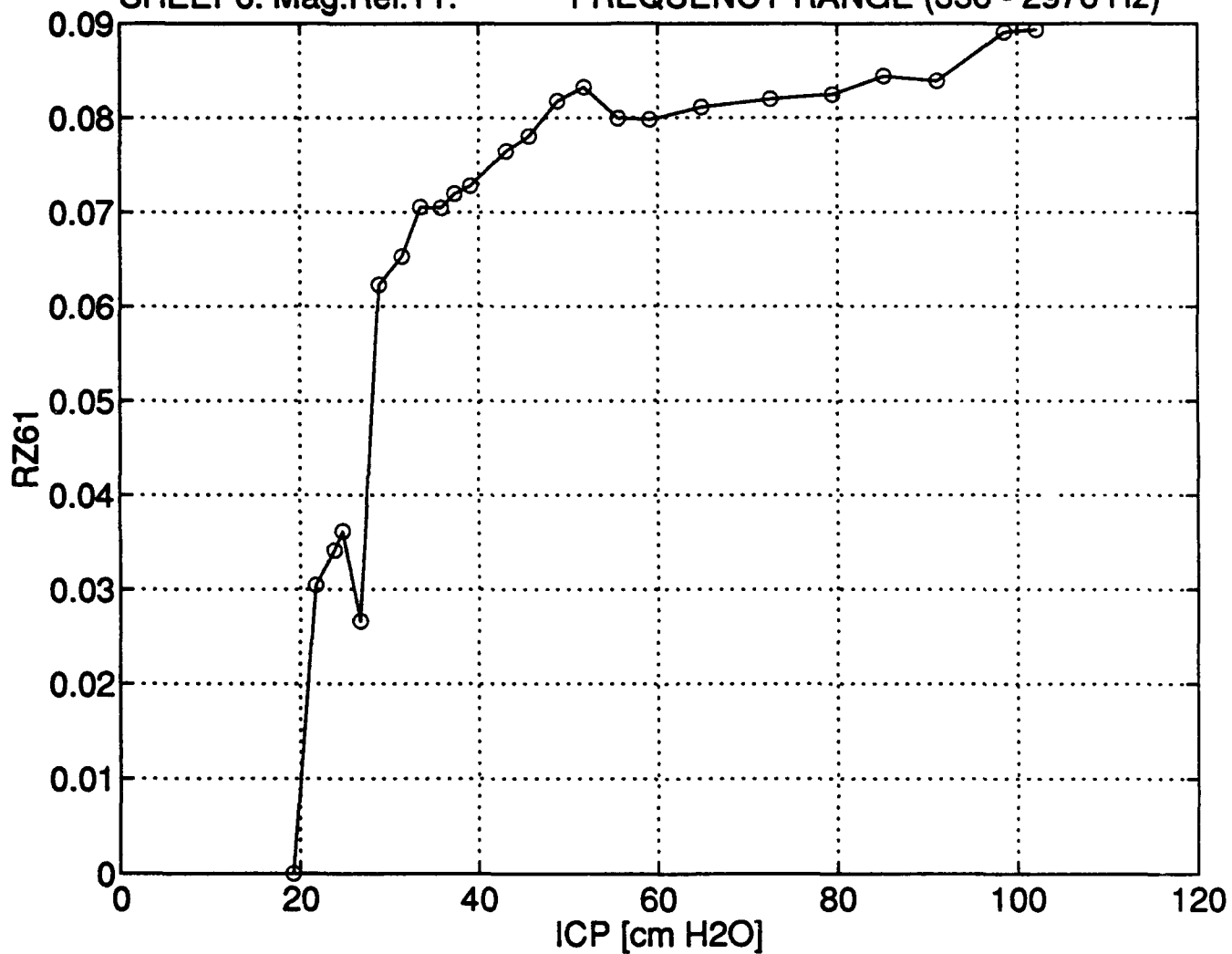
MAGNITUDE OF RELATIVE TRANSFER IMPEDANCE 1, SHEEP6
FREQUENCY RANGE (2736 - 4096 Hz)
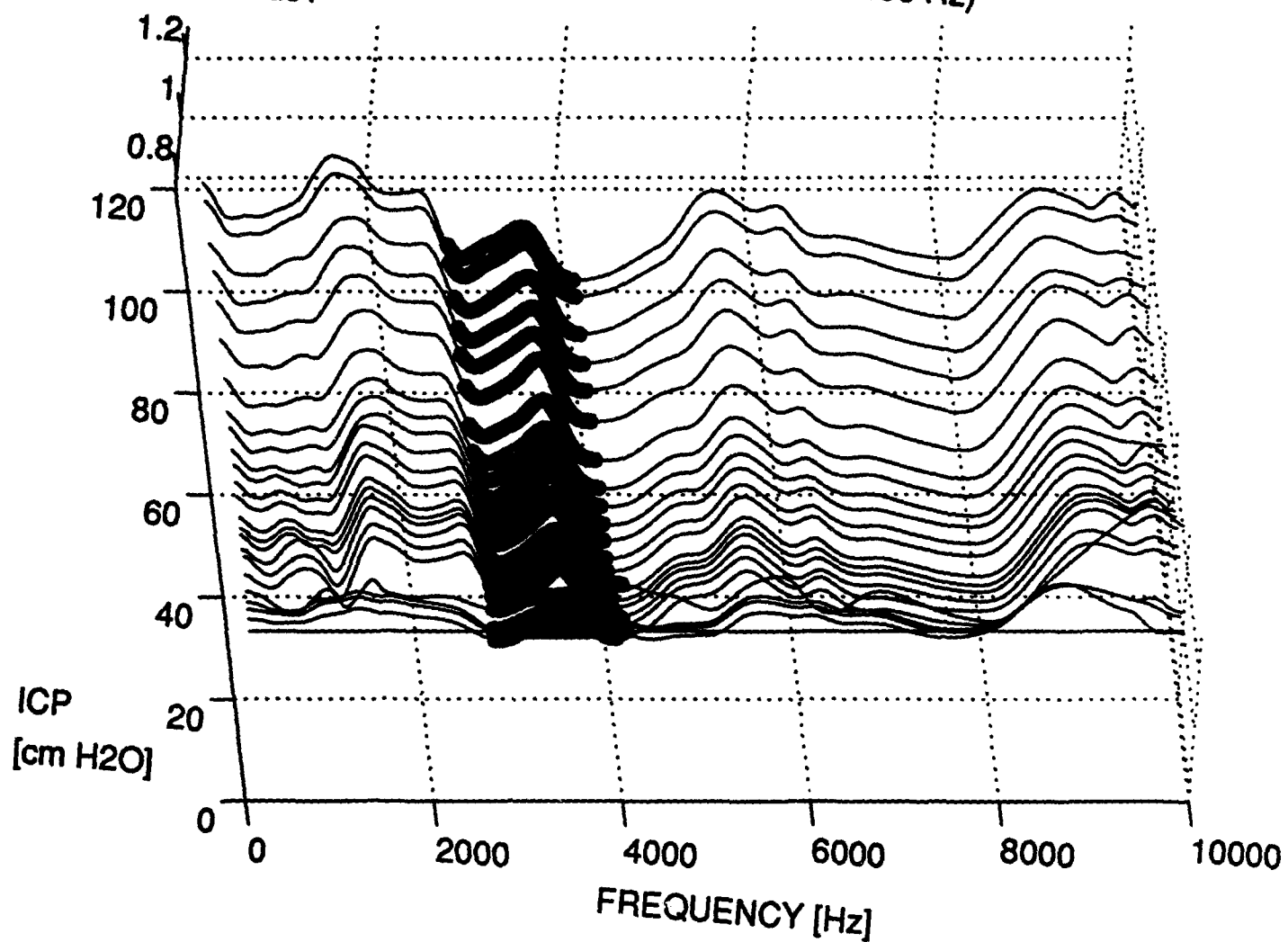
MAGNITUDE STANDARD DEVIATION vs. ICP
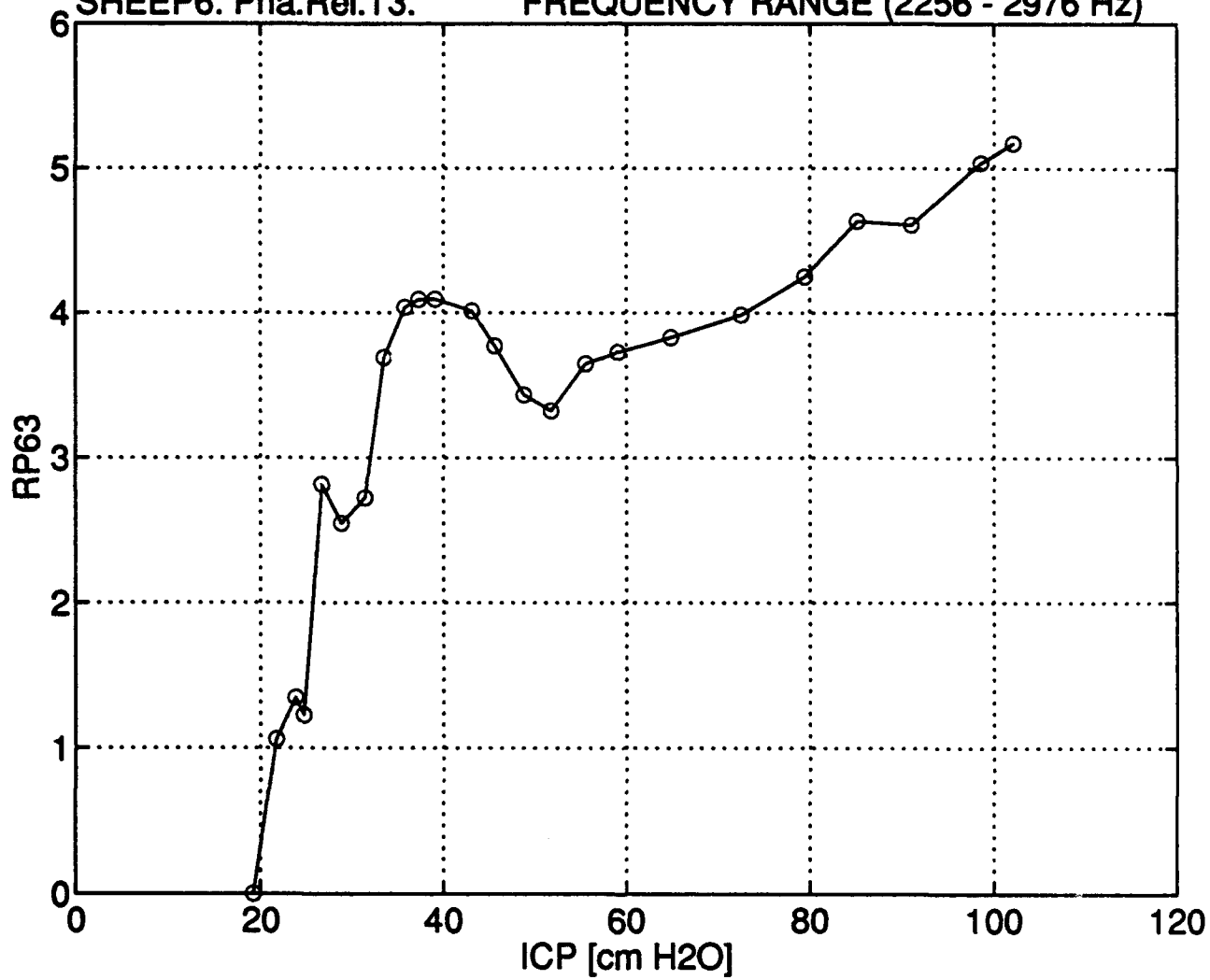SHEEP6: Mag.Rel.T1.   FREQUENCY RANGE (2736 - 4096 Hz)

MAGNITUDE OF RELATIVE TRANSFER IMPEDANCE 1, SHEEP6
FREQUENCY RANGE (4096 - 6896 Hz)
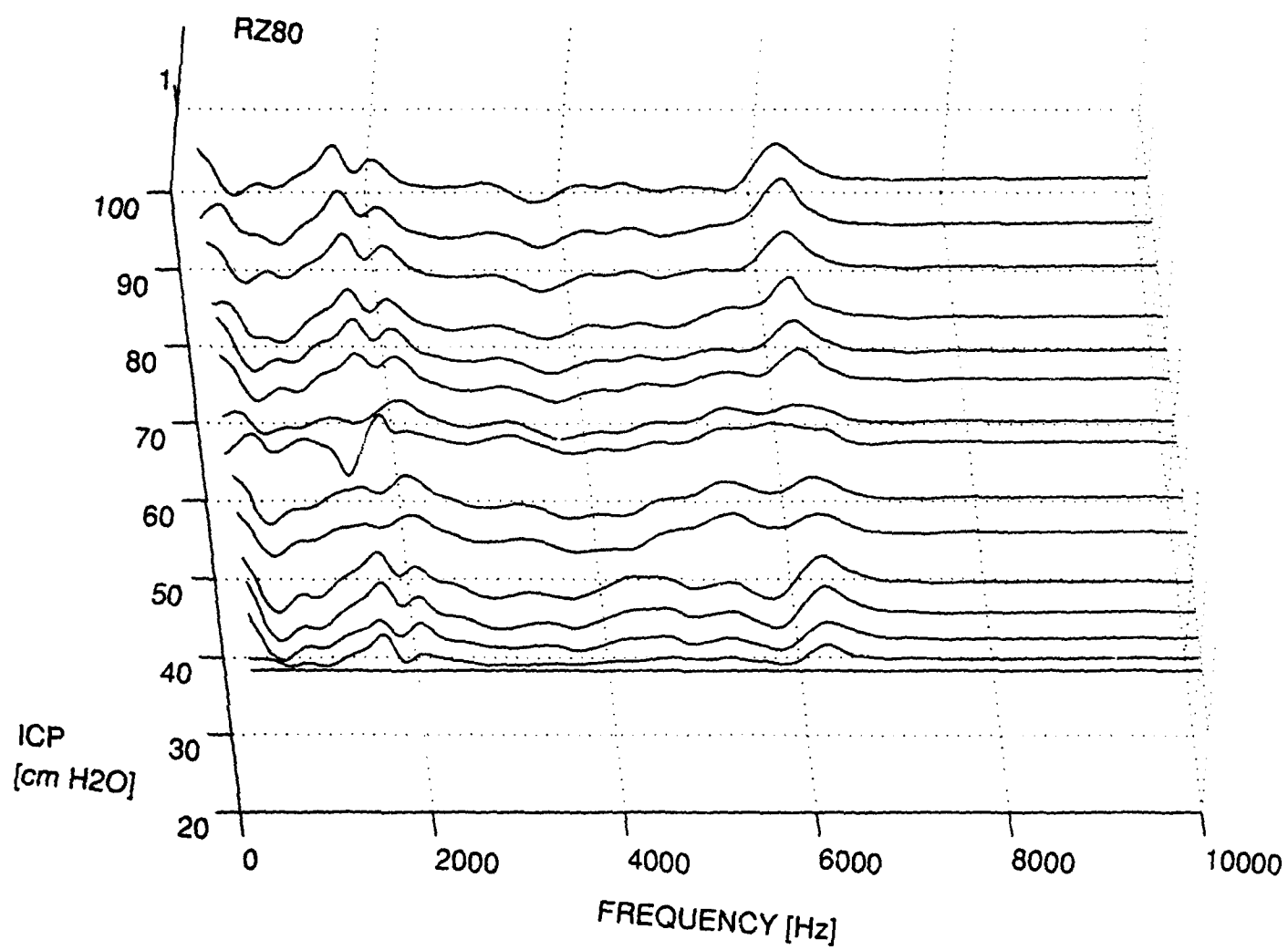
MAGNITUDE STANDARD DEVIATION vs. ICP
SHEEP6: Mag.Rel.T1.   FREQUENCY RANGE (4096 - 6896 Hz)

MAGNITUDE OF RELATIVE TRANSFER IMPEDANCE 1, SHEEP6
FREQUENCY RANGE (8016 - 9616 Hz)
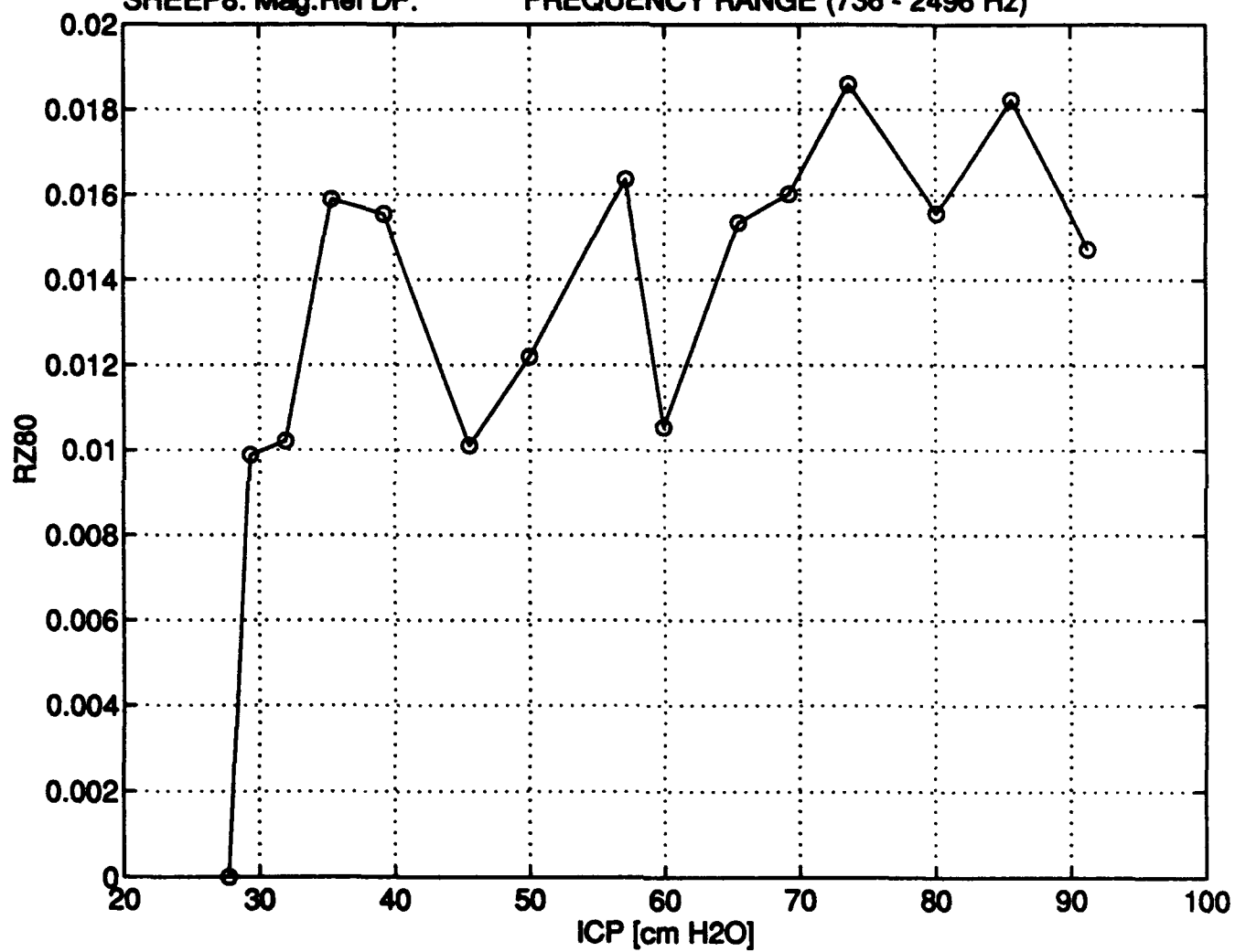
MAGNITUDE STANDARD DEVIATION vs. ICP
SHEEP6: Mag.Rel.T1.   FREQUENCY RANGE (8016 - 9616 Hz)

MAGNITUDE OF RELATIVE TRANSFER IMPEDANCE 2, SHEEP6

MAGNITUDE OF RELATIVE TRANSFER IMPEDANCE 2, SHEEP6
FREQUENCY RANGE (296 - 2656 Hz)

RZ62

1.2
1.
120
100
80
60
40

ICP   20
[cm H2O]

0

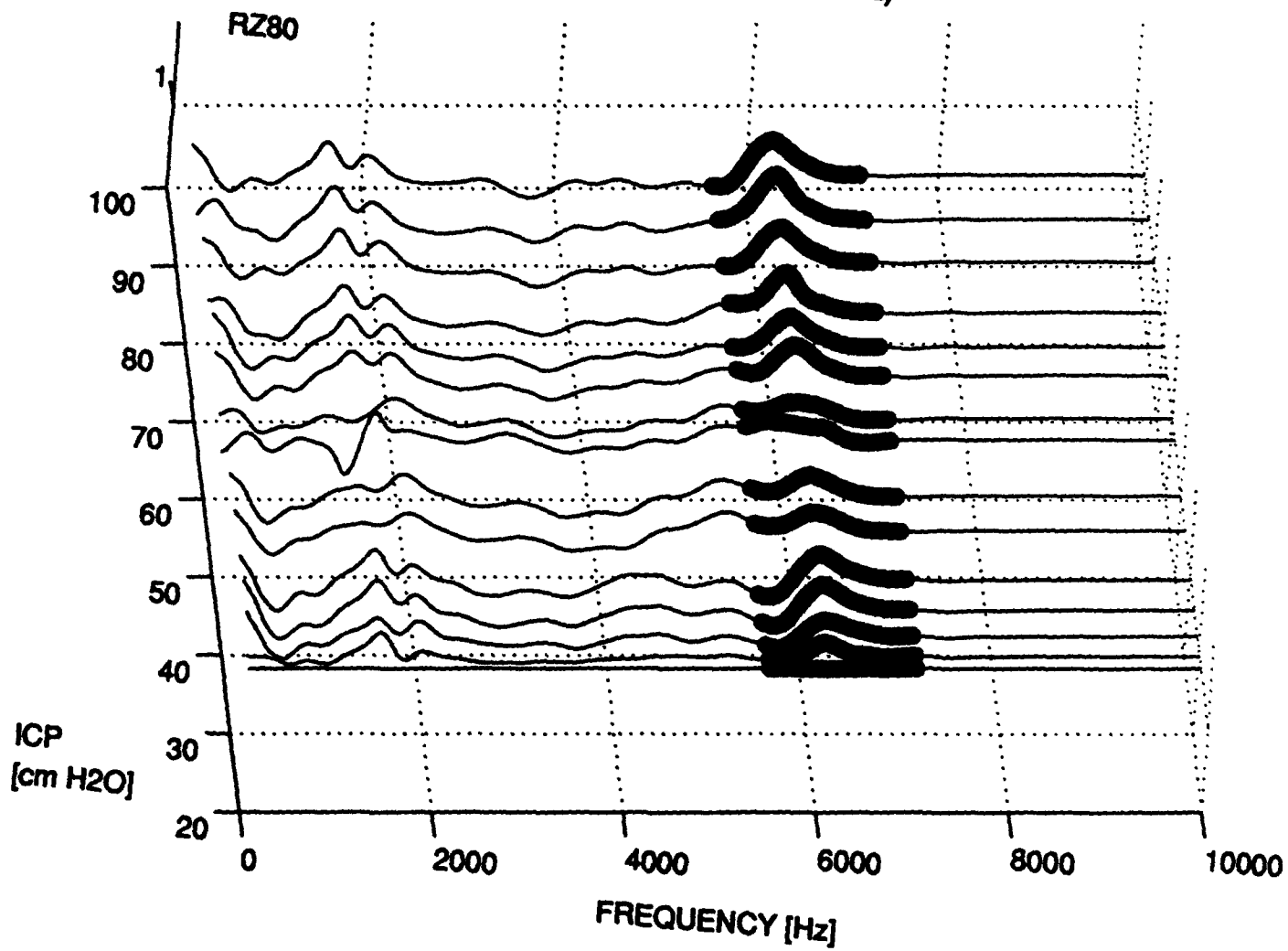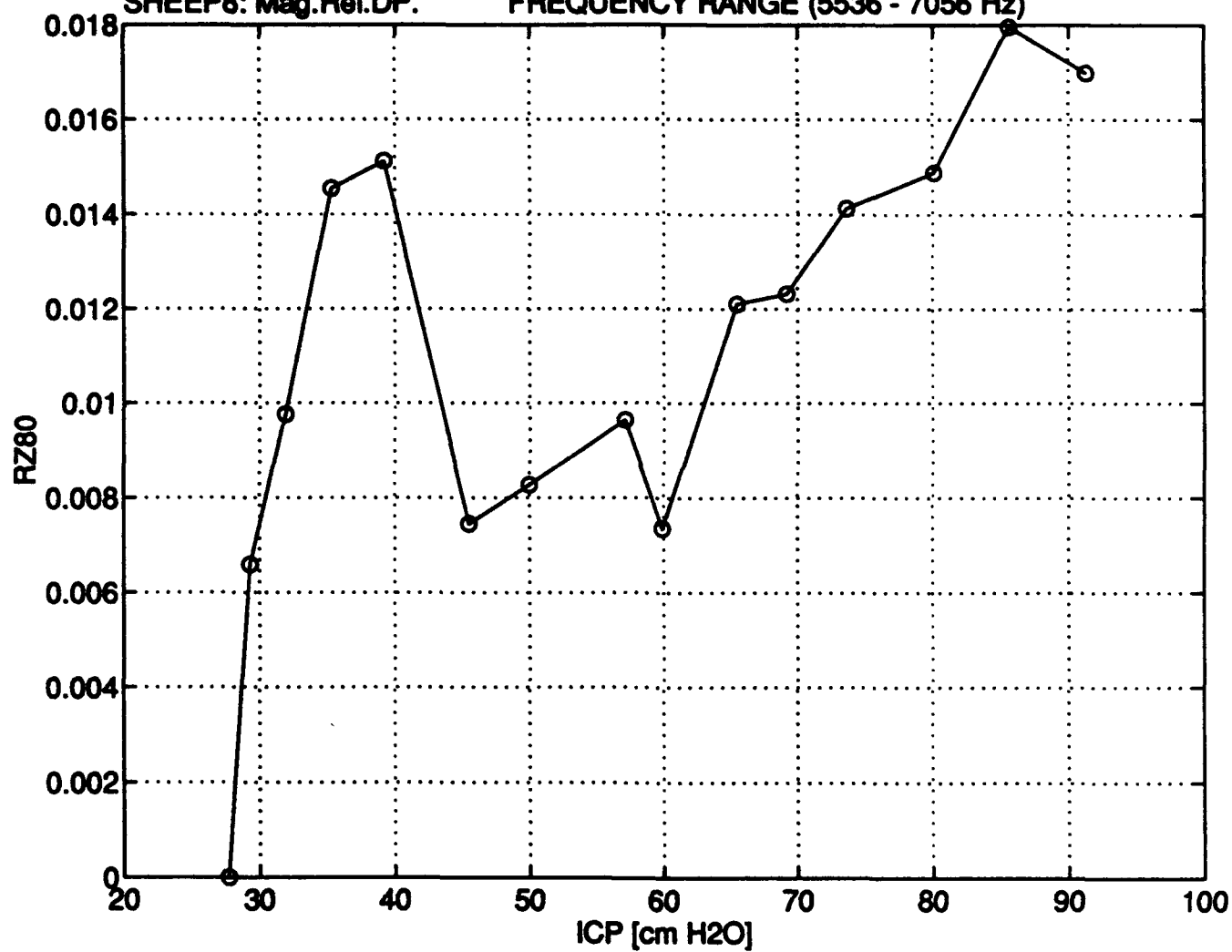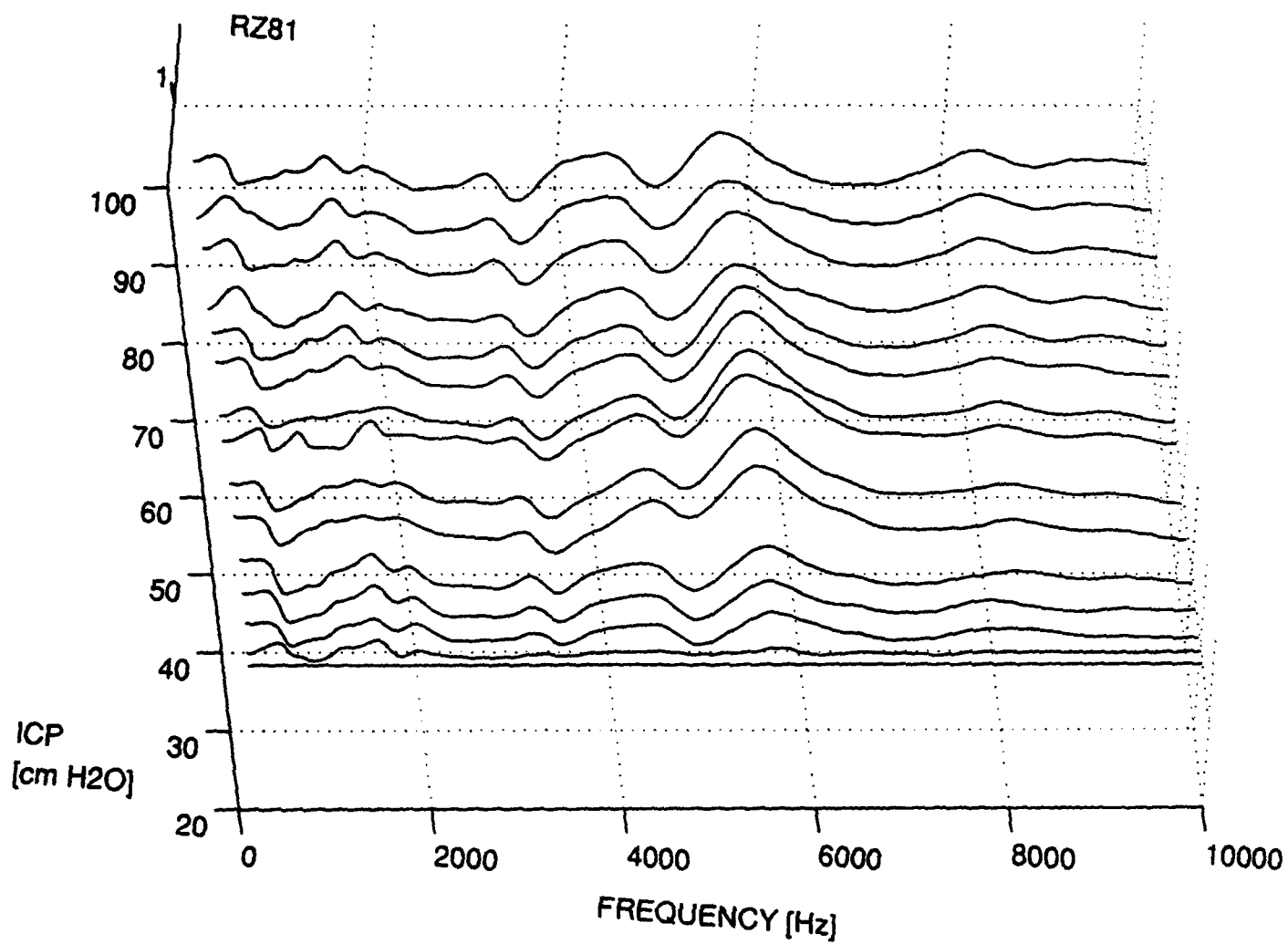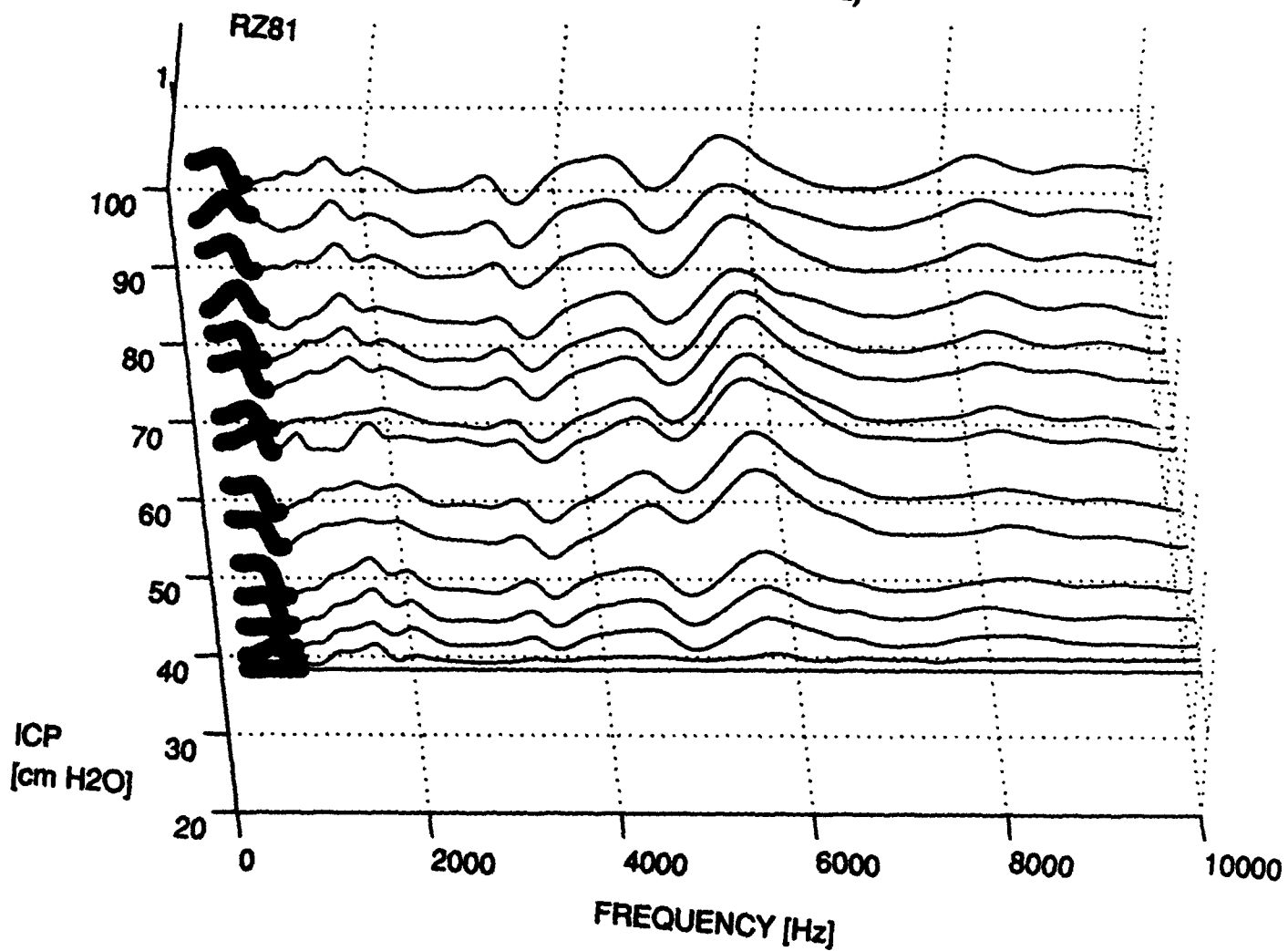0   2000   4000   6000   8000   10000
FREQUENCY [Hz]

MAGNITUDE STANDARD DEVIATION vs. ICP
SHEEP6: Mag.Rel.T2.   FREQUENCY RANGE (296 - 2656 Hz)

MAGNITUDE OF RELATIVE TRANSFER IMPEDANCE 2, SHEEP6
FREQUENCY RANGE (2896 - 4896 Hz)

RZ62

ICP
[cm H2O]

FREQUENCY [Hz]

MAGNITUDE STANDARD DEVIATION vs. ICP
SHEEP6: Mag.Rel.T2.   FREQUENCY RANGE (2896 - 4896 Hz)

MAGNITUDE OF RELATIVE TRANSFER IMPEDANCE 3, SHEEP6

RZ63

1.4
1.2
1
0.8
120
100
80
60
40

ICP
[cm H2O]

20

0

0   2000   4000   6000   8000   10000
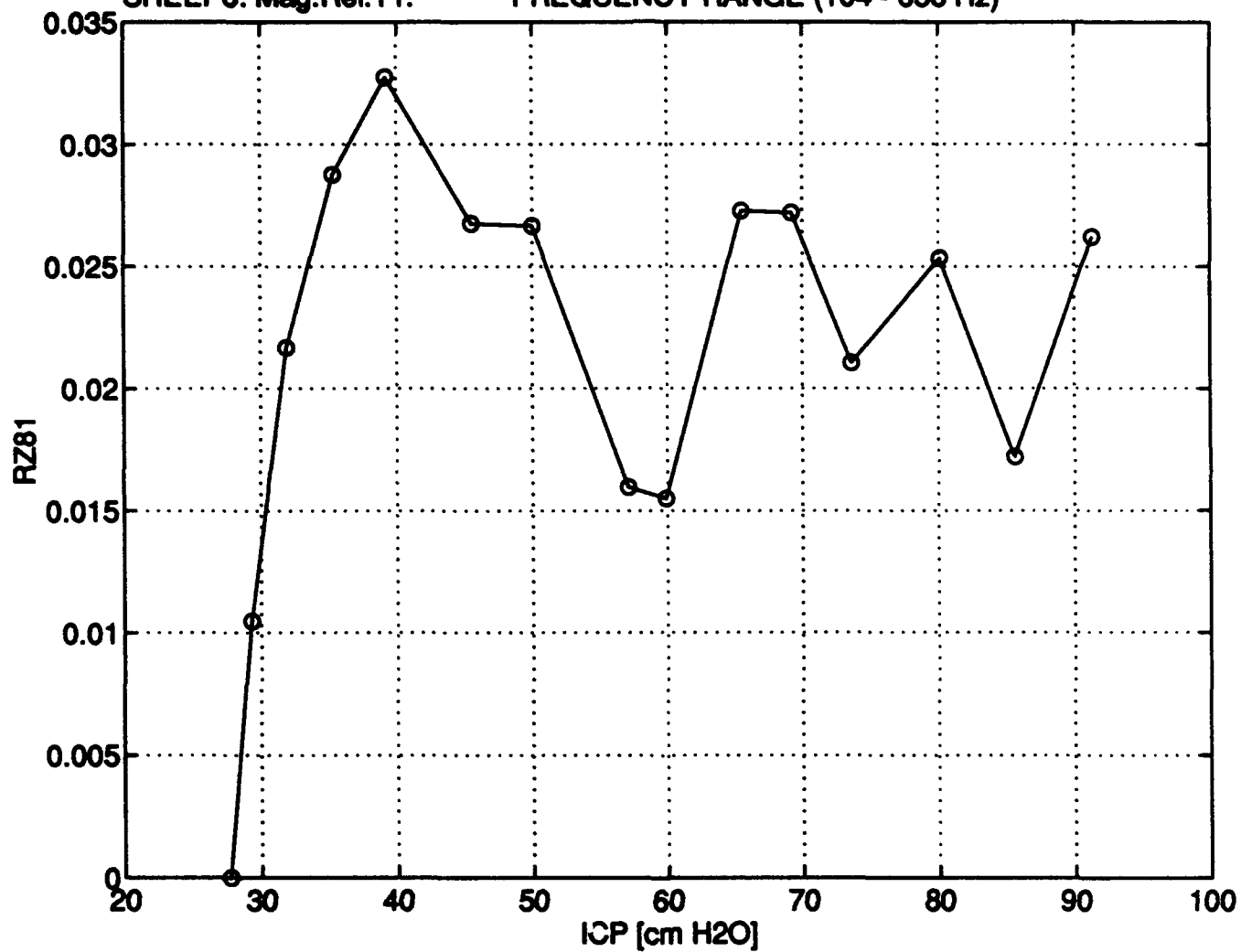
FREQUENCY [Hz]

MAGNITUDE OF RELATIVE TRANSFER IMPEDANCE 3, SHEEP6
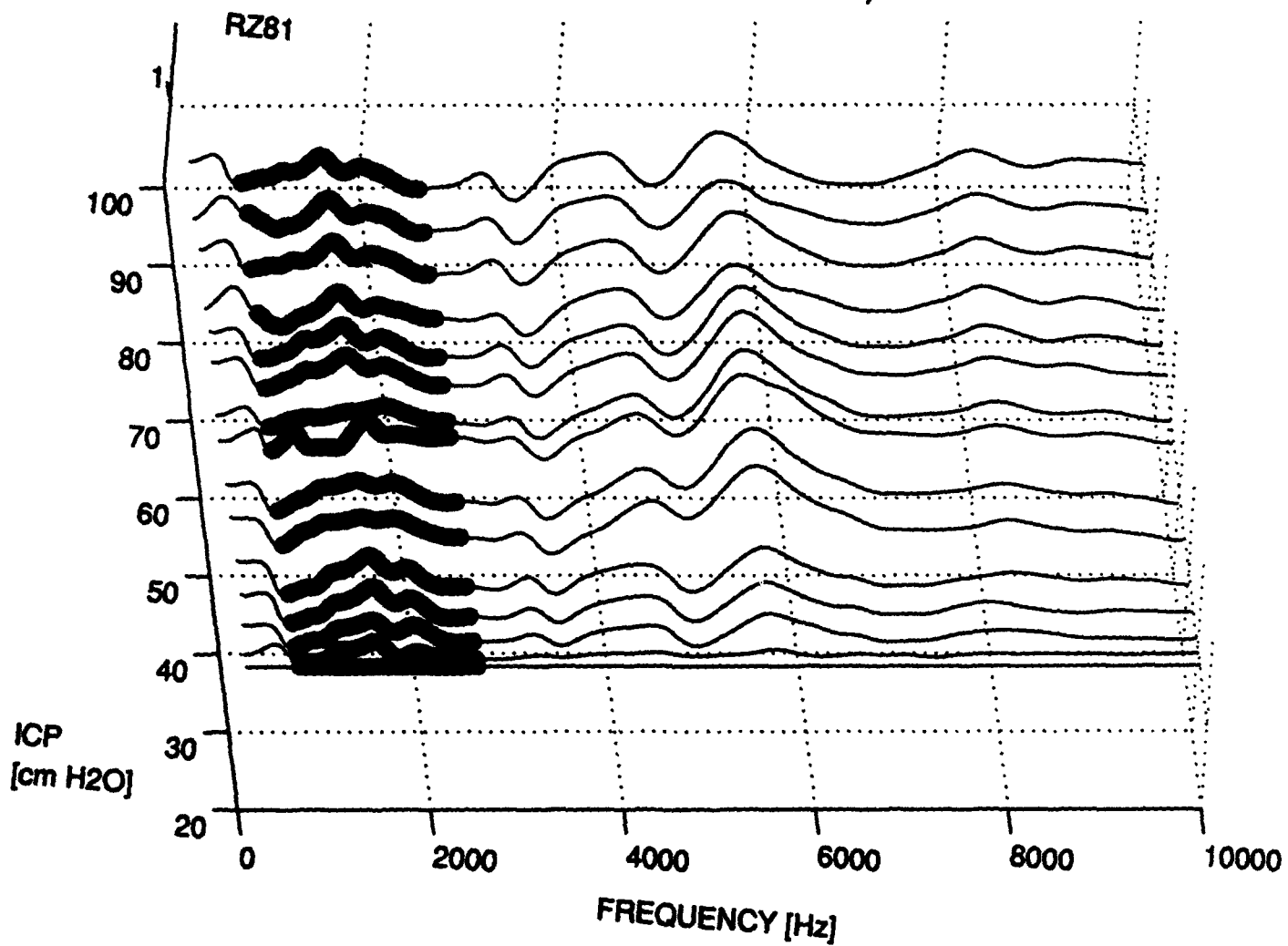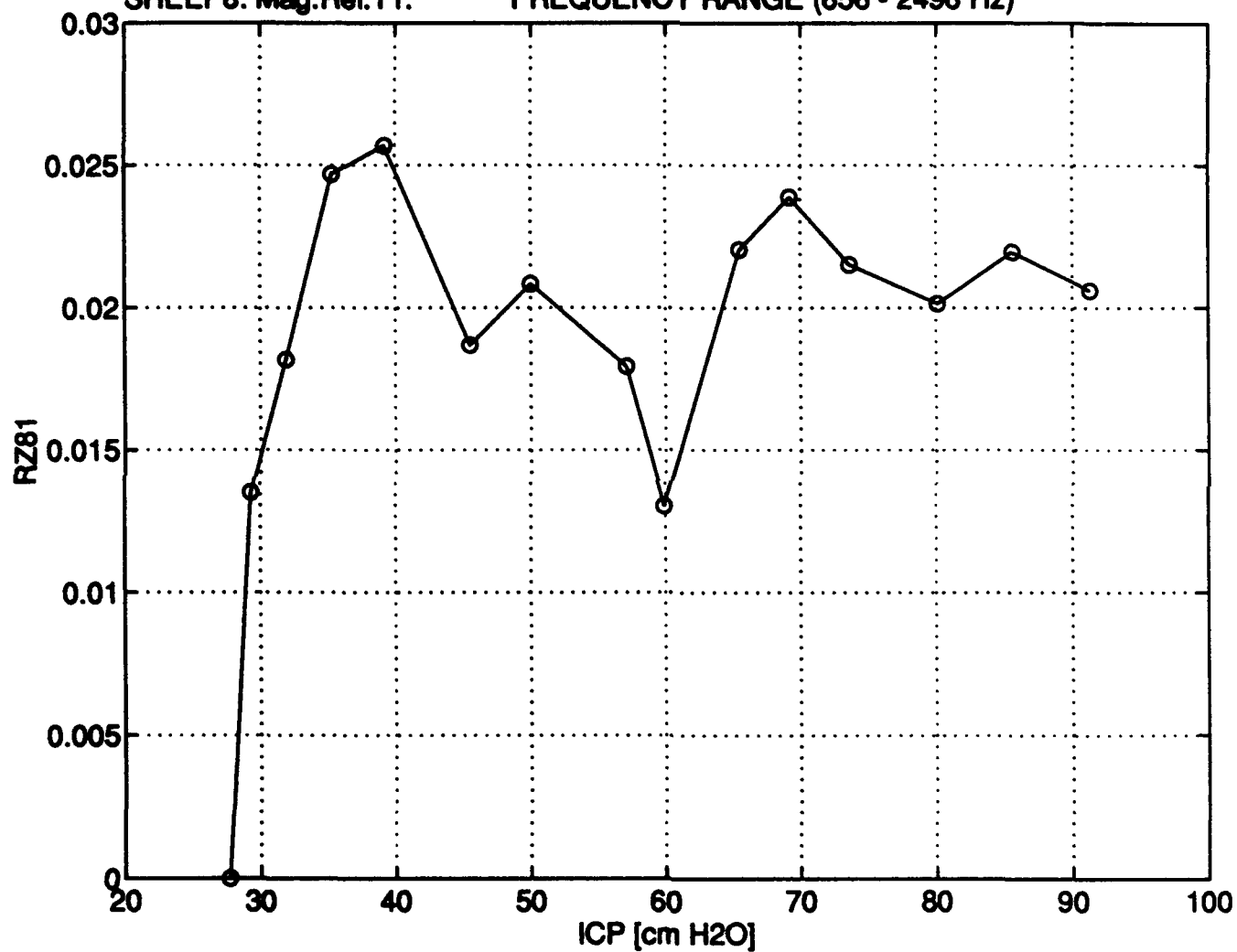FREQUENCY RANGE (736 - 2496 Hz)

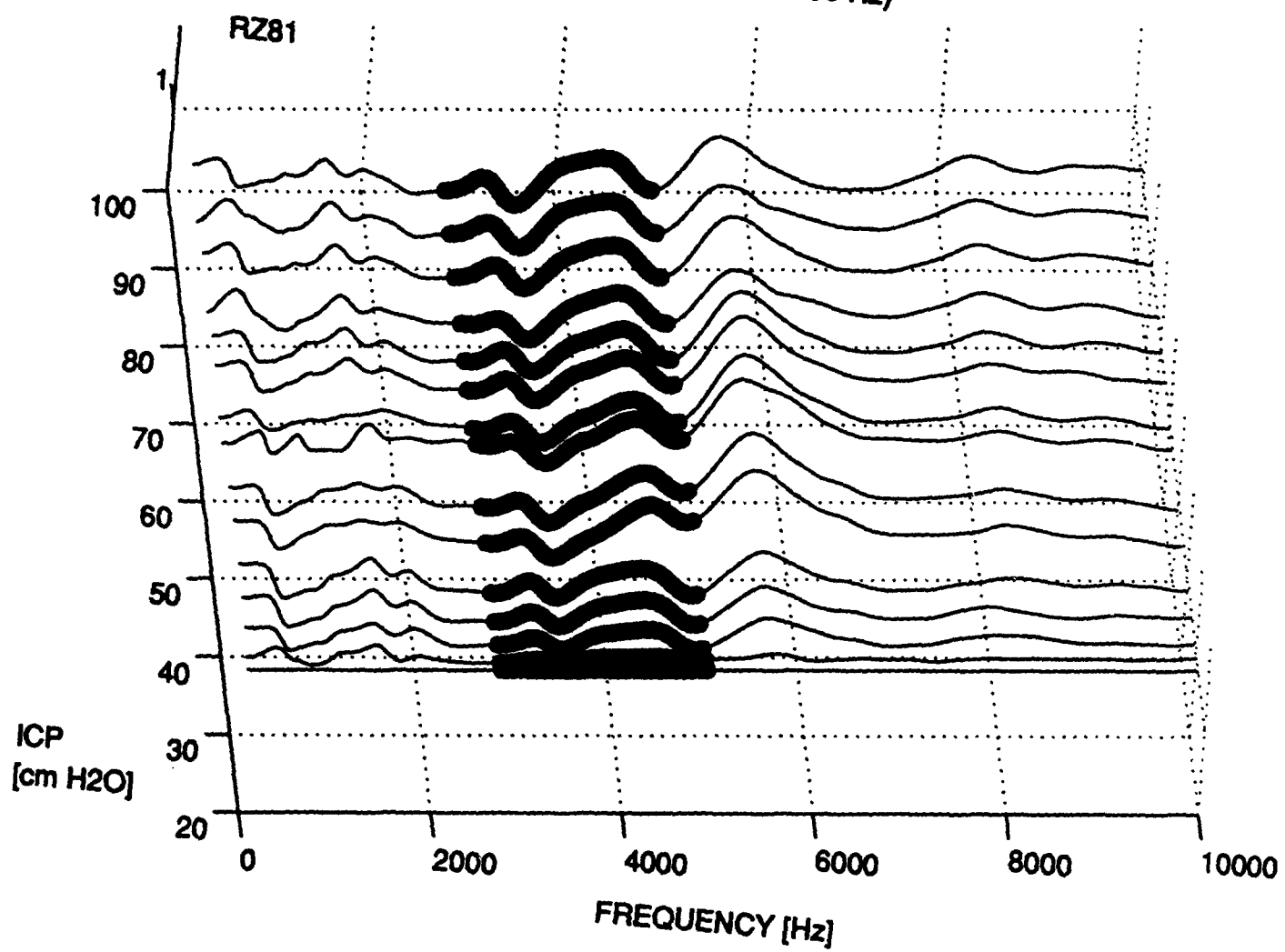MAGNITUDE STANDARD DEVIATION vs. ICP
SHEEP6: Mag.Rel.T3.   FREQUENCY RANGE (736 - 2496 Hz)

MAGNITUDE OF RELATIVE TRANSFER IMPEDANCE 3, SHEEP6
FREQUENCY RANGE (2496 - 3296 Hz)

RZ63

ICP
[cm H2O]

FREQUENCY [Hz]

MAGNITUDE STANDARD DEVIATION vs. ICP
SHEEP6: Mag.Rel.T3.   FREQUENCY RANGE (2496 - 3296 Hz)
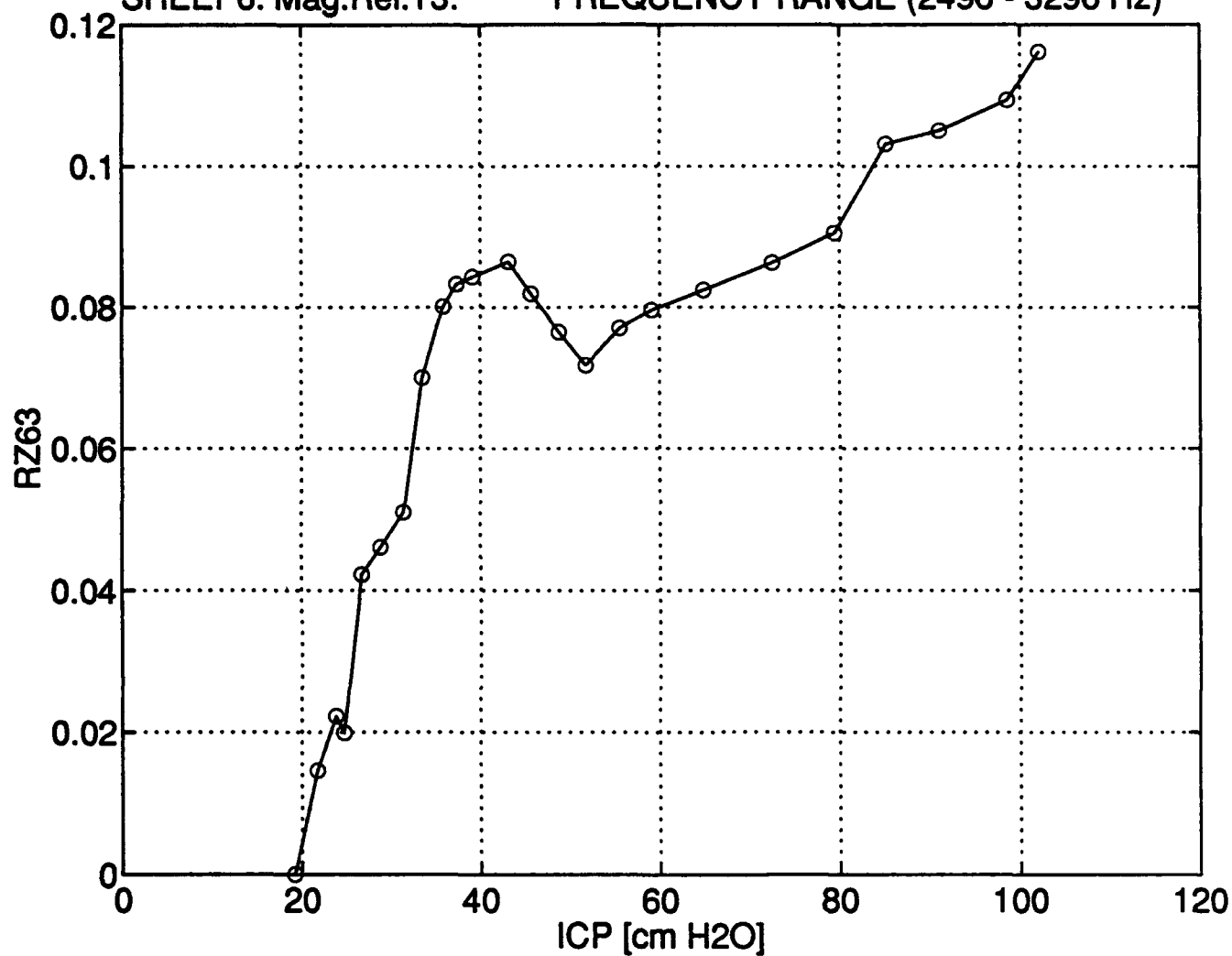
PHASE OF RELATIVE DRIVING POINT IMPEDANCE, SHEEP6

PHASE OF RELATIVE DRIVING POINT IMPEDANCE, SHEEP6
FREQUENCY RANGE (416 - 2096 Hz)

PHASE STANDARD DEVIATION vs. ICP
SHEEP6: Pha.Rel.DP.   FREQUENCY RANGE (416 - 2096 Hz)

PHASE OF RELATIVE DRIVING POINT IMPEDANCE, SHEEP6
FREQUENCY RANGE (4096 - 7296 Hz)

PHASE STANDARD DEVIATION vs. ICP
SHEEP6: Pha.Rel.DP.   FREQUENCY RANGE (4096 - 7296 Hz)
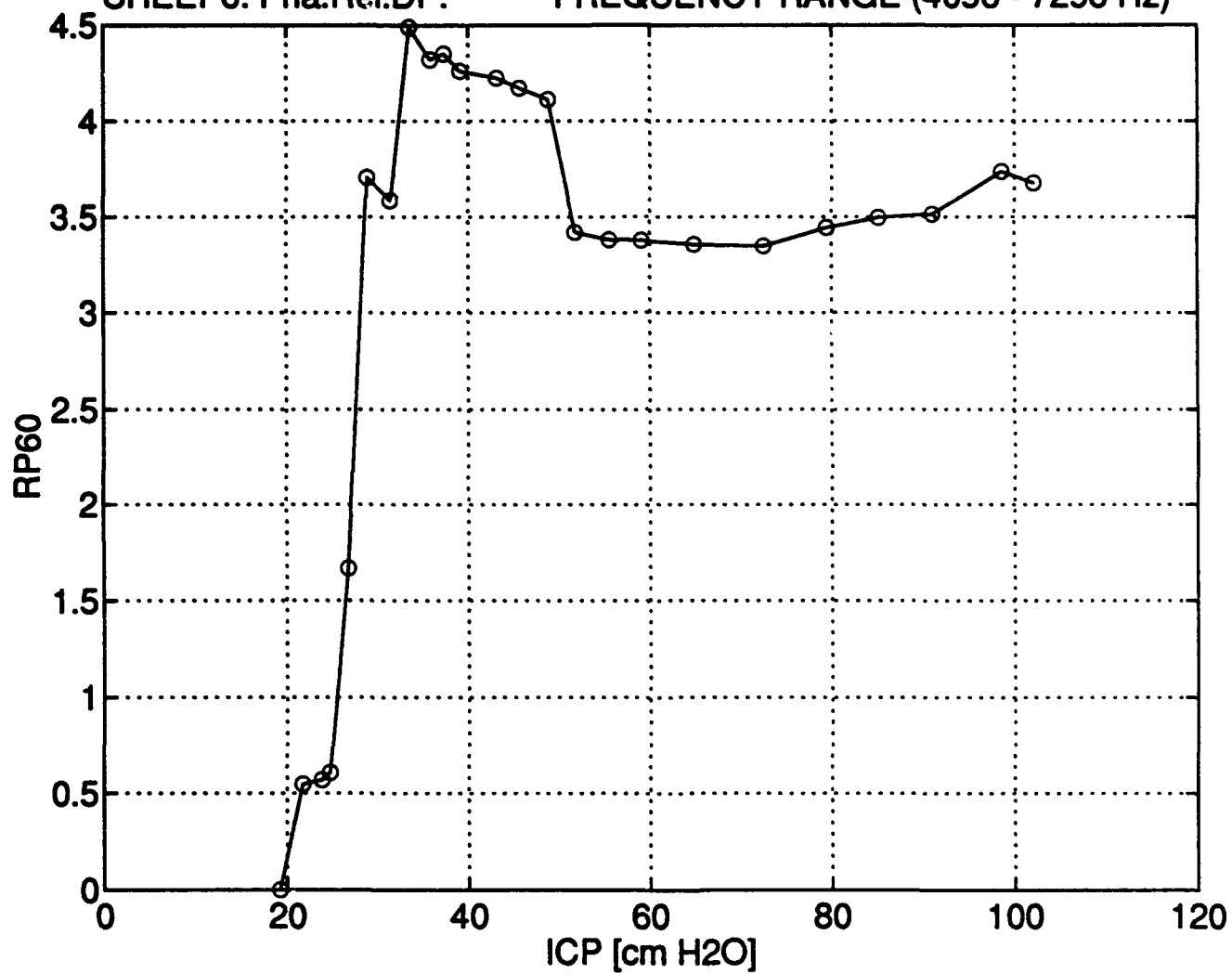
PHASE OF RELATIVE TRANSFER IMPEDANCE 1, SHEEP6

PHASE OF RELATIVE TRANSFER IMPEDANCE 1, SHEEP6
FREQUENCY RANGE (976 - 2096 Hz)

PHASE STANDARD DEVIATION vs. ICP
SHEEP6: Pha.Rel.T1.   FREQUENCY RANGE (976 - 2096 Hz)

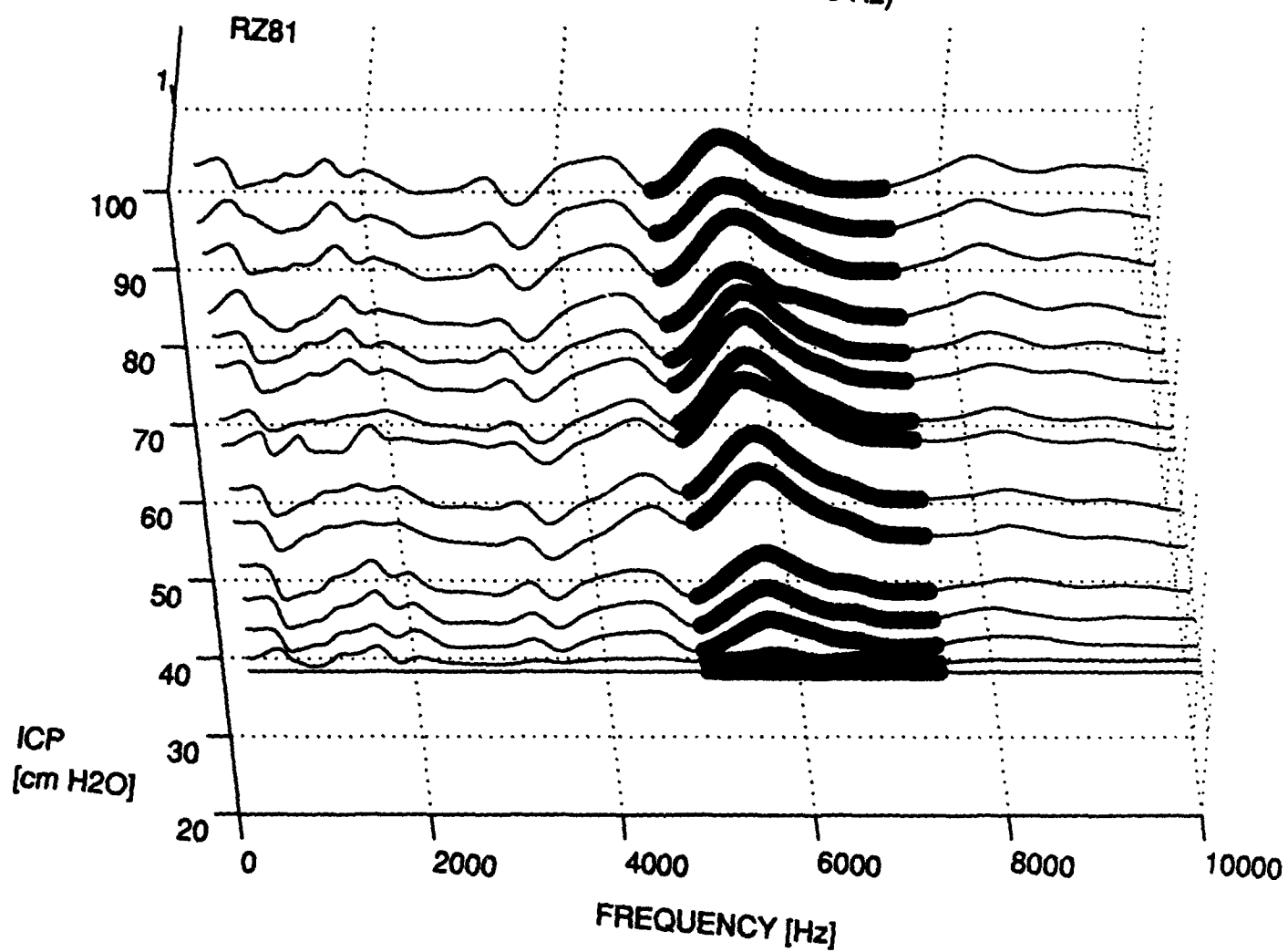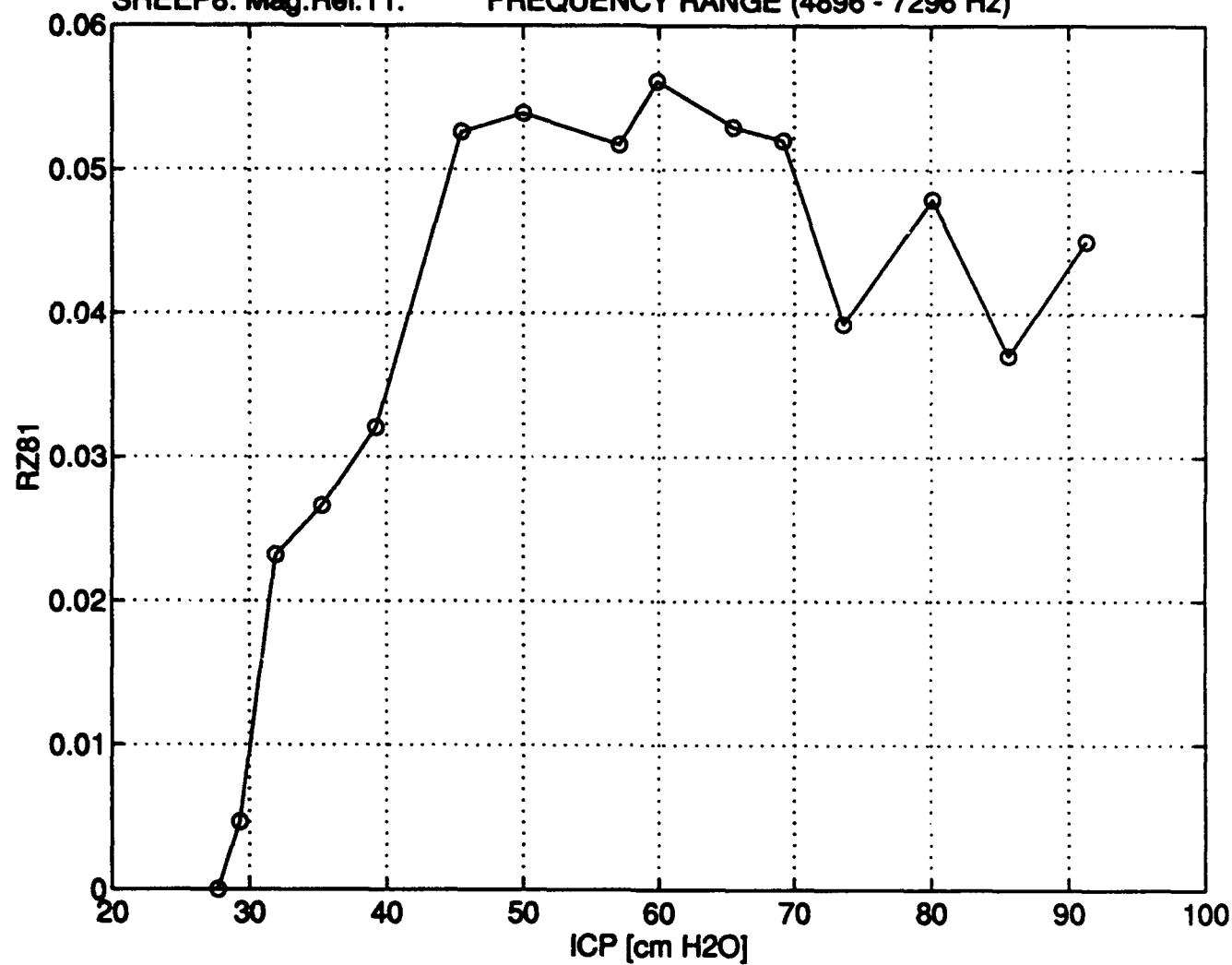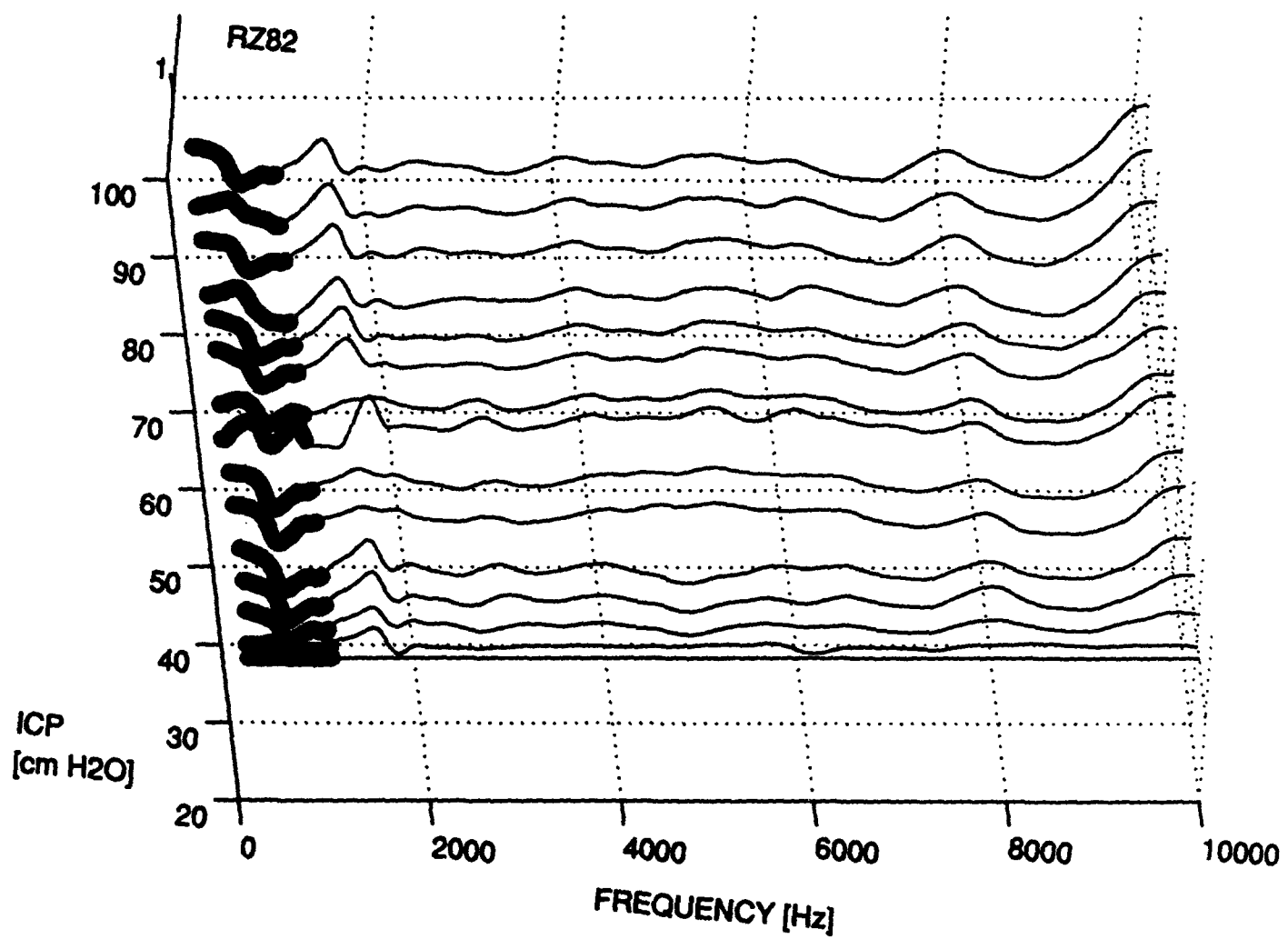PHASE OF RELATIVE TRANSFER IMPEDANCE 1, SHEEP6
FREQUENCY RANGE (2496 - 3696 Hz)

PHASE STANDARD DEVIATION vs. ICP
SHEEP6: Pha.Rel.T1.   FREQUENCY RANGE (2496 - 3696 Hz)

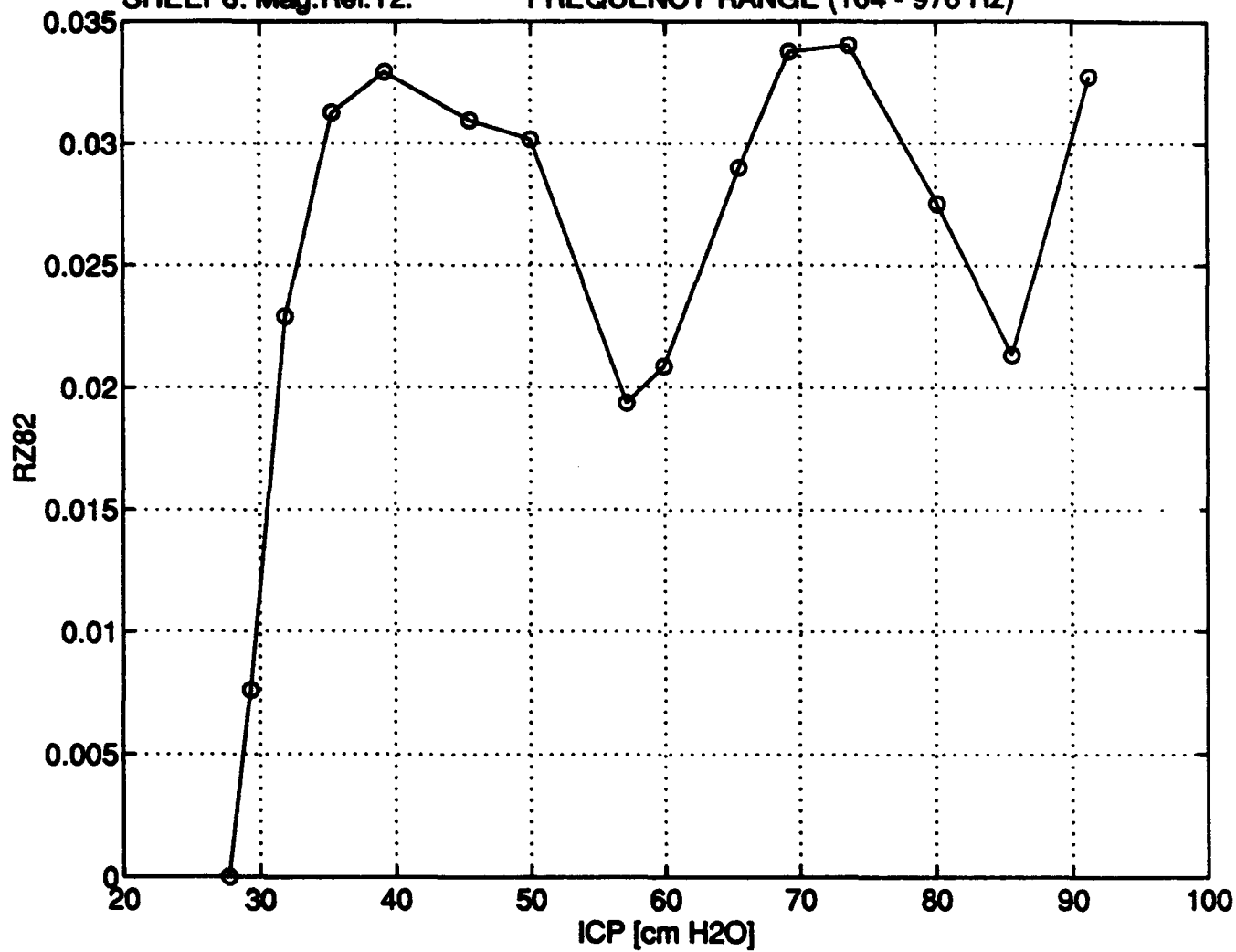PHASE OF RELATIVE TRANSFER IMPEDANCE 1, SHEEP6
FREQUENCY RANGE (3696 - 5936 Hz)

PHASE STANDARD DEVIATION vs. ICP
SHEEP6: Pha.Rel.T1.   FREQUENCY RANGE (3696 - 5936 Hz)

PHASE OF RELATIVE TRANSFER IMPEDANCE 1, SHEEP6
FREQUENCY RANGE (6336 - 9696 Hz)

PHASE STANDARD DEVIATION vs. ICP
SHEEP6: Pha.Rel.T1.   FREQUENCY RANGE (6336 - 9696 Hz)

PHASE OF RELATIVE TRANSFER IMPEDANCE 2, SHEEP6

PHASE OF RELATIVE TRANSFER IMPEDANCE 2, SHEEP6
FREQUENCY RANGE (104 - 1616 Hz)

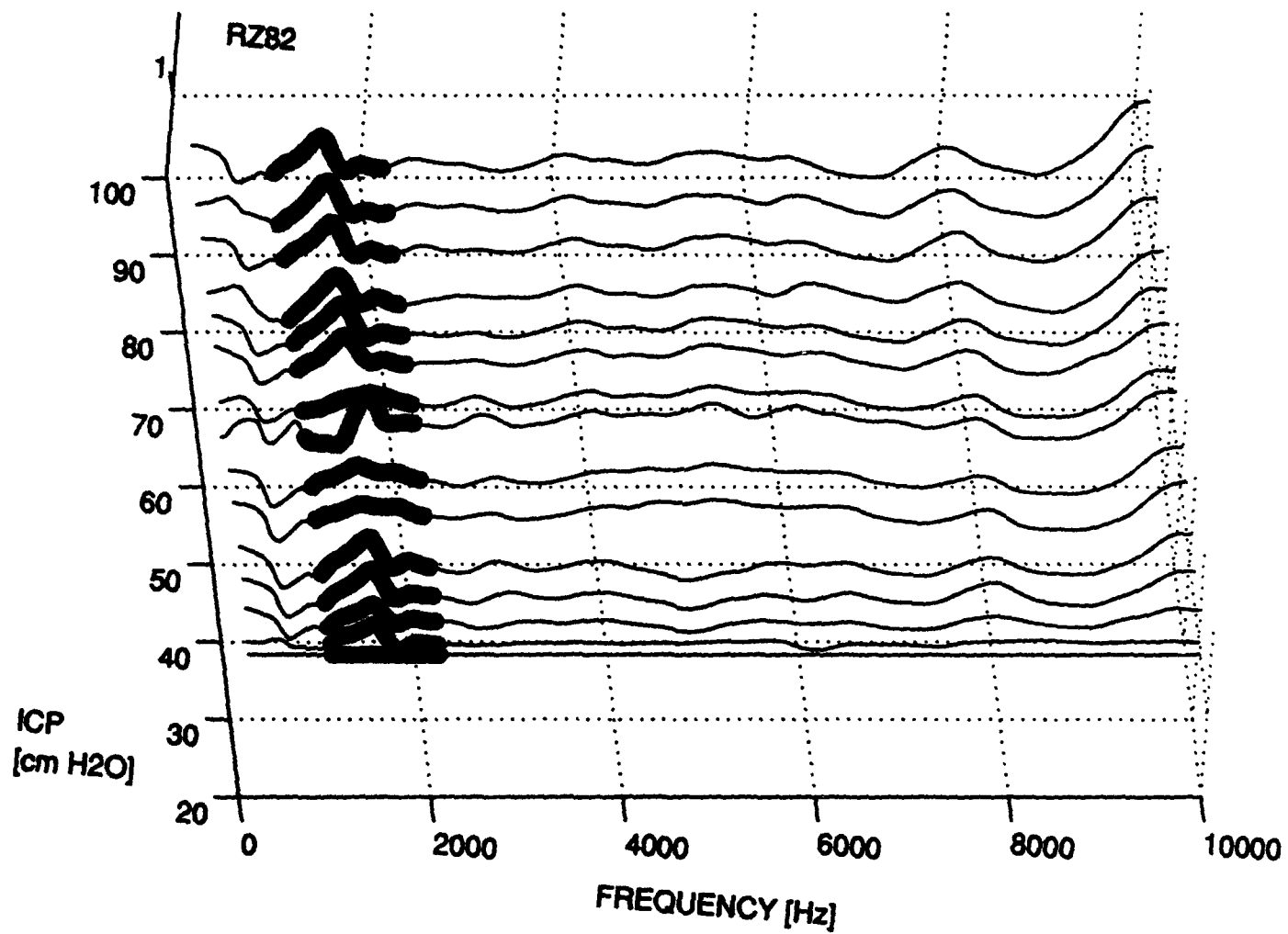PHASE STANDARD DEVIATION vs. ICP
SHEEP6: Pha.Rel.T2.   FREQUENCY RANGE (104 - 1616 Hz)

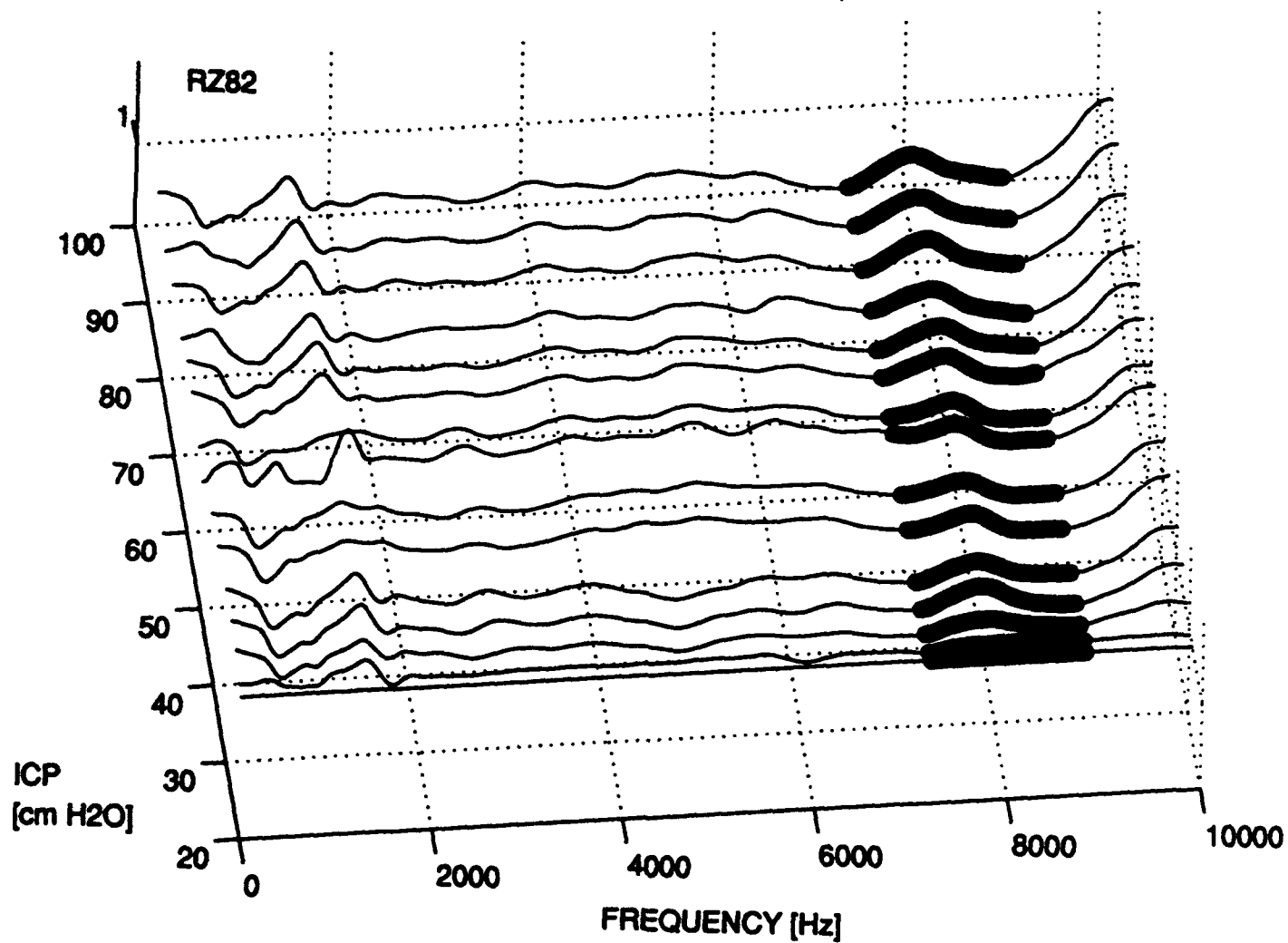PHASE OF RELATIVE TRANSFER IMPEDANCE 2, SHEEP6
FREQUENCY RANGE (2256 - 4336 Hz)

RP62 [deg]

ICP
[cm H2O]

FREQUENCY [Hz]

PHASE STANDARD DEVIATION vs. ICP
SHEEP6: Pha.Rel.T2.   FREQUENCY RANGE (2256 - 4336 Hz)

PHASE OF RELATIVE TRANSFER IMPEDANCE 3, SHEEP6

PHASE OF RELATIVE TRANSFER IMPEDANCE 3, SHEEP6
FREQUENCY RANGE (176 - 2096 Hz)
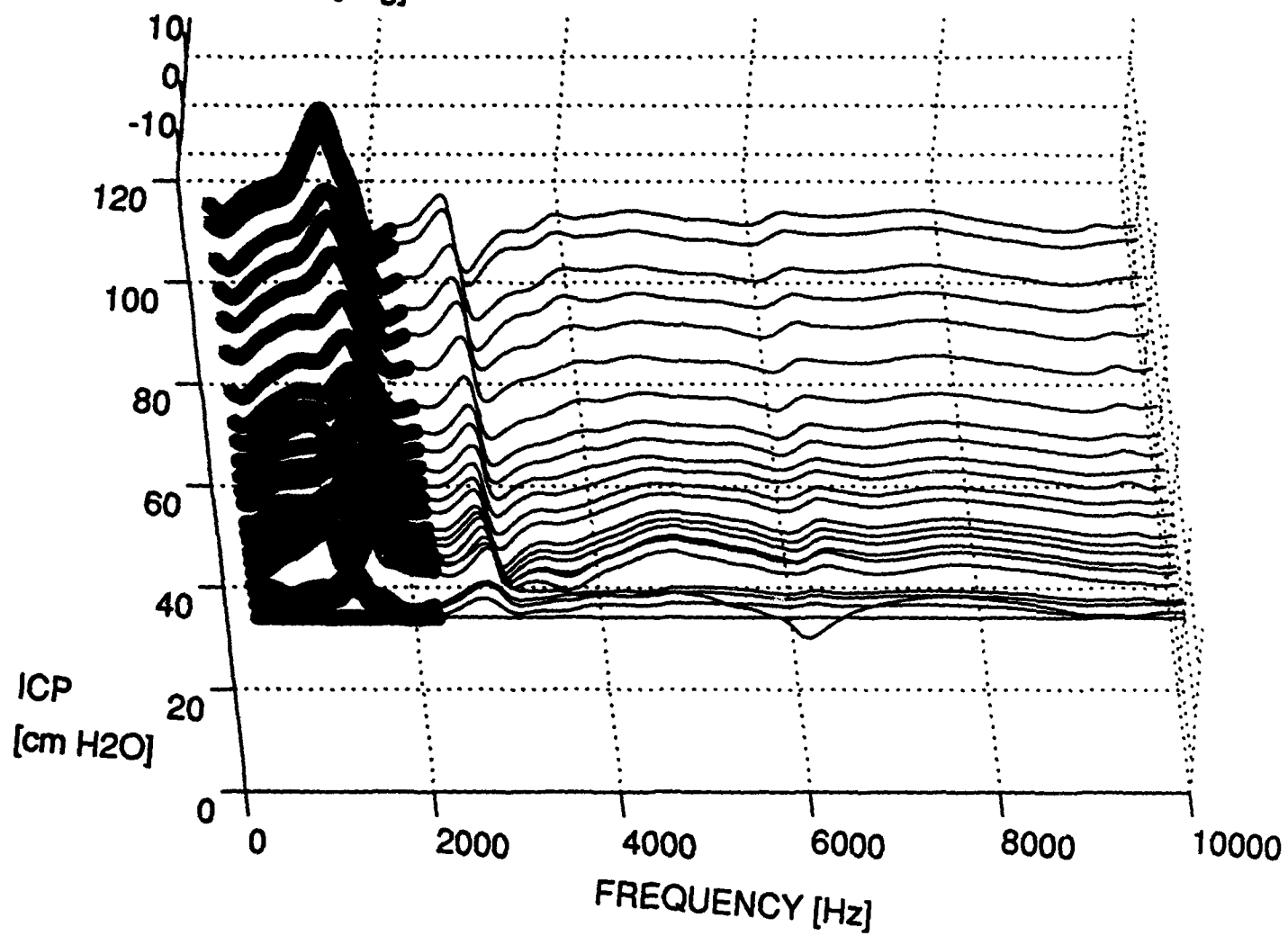
PHASE STANDARD DEVIATION vs. ICP
SHEEP6: Pha.Rel.T3.   FREQUENCY RANGE (176 - 2096 Hz)

PHASE OF RELATIVE TRANSFER IMPEDANCE 3, SHEEP6
FREQUENCY RANGE (2256 - 2976 Hz)

RP63 [deg]

PHASE STANDARD DEVIATION vs. ICP
SHEEP6: Pha.Rel.T3.   FREQUENCY RANGE (2256 - 2976 Hz)

MAGNITUDE OF RELATIVE DRIVING POINT IMPEDANCE, SHEEP8

RZ80

ICP
[cm H2O]

FREQUENCY [Hz]

MAGNITUDE OF RELATIVE DRIVING POINT IMPEDANCE, SHEEP8
FREQUENCY RANGE (736 - 2496 Hz)
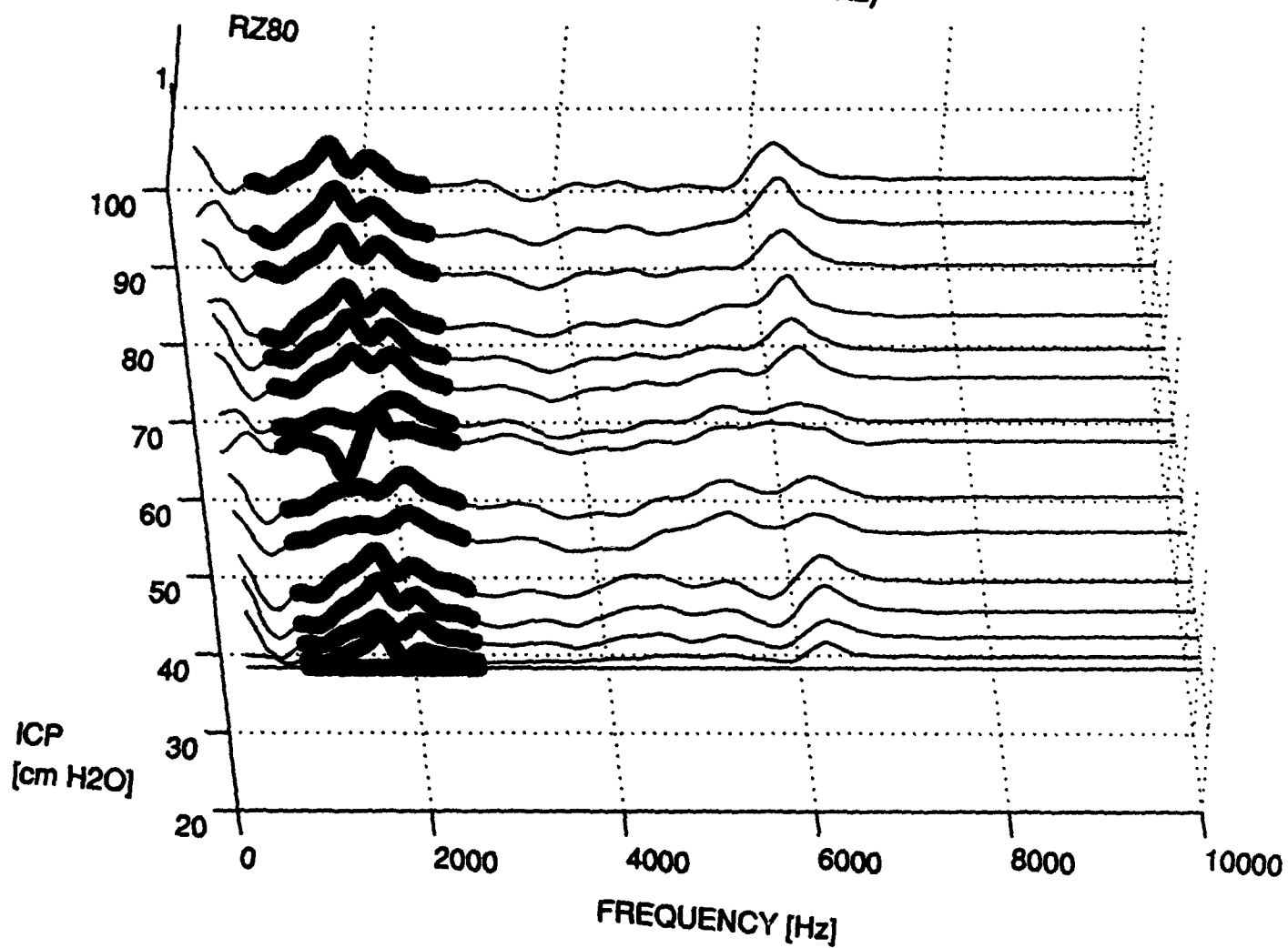
MAGNITUDE STANDARD DEVIATION vs. ICP
SHEEP8: Mag.Rel DP.   FREQUENCY RANGE (736 - 2496 Hz)

MAGNITUDE OF RELATIVE DRIVING POINT IMPEDANCE, SHEEP8
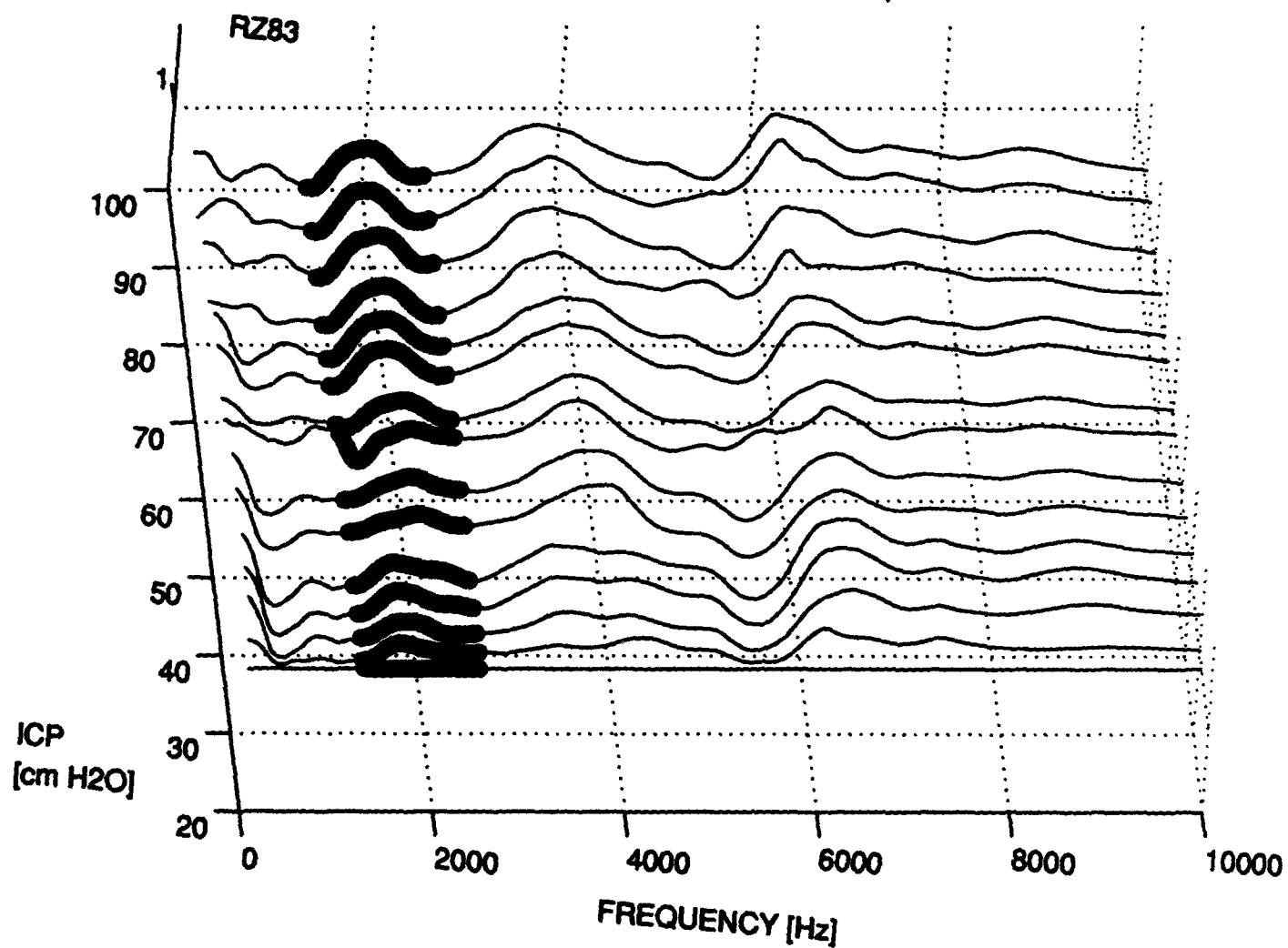FREQUENCY RANGE (5536 - 7056 Hz)

MAGNITUDE STANDARD DEVIATION vs. ICP
SHEEP8: Mag.Rel.DP.   FREQUENCY RANGE (5536 - 7056 Hz)

MAGNITUDE OF RELATIVE TRANSFER IMPEDANCE 1, SHEEP8

MAGNITUDE OF RELATIVE TRANSFER IMPEDANCE 1, SHEEP8
FREQUENCY RANGE (104 - 656 Hz)

MAGNITUDE STANDARD DEVIATION vs. ICP
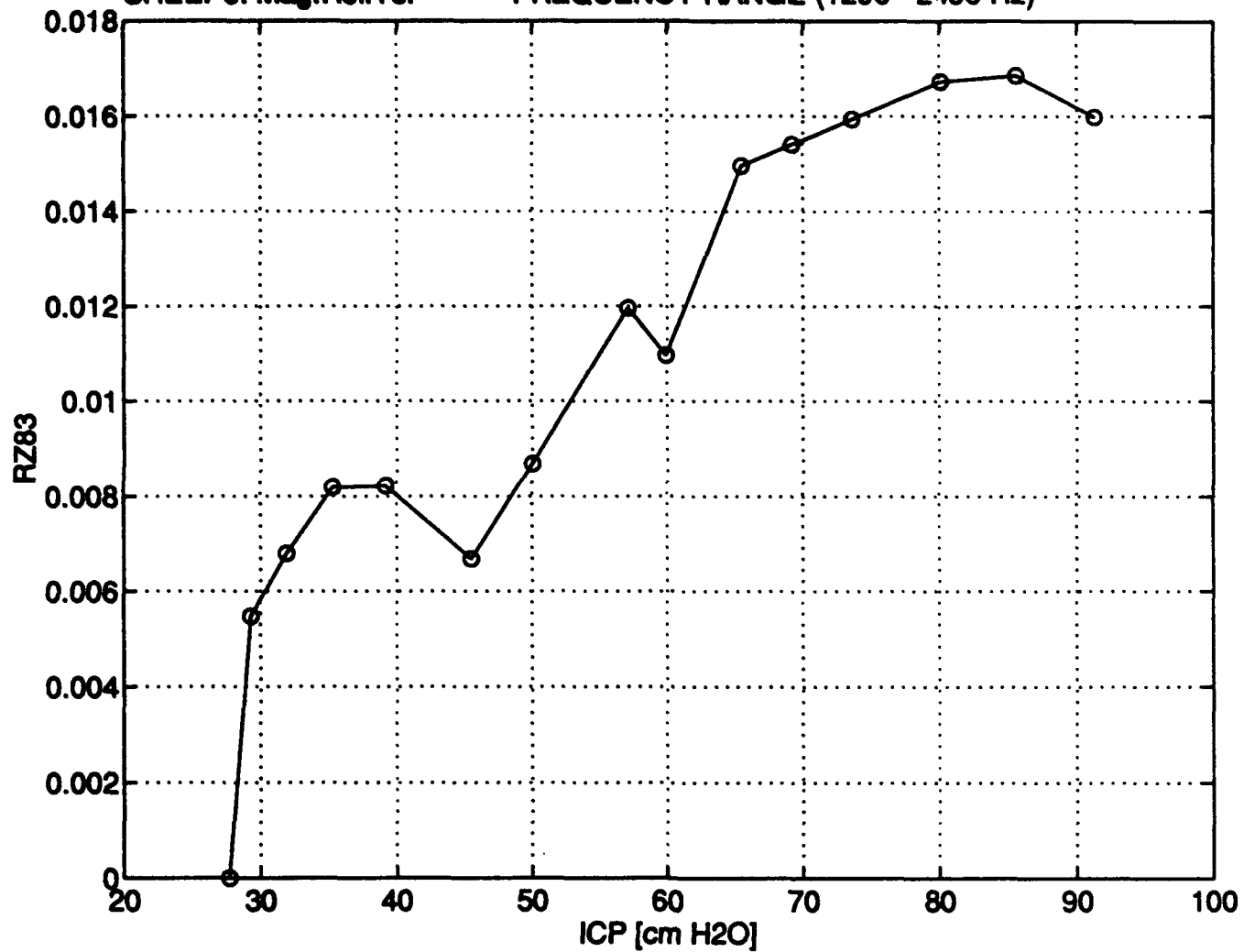SHEEP8: Mag.Rel.T1.   FREQUENCY RANGE (104 - 656 Hz)

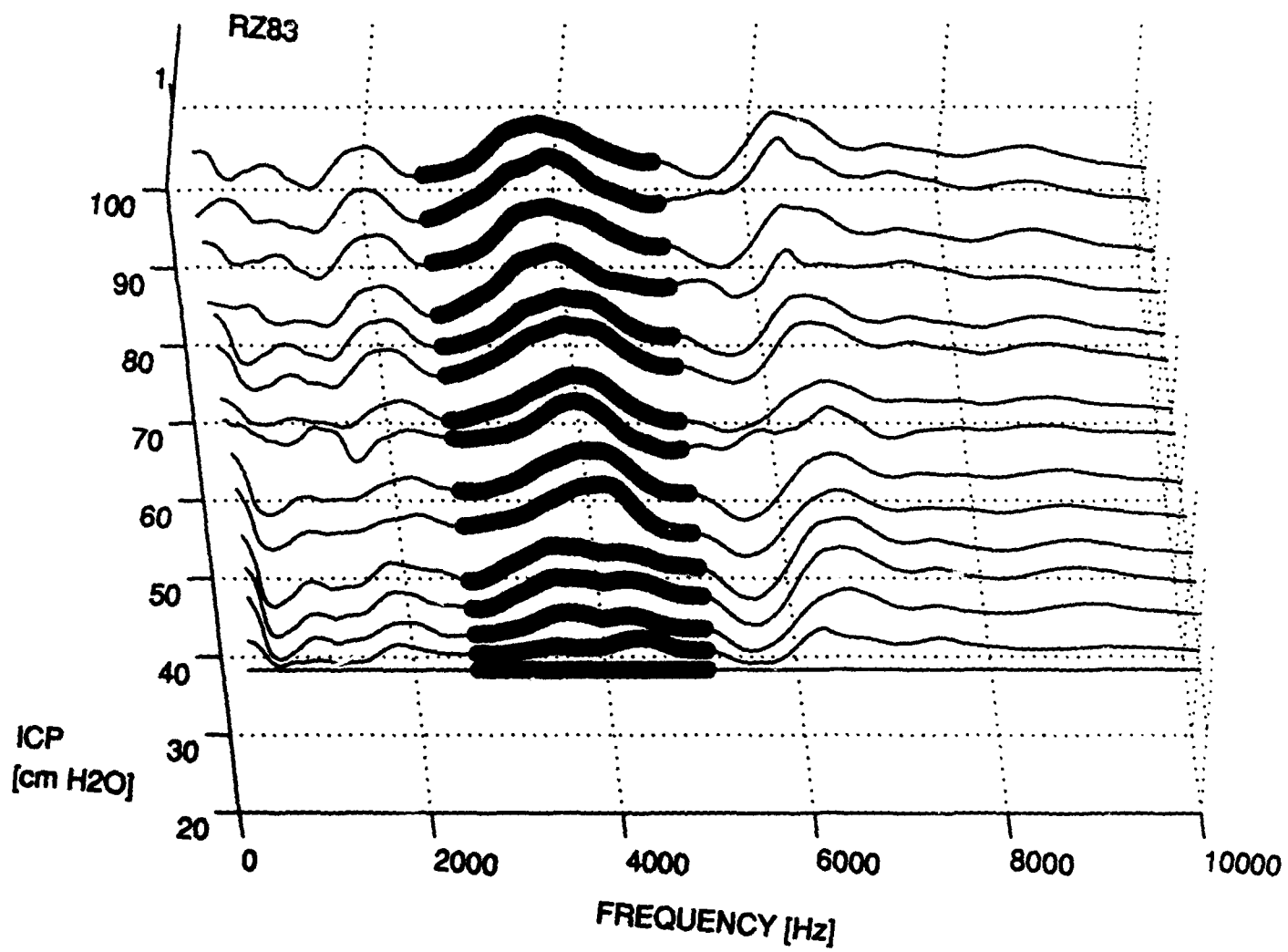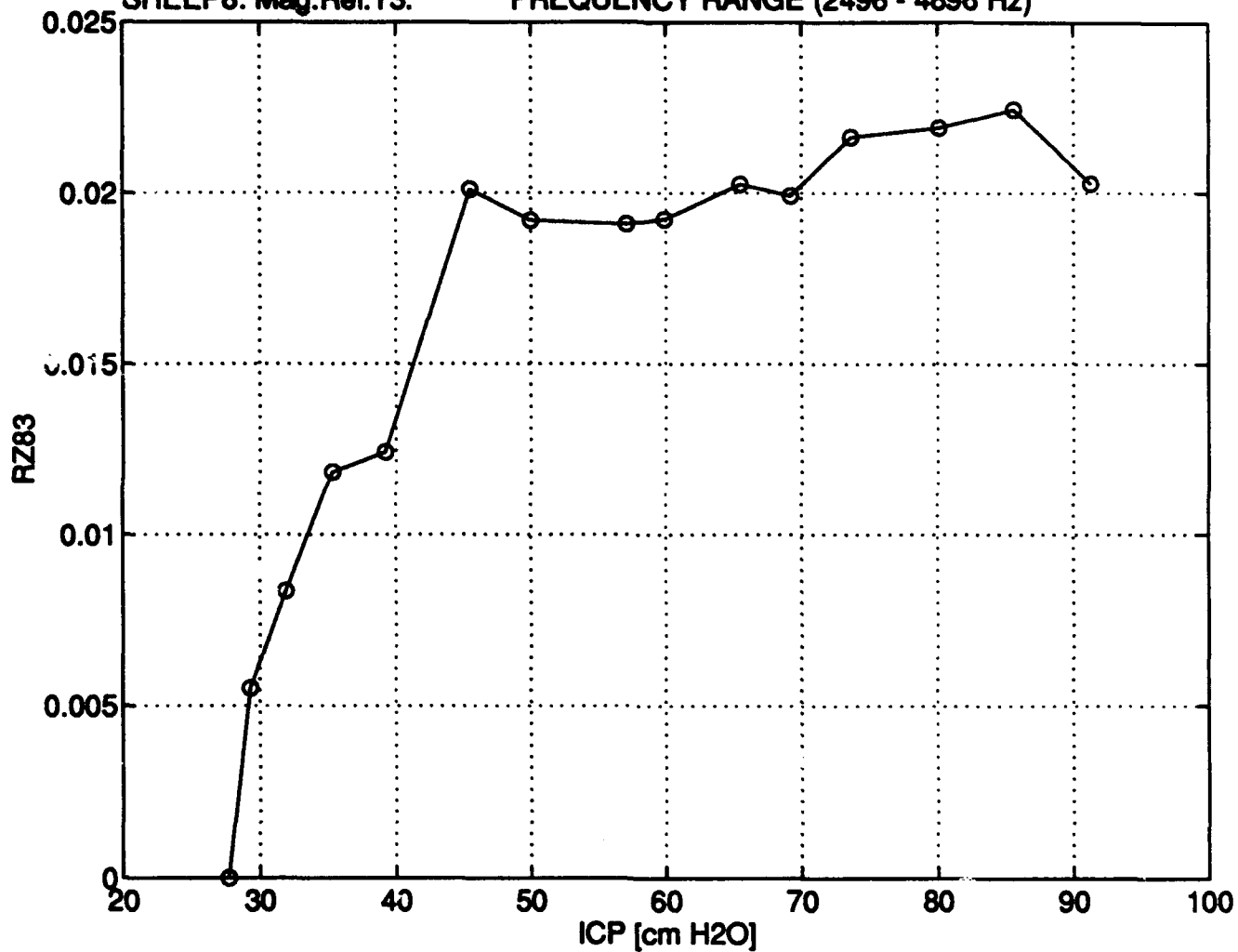MAGNITUDE OF RELATIVE TRANSFER IMPEDANCE 1, SHEEP8
FREQUENCY RANGE (656 - 2496 Hz)

RZ81

ICP
[cm H2O]

FREQUENCY [Hz]

MAGNITUDE STANDARD DEVIATION vs. ICP
SHEEP8: Mag.Rel.T1.   FREQUENCY RANGE (656 - 2496 Hz)

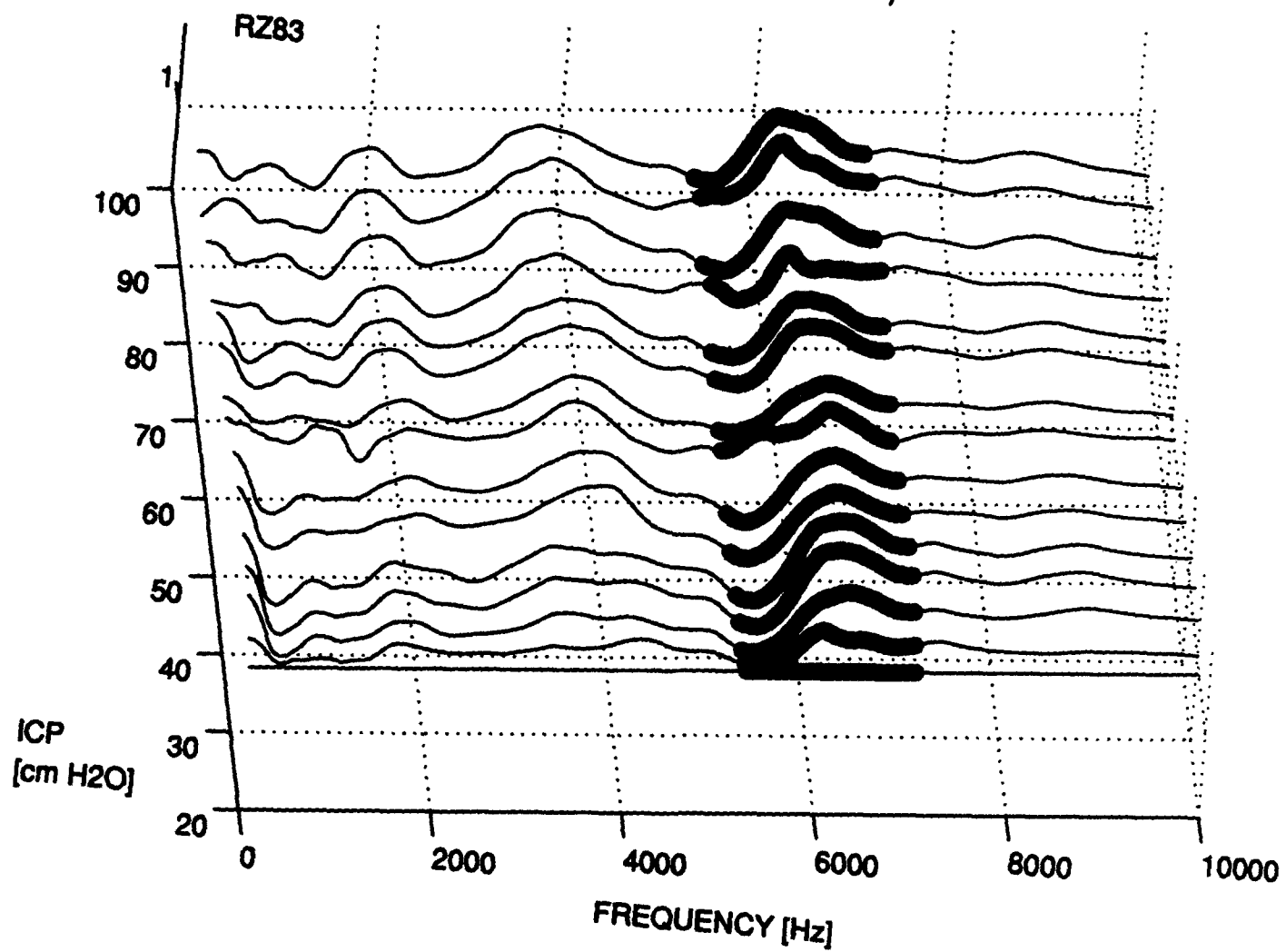MAGNITUDE OF RELATIVE TRANSFER IMPEDANCE 1, SHEEP8
FREQUENCY RANGE (2736 - 4896 Hz)

MAGNITUDE STANDARD DEVIATION vs. ICP
SHEEP8: Mag.Rel.T1.   FREQUENCY RANGE (2736 - 4896 Hz)
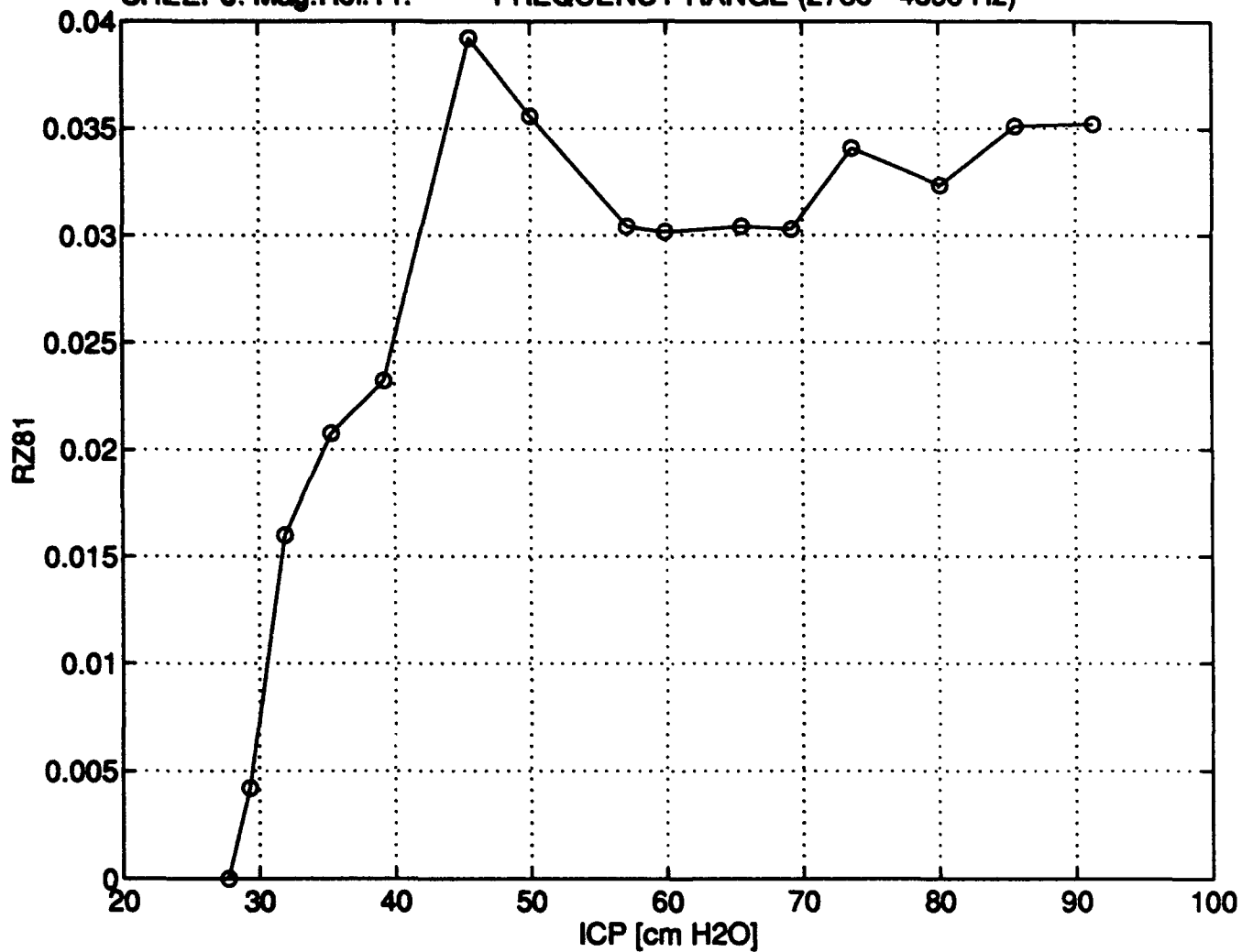
MAGNITUDE OF RELATIVE TRANSFER IMPEDANCE 1, SHEEP8
FREQUENCY RANGE (4896 - 7296 Hz)
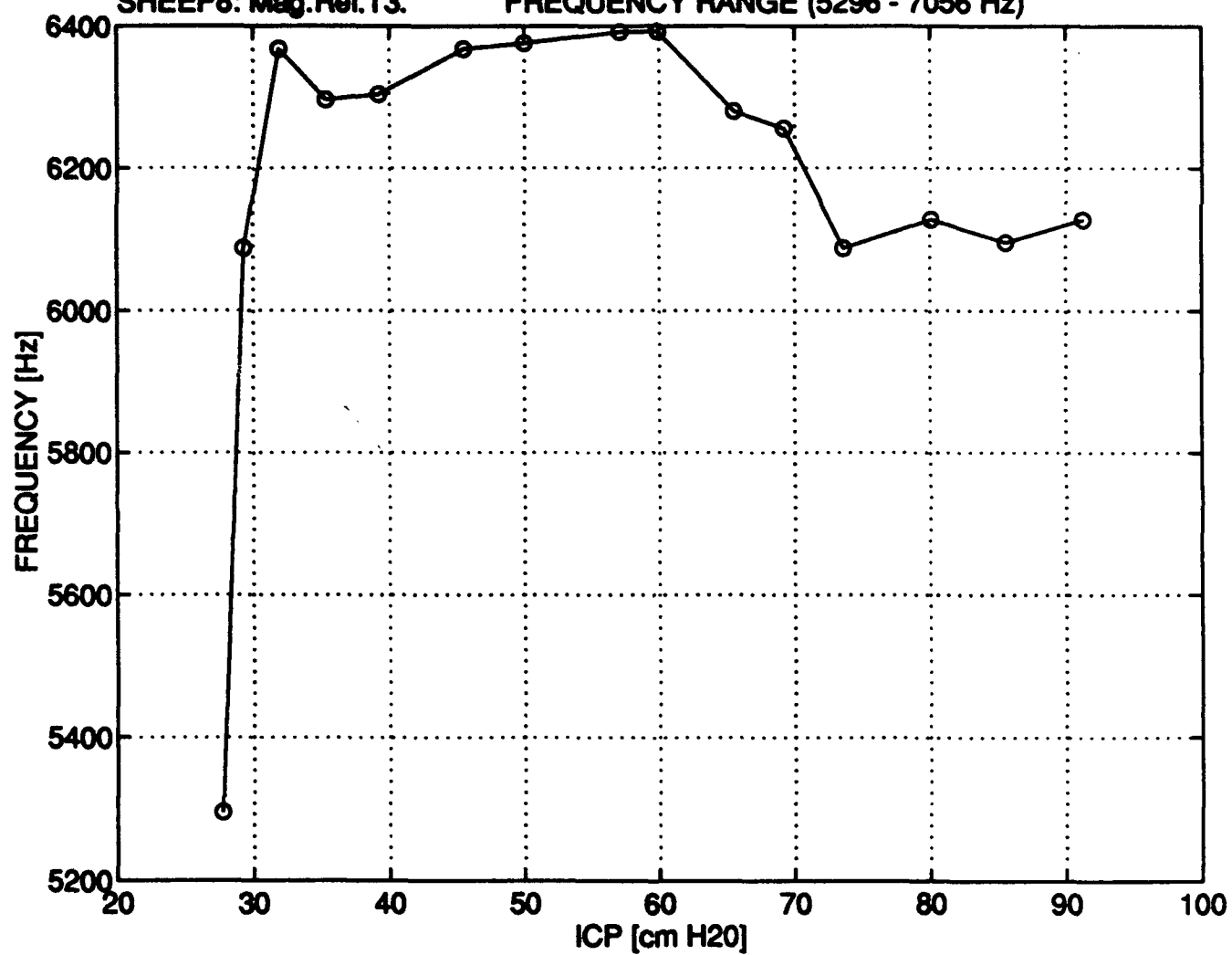
MAGNITUDE STANDARD DEVIATION vs. ICP
SHEEP8: Mag.Rel.T1.   FREQUENCY RANGE (4896 - 7296 Hz)

MAGNITUDE OF RELATIVE TRANSFER IMPEDANCE 2, SHEEP8

MAGNITUDE OF RELATIVE TRANSFER IMPEDANCE 2, SHEEP8
FREQUENCY RANGE (104 - 976 Hz)

RZ82

ICP
[cm H2O]

FREQUENCY [Hz]

MAGNITUDE STANDARD DEVIATION vs. ICP
SHEEP8: Mag.Rel.T2.   FREQUENCY RANGE (104 - 976 Hz)

MAGNITUDE OF RELATIVE TRANSFER IMPEDANCE 2, SHEEP8
FREQUENCY RANGE (976 - 2096 Hz)

MAGNITUDE STANDARD DEVIATION vs. ICP
SHEEP8: Mag.Rel.T2.   FREQUENCY RANGE (976 - 2096 Hz)
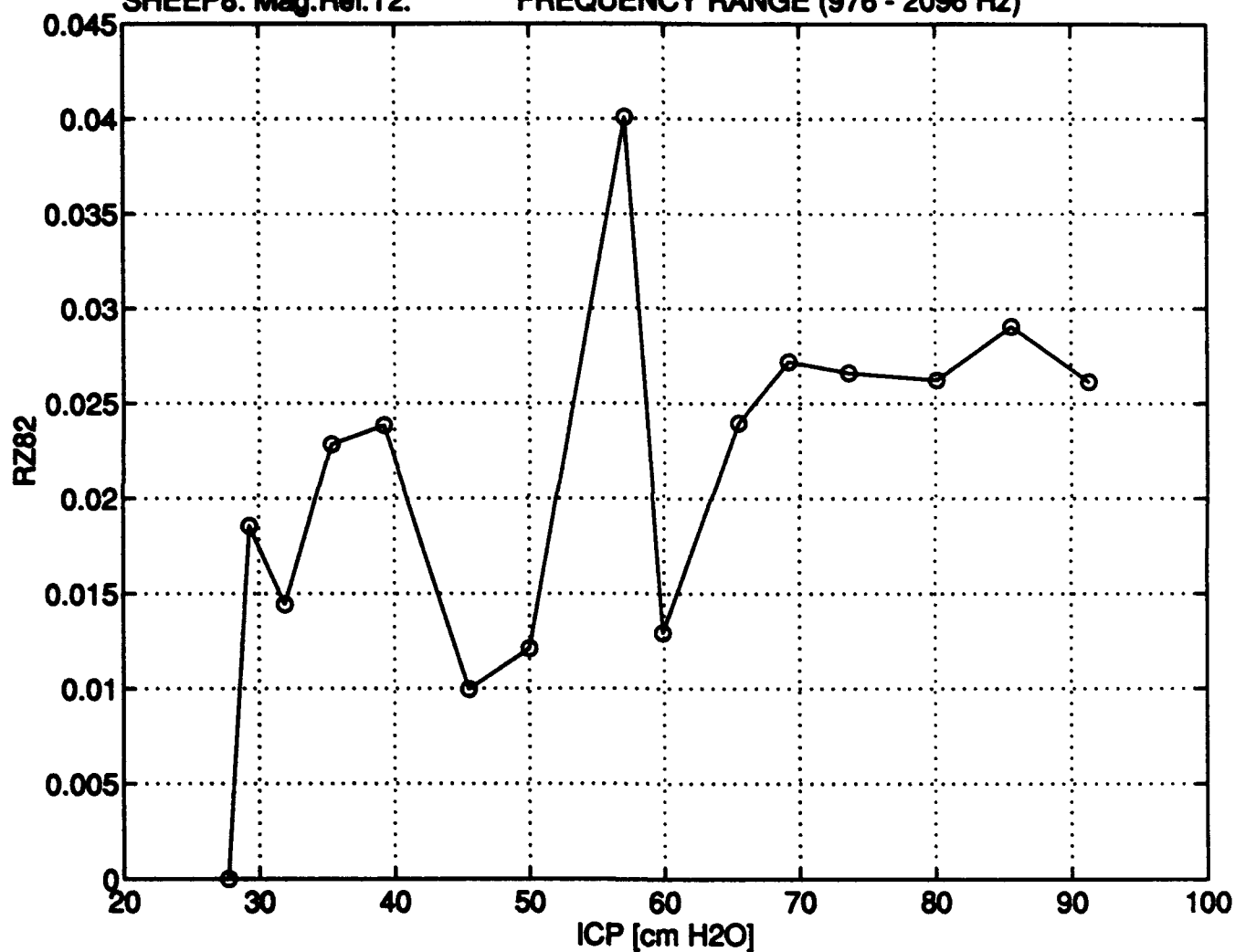
MAGNITUDE OF RELATIVE TRANSFER IMPEDANCE 2, SHEEP8
FREQUENCY RANGE (7296 - 8896 Hz)

MAGNITUDE STANDARD DEVIATION vs. ICP

SHEEP8: Mag.Rel.T2.   FREQUENCY RANGE (7296 - 8896 Hz)
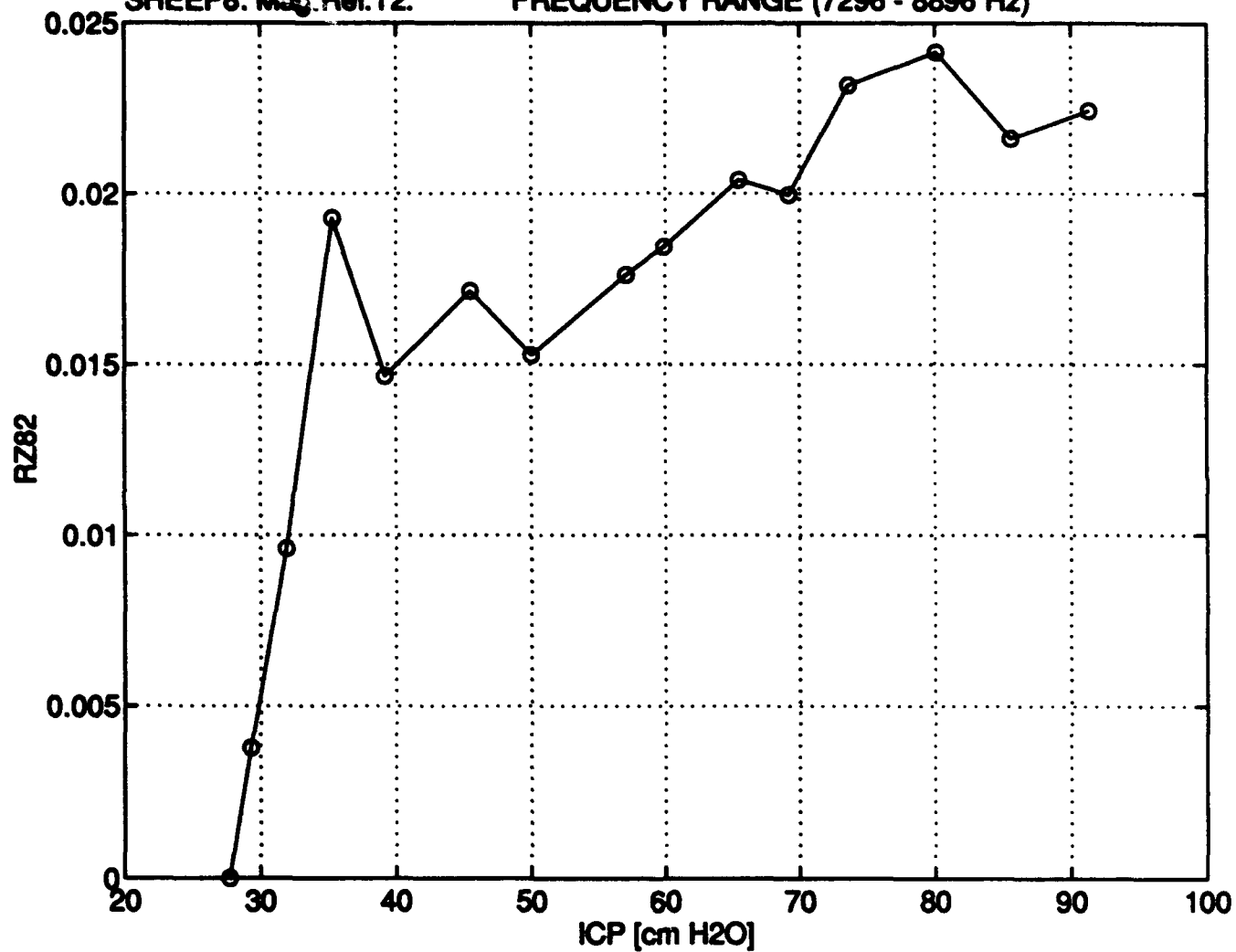
MAGNITUDE OF RELATIVE TRANSFER IMPEDANCE 3, SHEEP8
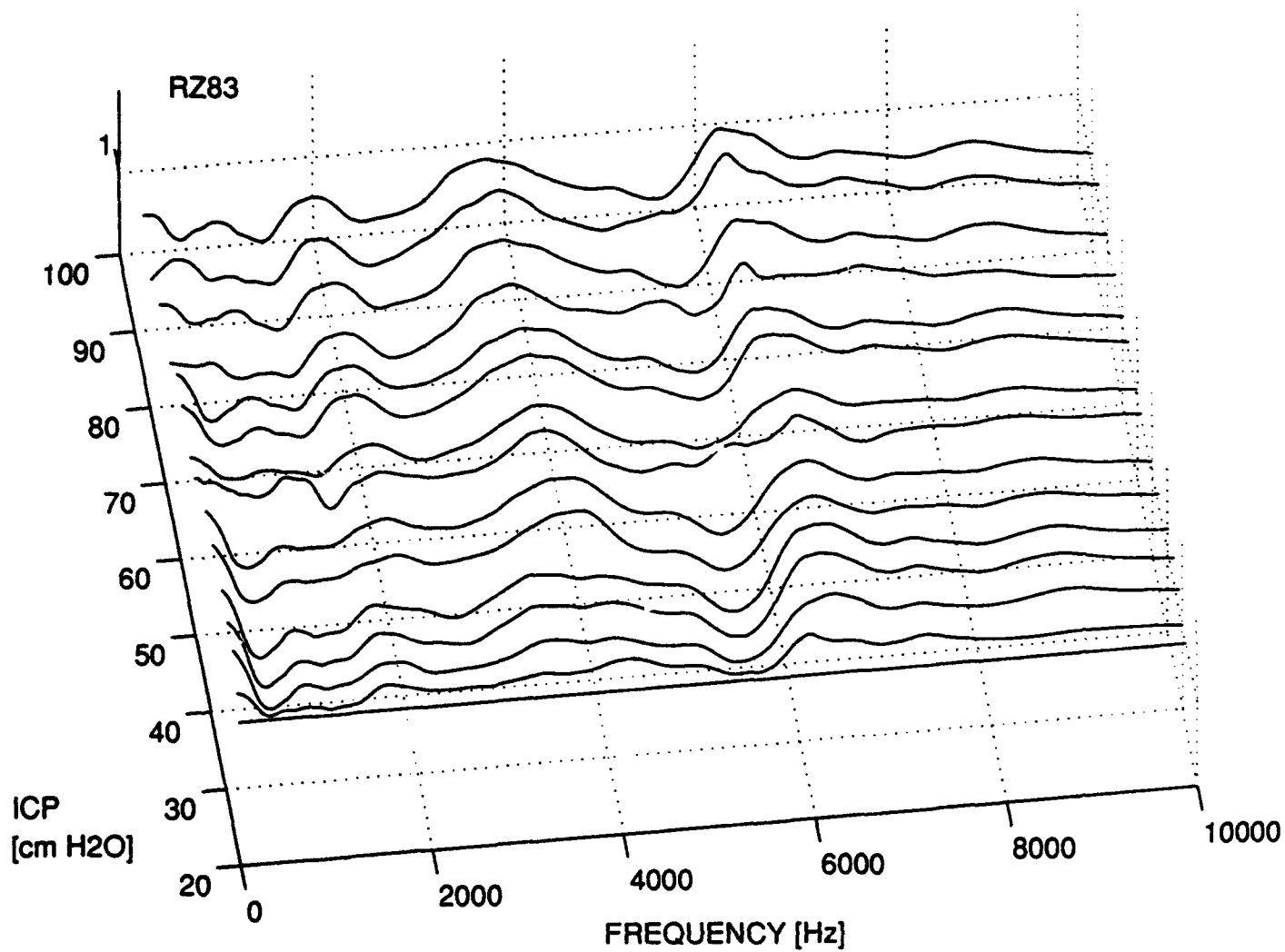
MAGNITUDE OF RELATIVE TRANSFER IMPEDANCE 3, SHEEP8
FREQUENCY RANGE (104 - 576 Hz)
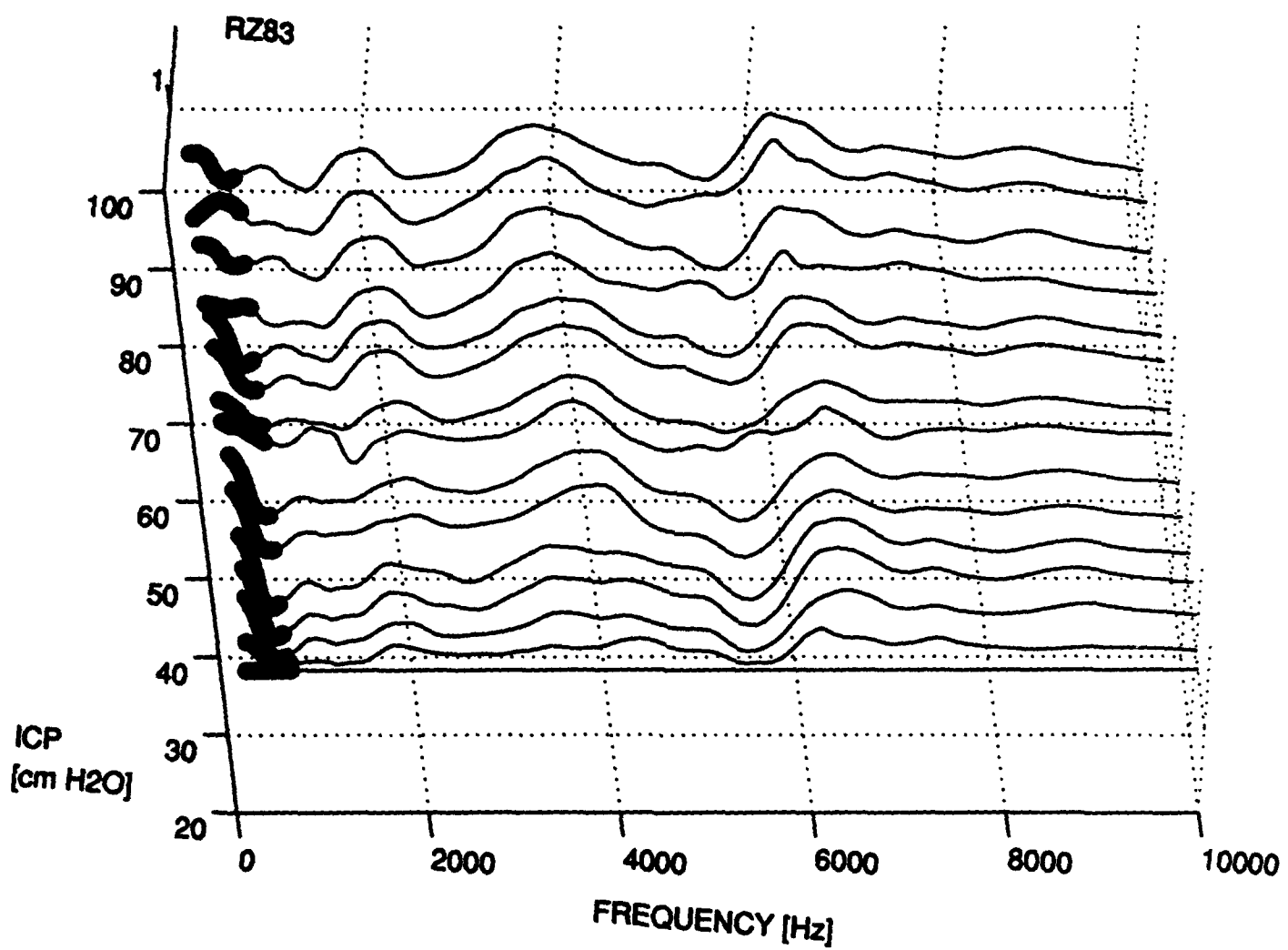
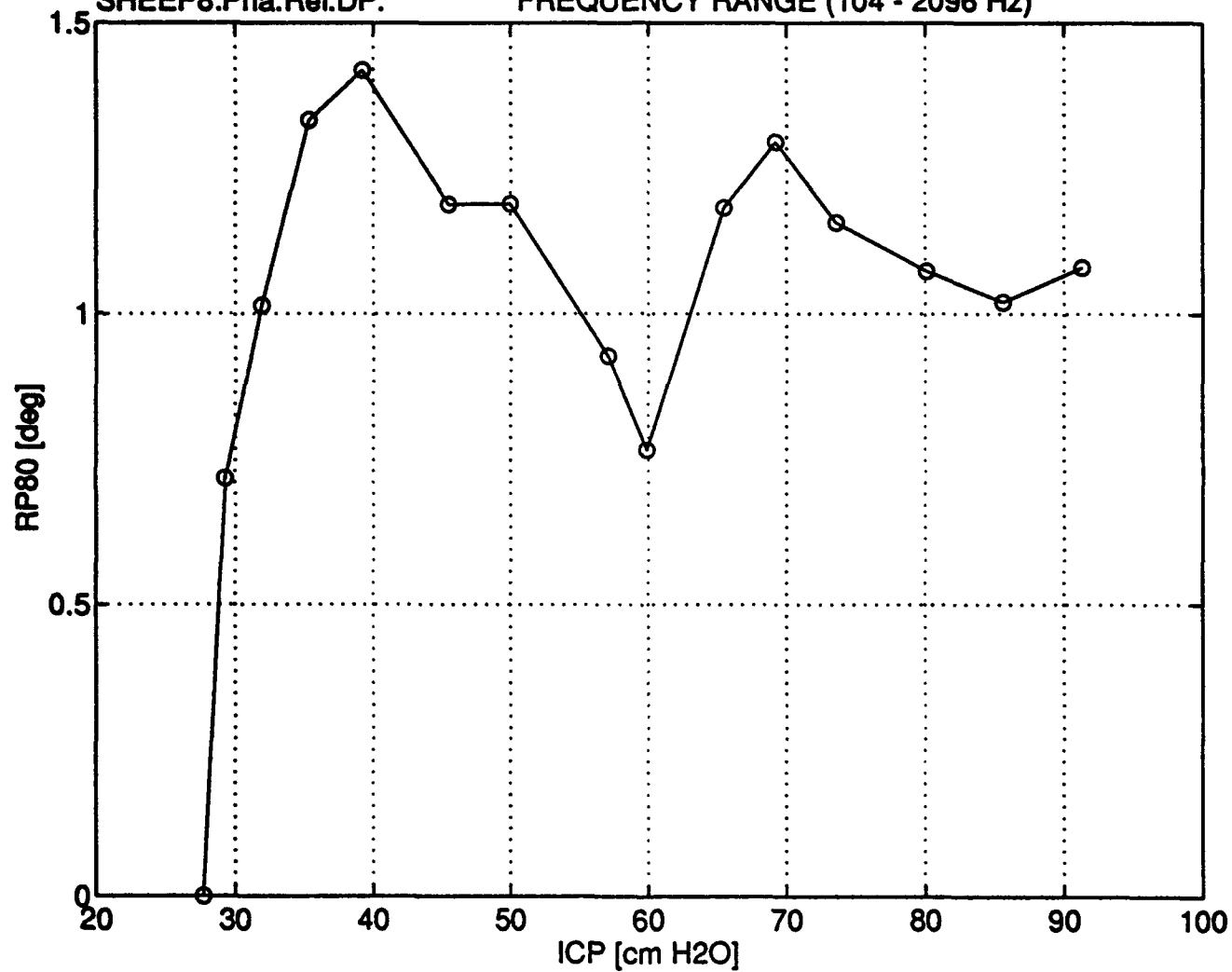MAGNITUDE STANDARD DEVIATION vs. ICP
SHEEP8: Mag.Rel.T3.   FREQUENCY RANGE (104 - 576 Hz)
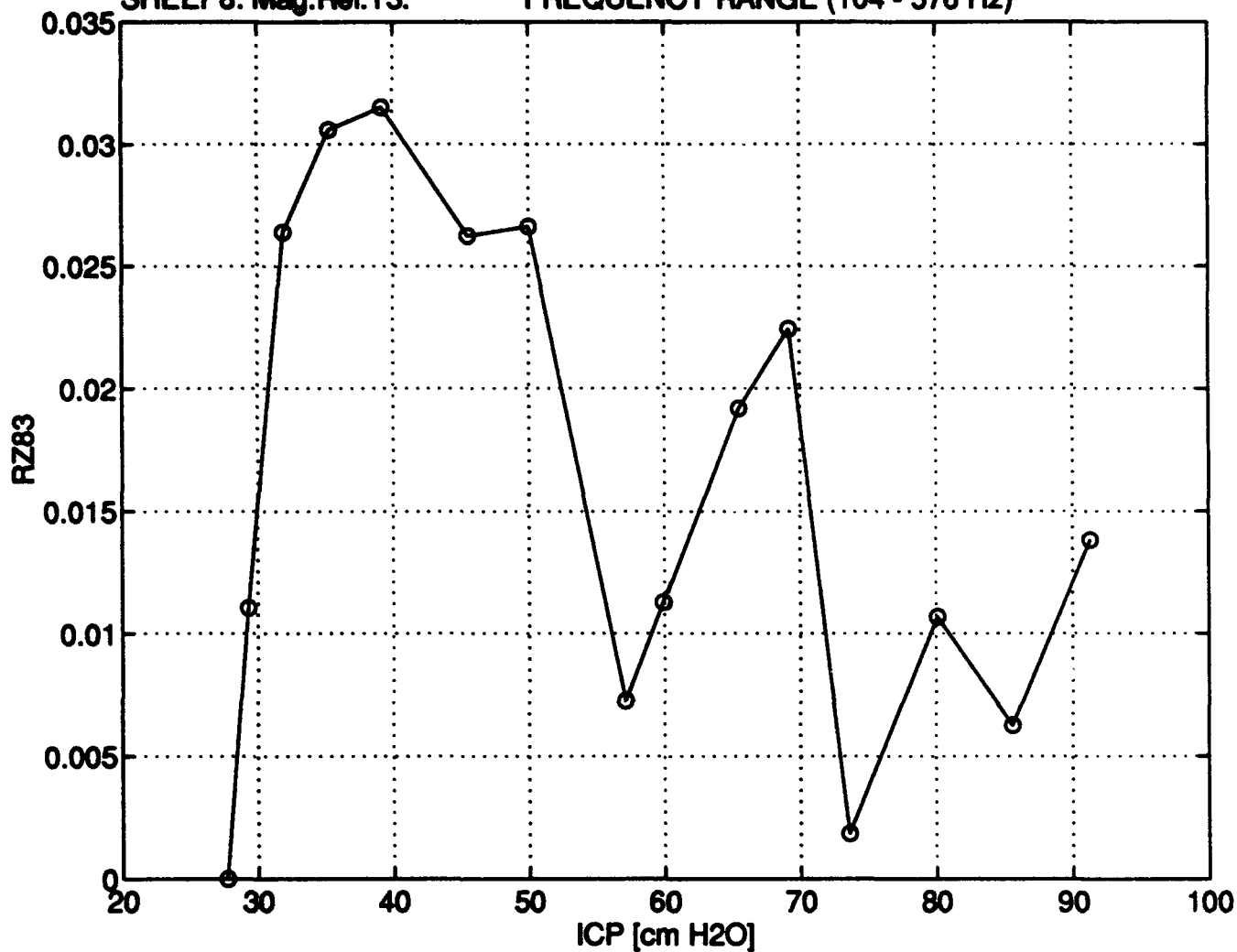
MAGNITUDE OF RELATIVE TRANSFER IMPEDANCE 3, SHEEP8
FREQUENCY RANGE (1296 - 2496 Hz)

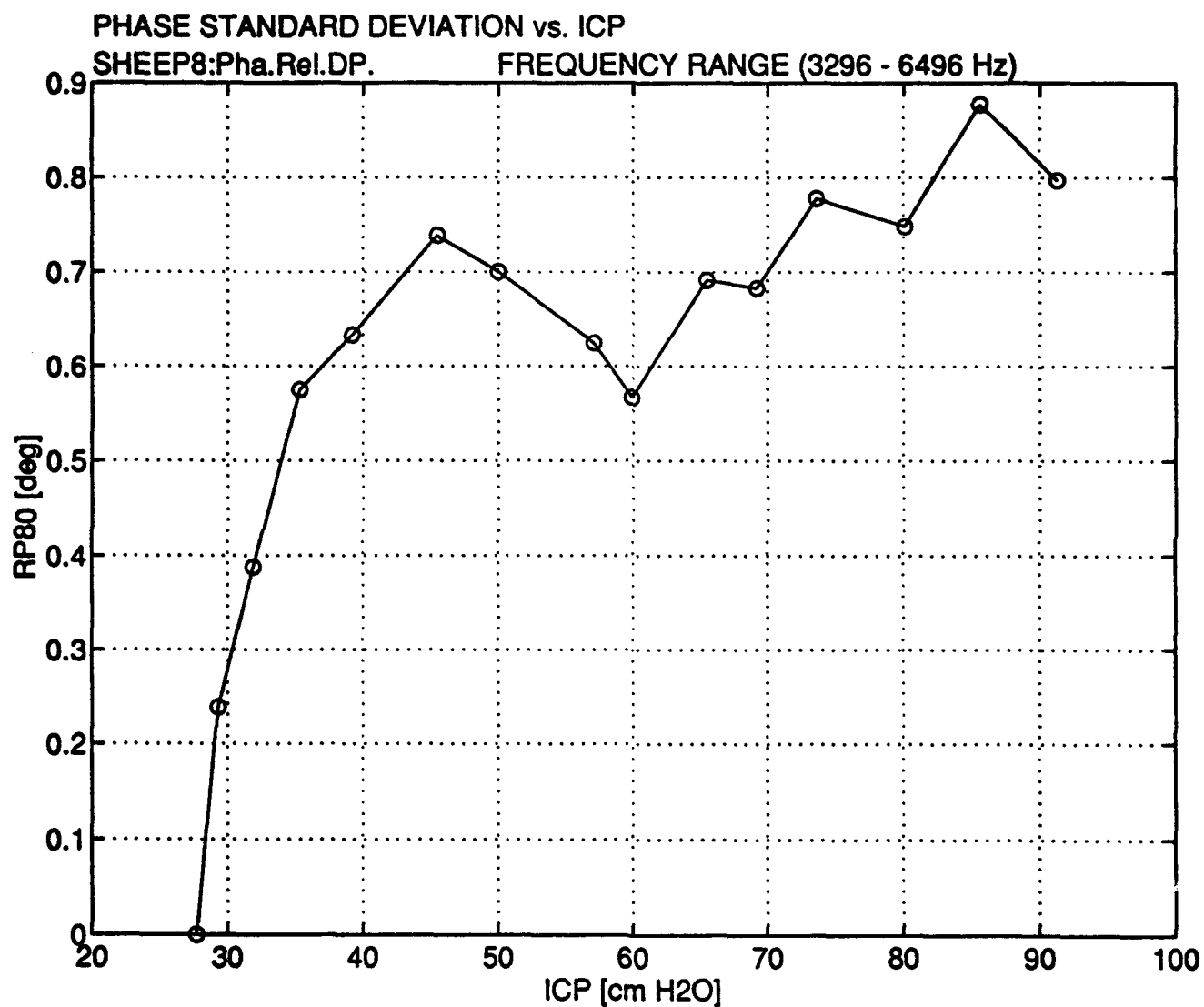MAGNITUDE STANDARD DEVIATION vs. ICP
SHEEP8: Mag.Rel.T3.   FREQUENCY RANGE (1296 - 2496 Hz)

MAGNITUDE OF RELATIVE TRANSFER IMPEDANCE 3, SHEEP8
FREQUENCY RANGE (2496 - 4896 Hz)

MAGNITUDE STANDARD DEVIATION vs. ICP
SHEEP8: Mag.Rel.T3.   FREQUENCY RANGE (2496 - 4896 Hz)

MAGNITUDE OF RELATIVE TRANSFER IMPEDANCE 3, SHEEP8
FREQUENCY RANGE (5296 - 7056 Hz)

MAGNITUDE MAXIMUM vs. ICP
SHEEP8: Mag.Rel.T3.   FREQUENCY RANGE (5296 - 7056 Hz)
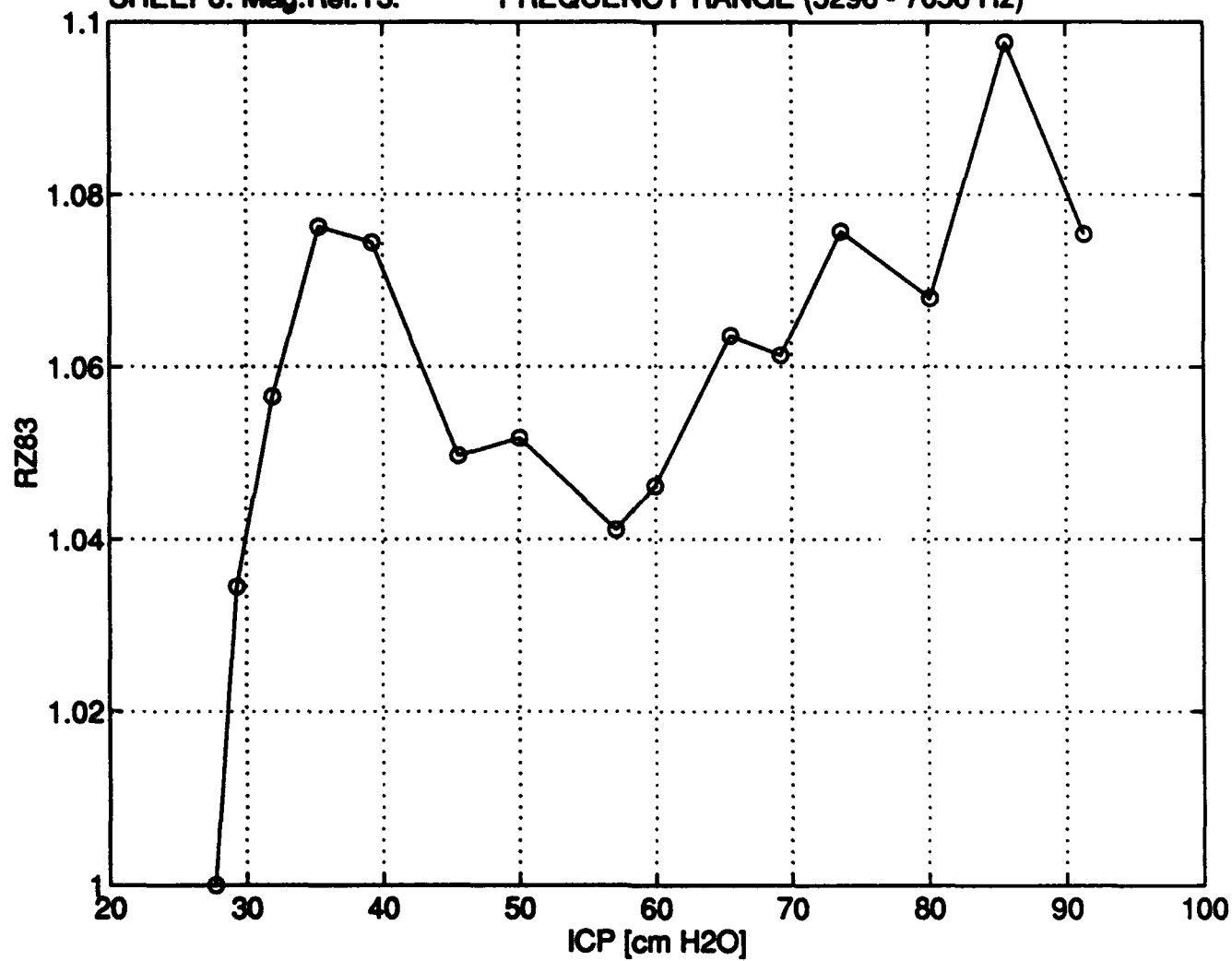
LOCATIONS OF MAGNITUDE MAXIMUM vs. ICP
SHEEP8: Mag.Rel.T3.   FREQUENCY RANGE (5296 - 7056 Hz)

MAGNITUDE MINIMUM vs. ICP
SHEEP8: Mag.Rel.T3.   FREQUENCY RANGE (5296 - 7056 Hz)
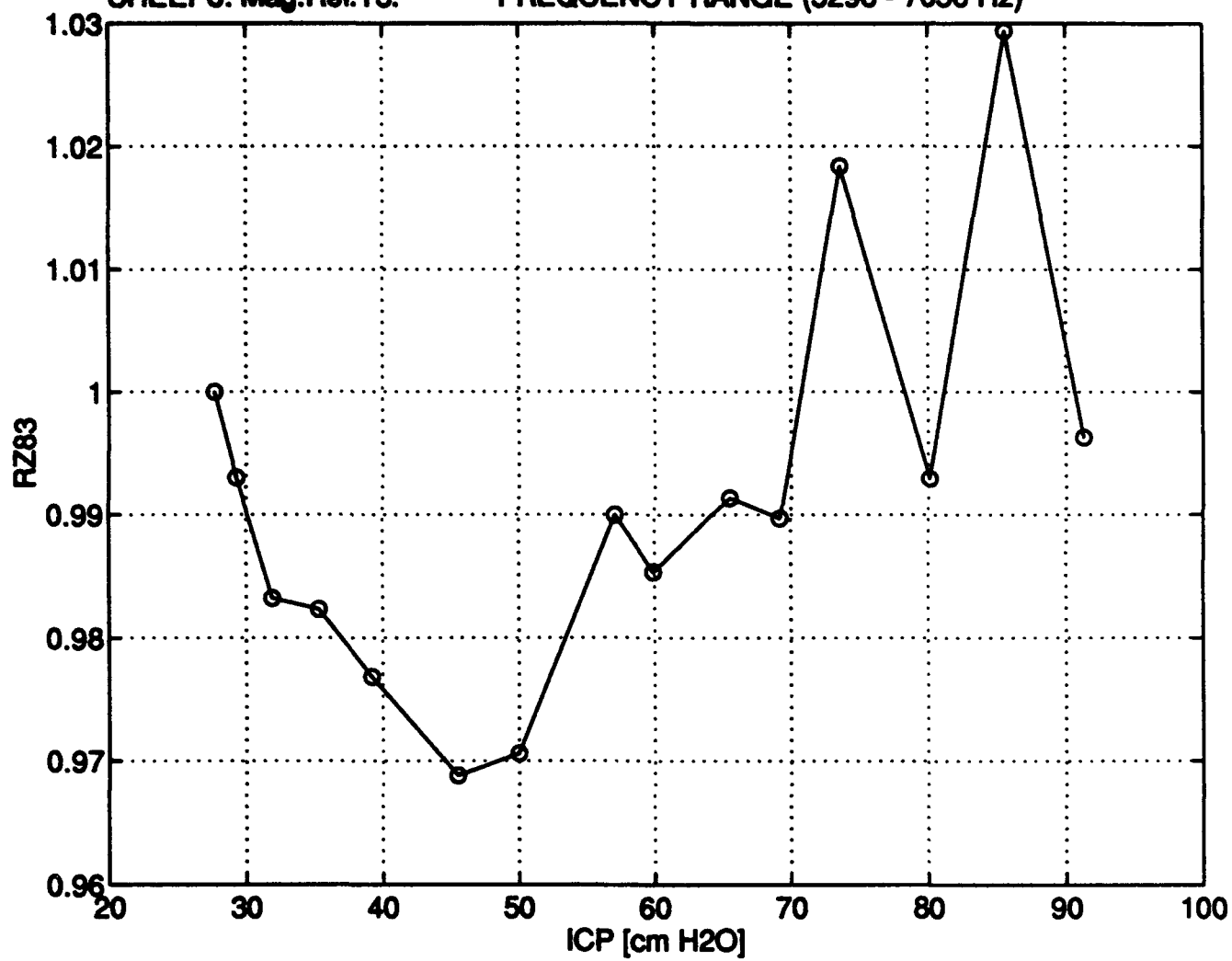
LOCATIONS OF MAGNITUDE MINIMUM vs. ICP
SHEEP8: Mag.Rel.T3.   FREQUENCY RANGE (5296 - 7056 Hz)
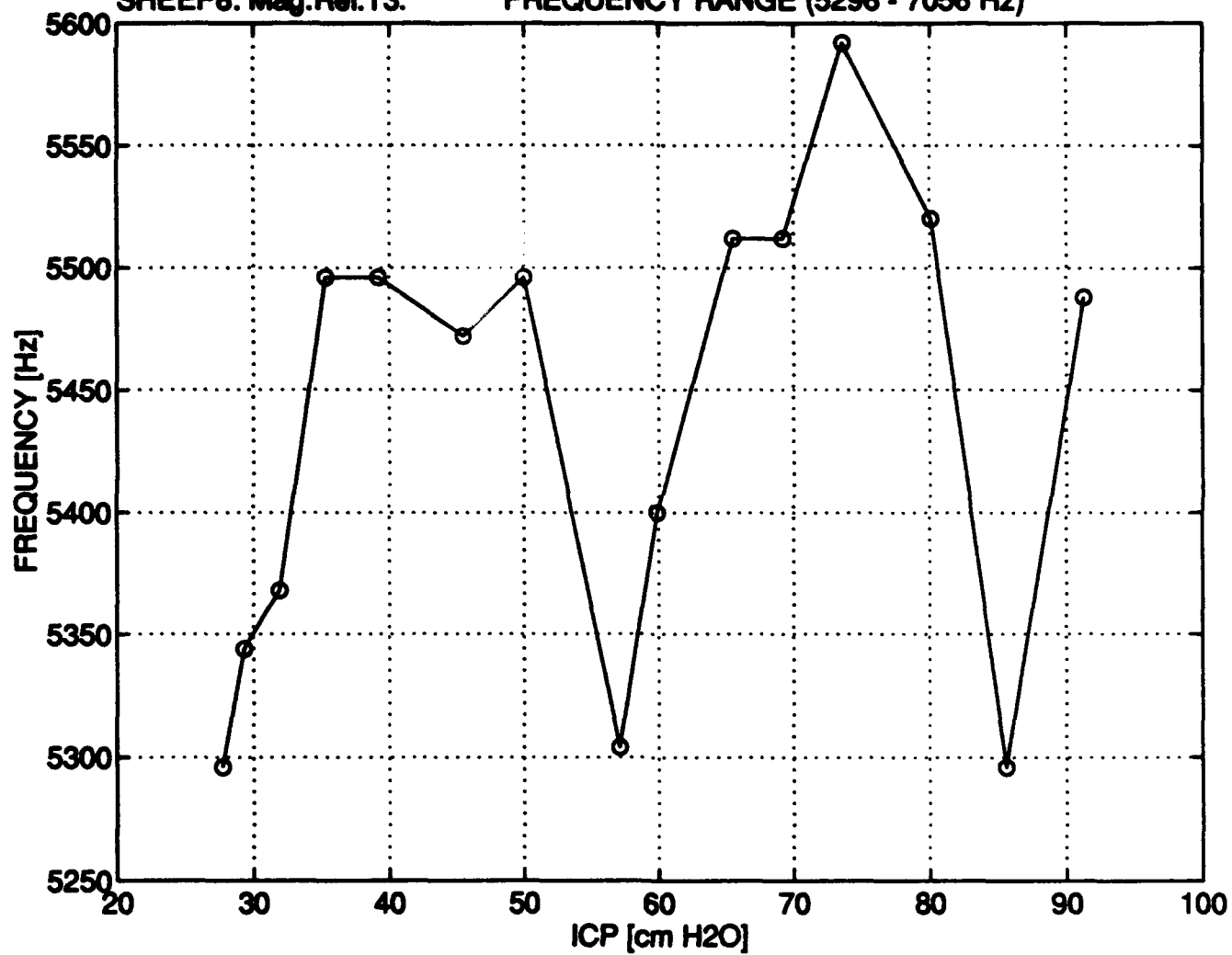
MAGNITUDE MEAN VALUE vs. ICP

SHEEP8: Mag.Rel.T3.   FREQUENCY RANGE (5296 - 7056 Hz)
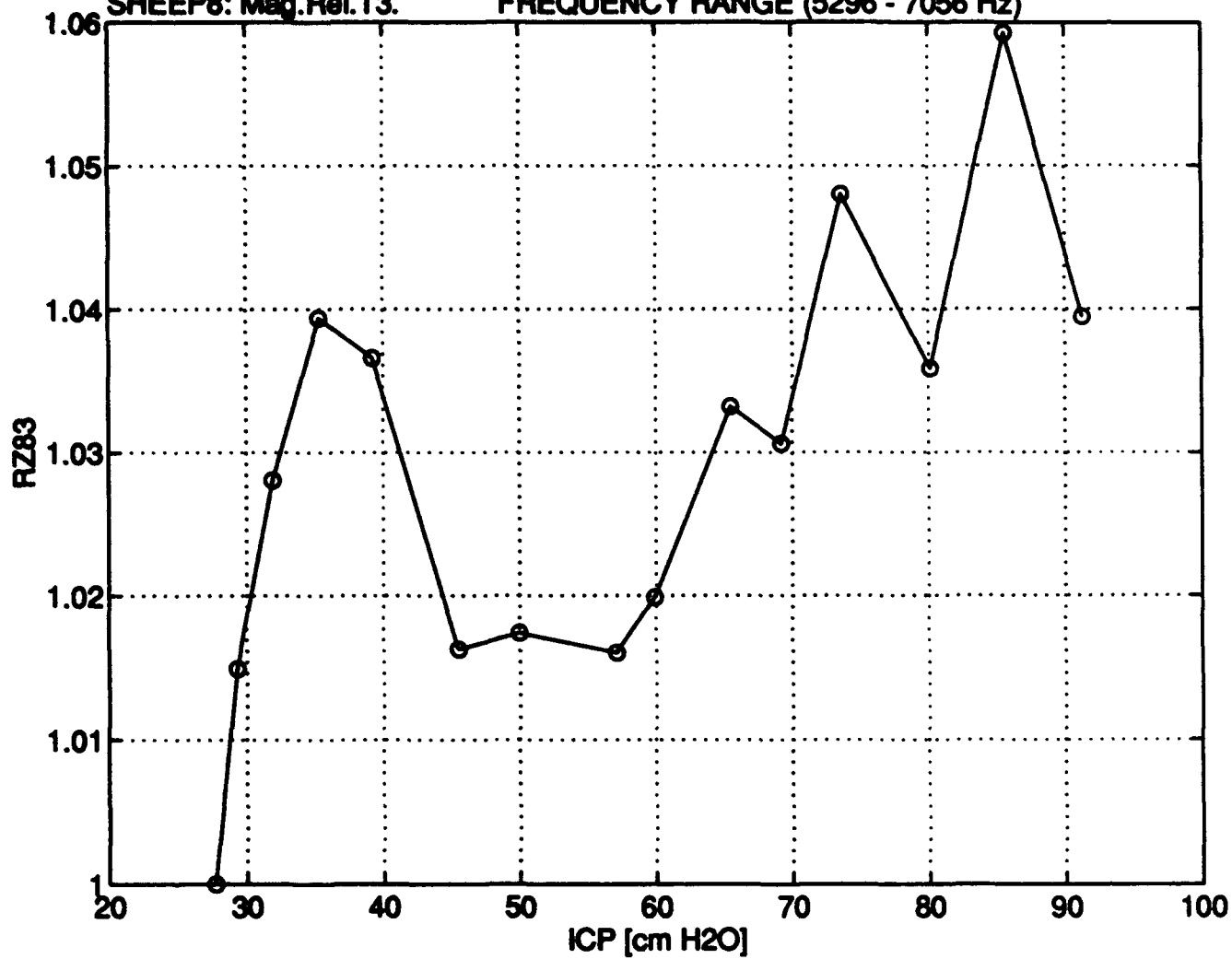
MAGNITUDE TRANSITION (max-min) vs. ICP
SHEEP8: Mag.Rel.T3.   FREQUENCY RANGE (5296 - 7056 Hz)
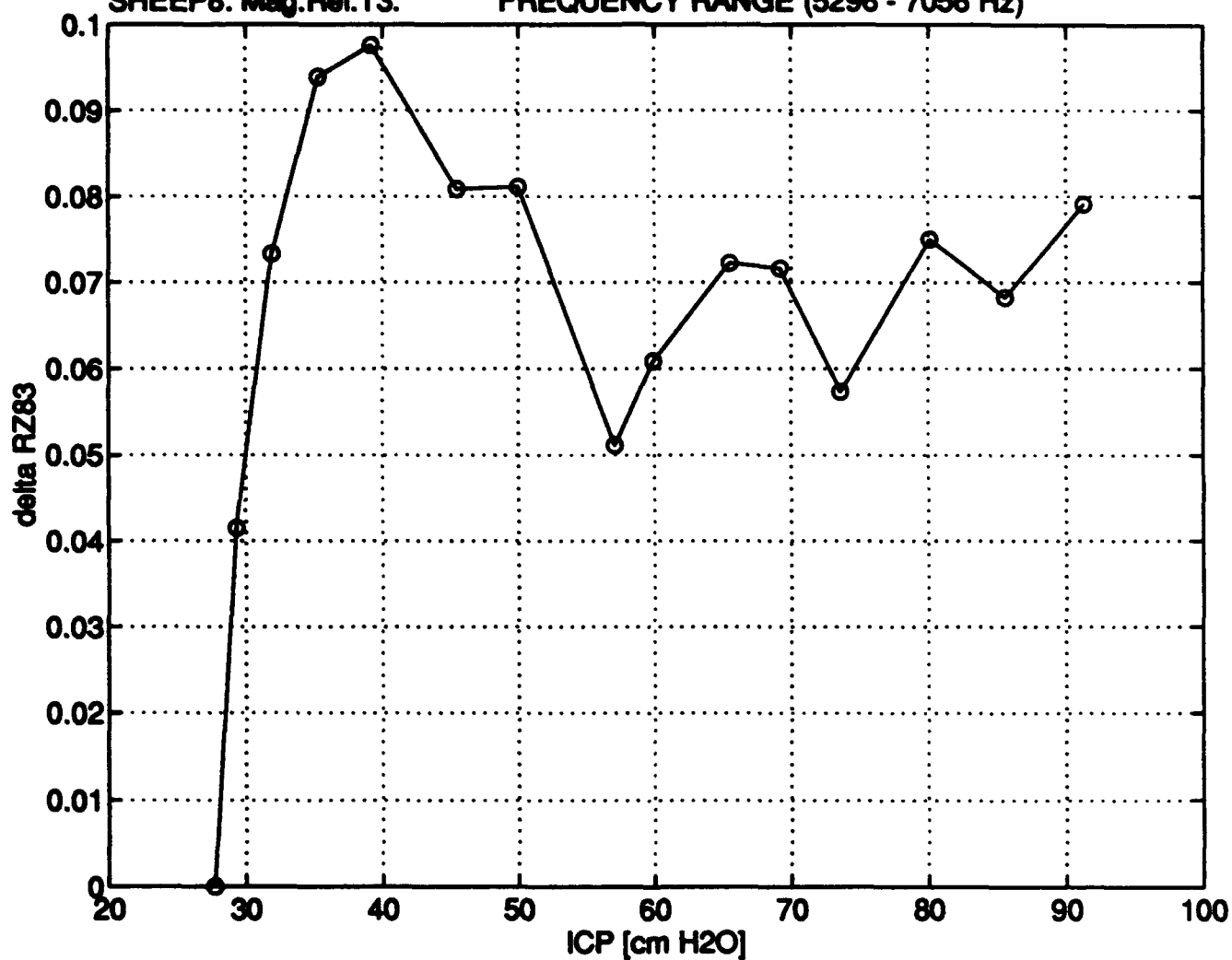
PHASE OF RELATIVE DRIVING POINT IMPEDANCE, SHEEP8
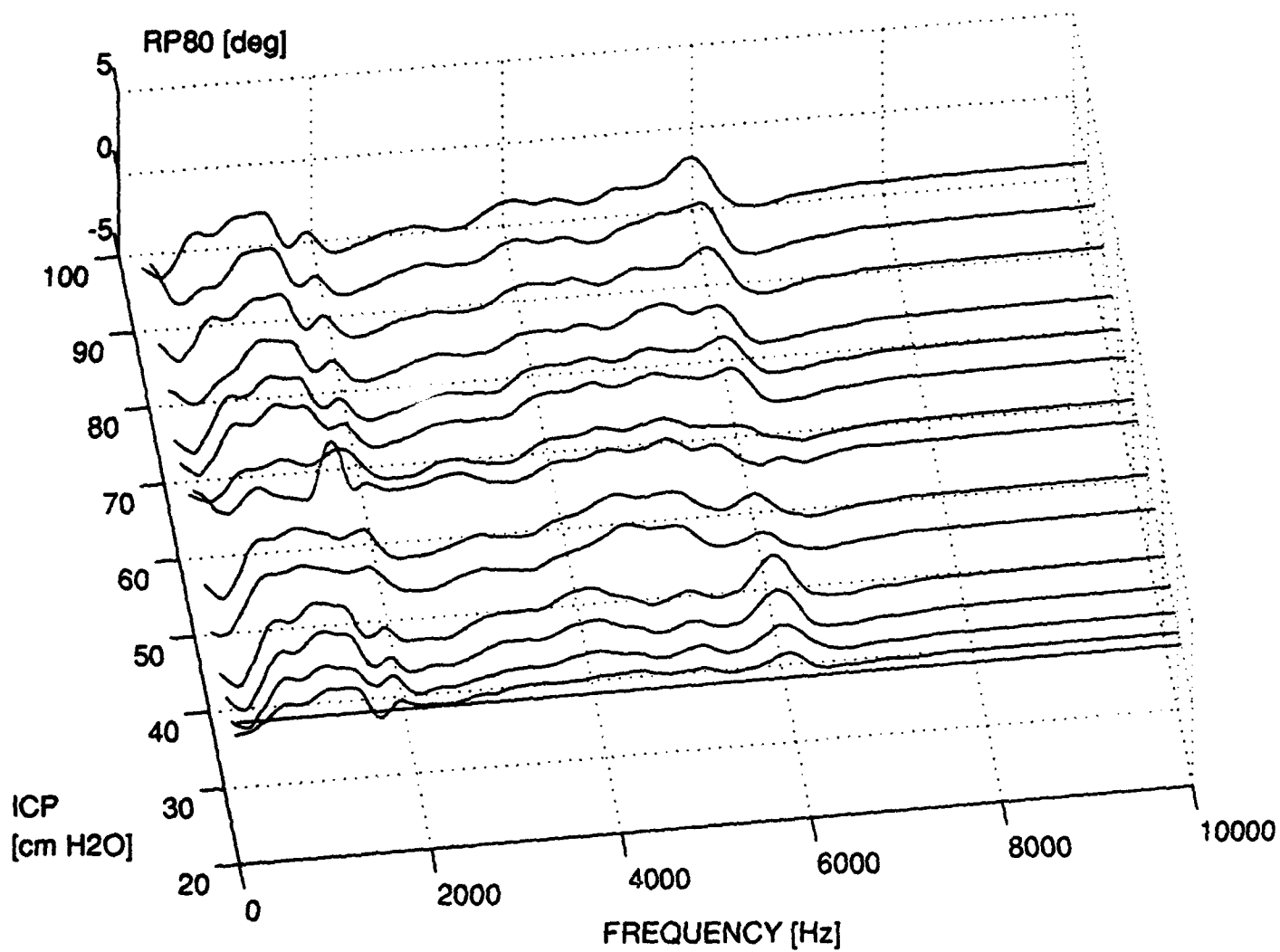
PHASE OF RELATIVE DRIVING POINT IMPEDANCE, SHEEP8
FREQUENCY RANGE (104 - 2096 Hz)
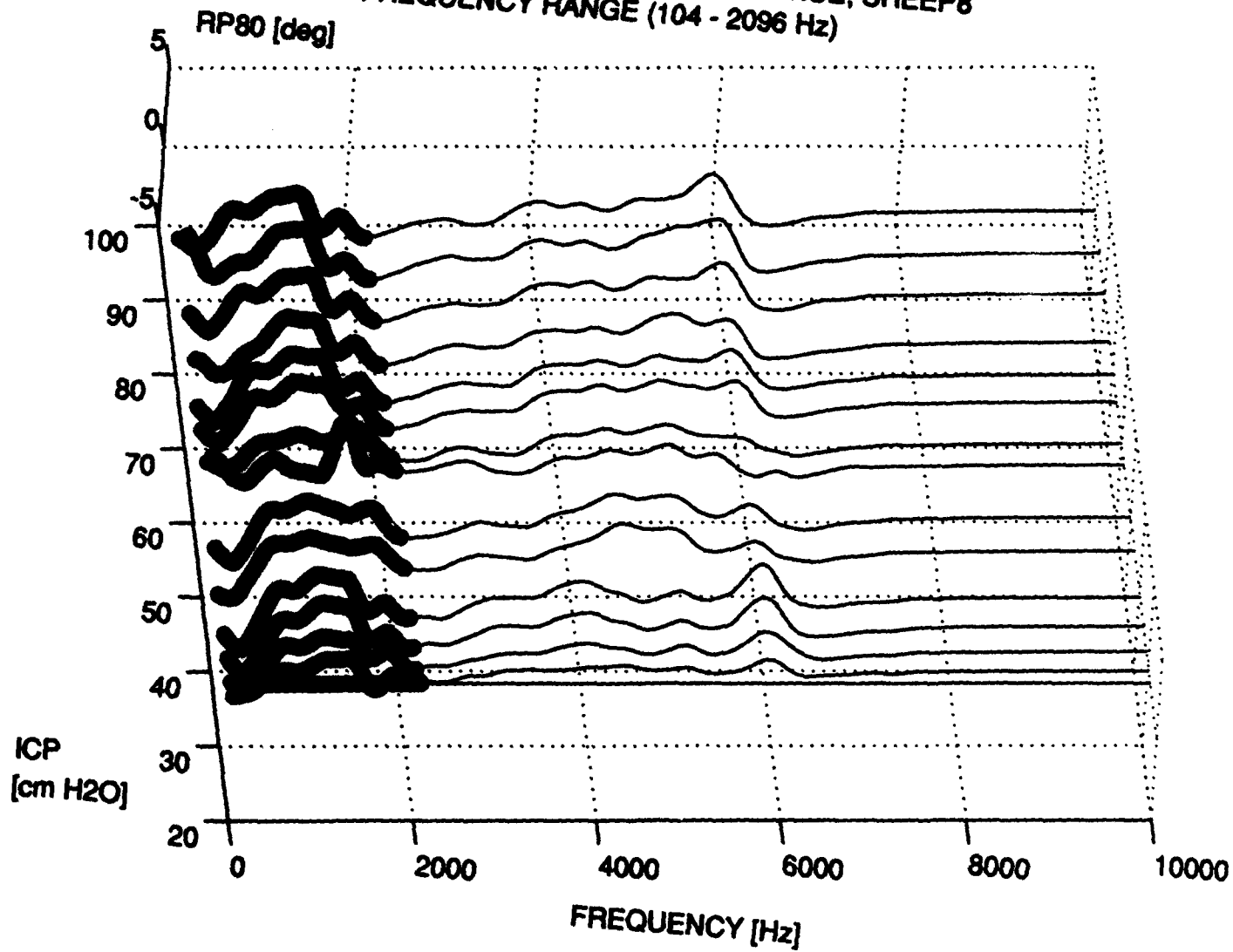
PHASE STANDARD DEVIATION vs. ICP
SHEEP8:Pha.Rel.DP.   FREQUENCY RANGE (104 - 2096 Hz)

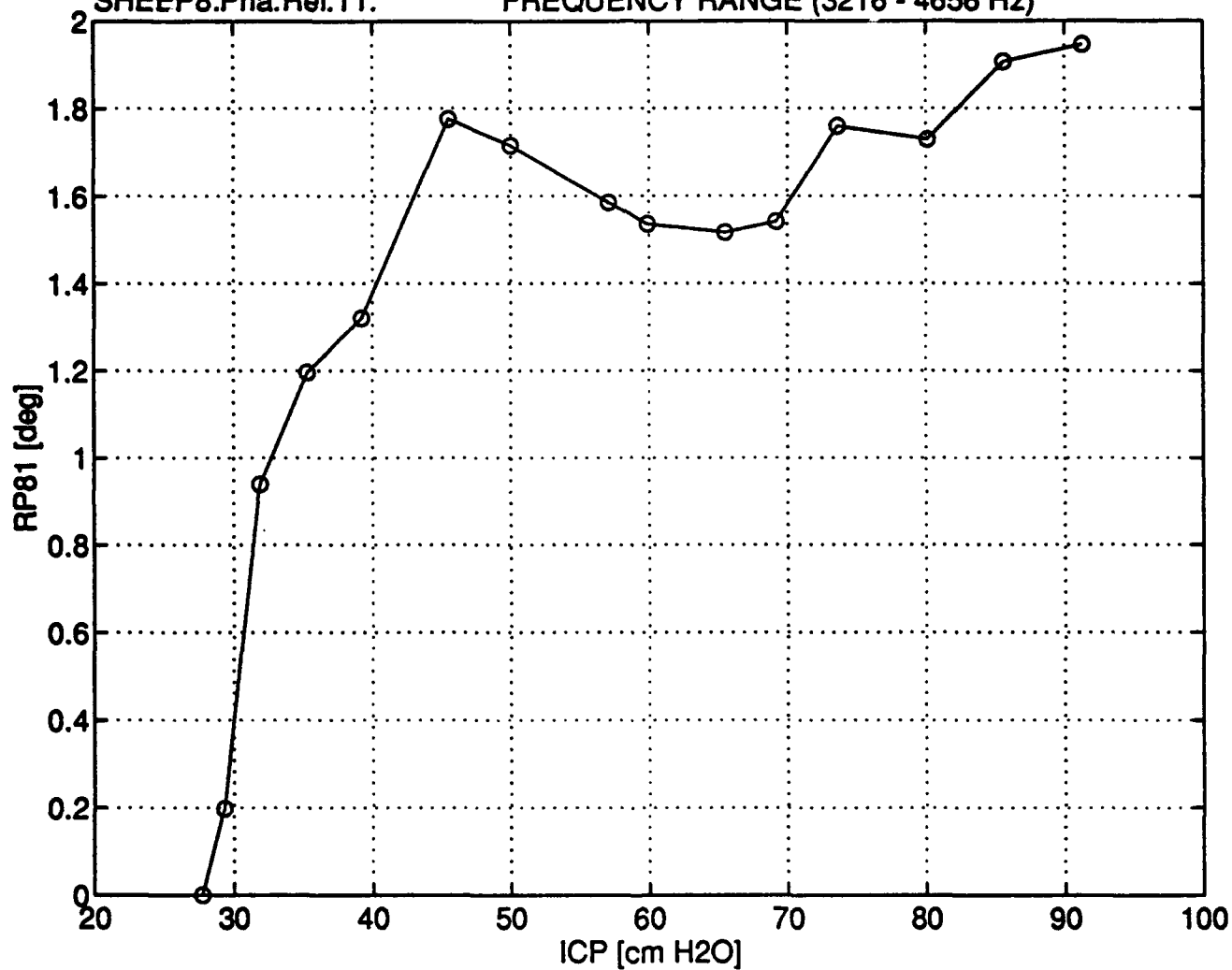PHASE OF RELATIVE DRIVING POINT IMPEDANCE, SHEEP8
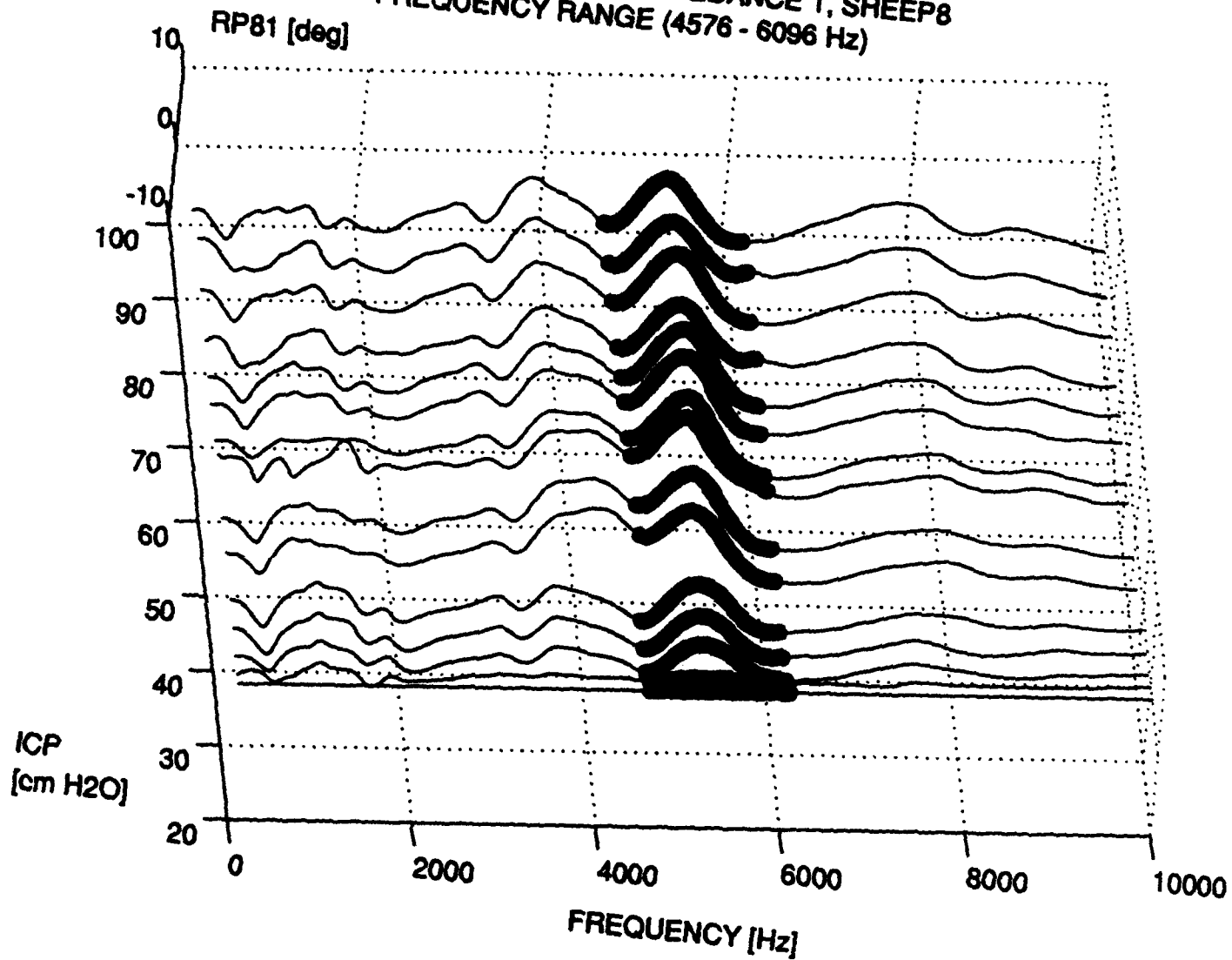FREQUENCY RANGE (3296 - 6496 Hz)

PHASE STANDARD DEVIATION vs. ICP
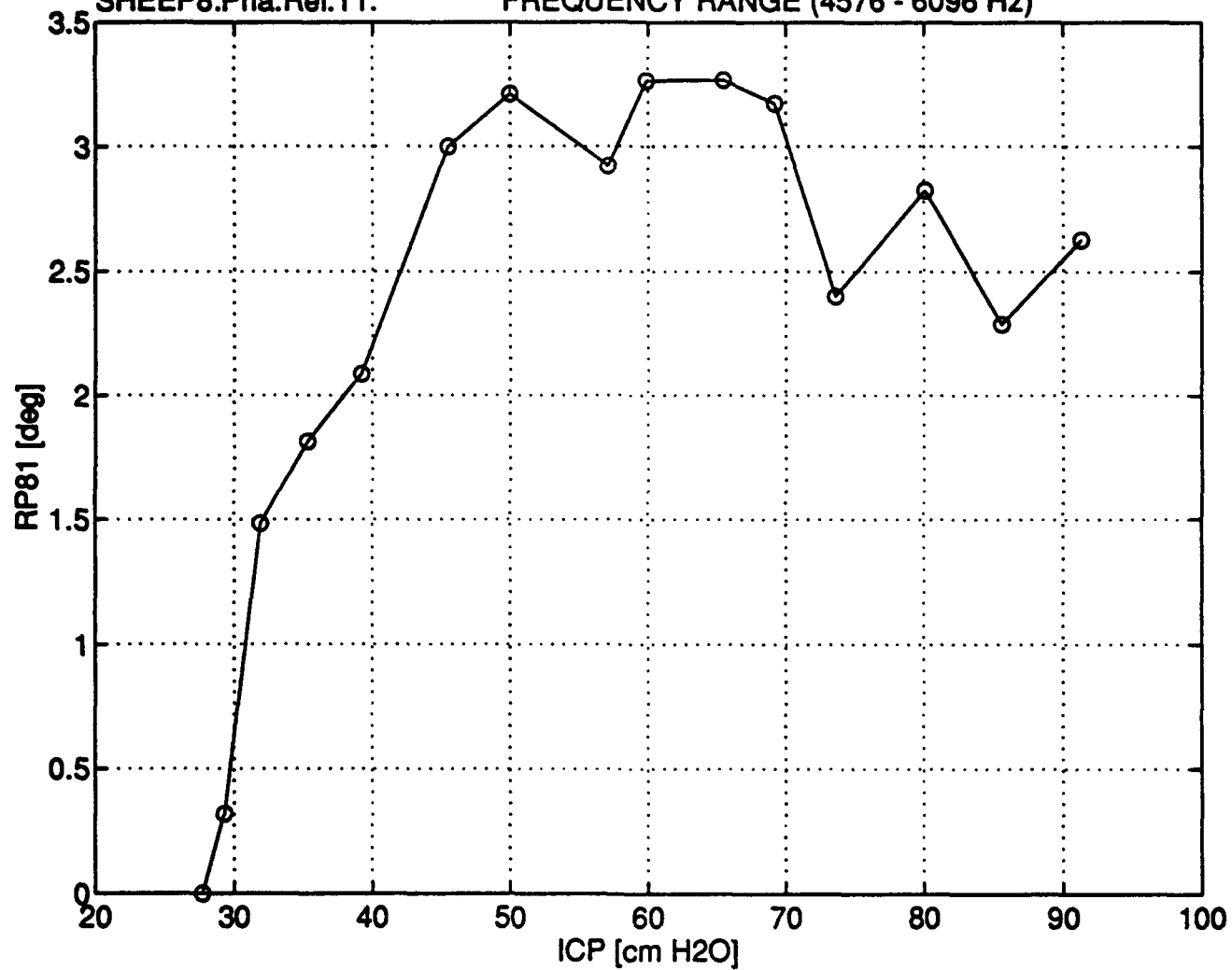SHEEP8:Pha.Rel.DP.   FREQUENCY RANGE (3296 - 6496 Hz)
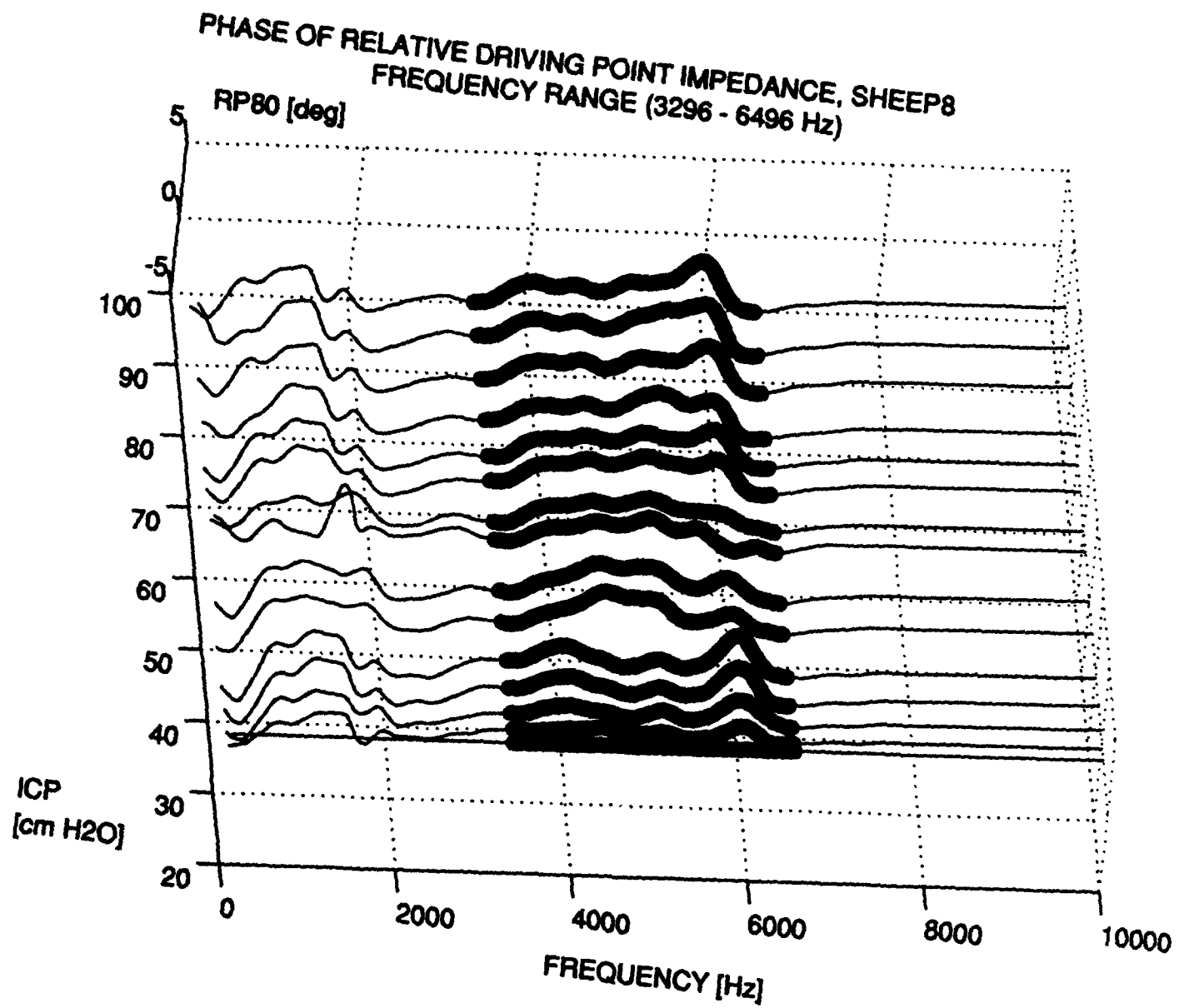
PHASE OF RELATIVE TRANSFER IMPEDANCE 1, SHEEP8

PHASE OF RELATIVE TRANSFER IMPEDANCE 1, SHEEP8
FREQUENCY RANGE (104 - 2096 Hz)
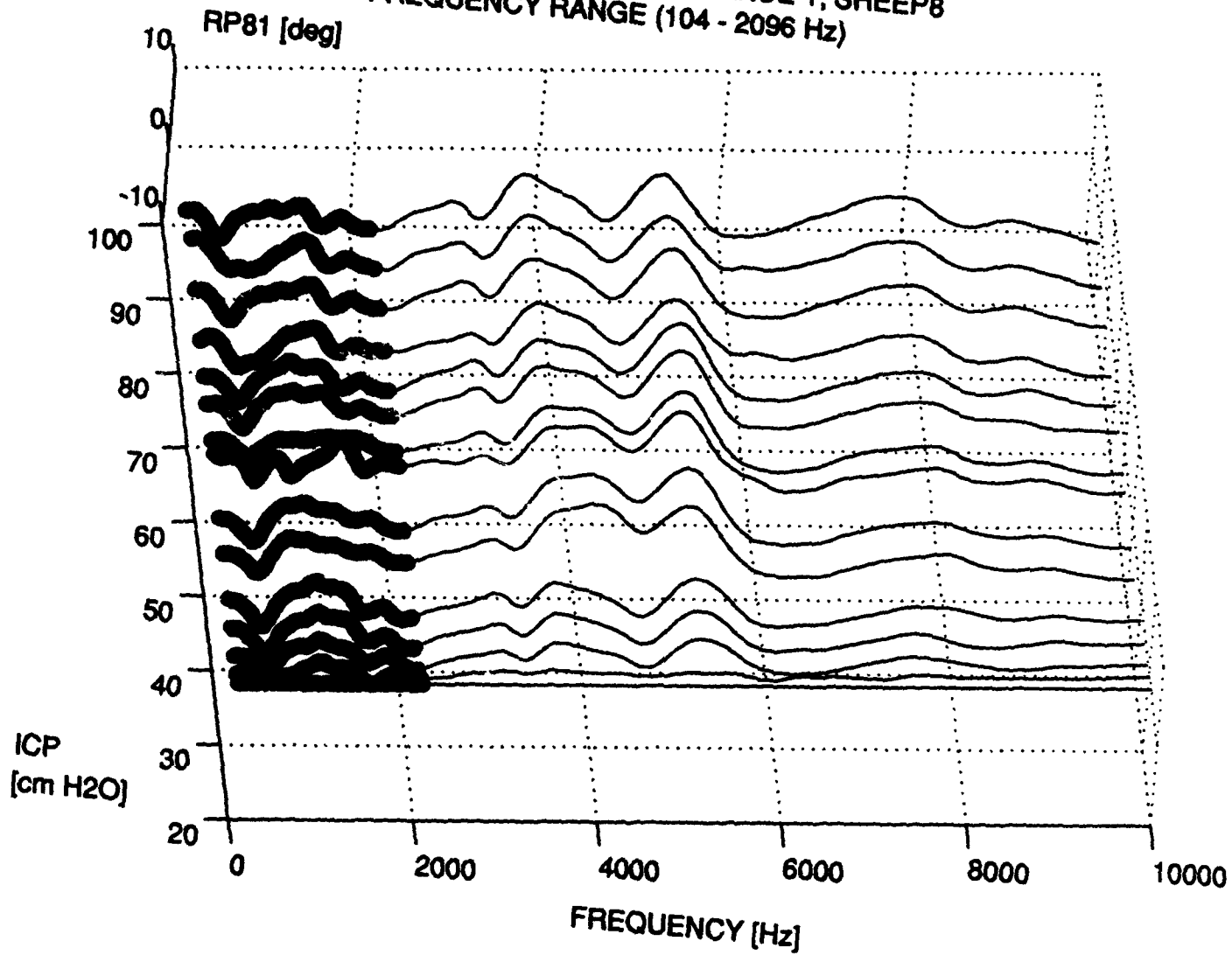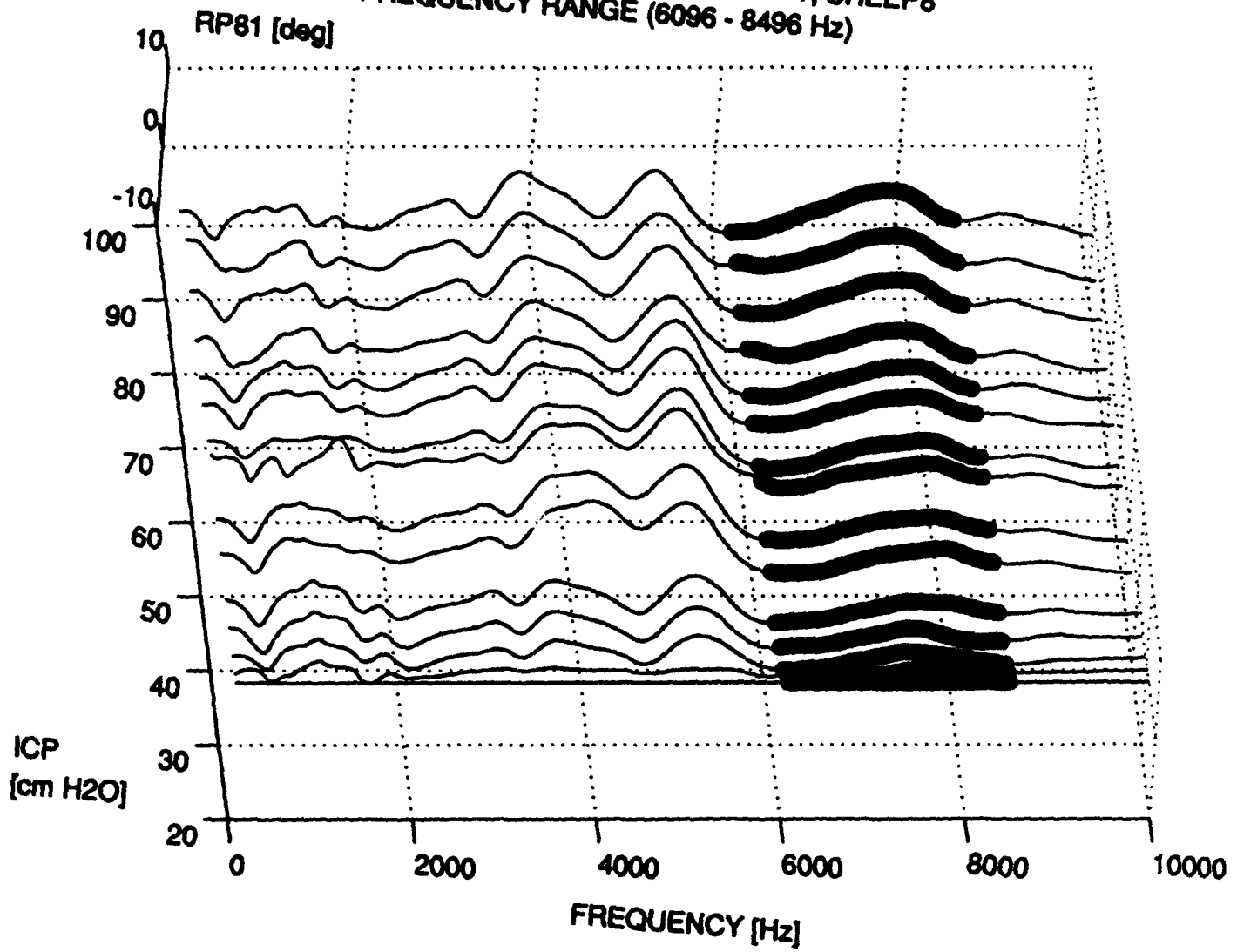
RP81 [deg]

ICP
[cm H2O]

FREQUENCY [Hz]

PHASE STANDARD DEVIATION vs. ICP
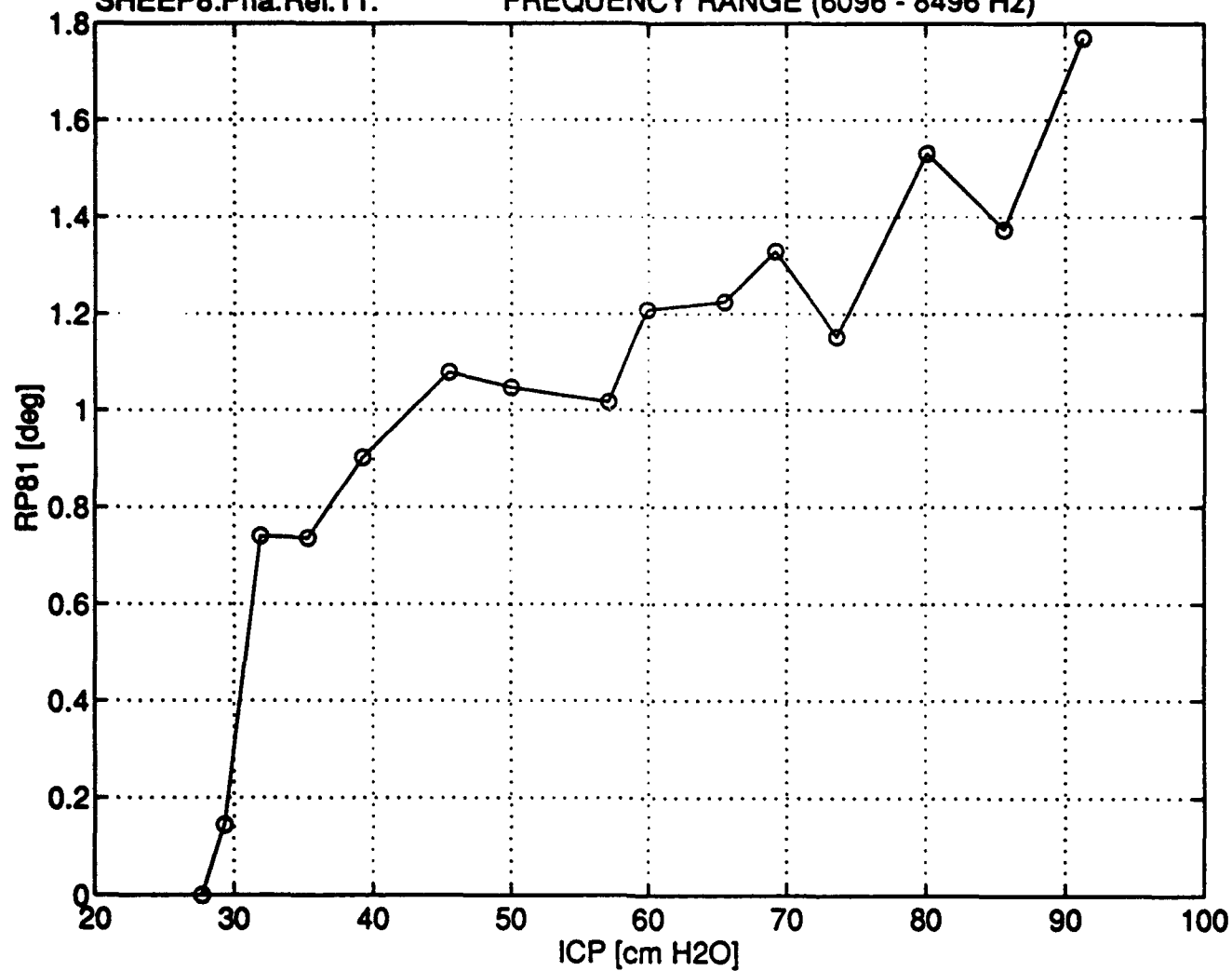SHEEP8:Pha.Rel.T1.   FREQUENCY RANGE (104 - 2096 Hz)
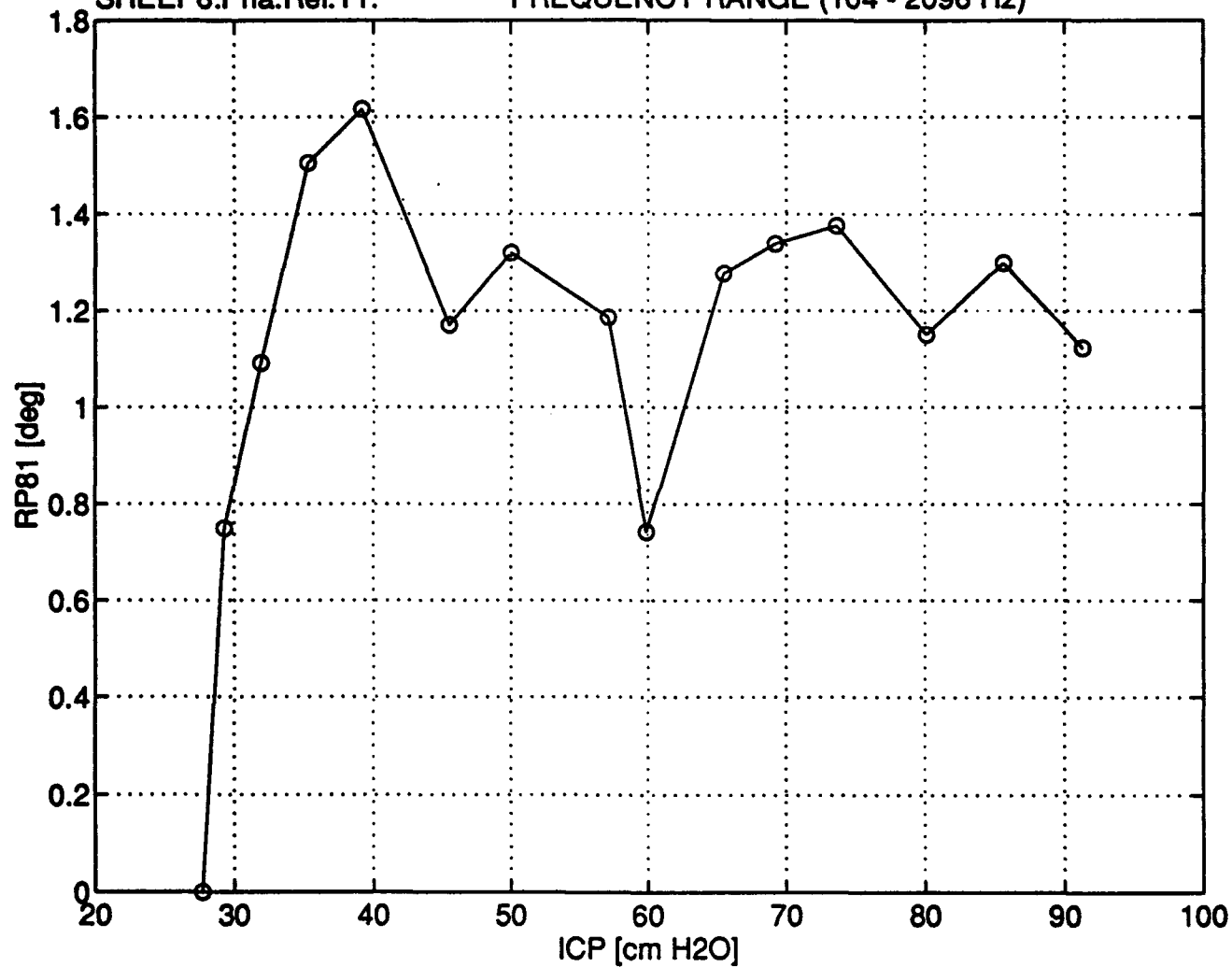
PHASE OF RELATIVE TRANSFER IMPEDANCE 1, SHEEP8
FREQUENCY RANGE (3216 - 4656 Hz)
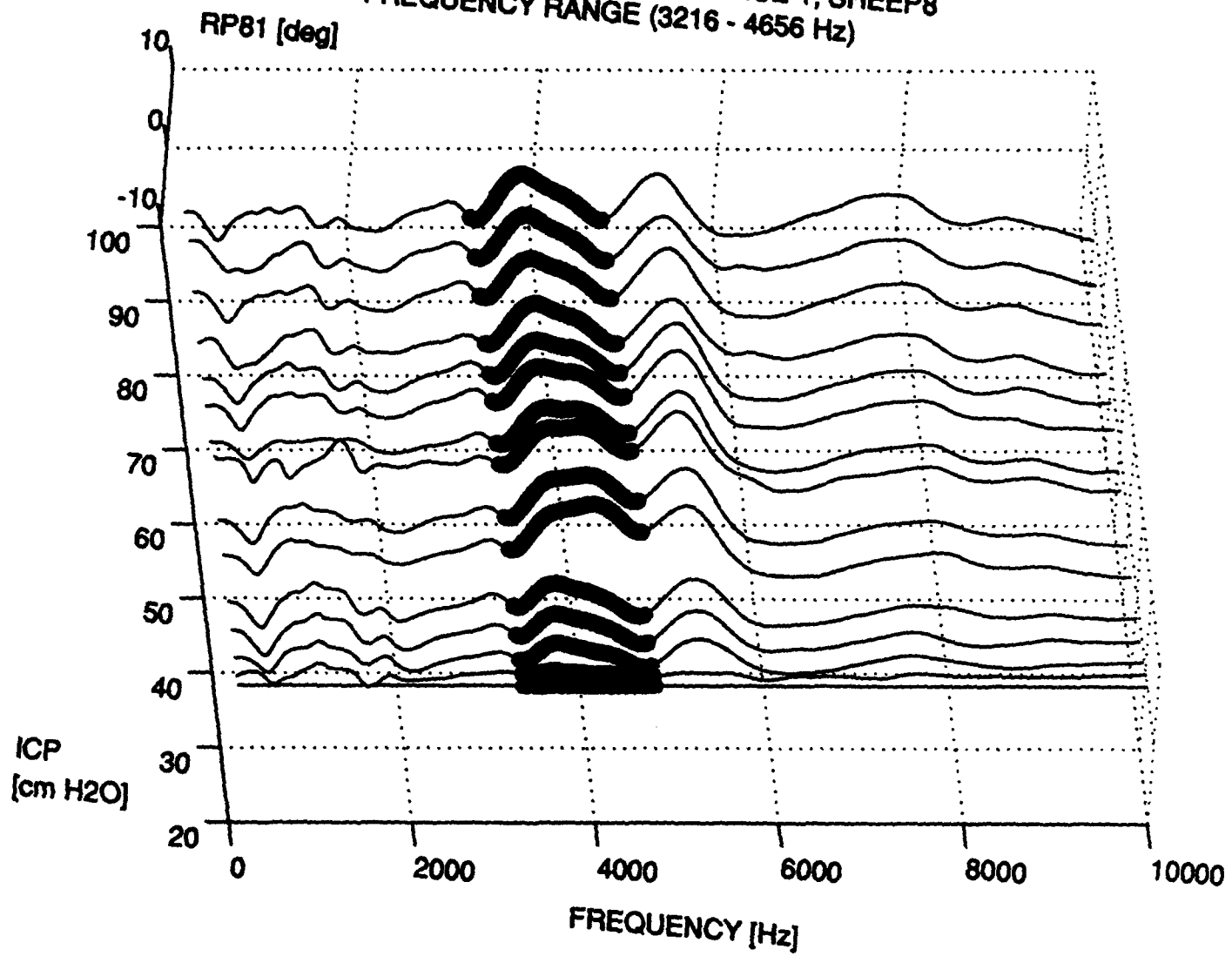
PHASE STANDARD DEVIATION vs. ICP
SHEEP8:Pha.Rel.T1.   FREQUENCY RANGE (3216 - 4656 Hz)

PHASE OF RELATIVE TRANSFER IMPEDANCE 1, SHEEP8
FREQUENCY RANGE (4576 - 6096 Hz)

RP81 [deg]

ICP
[cm H2O]

FREQUENCY [Hz]

PHASE STANDARD DEVIATION vs. ICP

SHEEP8:Pha.Rel.T1.   FREQUENCY RANGE (4576 - 6096 Hz)

PHASE OF RELATIVE TRANSFER IMPEDANCE 1, SHEEP8
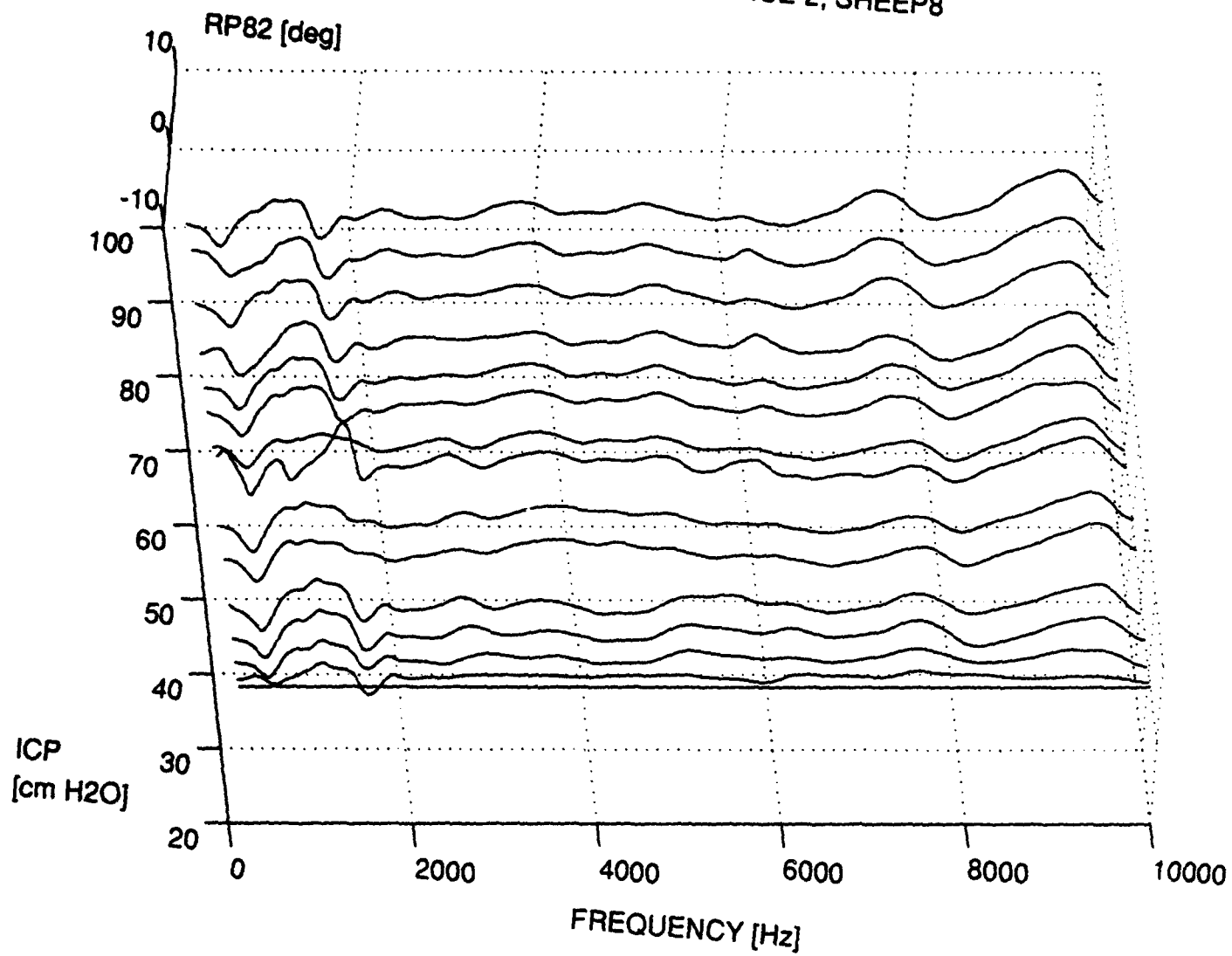FREQUENCY RANGE (6096 - 8496 Hz)

PHASE STANDARD DEVIATION vs. ICP
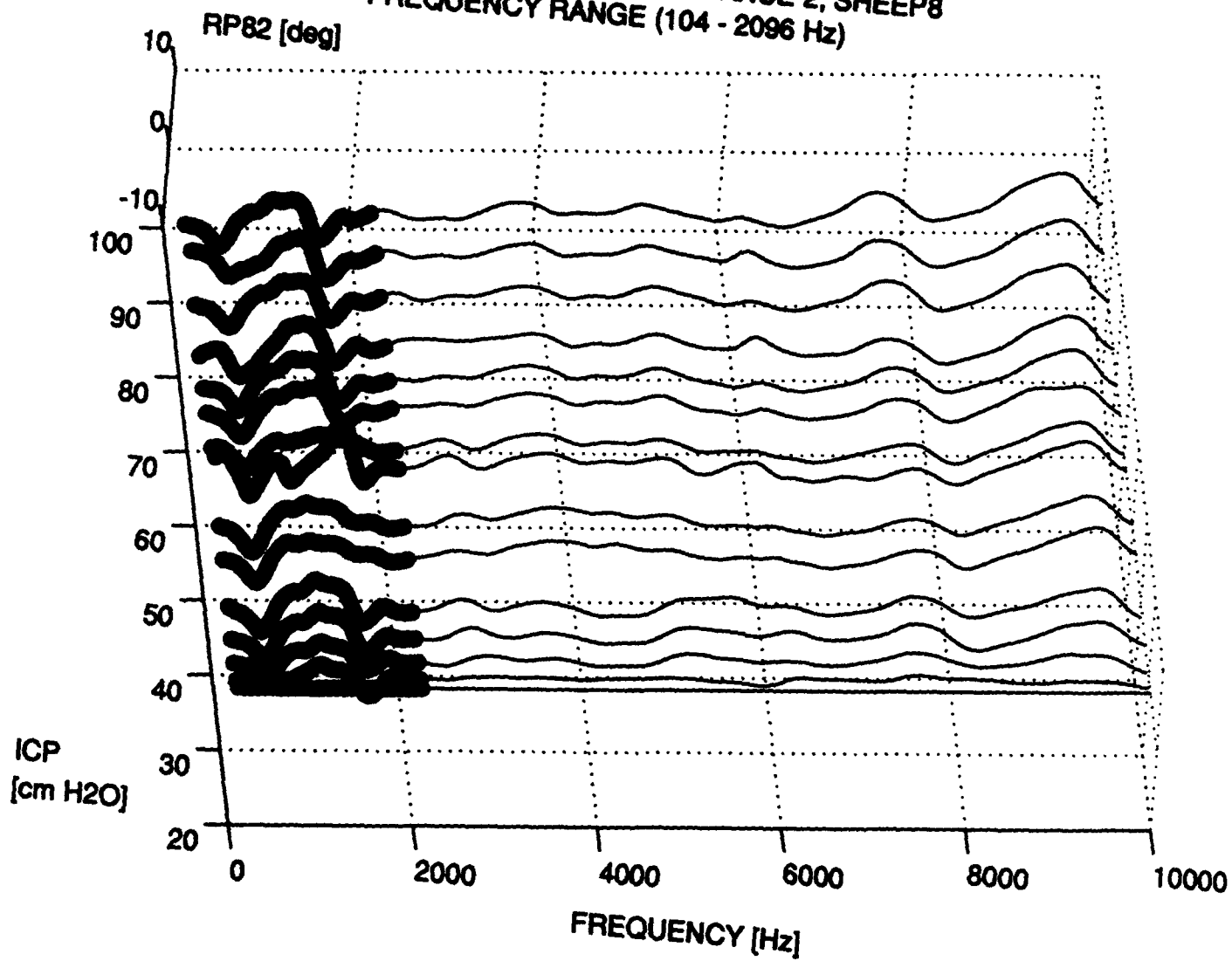SHEEP8:Pha.Rel.T1.   FREQUENCY RANGE (6096 - 8496 Hz)
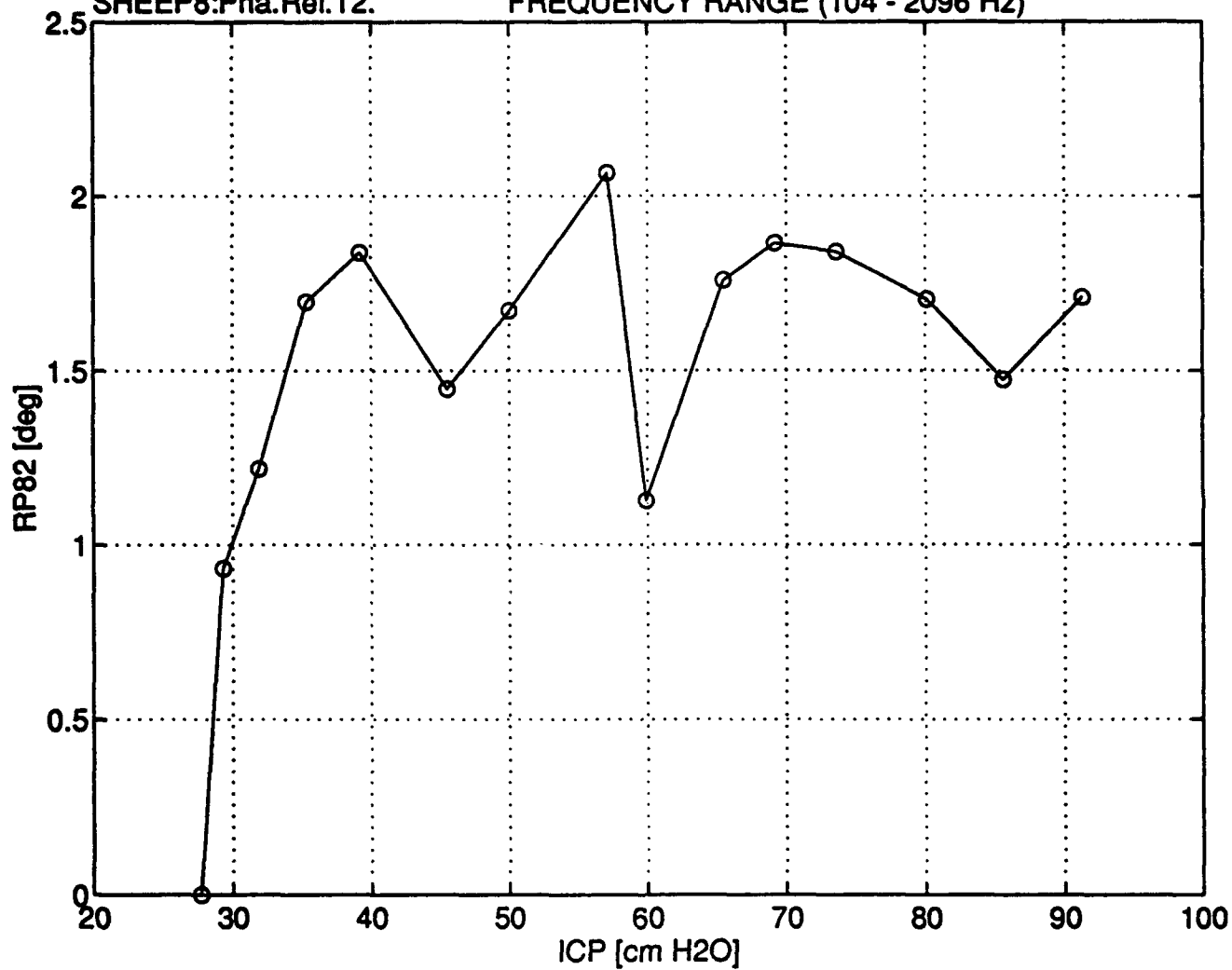
PHASE OF RELATIVE TRANSFER IMPEDANCE 2, SHEEP8

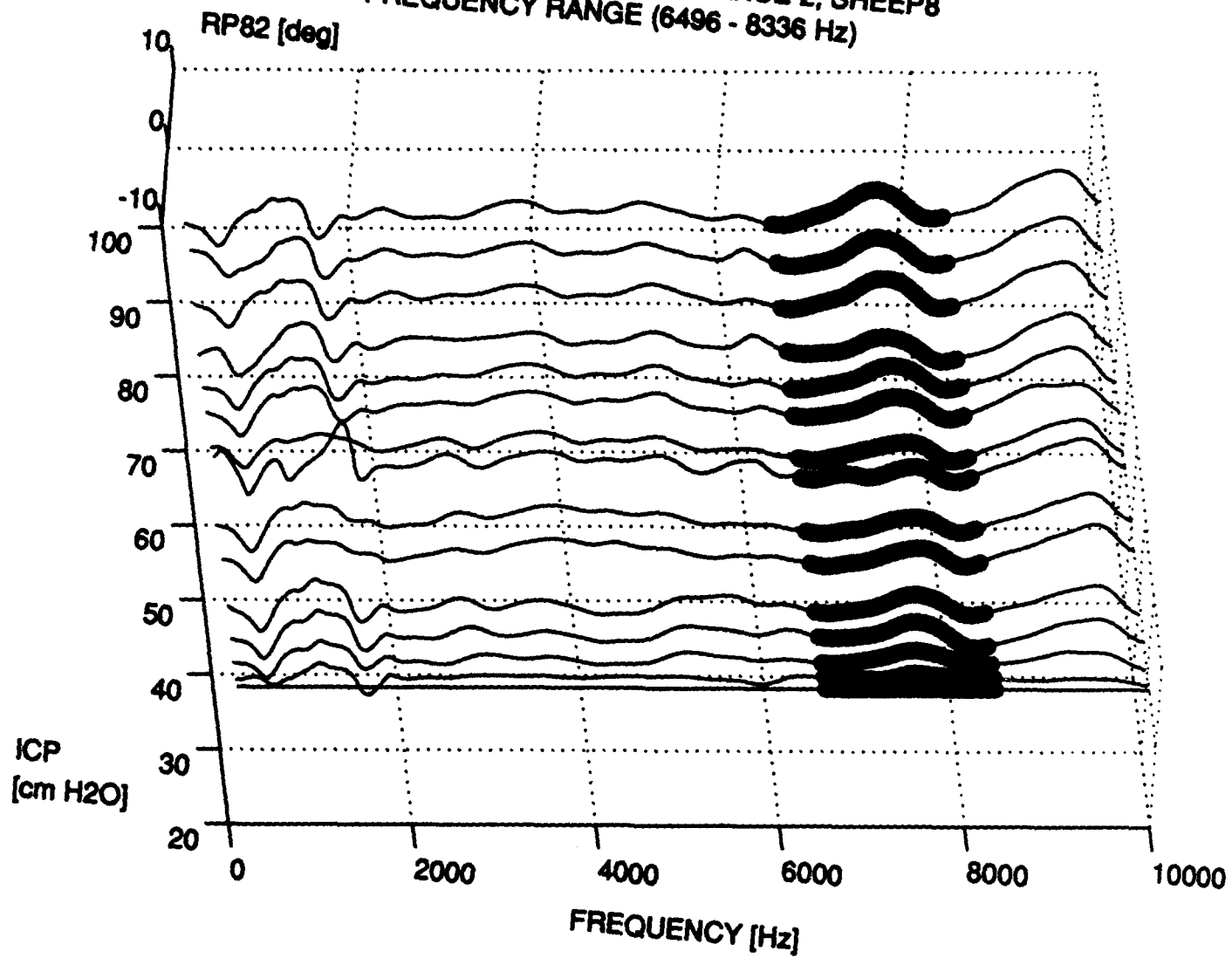PHASE OF RELATIVE TRANSFER IMPEDANCE 2, SHEEP8
FREQUENCY RANGE (104 - 2096 Hz)

PHASE STANDARD DEVIATION vs. ICP

SHEEP8:Pha.Rel.T2.   FREQUENCY RANGE (104 - 2096 Hz)

PHASE OF RELATIVE TRANSFER IMPEDANCE 2, SHEEP8
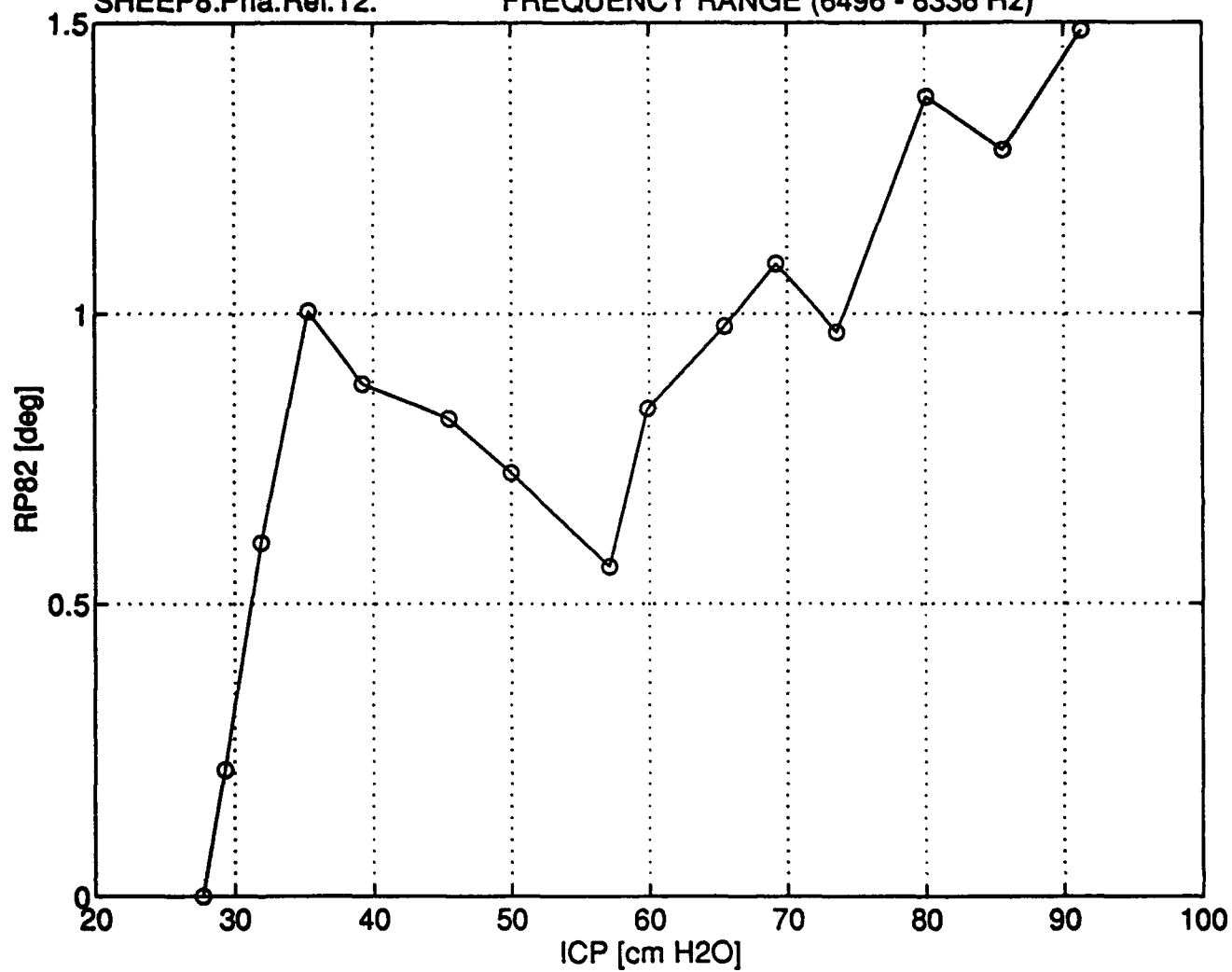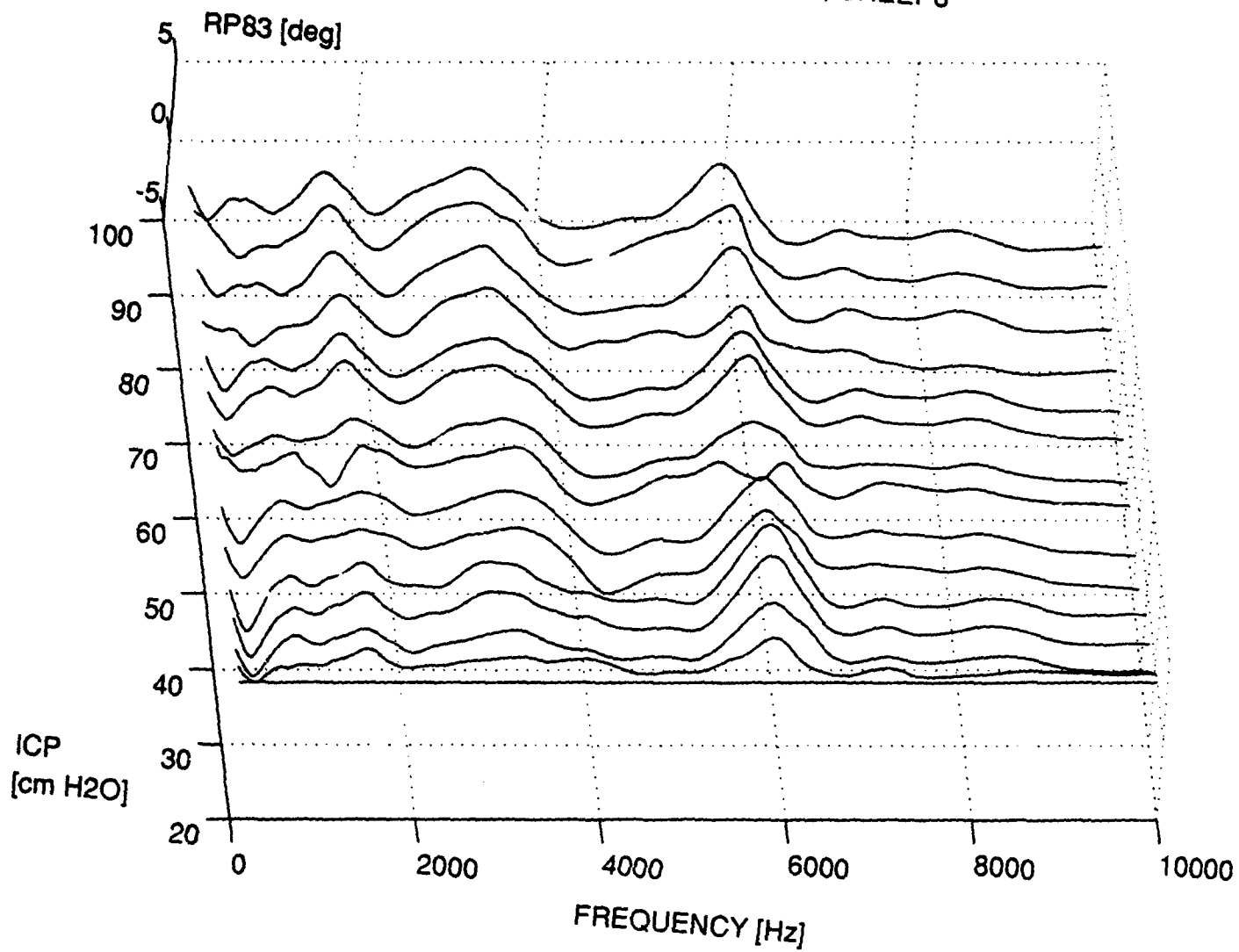FREQUENCY RANGE (6496 - 8336 Hz)

PHASE STANDARD DEVIATION vs. ICP
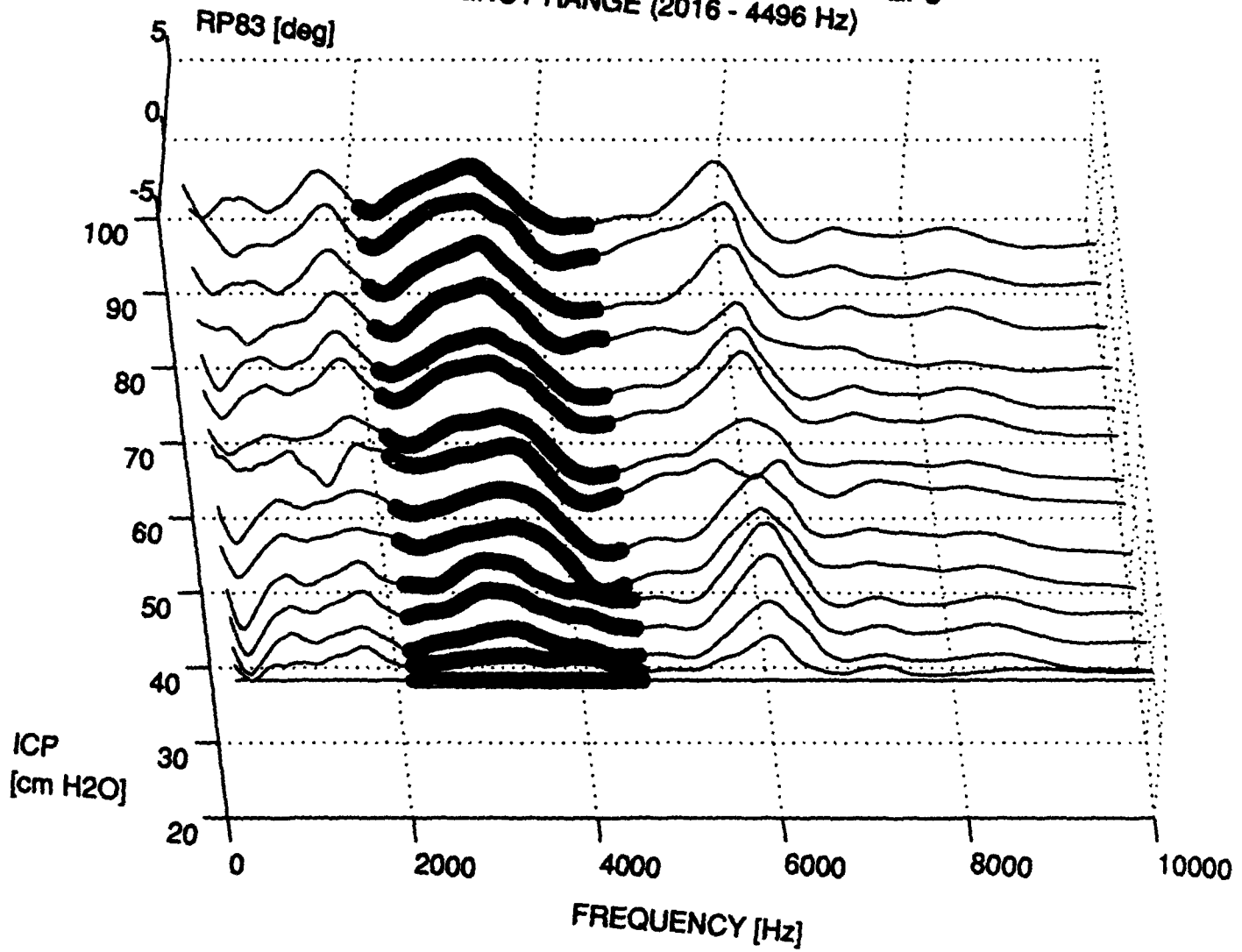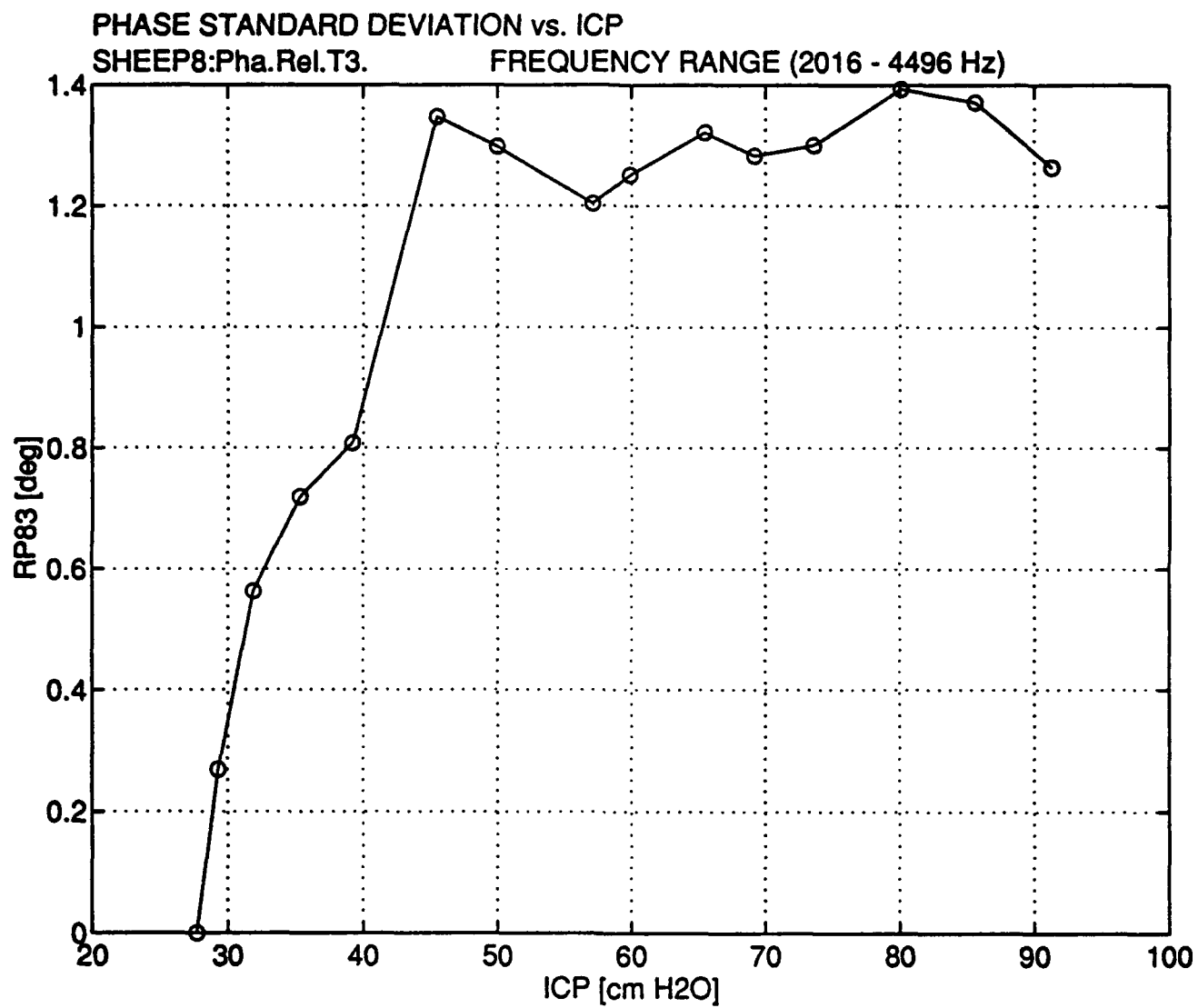SHEEP8:Pha.Rel.T2.   FREQUENCY RANGE (6496 - 8336 Hz)

PHASE OF RELATIVE TRANSFER IMPEDANCE 3, SHEEP8

RP83 [deg]

ICP
[cm H2O]

FREQUENCY [Hz]

PHASE OF RELATIVE TRANSFER IMPEDANCE 3, SHEEP8
FREQUENCY RANGE (2016 - 4496 Hz)

PHASE STANDARD DEVIATION vs. ICP
SHEEP8:Pha.Rel.T3.   FREQUENCY RANGE (2016 - 4496 Hz)
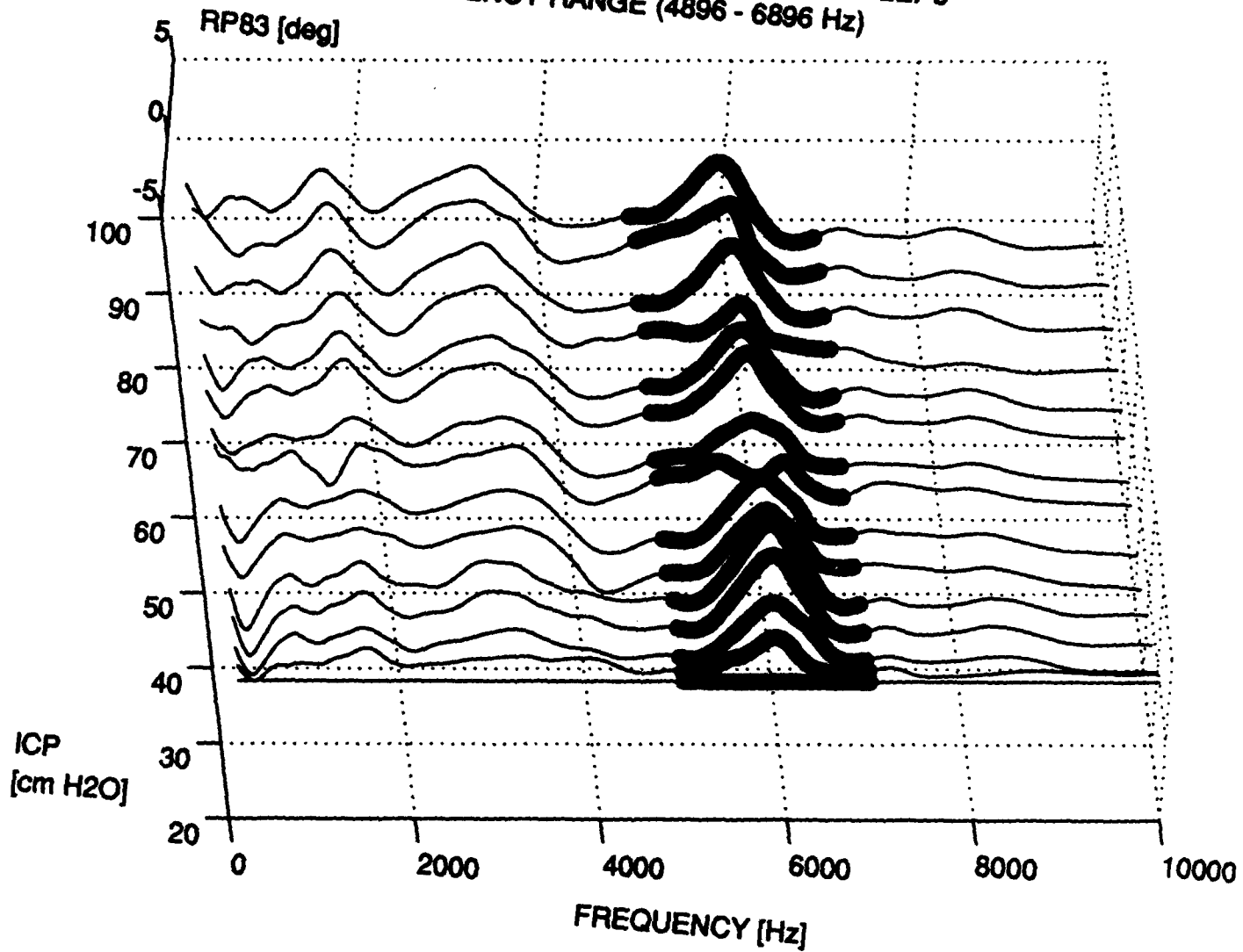
PHASE OF RELATIVE TRANSFER IMPEDANCE 3, SHEEP8
FREQUENCY RANGE (4896 - 6896 Hz)

PHASE STANDARD DEVIATION vs. ICP

SHEEP8:Pha.Rel.T3.   FREQUENCY RANGE (4896 - 6896 Hz)